THE UNIVERSITY *of* EDINBURGH

The role of peritoneal mesothelial cells and the inflammatory response in peritoneal fibrosis

Xuan Wu

Thesis Submitted for Doctor of Philosophy

University of Edinburgh

Edinburgh 2011

DECLARATION

I hereby declare that I am the author of this thesis and that I did all the work described herein, unless otherwise specified. All sources have been acknowledged by the means of references.

Xuan Wu

ACNOWLEDGEMENTS

It is a great opportunity for me to thank people who help me get through these unforgettable three years. Firstly, I would like to specially acknowledge my principal supervisor Professor J. Ian Mason for all his support, advice and assistance throughout these years. I would like to thank him for being such a wonderful mentor, supporting my work and ideas as well as his great contribution during the writing parts of this thesis. I would also like to thank my second supervisor, Professor Stephen G. Hillier for all his support during my study, as well as the generous help and encouragement he offered me in my daily life. I would also like to thank my third supervisor Dr Chris Harlow for his dedicated contribution to my work and valuable discussions during conduction of experiments and writing up of this thesis. Special thanks to Professor Hilary O. Critchley, Dr Scott Fegan and Dr Andrew Horne for their contribution to the recruitment of primary cells (project LREC numbers 04-51103-36). I am also grateful to Mrs Deborah Price, Dr Forbes Howie and Mrs Anne Grant for technical assistance and training during the time of my studies. I also want to thank Xia Ren, PhD student in our lab, for her great help. Many thanks to Mrs Catherine Murray and Mrs Sharon McPherson for assistance in primary tissue collection. Thank you to Dr Fiona Gardiner who is happy to solve any problems I met in the lab. A huge thank you to all the people in the MRC/Centre for Reproductive Health (CRH) at the University of Edinburgh for all the help and fun I had in the last four years.

I do much appreciate financial support from the College of Medicine and Veterinary Medicine PhD scholarship, University of Edinburgh; and the Overseas Research Students Awards Scheme, UK.

Finally, I extremely appreciate my super parents. Without their love and support, I couldn't have such a wonderful life.

ABSTRACT

Post-operative adhesion is a common complication after abdominal surgery, with high impact on patient wellbeing and healthcare costs. The repair of peritoneum is a complex process involving orderly phases which share some common features to normal wound healing. These include coagulation, infiltration of inflammatory cells, cell proliferation, extracellular matrix (ECM) deposition and remodelling, often with overlap between phases. The unique feature of peritoneal repair is that both small and large peritoneal wounds heal in a similar time. The peritoneum is a monolayer of elongated, flattened, squamous-like peritoneal mesothelial cells (PMC). Local mesothelial cell proliferation, centripetal cell migration from the wound edge, as well as incorporation of free-floating mesothelial cells may all contribute to repair of injured peritoneum. To date, the only well-characterised pathologic mechanism underlying post-operative adhesion formation at the molecular level is the formation of the fibrin layer and regulation of peritoneal fibrinolytic capacity. However, the contributions of collagen deposition and ECM remodelling to the peritoneal repair mechanism are not well understood. This thesis focuses on the role of PMC in the regulation of ECM deposition and remodelling in response to inflammatory stimuli in both *in vivo* and *in vitro* models, aiming to identify other key pro-fibrotic factors involved in the development of post-operative adhesion.

We first identified that lysyl oxidase (LOX) played a key role in the progression of peritoneal fibrosis by regulating collagen cross-linking and deposition *in vivo*. The inhibition of LOX enzyme activity prevented the formation of fibrotic tissue by reducing collagen deposition. Meanwhile, dexamethasone (DEX) treatment also minimized the fibrotic response. Furthermore, *in vitro* studies showed that the induction of collagen deposition factors in PMC, including LOX and pro-collagen I, required both IL-1 and TGF-β signalling pathways. Thus, the combination of IL-1 +

TGF-β was adopted in an *in vitro* model to mimic the inflammatory environment during peritoneal repair. Treatment of PMC with IL-1+TGF-β caused an epithelial-to-mesenchymal transition (EMT). These transformed PMC had enhanced cell motility and were more adherent to fibronectin. Finally, a real-time quantitative PCR-based microarray was used for genomic analysis of ECM-adhesion-related PMC genes in response to IL-1 and TGF-β treatment. The results showed that IL-1 was more involved in regulating ECM degradation by inducing expression of matrix metalloproteinase (MMP) genes, whereas TGF-β mainly affected genes involved in ECM deposition, including collagens and other ECM components. However, both cytokines were shown to regulate some key genes involved in the development of adhesion, including COL16A1, COL7A1, FN1, ITGA5, and TGFB1. Moreover, IL-1 was shown to reduce ITGA4 and ITGB6 expression affecting adherence of PMC to basement membrane, while TGF-β increased MMP14 and MMP16 expression, which could facilitate invasion of EMT-transformed PMC to the site of tissue repair.

In summary, this thesis indicates that LOX plays an important role in peritoneal fibrosis. Secondly, a combination of IL-1 and TGF-β1 treatment demonstrates how these factors can act in concert to orchestrate tissue remodelling during peritoneal repair. Finally, genomic analysis of ECM-adhesion genes increases our understanding of aspects of the pathology of post-operative adhesion and identifies novel potential therapeutic targets to prevent adhesion formation.

LIST OF FIGURES

LIST OF TABLES

LIST OF ABBREVIATIONS

11b-HSD	11b-hydroxysteroid dehydrogenase
ABC	avidin-biotin complex
ACP	aldol condensation product
ADAMTS1	a disintegrin and metalloproteinase with thrombospondin motifs 1
AP-1	activating protein-1
ASK-1	apoptosis signal-regulated kinase-1
ATCC	American Type Culture Collection
BAPN	β-aminopropanenitrile
BC	buffy Coat
bHLH	basic helix-loop-helix
BM	basement membrance
BSA	bovine albumin serum
BSO	bilateral salpingo-oophorectomy
CA-IL-1α	cell-associated IL-1α
CAMs	cell adhesion molecules
CBP	CREB-binding protein
CNT	carbon nanotubes
CREB	cAMP response element-binding protein
CTGF	connective tissue growth factor
DAB	diaminobenzidine
DBPS	dulbecco's phosphate-buffered saline
deLNL	dehydrolysinonorleucine
DEX	dexamethasone
Diag Lapscpy	diagnostic laparoscopy
ECM	extracellular matrix
EGF	epidermal growth factor
EMT	epithelial-mesenchymal transition
ERK	extracellular signal-regulated kinase
F	cortisol
FAK	focal adhesion kinase
FBGC	foreign body giant cell
FBS	fetal Bovine Serum
FGF	fibroblast growth factor
GC	glucocorticoids
GM-SCF	granulocyte–macrophage colony stimulating factor
GR	glucocorticoid receptor
GRE	GC-response elements
GRO-a	growth-related oncogene-a
G-SCF	granulocyte colony stimulating factor
H&E	hematoxylin and eosin
HB-EGF	heparin-binding EGF

HGF	hepatocyte growth factor
HMB	heavy menstrual bleeding
HMB	heavy menstrual bleeding
HRP	horseradish peroxidise
HSP	heat shock protein
i.p	intra-peritoneal
ICAM-1	intercellular adhesion molecule
IFN-γ	interferon-γ
IKKs	IκB kinases
IL	interleukin
IL-1R	IL-1 receptor
IL-1ra	IL-1 receptor antagonist
IL-1α	interleukin 1 alpha
IMB	irregular menstrual bleeding
IMDM	Iscove's Modified Dulbecco's medium
IP-10	IFN-g-inducible protein-10
IRAK	IL-1 receptor-associated kinase
IκB	nuclear factor of kappa light polypeptide gene enhancer in B-cells inhibitor
JNK	c-Jun N-terminal kinase
Lap Ster	laparoscopic sterilisation
LFA-1	lymphocyte function-associated antigen-1
LIF	left Iliac Fossa
LOX	lysyl oxidase
LOXL	LOX-like
LPS	Lipopolysaccharide
LTBP	latent TGF-β binding proteins
LTQ	lysine tyrosylquinone
MA-IL-1	membrane-associated IL-1
MAPK	mitogen-activated protein kinases
MCP-1	monocyte chemoattractant protein-1
M-CSF	macrophage colony-stimulating factor
MEKK	mitogen-activated protein kinase/Erk kinase kinase;
MKK	mitogen-activated protein kinase kinase
MKP-1	MAPK phosphatase 1
MMP	matrix metalloproteinase
NA	not applicable
NEMO	NF-κB essential modulator
NF-κB	nuclear factor kappa-light-chain-enhancer of activated B cells
nGRE	negative GRE
NGS	normal goat serum
NO	nitric oxide
NT	multi-wall carbon nanotubes

NTC	no template control
OSE	ovarian surface epithelial
PAI	plasminogen activator inhibitors
PBMC	peripheral blood mononuclear cells
PDGF	platelet-derived growth factor
PMA	phorbol myristate acetate
PMC	peritoneal mesothelial cells
PMN	polymorphonuclear leukocytes
PR	progesterone receptor
RER	rough endoplastic reticulum
RIF	right Iliac Fossa
RIP-1	receptor-interacting protein-1
RSO	right salpingo-oophorectomy
SARA	smad anchor for receptor activation
SDF-1	stromal cell-derived factor-1
STAH	subtotal abdominal hysterectomy
STAT	signal transduction activator of transcription
SWNT	single-walled nanotube
TACE	TNF alpha converting enzyme
TAH	total abdominal hysterectomy,
TAK	TGF-β activated kinase
TBS	tris-buffered saline
TBST	tris-buffered saline supplemented with Tween
TGF-β1	transforming growth factor beta 1
TGF-βR	TGF-β type receptors
TIMP	tissue inhibitors of metalloproteinase
TIR	toll-like/IL-1 receptor
TNF-R	TNF receptor
TNF-α	tumor necrosis factor-alpha
tPA	tissue plasminogen activators
TRADD	TNF-receptor type 1 associated death domain-containing adaptor protein
TRAF	TNF receptor-associated factors
uPA	urokinase plasminogen activators
VCAM	vascular cell adhesion molecule
VEGF	vascular endothelial growth factor
VSMCs	vascular smooth muscle cells
ZO-1	zonula occludens-1

TABLE OF CONTENTS

Chapter 1

General Introduction

The aim of this thesis is to examine the central role of mesothelial-cell-secreted Lysyl Oxidase (LOX) in the fibrotic response associated with peritoneal fibrosis following inflammatory injury, using *in vivo* and *in vitro* models. Other factors involved in the fibrotic process will be identified using a PCR-based microarray to analyse cytokine-induced effects on a panel of ECM-associated genes. Understanding the factors regulating peritoneal fibrosis may inform the development of therapeutic agents to limit the development of fibrosis associated with surgery and disease. This review of the relevant literature sets a background to the experimental studies described in subsequent chapters of the thesis.

1.1 Clinical aspects of peritoneal fibrosis and adhesion within the abdominal cavity

Post-operative peritoneal adhesions are very common complications after abdominal surgery (Parker et al., 2005) (Figure 1.1). They can cause bowel obstruction, infertility, and extreme pelvic pain that dramatically impact quality of life and healthcare costs (Parker et al., 2005). Although the problem has been extensively studied *in vitro* and *in vivo*, to date the pathology is still not fully understood. Clinically oriented guidelines for the diagnosis, treatment and options for reducing adhesion still need further investigation. Intra-abdominal adhesions may be congenital or acquired. Congenital adhesions can be attributed to abnormal physiological organogenesis or embryonal development of the abdominal cavity. For example, a frequent observation is the attachment of the sigmoid colon to the left abdominal wall. Fortunately they are rare and usually asymptomatic (Liakakos et al., 2001). Patients who have not undergone surgery still may develop post-inflammatory adhesions (Weibel and Majno, 1973). These are mainly caused by intra-abdominal inflammation linked to diseases such as endometriosis, peritonitis, radiotherapy,

Chlamydia trachomatis infection (Taylor-Robinson et al., 2009), or long-term peritoneal dialysis (Liakakos et al., 2001; Cheong et al., 2001; Monk et al., 1994).

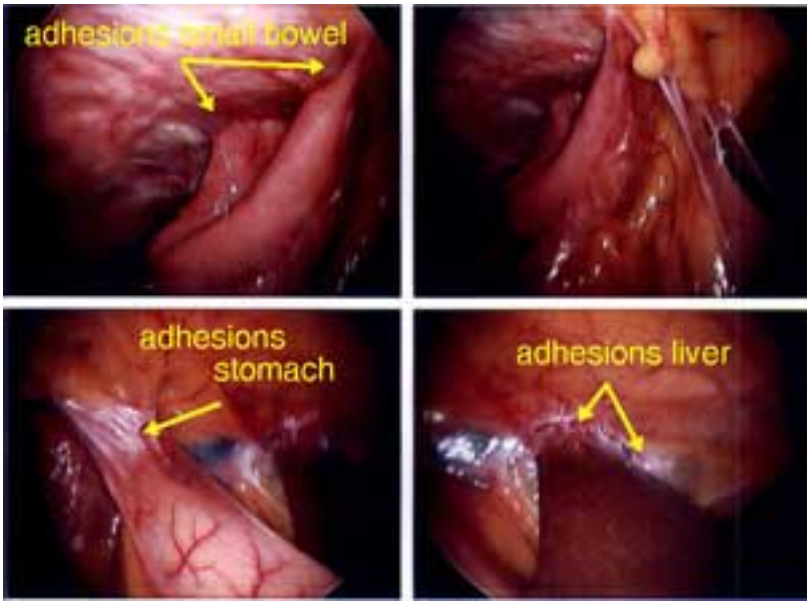

Figure 1.1. Postoperative adhesions following open surgery

Although there can be many causes for intra-abdominal adhesions as mentioned above, the major cause is associated with surgery. The incidence of such peritoneal adhesion in patients following general abdominal surgery ranges from 63% to 97% (Menzies and Ellis, 1990; Group., 1991). They develop as a result of unusual wound healing and are influenced by many factors (Table 1.1).

Table 1.1. Overview of factors that influence the formation of adhesions. Adapted from (Bruggmann et al., 2010).

Factors influence the formation of adhesions	
• Complexity of operation	(DeCherney and diZerega, 1997)
• Extent of peritoneal trauma	(Dijkstra et al., 2000; Menzies, 1993)
• Previous illness (e.g., diabetes)	(Liakakos et al., 2001)
• Poor nutritional status	(Liakakos et al., 2001)
• Intra-abdominal placement of foreign bodies (e.g. meshes)	(Liakakos et al., 2001)
• Excessive coagulation with tissue necrosis	(Drollette and Badawy, 1992)
• Accompanying bacterial infection	(Liakakos et al., 2001)
• Laparoscopy – Dehydration owing to high insufflation pressure and compression of capillary flow	(Yesildaglar and Koninckx, 2000; Molinas and Koninckx, 2000)
• Laparoscopy – Dehydration owing to dry gas	(Ott, 2008)
• Laparoscopy – Mesothelial hypoxia owing to use of CO_2	(Molinas et al., 2001)
• Laparotomy – Dehydration owing to light and heat	(Drollette and Badawy, 1992)
• Laparotomy – Exposure to foreign material (e.g., glove powder)	(Torre et al., 2002; Luijendijk et al., 1996)
• Laparotomy – Mesothelial dehydration and abrasion from use of dry abdominal drapes	(Dijkstra et al., 2000; Menzies, 1993)

A considerable number of these patients experience serious complications, including bowel obstruction (Menzies, 1993; Beck et al., 1999), female secondary infertility (Hershlag et al., 1991) and re-operative complications (Holmdahl and Risberg, 1997). The greater omentum is involved in 80% of cases of postoperative intra-abdominal adhesion and around 50% with the bowel (Menzies and Ellis, 1990). The symptoms caused by these adhesions include meteorism, digestive disorders, infertility, intestinal obstruction, irregular bowel movements, and chronic abdominal pain. Ovarian (Pittaway et al., 1985) and peritubal (Stovall et al., 1989; Molloy et al., 1987) adhesions can also be found in over 90% of patients after gynaecological adnexal surgery. These can reduce mobility, cause mechanical blockage of the Fallopian

tubes, and eventually lead to follicular entrapment. Such adhesions may also interfere with oocyte transport, increasing the risk of ectopic pregnancy (Molloy et al., 1987). Readmission for patients who have had postoperative abdominal adhesion is another huge problem in terms of both patient morbidity and healthcare costs. Awareness of such problems has increased in recent years. A comprehensive epidemiological study was undertaken in Scotland in 1986 to determine the frequency of adhesion-related complications in patients undergoing open lower abdominal surgery (Parker et al., 2001) . The study showed that over a 10 year period, up to 33% of patients were readmitted to hospital for an average of 2.2 occasion, due to a disorder directly or possibly related to adhesions, or for surgery complicated by adhesions. Over £500 million was spent in UK over 10 years for adhesion-related readmission following lower abdominal surgery (Wilson et al., 2002). In a more recent study (Parker et al., 2004), the rates of adhesion-related readmissions following colorectal surgery were found to be very similar between 1986 and 1996-1997. The rate of directly or possibly related readmissions 4 years after colorectal surgery was 25.5% in the former and 29.7% in the latter. This suggested there was no improvement in reduction of adhesion-related readmission despite advances in surgical technique that had occurred. In order to address the problem more specifically, another study (Parker et al., 2005) investigated the risk of adhesions associated with specific types of abdominal surgery and with patient characteristics. In this study, researchers used data from the Scottish National Health Service medical record linkage database to assess the risk of the adhesion-related readmissions following open lower abdominal surgery between April 1996–March 1997. They found a nearly 5% risk of readmission directly related to adhesions in the 5 years following surgery among patients undergoing lower abdominal surgery (excluding appendectomy). Panproctocolectomy and ileostomy surgery appear to be associated with the greatest risk of an adhesion-related readmission. Previous surgery (within 5 years) and patient age (< 60 years) were also identified as important risk factors, as double readmission

risk was found in patients who had had undergone abdominal or pelvic surgery within the previous 5 years and in the patients aged < 60 years as well. This study will help to identify the patients who might have a high risk to get an adhesion related readmission.

Based on pathophysiological mechanisms of origin, various strategies have more recently been taken to reduce adhesions (Table 1.2). Nowadays anti-inflammatory agents, fibrinolytics, and antibiotic solutions are used to prevent adhesion formation (Metwally et al., 2006; Kamel, 2010). Moreover other solutions, such as colloids (dextran) or crystalloid solutions (Ringer lactate or saline), have been used to separate peritoneal surfaces either alone or with corticosteroids or heparin. However, clinical data have yet to demonstrate a clear benefit of these substances in adhesion reduction (Metwally et al., 2006). Other materials have also been employed that form a physical barrier between the peritoneum and organs. For example, cross-linked esters of hyaluronic acid form a viscous gel that is applied to traumatized peritoneal surfaces after abdominal pelvic surgery to keep them separate during the healing process (Mais et al., 2006); carboxymethyl cellulose and polyethyleneoxide form a gel-like resorbent barrier for sealing peritoneal surfaces and preventing future adhesions (diZerega et al., 2007); oxidized regenerated cellulose is used as a resorbant membrane applied to injured surfaces (Ahmad et al., 2008). In summary, however despite many developments in adhesion prevention, there is no consensus on a reliable, consistent method for the prevention/reduction of adhesion formation. Further high-quality studies are therefore required.

Table 1.2. Practical tips: general strategies for reduction of adhesions. Table adapted from (Parker et al., 2005)

●Preference for tissue-sparing and micro-invasive surgical techniques
●Minimization of operating time and of heat and light
●Avoidance of peritoneal trauma by superfluous contact and coagulation
●Limited placement of intra-abdominal foreign bodies such as patches, meshes, and suture material
●Use of moistened abdominal drapes and swabs and occasional application of saline solution to minimize dehydration of mesothelial surfaces
●Irrigation of the abdominal cavity to remove residual intra-abdominal blood depots
●Reduction of infection risk by ensuring sterile working conditions and giving antibiotics as required
●Laparotomy: preferential use of latex- and powder-free gloves
●Laparoscopy: use of humidified gases at appropriately low insufflation pressure
●High-risk patients: use of barrier techniques or peritoneal instillation after appropriate explanation

1.2 Biological function of mesothelium and peritoneal mesothelial cells in the peritoneal cavity

The mesothelium was first described by Bichat in 1827 (Whitaker et al., 1982), as a single layer of flattened cells lining the serous cavities. In embryological studies, mesothelium was found to develop from the mesodermal tissue between 8 and 18 days of gestation, depending on species (Tiedemann, 1976; Hesseldahl and Larsen, 1969). In humans, this occurs around day 14. The mesothelium has been shown to cover three serosal cavities: pleural, pericardial and peritoneal cavities. In the male, it also lines the sac that surrounds the testes. The mesothelium is further defined as visceral mesothelium and parietal mesothelium. The former mainly covers the internal organs, whereas the later is referred to that which lines the body wall. Both morphological and histochemical studies have confirmed that the mesothelium is essentially similar, irrespective of species or anatomical site (Whitaker et al., 1982; Kluge and Hovig, 1967a; Kluge and Hovig, 1967b; Baradi and Rao, 1976; Baradi

and Hope, 1964; Tsilibary and Wissig, 1977; Gaudio et al., 1988; Raftery, 1973a; Whitaker et al., 1980). Despite the longstanding acknowledged existence of the mesothelium, its importance has only recently been recognised. Not only is the mesothelium a protective layer for preventing organs from sticking together, but it also plays an important role in regulating serosal response to injury, infection and disease.

The mesothelium consists of a monolayer of elongated, flattened, squamous-like mesothelial cells (Figure 1.2). The terminology arose because these cells not only display many epithelial characteristics including a polygonal cell shape, cytokeratin expression, and the ability to secrete a basement membrane, but also share some features of mesenchymal cells including expression of vimentin, desmin and, upon stimulation, alpha smooth muscle actin (Czernobilsky et al., 1985; Afify et al., 2002). These cells are approximately 25μm in diameter and rest on a thin basement membrane with underlying connective tissue. The predominant mesothelial cells present a squamous-like cell phenotype; but they can also present a cuboidal morphology which can be found in some areas, including the parenchymal organs (liver, spleen), the 'milky spots' of the omentum and the peritoneal side of the diaphragm (Wang, 1974; Michailova et al., 1999). Although they are both described as mesothelial cells, ultrastructural analysis has shown some differences between these two types of cells. Squamous-like cells have a round or ovoid nucleus, which is usually larger than that of the cuboidal cells and contain a prominent nucleolus (Baradi and Hope, 1964; Wang, 1974; Baradi and Campbell, 1974). In addition, squamous-like cells have few mitochondria, a poorly developed Golgi apparatus and little rough endoplastic reticulum (RER); whereas cuboidal cells contain abundant mitochondria, RER, and a well developed Golgi apparatus. A greater number of microfilaments are also found in the cuboidal cells compared to squamous ones (Baradi and Hope, 1964; Wang, 1974; Baradi and Campbell, 1974; Kluge and Hovig,

1967a). These features indicate that the cuboidal cells may be more metabolically active than the squamous ones. Interestingly, cuboidal cells, or morphologically similar ones, can be found after injury or stimulation of the serosal surfaces, which is suggestive of a more active role of cuboidal cells during serosal repair (Whitaker and Papadimitriou, 1985; Mutsaers et al., 2002).

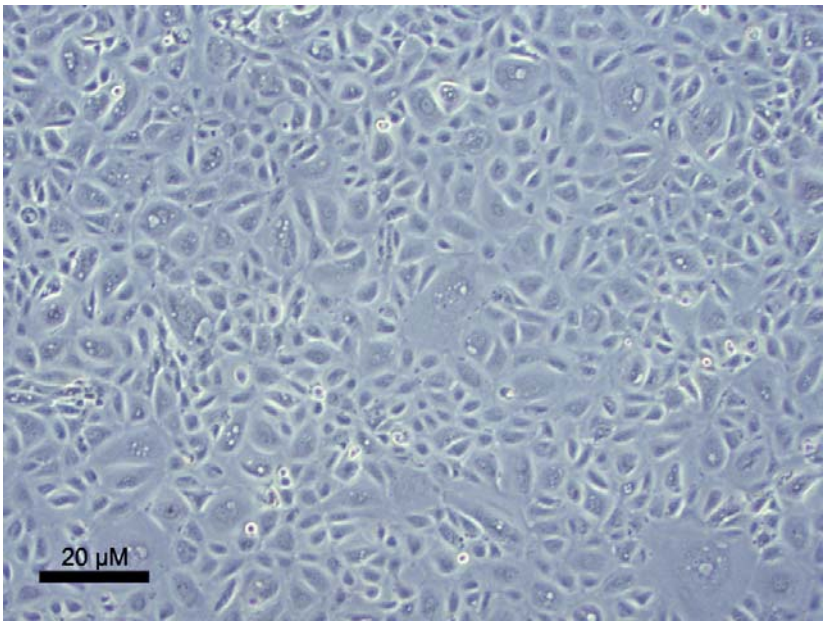

Figure 1.2. Phase contrast image showing a monolayer of peritoneal mesothelial cells in primary cell culture.

The luminal surface of the mesothelial cells has a well developed microvillous border, projecting from the apical surface. The microvilli are up to 3µm in length; but vary in shape, length and density between adjacent cells and between different organs (Andrews and Porter, 1973; Tsilibary and Wissig, 1977; Michailova et al., 1999). They help to trap protein from peritoneal fluid and to minimize the shear between neighbouring mesothelial surfaces. Interestingly, the number of microvilli expressed on each cell is also shown to depend on the surrounding physiological situation, that could be a functional adaptation of the microvilli (Madison et al., 1979). The mesothelial cells also have a well-developed system of vesicles and vacuoles. Most of them are micropinocytic; but a few multivesicular bodies and large

vacuoles can also be found. It has been shown that visceral mesothelium has more vesicles than the parietal mesothelium. These vesicles are often found along the luminal cell surface, in contact with the plasmalemma (Fukata, 1963; Kluge and Hovig, 1967a; Fedorko and Hirsch, 1971; Cotran and Karnovsky, 1968), and function in transporting fluids and particulates through the mesothelium by pinocytic transport (Cotran and Karnovsky, 1968; Leak and Rahil, 1978; Fedorko and Hirsch, 1971).

Mesothelial cells have well-developed cell-cell junctional complexes including tight junctions, adherens junctions, gap junctions and desmosomes (Kluge and Hovig, 1967b; Pelin et al., 1994). Tight junctions are thought to be important for the formation of cell surface polarity, as well as the development and maintenance of a semi-permeable diffusion barrier. Adherens junctions are crucial to form the structural and adhesive support of the cell layer, while gap junctions contribute to the establishment of aqueous inter-cellular channels. A number of protein components are involved in the build up of these junctional complexes, including E-, N- and P-cadherins (Yap et al., 1997; Simsir et al., 1999). N-cadherin has been shown to predominate (Simsir et al., 1999). Mesothelial cells also express membrane-associated zonula occludens-1 (ZO-1) (Foley-Comer et al., 2002). At the junctions between mesothelial cells, another important functional construction called ‘stomata’ has been described (Wang, 1975). It is postulated that these stomata may help the movement of fluid and particulate matter to and from the serous cavities. These stomatal openings are normally 3-12 μm in diameter and are controlled by actin filaments (Tsilibary and Wissig, 1983), but their size can increase during inflammation (up to more than 20μm). The stomata are generally found in the areas where cuboidal mesothelial cells are present, such as the peritoneal side of the diaphragm or the omental milky spots. The opening of stomata allow rapid removal of fluid, cells, bacteria and other particles from the serosal cavities to the underlying

submesothelial lymphatic system; indicating an important role of stomata in peritoneal clearance. In the meantime, it also provides a direct link between the pleural and abdominal cavities (Ohtani et al., 1995; Ohtani and Ohtani, 1997), which may account for the entry of inhaled materials into the abdominal cavity leading to fibrosis or malignant mesothelioma.

Not only can the stomata aid the transport of the fluid within the cavities, but mesothelium itself also plays an important role in transport across the serosal cavities. It has been shown that microvilli can bind fluids and aid adsorption by their glycosaminoglycan covering (Wang, 1974). Many tracing studies have also demonstrated that particulates and solutes can be actively transported across the mesothelium by pinocytic vesicles (Fukata, 1963; Fedorko and Hirsch, 1971; Leak and Rahil, 1978). In addition, mesothelial cells can increase the number of plasmalemmal vesicles, which facilitates clearance of extracellular fluid under elevated fluid pressure (Shumko et al., 1993).

Mesothelial cells also play an important role in inflammatory responses within the serosal cavities. It has been shown that mesothelial cells can secret various pro-, anti-inflammatory and immunomodulatory factors. These include prostaglandins, prostacyclin, nitric oxide (NO) and reactive nitrogen and oxygen species, chemokines, anti-oxidant enzymes, cytokines and growth factors, extracellular matrix (ECM) molecules and products of the coagulation cascade.

The production of these factors is mainly due to a variety of stimuli including bacterial endotoxins, cytokines, asbestos, or instilled agents, with the purpose of restoring normal mesothelial architecture and function (Antony et al., 1993; Boylan et al., 1992; Antony et al., 1995). For example, it has been shown that lipopolysaccharide (LPS) and zymosan can stimulate tumour necrosis factor (TNF)-α,

interleukin (IL)-1β, and IL-10 production from cultured rat peritoneal mesothelial cells (Yao et al., 2004). Disorder of production of these cytokines might further contribute to peritonitis (Yao et al., 2004). Studies also show that mesothelial cells can eliminate bacteria by phagocytosis resulting in IL-8 release (Visser et al., 1995; Visser et al., 1996). Phagocytosis also occurs during engulfment of asbestos fibres by these cells (Antony et al., 1995). Furthermore, talc and asbestos have been shown to stimulate mesothelial cells to secrete IL-8 and monocyte chemoattractant protein-1 (MCP-1), production of which can be further increased in the presence of IL-1β or TNF-α (Tanaka et al., 2000; Nasreen et al., 1998). Neutralizing studies, using specific MCP-1 and IL-8 antibodies, have demonstrated that cell-derived MCP-1 and IL-8 play important roles in chemotactic activity (Antony et al., 1995). Other chemotactic factors are also produced by mesothelial cells including stromal cell-derived factor-1 (SDF-1) (Coulomb-L'Hermin et al., 1999) and eotaxin (Katayama et al., 2002). The former can stimulate the growth of B lymphocyte precursors and account for the accumulation of B1 lymphocytes in the cavities (Coulomb-L'Hermin et al., 1999; Foussat et al., 2001). Eotaxin can be produced by mesothelial cells in response to TNF-α and IL-4, and is considered as a chemokine for eosinophils (Katayama et al., 2002; Georas et al., 2002). Studies have also shown that mesothelial cells can produce IL-6 and macrophage colony stimulating factor (M-CSF). Elevated levels of IL-6 are expressed by mesothelial cells in response to TNF-α and IL-1β (Topley et al., 1993). The expression of endogenous IL-6 can regulate the levels of pro-inflammatory factors in both local and systemic acute inflammatory responses (Xing et al., 1998). In addition, release of transforming growth factor-β (TGF-β) isoforms 1 and 2 from mesothelial cells is found in response to IL-1β (Offner et al., 1996). Furthermore, mesothelial cells also secret NO and other reactive radical species in response to cytokines, bacterial products and asbestos, including $O_2^{-}\cdot$, NO· and H_2O_2 (Chen et al., 2000; Choe et al., 1998; Owens and Grisham, 1993). Such reactive species can cause cell death to occur when the

mesothelial cells are challenged by other toxic elements, which allow the cells to initiate a self-clean and regeneration process.

As discussed above, mesothelial cells produce a variety of chemokines during serosal inflammation. Interestingly, these chemokines were found to be secreted more in the apical side of mesothelial cells than that of the basolateral side (Zeillemaker et al., 1995; Nasreen et al., 2001). Such polarized secrtion by mesothelial cells forms a chemotactic gradient from the basolateral to apical side of the cells (Zeillemaker et al., 1995; Nasreen et al., 2001). This accounts for the recruitment of inflammatory cells into the serosal cavities from underlying tissue, such as vascular and lymphatic vessels (Li et al., 1998). Studies have shown that blocking such gradients, with antibodies for respective chemokines, can inhibit the transmesothelial migration of neutrophils and monocytes through the mesothelial monolayer (Li et al., 1998; Nasreen et al., 2001). In addition to secreting chemokines for inflammatory cell recruitment, mesothelial cells also produce specific integrins and adhesion molecules to facilitate the migration of inflammatory cells. For example, mesothelial cells can express intercellular adhesion molecule (ICAM-1), which interacts with lymphocyte function-associated antigen-1 (LFA-1) on the surface of leucocytes (Nasreen et al., 2001; Jonjic et al., 1992). The interaction leads to cell-cell adherence and contributes to the transmigration of leucocytes through mesothelial cell monolayers (Liberek et al., 1996). It was shown that ICAM-1 is only expressed on the microvilli of mesothelial cells (Liang and Sasaki, 2000). This suggested another important role of microvilli in regulating leucocytes migration through the mesothelium.

Finally, mesothelial cells secrete a variety of growth factors and ECM molecules that are critical for tissue repair. For example, TGF-β 1/2 are synthesized by mesothelial cells and regulated by IL-1β (Offner et al., 1996). Hypoxia, which is normally caused by tissue ischemia after injury, is also found to increase TGF-β 1/2 mRNA levels

(Offner et al., 1996). TGF-β2 can further stimulate mesothelial cells to produce vascular endothelial growth factor (VEGF) (Gary Lee et al., 2002), an important factor involved in angiogenesis. The inflammatory factors produced by mesothelial cells; including TGF-β, platelet-derived growth factor (PDGF), fibroblast growth factor (FGF), TNF-α and IL-1; are mitogenic for human mesothelial cells in *vitro and in vivo* (Gabrielson et al., 1988; Laveck et al., 1988; Mutsaers et al., 1997). These indicate an active autocrine regulation mechanism of mesothelial cell contribution to tissue repair. In addition, mesothelial cells can synthesize a variety of ECM components. Studies have shown that cultured rat mesothelial cells can produce collagen types I, III and IV, elastin, fibronectin and laminin (Rennard et al., 1984; Laurent et al., 1988; Owens and Grimes, 1993), which is likely the same in human cells. Furthermore, mesothelial cells can organize these components into complex structures that reassemble to form the ECM *in vivo* (Rennard et al., 1984). The production of these molecules from mesothelial cells is regulated by many cytokines and growth factors, including IL-1β, TGF-β, TNF-α, epidermal growth factor (EGF) and PDGF (Owens and Grimes, 1993; Owens and Grisham, 1993; Kuwahara et al., 1994; Perfumo et al., 1996). Other studies have shown that collagen synthesis is increased in the cells in response to peritoneal effluents obtained from patients with acute peritonitis (Perfumo et al., 1996). This indicates an important role of peritoneal fluid in the regulation of tissue repair. Mesothelial cells also contribute to tissue remodelling by secreting matrix metalloproteinases (MMPs) and tissue inhibitors of metalloproteinases (TIMPs) (Marshall et al., 1993; Rougier et al., 1997; Ma et al., 1999), which are very important factors involved in collagen degradation (see section 1.5.4). It has been proposed that the regulation of the balance of these inflammatory molecules, together with the ECM factors, leads either to normal tissue repair or to fibrosis and adhesion formation. A summary of the factors produced by human mesothelial cells is listed in Table 1.3, with their respective stimuli.

Table 1.3. Factors produced by human mesothelial cells. Table adapted from (Mutsaers, 2002).

Molecules	Stimulus	References
Cytokines		
IL-1	EGF, TNF-α, LPS	(Demetri et al., 1989; Lanfrancone et al., 1992)
IL-6	TNF-α, IL-1	(Fujino et al., 1996; Topley et al., 1993)
CSF (G,M,GM)	IL-1, TNF-α, EGF, LPS	(Demetri et al., 1989; Lanfrancone et al., 1992)
Chemokines		
IL-8	IL-1, TNF-α, LPS, macrophage CM, asbestos, talc	(Visser et al., 1995; Betjes et al., 1993)
MCP-1	IL-1, TNF-α, IFN-γ, LPS	(Visser et al., 1998a; Haslinger et al., 2001)
RANTES	IL-1, TNF-α, IFN-γ	(Visser et al., 1998a)
GRO-α	IL-1, TNF-α, IFN-γ	(Visser et al., 1998a)
IP-10	IL-1, TNF-α, IFN-γ	(Visser et al., 1998a)
Eotaxin	IL-4, TNF-α	(Katayama et al., 2002)
Growth factors		
TGF-β	IL-1, hypoxia	(Offner et al., 1996; Saed et al., 2000)
FGF	IL-1	(Cronauer et al., 1999)
HB-EGF	IL-1, TNF-α	(Jayne et al., 2000; Faull et al., 2001)
VEGF	IL-1, TNF-α, TGF-β	(Jayne et al., 2000; Gary Lee et al., 2002)
HGF	N/A	(Warn et al., 2001)
ECM-related molecules		
Collagen I	IL-1, TNF-α, EGF, PDGF	(Owens and Grimes, 1993; Saed et al., 1999; Yang et al., 1999)
Collagen III	TGF-β, EGF, PDGF, hypoxia	(Saed et al., 1999; Harvey and Amlot, 1983; Rennard et al., 1984)
Fibronectin	IL-1	(Yang et al., 1999; Rennard et al., 1984)
Hyaluronan	IL-1, EGF, PDGF	(Yung et al., 2000; Heldin and Pertoft, 1993)
Surfactant	N/A	(Beavis et al., 1994)

Molecules	Stimulus	References
Biglycan	N/A	(Yung et al., 1995)
Decorin	N/A	(Yung et al., 1995)
MMP	TGF-β, PMA	(Ma et al., 1999; Rougier et al., 1997; Marshall et al., 1993)
TIMP	TGF-β, PMA	(Ma et al., 1999; Rougier et al., 1997; Marshall et al., 1993)
Integrin (α1-6, β1, β3, α4β3)	EGF	(Liaw et al., 2001; Leavesley et al., 1999)
Coagulation cascade proteins		
Tissue factor	N/A	(Bottles et al., 1997)
tPA	TNF-α	(Idell et al., 1992; Sitter et al., 1995; Sitter et al., 1999)
uPA	TGF-β	(Rougier et al., 1998; Falk et al., 2000)
PAI	IL-1, TNF-α, TGF-β, thrombin, LPS	(Sitter et al., 1999; Sitter et al., 1995; Rougier et al., 1998)
Adhesion molecules		
ICAM	IL-1, TNF-α, IFN-γ	(Jonjic et al., 1992; Cannistra et al., 1994; Liberek et al., 1996)
VCAM	IL-1, TNF-α, IFN-γ, LPS	(Jonjic et al., 1992; Cannistra et al., 1994; Liang and Sasaki, 2000)
E-cadherin	N/A	(Simsir et al., 1999)
N-cadherin	N/A	(Simsir et al., 1999)
Other molecules		
Cyclo-oxygenase/ prostaglandins	IL-1, TNF-α, thrombin, macrophage CM	(Baer and Green, 1993; Topley et al., 1994; Hott et al., 1994)
HSP	IL-1, TNF-α	(Lopez-Cotarelo et al., 2000)
NO	Combination of IL-1, TNF-α, IFN-γ, LPS	(Chen et al., 2000)
Reactive species scavengers	Asbestos	(Janssen et al., 1994)

Abbreviation: IL, interleukin; EGF, epidermal growth factor; HB-EGF, heparin-binding EGF; VEGF, vascular EGF; TNF-α, tumour necrosis factor-α; LPS, lipopolysaccharide; IFN-γ, interferon-γ; G-, M-, GM-CSF, granulocyte, macrophage and granulocyte–macrophage colony stimulating factor, respectively; MCP-1, monocyte chemoattractant protein-1; GRO-a, growth-related oncogene-a; IP-10, IFN-g-inducible protein-10; PDGF, platelet-derived growth factor; FGF, fibroblast growth factor; HGF, hepatocyte growth factor, respectively; PMA, phorbol myristate acetate; MMP, matrix metalloproteinases; TIMP, tissue-specific inhibitors of metalloproteinases; PAI, plasminogen activator inhibitors; tPA, uPA, tissue and urokinase plasminogen activators, respectively; ICAM, intercellular adhesion molecule; VCAM, vascular cell adhesion molecule; HSP, heat shock protein; NO, nitric oxide.

1.3 Mechanism of peritoneal repair and post-operative adhesion

1.3.1 Normal wound healing, scar formation and fibrosis

Injury to cells and tissue is common to almost every accident and disease. The damage will normally initiate the healing process, which can be broadly separated into tissue regeneration and tissue repair. Tissue regeneration normally involves a complete reconstitution of lost or injured tissue and helps to restore normal tissue function. In contrast, tissue repair could lead to dysfunction in the original tissue, as it may restore the original tissue with inclusion of aberrant components, such as scar tissue. Tissue regeneration, such as the growth of an amputated limb in amphibians or liver regeneration, can be found in mammals but happens rarely. It has been shown that the regrowth process always involves compensatory growth, e.g., in kidney repair (Mene et al., 2003). Growth factors and stem cells also play very important roles in this process. Tissue repair is a much more common event that occurs during the healing process. Since most tissues cannot heal solely by self-regeneration, the healing is always associated with a mix of self-regeneration and replacement of other components, including connective tissue. Thereby, tissue repair can lead to the formation of a scar at the injury site. In post-operative repair, it may provoke adhesion formation. Fibrotic tissue will cause dysfunction of the original tissue and lead to many further problems. Therefore, a deeper understanding of the healing process, particularly the tissue repair process, will help to find a resolution for tissue fibrosis.

As the repair process is more or less the same in different tissues, cutaneous wound healing is used as an example to introduce the general process of tissue repair. The healing process can be generally divided into sequential phases, commonly with

overlap between each phase (Hunt et al., 2000). First, the injury causes rapid activation of a coagulation process, which results in the formation of a blood clot at the injured site (Robson et al., 2001). The clot is formed by entrapped blood cells, fibrin, fibronectin and other complement components. It not only helps to stop bleeding, but also serves as a scaffold for the recruitment of inflammatory cells (Robson et al., 2001; Lawrence, 1998). For example, neutrophils are shown to appear on the injured site within 24 h to clean up the damaged tissue and invading bacteria (Werner and Grose, 2003). Subsequently granulation tissue is formed by the proliferation of fibroblasts and vascular endothelial cells (Witte and Barbul, 1997; Zhang et al., 1997). The granulation tissue progressively invades the injured space and replaces lost tissue, a hallmark of tissue repair. One of the notable features of granulation tissue is that it is often edematous, due to the leakage of newly forming blood vessels. This might assist however more ready access of other components to the injury site, facilitating the repair. In the meantime, neutrophils are replaced by macrophages from 48 to 96 h after injury (Hart, 2002). As the key inflammatory cells in the healing process, macrophages are capable of clearing the damaged tissue, fibrin and other foreign material (Werb et al., 1980). In addition, macrophages can produce a series of factors including PDGF, EGF, TGF-β, FGF, VEGF, IL-1 and TNF (Lingen, 2001; Delavary et al., 2011). These factors can promote fibroblast migration and proliferation, angiogenesis and ECM deposition. ECM deposition follows after granulation tissue formation. The ECM components can be produced by a variety of cells presenting in the injured site, including fibroblast cells (Myllyharju and Kivirikko, 2001), macrophages (Delavary et al., 2011), and epithelial cells (Myllyharju and Kivirikko, 2001). A predominant ECM is found within the injury area replacing the granulation tissue, with re-epithelialization beginning later on the surface of the tissue. The mediators for the epithelialization are thought to be HGF, HB-EGF, FGF-7 and IL-6 (Werner and Grose, 2003). In large wound areas, wound contraction helps to close the wound by decreasing the gap between the edges of the

wound. This process is mediated by myofibroblasts at the edge of the wound (Clark et al., 1989; Montesano and Orci, 1988). These cells have similar ultrastructual characteristics to smooth muscle cells. They contract the wound physically and also secrete large amounts of ECM components, including collagen I, fibronectin and tenascin-C (Darby and Hewitson, 2007). Myofibroblasts are thought to originate from tissue fibroblasts (Quan et al., 2006), promoted by factors secreted by macrophages at the wound sites, including TGF-β, PDGF and FGF-2. However, some studies suggest they may also originate from bone marrow precursors known as fibrocytes, or from epithelial cells through the epithelial-to-mesenchymal transition (Zeisberg et al., 2007; Kalluri and Neilson, 2003). The last step involved in tissue repair is the remodelling of connective tissue. Repair of injured tissue always leads to large amounts of ECM components being deposited at the wound site to replace lost tissue (Velnar et al., 2009). Therefore, the balance between ECM synthesis and degradation mediates in the remodeling of the connective tissue, a very important process for the completion of tissue repair. We already know that many growth factors contribute to ECM synthesis including TGF-β (Buck et al., 1996). The mediators of the ECM degradation involve the MMP family of enzymes. (Nagase and Woessner, 1999). The MMP family has more than 20 members, all having a conserved 180-residue zinc-protease domain (Visse and Nagase, 2003). They include interstitial collagenases (MMP-1, -2,-3), gelatinases (MMP-2 and -9), and stromelysins (MMP-3, -10, and -11) (Visse and Nagase, 2003).

MMPs can act on a variety of ECM components, such as collagen types I, II, III, fibronectin and laminin. Most MMPs are produced by fibroblasts, macrophages, neutrophils and some epithelial cells (Vu and Werb, 2000). Their production can be up-regulated by growth factors (PDGF, FGF), cytokines (IL-1, TNF) and phagocytosis in macrophages (Werb et al., 1980; Circolo et al., 1991; Goetzl et al., 1996), but be inhibited by TGF-β (Sporn and Roberts, 1992) and steroids (Green and

Friedland, 2007). They can readily degrade the ECM components because of their high enzymatic activity. Therefore, tight regulation of the high activity of the MMPs is maintained by tissue inhibitors of metalloproteinases (TIMPs). TIMPs are produced by most mesenchymal cells and can prevent uncontrolled action of the MMPs (Brew et al., 2000). More details about the MMPs and TIMPs will be discussed in section 1.5.4. We can conclude that the key feature involved in tissue remodelling is the regulation of ECM synthesis and degradation. This process seems to be mostly mediated by growth factors, MMPs and TIMPs present at the area of injury.

The final process of repair involves scar formation at the injured site. This is composed of spindle-shaped fibroblasts, dense collagen, fragments of elastic tissue, small vascular vessels and other ECM components (O'Kane, 2002). Fibrosis is defined by the overgrowth, hardening, and/or scarring of various tissues and is attributed to excess deposition of extracellular matrix components, mainly collagen (Wynn, 2008). Although the terms scarring and fibrosis are interchangeable, fibrosis mainly relates to severe collagen deposition in chronic disease. The pathology of fibrosis associated with chronic disease is quite similar to the mechanisms of skin wound healing discussed above. However, the skin wound healing is always completed by orderly healing steps, which are promoted by acute inflammatory responses. In contrast, the chronic diseases caused by infections, autoimmune reactions and severe trauma always lead to chronic inflammation. The persistant stimulus in the chronic inflammatory response can lead to a disorderly repair process with much longer periods in each healing phase. Adverse chronic inflammation will be discussed later in section 1.4.2. The cellular and molecular mechanisms of fibrosis involve various cell types and inflammatory factors. One of the key cellular mediators of fibrosis are myofibroblasts, as they can promote wound contraction and produce a large quantity of ECM components (Quan et al., 2006; Follonier Castella

et al., 2010). Other cellular mediators including lymphocytes and monocytes also contribute to fibrosis, as these cells sustain the production of growth factors and fibrogenic cytokines during the chronic inflammatory process (Wynn and Barron, 2010; Wynn, 2004). Therefore, the molecular mechanism(s) of fibrosis is relative to the persistant presence of various growth factors and fibrogenic cytokines, including TGF-β, PDGF, IL-4 and IL-13 (Wynn, 2008).

TGF-β has been recognized as the most important factor contributing to fibrosis. Studies have shown that inhibition of TGF-β can suppress fibrosis in many disease models (Lee et al., 2001; Daniels et al., 2004). The function of TGF-β and its signalling pathway(s) will be discussed in more detail in section 1.4.3.3. Additionally, cytokines IL-4 and IL-13 also have distinct roles in the regulation of fibrosis. For example, studies indicate that IL-4 is another potent profibrotic cytokine which is nearly twice as effective as TGF-β (Fertin et al., 1991). Receptors for IL-4 are found on many human and mouse fibroblast cells (Sempowski et al., 1994; Doucet et al., 1998). The activation of these receptors can increase the production of ECM factors, including types I and III collagen and fibronectin (Sempowski et al., 1994; Doucet et al., 1998). Blocking IL-4 led to a significant reduction in the development of hepatic fibrosis in mice (Cheever et al., 1994). IL-13 is another cytokine that has been identified as a predominant factor in several experimental models of fibrosis (Blease et al., 2001; Kumar et al., 2002; Keane et al., 2007; Kolodsick et al., 2004). On the other hand, over-expression of IL-13 in the lung induced significant subepithelial airway fibrosis in mice without any other additional inflammatory stimulus (Zhu et al., 1999), while anti-IL-13 treatment markedly reduced collagen deposition in the lungs of animal challenged with *A. fumigatus* conidia (Blease et al., 2001) or bleomycin (Belperio et al., 2002).

In summary, tissue repair is a complex process normally including orderly phases as we discussed above. Development of scar after tissue repair is quite common, since the injured tissue has always been replaced with a large amount of ECM components, mainly collagen. Fibrosis is most often linked to chronic inflammation, with persistant activation of profibrotic cells and factors. The resolution of inflammatory responses, as well as the balance between ECM synthesis and degradation, is critical to prevent tissue fibrosis.

1.3.2 Peritoneal repair

Peritoneal repair shares some common features to normal wound healing, including an inflammatory response, cell proliferation, extracellular matrix (ECM) deposition, angiogenesis and the fibrinolytic system. The unique feature of peritoneal repair is, however, that both small and large peritoneal wounds heal in a similar amount of time (Hubbard et al., 1967). Irrespective of the size of the wound area, peritoneal repair is normally completed within 7-10 days of the initial injury, being complete when the wound area is covered by cells displaying all the characteristics of mesothelial cells. It is suggested that unlike normal wound healing, such as that occurring in epithelium, peritoneum does not repair solely by proliferation and centripetal migration of cells from the wound edge. Many studies have been undertaken to address the mechanism regulating the peritoneal repair process. The general process has been defined (Hubbard et al., 1967). In this study, a midline incision was made and defects in the parietal peritoneum were created in Wistar rats, albino rabbits, and mongrel dogs. The healing process was investigated at 12 hours, and at daily intervals up to 7 days. The findings were quite similar in dogs, rabbits, and rats. At 24 hours the injury tissue was covered by a thin layer of fibrin. Infiltration of inflammatory cells including polymorphonuclear cells, eosinophils, lymphocytes and monocytes was found across the injured area (see Figure 1.3A).

Injured muscle fibres in the depths of the wound were removed by phagocytosis. By day 2 occasional fibroblasts were found within the injury area but mononuclear cells predominated in the whole injury site indicating a continued inflammatory response (Figure 1.3B). On day 3 most inflammatory cells had disappeared except for a few macrophages which indicated that the main inflammatory response was complete. Fibroblast-like cells replaced the fibrin layer to cover the surface of injury tissue (Figure 1.3C). Numerous mitoses were seen indicative of a regenerative process. From 4 to 6 days (Figure 1.3D-E), the number of fibroblasts decreased. Regeneration of peritoneum was found on the surface of the injury area and collagen deposition was found to replace the underlying fibroblasts. At 7 days (Figure 1.3F) the repair process was generally complete with an intact peritoneal mesothelium on the surface and underlying connective tissue consisting of mainly fibroblasts and collagen. The repaired tissue was quite similar to the normal tissue (Figure 1.3G) except for fewer fibroblasts in the deeper layers and a greater amount of collagen. In summary, the sequential peritoneal repair process includes the following steps: (1) A coagulation phase covering injured tissue with fibrin; (2) An inflammation phase with inflammatory cell infiltration; (3) A fibroplasias phase with fibroblast-like cells infiltration; (4) ECM remodelling phases with ECM deposition and degradation; and (5) Regeneration of peritoneum.

Figure 1.3. Sections of peritoneal tissues during wound repair. A. The centre of a peritoneal defect at 24 hours (X450); B. The centre of a peritoneal defect at 2 days. (X 450); C. The centre of a peritoneal defect at 3 days. (X 450); D. The centre of a peritoneal defect at 5 days. (X 450); E. The centre of a peritoneal defect at 6 days, collagen shown by Masson staining. (X 450); F. The centre of a peritoneal defect at 7 days. (X 450); G. A section of normal peritoneum. Figure adapted from (Hubbard et al., 1967)

A (24 h)

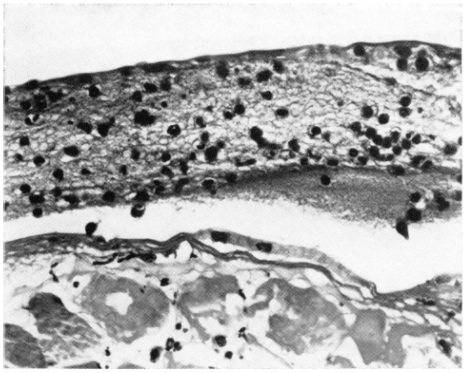

B (2 days)

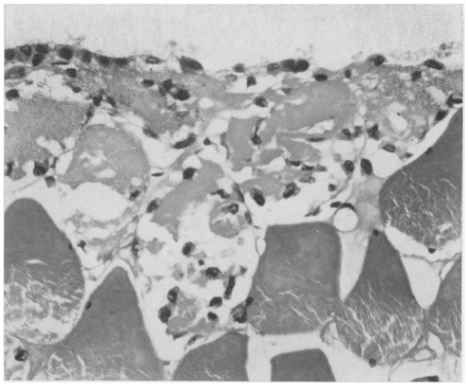

C (3 days)

D (5 days)

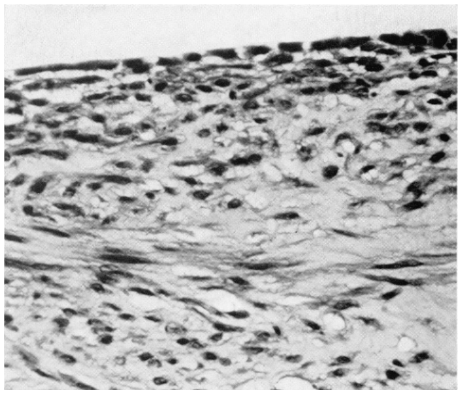

E (6 days)

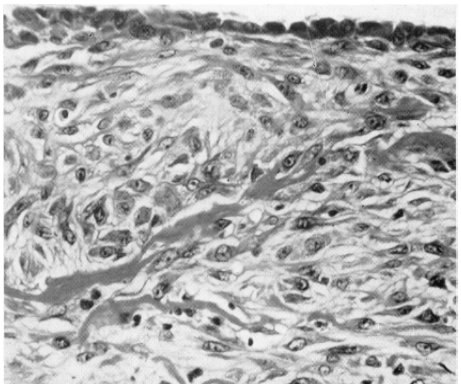

F (7 days)

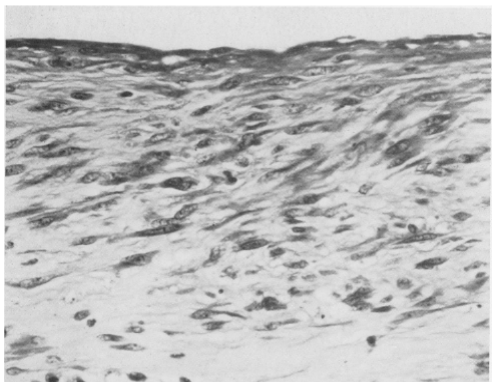

G (normal)

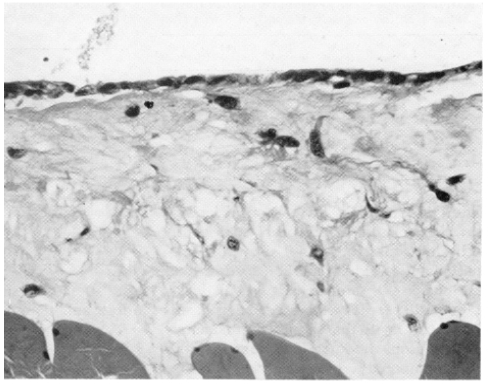

Although the general repair process discussed above appeared quite similar to a normal healing process, the regeneration of peritoneal mesothelium was still undefined since both small and large defects in the mesothelium were found to heal at the same rate. It has been shown that mesothelial cells at the edge of injured areas undergo cell proliferation and temporarily transform into spindle-shaped cells that migrate on to the denuded wound area (Whitaker and Papadimitriou, 1985; Mutsaers et al., 2000). The normal mesothelium is a slowly renewing tissue with 0.16-0.5% of cells undergoing mitosis at any one time (Mutsaers et al., 2000; Fotev et al., 1987). However, they can be stimulated to divide by many agents as well as by direct physical damage. Furthermore, kinetic studies using [^{3}H]-thymidine as a marker for DNA synthesis confirmed that around 28% of mesothelial cells at the wound edge and on the opposing surface were dividing 24-48 h after injury (Figure 1.4A, B) (Mutsaers et al., 2000; Whitaker and Papadimitriou, 1985), whereas the centre of the wound reaches the maximum number by day 4 (Figure 1.4C). This suggested that local mesothelial cells proliferation and centripetal migration from the wound edge plays a very important role in peritoneal mesothelium healing. However it is clear that this is not the only mechanism accounting for the peritoneal repair. Irradiation(Whitaker and Papadimitriou, 1985; Fotev et al., 1987) and cell labelling studies (Fotev et al., 1987; Foley-Comer et al., 2002; Raftery, 1973b) have shown that macrophage transformation and a possible circulating bone marrow-derived mesothelial precursor are not involved. However, Campbell's group showed that bone marrow origin cells can differentiate into myofibroblasts within the peritoneal cavity in response to irritation from foreign bodies (Campbell et al., 2000). Several pro-fibrotic genes were found up-regulated in these myofibroblasts which can contribute to peritoneal repair (Le et al., 2010). In addition, other studies suggest that regenerating mesothelium might originate either from a sub-mesothelial mesenchymal precursor or free-floating mesothelial cells (Herrick and Mutsaers, 2004).

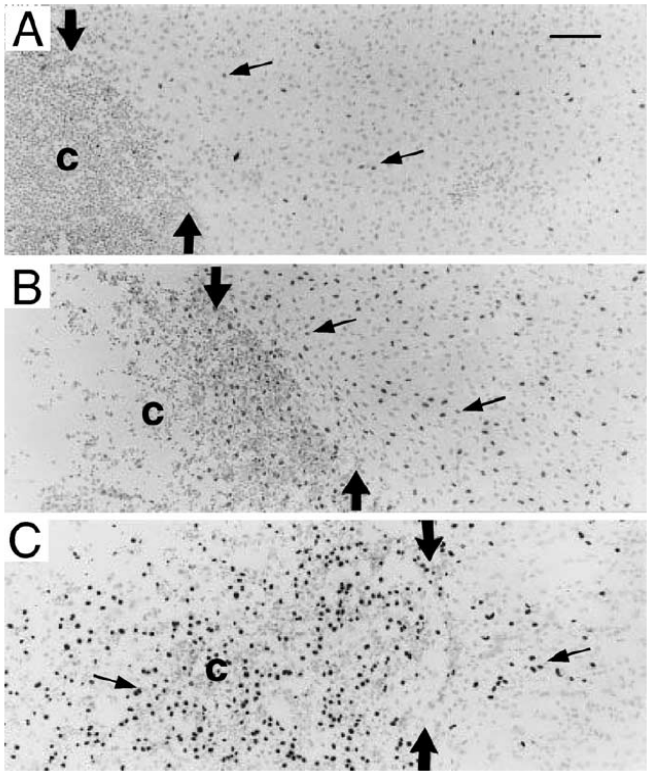

Figure 1.4. Surface imprints of [^{3}H]-TdR labelled serosal lesions at (A) 24 h, (B) 2 days, and (C) 4 days. Letter c: The centre of the lesion; Thick arrows: the margin between the centre and edge of the lesion; Small arrows: dark nuclei are labelled with silver grains (magnification X16). Bar 125 μm. Figure adapted from (Mutsaers et al., 2000).

The nature of the sub-mesothelial mesenchymal precursor remains controversial. One theory was advanced by researchers on discovering the presence of cells with epithelial-like characteristics in the subserosal layer of biopsies from various pathological conditions (Bolen et al., 1986; Bolen et al., 1987; Davila and Crouch, 1993; Dobbie, 1990). Bolen and co-workers have shown the best evidence for the existence of such precursor cells (Bolen et al., 1986; Bolen et al., 1987). They demonstrated that normal surface mesothelial cells expressed low and high molecular weight cytokeratins whereas submesothelial cells only expressed vimentin. However, submesothelial cells lost vimentin expression and acquired high and low molecular weight cytokeratins in the injured serosa. This suggested that the sub-mesothelial

cells were differentiating towards a mesothelial cell phenotype and thereby accounting for the regeneration of surface mesothelium. However, in a similar study, Whitaker and co-workers (Whitaker et al., 1992) could not reproduce these findings and doubted that the pattern seen by Bolen was a result of mature mesothelial cells migrating into the subserosal connective tissue. In addition, a kinetic study of mesothelial repair demonstrated that subserosal cells were not essential for mesothelial healing (Mutsaers et al., 2000). The study was suggestive that the surrounding uninjured mesothelial cells were more likely to contribute to mesothelium regeneration.

Furthermore, it has been suggested that the epithelial-like cells in the subserosal layer might originate from mesothelial cells through an epithelial-mensenchymal transition (EMT). EMT is a characteristic loss of the epithelial markers E-cadherin, ZO-1, and desmoplakins I and II; and acquisition of a mesenchymal phenotype, with up-regulation of the mesenchymal marker fibronectin and reorganization of actin stress fibres and vimentin (Miettinen et al., 1994). Thus, EMT changes an epithelial cell to one with a fibroblastic nature (Figure 1.5). EMT has a role in many fibrotic diseases by increasing cell migration, invasion and cell-ECM adhesion, such as in kidney fibrosis (Higgins et al., 2007) and biliary atresia fibrosis (Diaz et al., 2008). It has been shown that various growth factors, including EGF (Leavesley et al., 1999) and TGF-β (Miettinen et al., 1994), can induce mesothelial cells to change phenotype and express many mesenchymal markers. In culture, mesothelial cells present both mesenchymal and epithelial characteristics throughout early passages. Thus, these findings have been suggested that the inflammatory response can direct the phenotype of mesothelial cells at different stages of wound healing by the production of inflammatory factors, particularly TGF-β. The mechanism of TGF-β induced EMT will be further discussed in a later section (1.4.3.3)

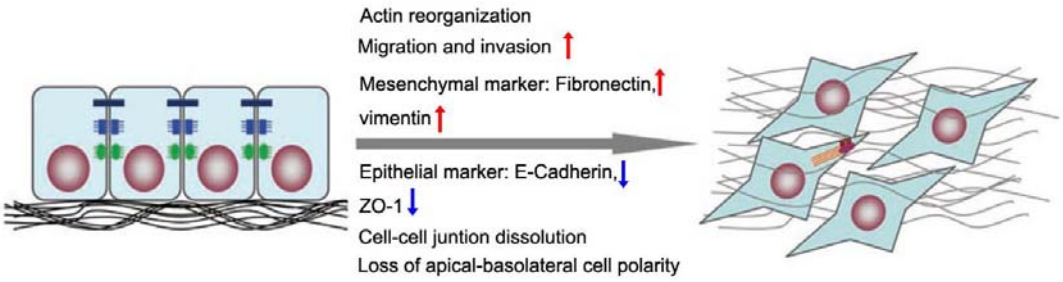

Figure 1.5. Epithelial-mesenchymal transition. EMT occurs when epithelial cells lose their epithelial cell characteristics, including dissolution of cell-cell junctions, i.e. tight junctions (black), adherens junctions (blue) and desmosomes (green), and loss of pical- basolateral polarity, and acquire a mesenchymal phenotype, characterized by actin reorganization and stress fibre formation (red), migration and invasion. Figure adapted from (Xu et al., 2009).

In a number of studies, free-floating mesothelial cells were proposed to contribute to peritoneal repair (Watters and Buck, 1973; Whitaker and Papadimitriou, 1985). A 12-fold increase in the number of viable free-floating mesothelial cells was found in the peritoneal lavage fluid recovered from experimental animals following injury to mesothelium compared to controls (Fotev et al., 1987). These cells were thought to originate from proliferative mesothelial cells adjacent to, or opposing, the serosal injury. Furthermore, it was shown that mesothelium healing was delayed following postoperative peritoneal lavages, possibly due to the removal of the free-floating cells (Tolhurst Cleaver et al., 1974). The most reliable evidence for the incorporation of free-floating mesothelial cells during serosal healing was presented by Foley-Comer and co-workers (Foley-Comer et al., 2002). The study used an *in vivo* cell tracking dye (1, 1'-dioctadecyl-3, 3, 3', 3'-tetramethylindo-carbacyanine perchlorate; DiI) to label cultured mesothelial cells, peritoneal lavage cells and control fibroblasts. The labelled cells were injected into experimental animals immediately following mesothelial injury. Labelled cultured mesothelial and peritoneal lavage cells, but not cultured fibroblasts, implanted onto the wound surface and began to proliferate. Furthermore, the implanted cells were shown to

incorporate into the regenerated mesothelium and form junctional complexes. These studies have clearly shown that free-floating mesothelial cells may play an important role in peritoneal mesothelium healing. They proposed that the free-floating cells might move down chemotactic gradients and attach to ECM components exposed beneath the mesothelium. The attached cells would then proliferate and reconstitute an intact mesothelial monolayer. However, how these cells become detached from the basement membrane and remain viable in the peritoneal fluid still requires further investigation.

In summary, peritoneal repair requires recruitment of inflammatory cells to the injured area and production of various inflammatory factors including growth factors and cytokines. The wound surface becomes covered by a fibrin layer, which is followed by the appearance of proliferative fibroblast cells to replace the fibrin layer as well as the underlying tissue. Meanwhile, collagen deposition is initiated to build up connective tissue. The repair process is completed on formation of an intact mesothelial cell layer on the surface. The regeneration of mesothelium may well be a consequence of both local mesothelial cell proliferation and centripetal migration from the wound edge, as well as the attachment of free-floating mesothelial cells in the peritoneal fluid.

1.3.3 Pathology of post-operative adhesion

So far, the well-established pathologic mechanism of post-operative adhesion involves the formation of the fibrin layer and the regulation of the peritoneal fibrinolysis capacity (Holmdahl et al., 1996). As discussed above, defects in the peritoneum are immediately covered by a thin layer of fibrin. This arises because damage to the peritoneum is followed by increased vascular permeability with exudation of fibrinogen and plasma fibronectin. The fibrinogen is then cleaved into

fibrin by the serine protease thrombin (Blomback et al., 1978). Fibrin is cross-linked by fibrin-stabilizing factor and binds to the tissue fibronectin at the wound sites, as well as plasma fibronectin, to form a fibrin clot (Blomback et al., 1978; Smith et al., 2007). The fibrin clot acts mainly to help close the wound and form a wound bed for the recruitment of inflammatory cells (Hermans and McDonagh, 1982). In normal peritoneal repair, the fibrin layer will be degraded by the endogenous fibrinolytic activity of the mesothelial cells within 72h (Sulaiman et al., 2002). At this stage, the mesothelial cells produce fibrinolytic mediators - plasminogen activators (PA), including the urokinase PA (uPA) and tissue PA (tPA) (Sulaiman et al., 2002). The PAs are serine proteases that catalyze the conversion of plasminogen to plasmin (Vassalli et al., 1991). Plasmin is responsible for fibrinolysis, direct degradation of extracellular matrix, and activation of MMPs (Vassalli et al., 1991). Meanwhile, mesothelial cells have been shown to produce fibrin stabilizing plasminogen activator inhibitor-1 and -2 (PAI-1 and PAI-2) (Idell et al., 1992; Rougier et al., 1998). It is suggested a fine balance between fibrin deposition and breakdown, that, if not regulated appropriately, can cause reduced fibrin clearance and result in adhesion formation (Holmdahl et al., 1998).

It has been shown that the balance between normal and fibrotic healing is regulated by the inflammatory response. The inflammatory factors (LPS, TNF-α, and IL-1) (Sitter et al., 1996; Whawell and Thompson, 1995) and fibrogenic mediators (TGF-β and thrombin) (Rougier et al., 1998; Falk et al., 2000; Mandl-Weber et al., 1999) have been shown to reduce production of PA by mesothelial cells while increasing the synthesis of PAI-1. Therefore, during chronic inflammation, a significant delay in fibrinolysis can be caused by a persistent inflammatory response. The undigested fibrin will easily conglutinate the opposite site of the mesothelium to the wound. Further, fibrin-rich adhesions become organized with invading fibroblasts, endothelial cells and macrophages with consequent collagen deposition and

angiogenesis. This will lead to permanent fibrous adhesions formed within a week in the injured areas (Figure 1.6).

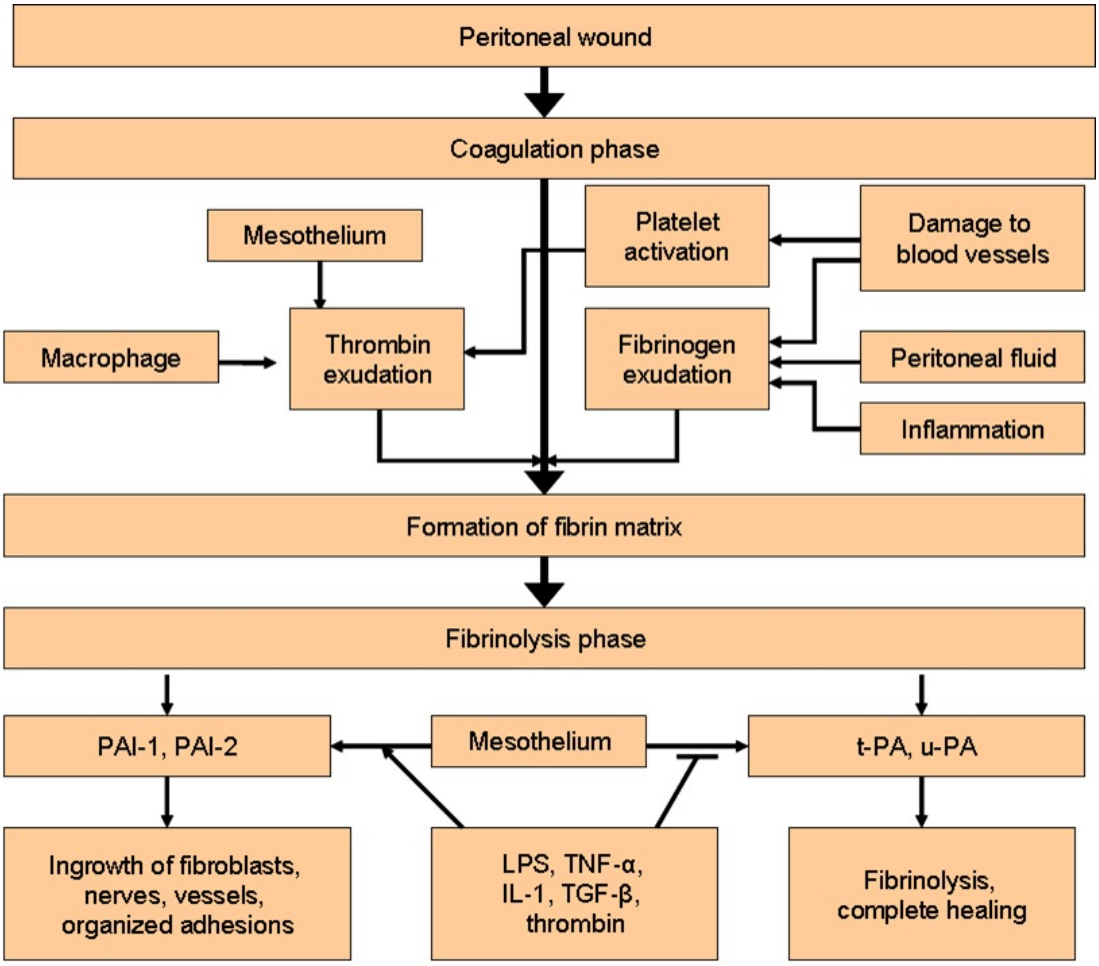

Figure 1.6. Fibrinolysis inter-relationships involved in the origin of post-operative adhesion. Figure adapted from (Bruggmann et al., 2010).

Other factors are also proposed to be involved in post-operative adhesion formation, including hypoxia. It has been shown that hypoxia can increase the production of lactate through the anaerobic glycolysis process (Shavell et al., 2009). The study demonstrated an elevated lactate concentration in the wound space immediately after injury. Lactate can act as an important stimulus for collagen formation and angiogenesis, and can then be a potent factor to promote adhesion formation by excessive collagen deposition and rapid angiogenesis. In addition, other studies have demonstrated that a specific neurokinin-1 receptor (NK-1R) antagonist, CJ-12,255

(Pfizer), can reduce adhesion formation in an experimental animal surgical model by increasing MMP activity in the peritoneum 24 hours after surgery (Cohen et al., 2007). These data also support the role of MMPs in post-operative adhesion formation. Although there are a number of studies regarding the pathology of post-operative adhesion formation, an understanding of its underlying mechanism is incomplete.

1.4 Inflammation and tissue fibrosis

1.4.1 Inflammatory response induced by tissue damage.

In a tissue repair process, the inflammatory response is commonly induced by infections at wound sites and sites of tissue damage, with the aim of eliminating both the initial cause of cell injury (e.g., microbes, toxins) and the consequences of these injuries (e.g., cell death and damaged tissue). Cellular response, as a consequence of inflammatory cells infiltration, plays a very important role in the inflammatory process. For example, neutrophils can help to clear microbes through phagocytosis and express proteinases that are involved in matrix degradation, enabling further cellular infiltration by macrophages and fibroblasts (Lingen, 2001). Macrophages have a variety of effects in damaged tissue clearance, fibroblast proliferation, and tissue remodeling. In addition, lymphocytes can migrate to the inflammatory site by chemotaxis, and interact with macrophages by producing the main macrophage activator – interferon-γ (IFN-γ). They are also capable of producing EGF, FGF and MMPs (Blotnick et al., 1994; Xia et al., 1996). Mast cells, which are widely distributed in connective tissues are also recruited to the wound site and can be activated to produce IL-4, a cytokine that stimulates fibroblast proliferation (Trautmann et al., 2000). However, the requirement for inflammatory cells in wound

repair may be not as essential as initially thought. Animal studies shows that neutrophil- or mast cells- knockdown mice are capable of completing normal wound repair (Simpson and Ross, 1972; Dovi et al., 2003; Egozi et al., 2003). In contrast, depletion of macrophages with antisera and steroids results in a serious disturbance in the repair process (Leibovich and Ross, 1975). It has been shown that debridement, the clearance of dead cells, fibrin and tissue debris from the wound, is compromised in the absence of macrophages, suggesting an essential role of macrophages in wound healing. However, in neonatal PU.1-knockout mice, a mouse model of neutrophil and macrophage knockout, an enhanced rate of re-epithelialization was found with absence of fibrosis (Martin et al., 2003). These findings suggest that inflammatory cells might disturb re-epithelialization by secondary tissue damage. Therefore, the effects of macrophages might represent a "double-edged sword" in wound repair. For example, a recent study showed that macrophage depletion blocked fibrosis in mouse liver after CCl_4-induced damage, whereas the same depletion disturbed matrix degradation and slowed down scar resolution during the recovery phase (Duffield et al., 2005).

In parallel with the cellular response, the inflammatory response also contains an orchestrated effect from other molecular mediators. The list of these inflammatory mediators includes, but is not limited to, cytokines, growth factors, proteases, kinins, and cellular metabolites. These mediators are soluble factors released by resident cells or by platelets and leukocytes infiltrating from blood vessels. The main factors in wound healing are considered to be cytokines and growth factors. Cytokines are recognized as the core factors involved in formation of post-operative adhesion including IL-1, TNF-α, and TGF-β. Therefore, as a focus of interest in this project, the functions and effects of these three cytokines will be discussed in more detail in section 1.4.3.

Growth factors also play an essential role in tissue repair. For example, connective tissue growth factor (CTGF) is an important downstream mediator for several inflammatory factors, including TGF-β (Leask, 2008; Schultz Jel et al., 2002). The role of CTGF is strongly associated with angiogenesis and ECM remodeling (Kular et al., 2011; Leask and Abraham, 2006). As a cofactor for TGF-β induced fibrogenesis, CTGF appears to create a favorable environment for fibrogenic stimuli to act (Mori et al., 1999; Shi-wen et al., 2006). In contrast, CTGF on its own is found to only weakly promote fibrosis (Kennedy et al., 2007). Functions of other growth factors involved in tissue repair are presented in Table 1.4. Although growth factors are equally important as cytokines, the effect of growth factors involved in post-operative adhesion is beyond the scope of this thesis.

Table 1.4. Growth factors involved in wound healing. Table adapted from (Kumar et al., 2005c)

Growth Factor	Source	Functions
Epidermal growth factor (EGF)	Platelets, macrophages, saliva, urine, milk, plasma	Mitogenic for keratinocytes and fibroblasts; stimulates keratinocyte migration and granulation tissue formation
Transforming growth factor alpha (TNF-α)	Macrophages, T lymphocytes, keratinocytes, and many tissues	Similar to EGF; stimulates replication of hepatocytes and certain epithelial cells
Hepatocyte growth factor (HGF)	Mesenchymal cells	Enhances proliferation of epithelial and endothelial cells, and of hepatocytes; increases cell motility
Vascular endothelial cell growth factor (VEGF)	Mesenchymal cells	Increases vascular permeability; mitogenic for endothelial cells
Platelet-derived growth factor (PDGF)	Platelets, macrophages, endothelial cells, keratinocytes, smooth muscle cells	Chemotaxis and activation for PMNs, macrophages, fibroblasts, and smooth muscle cells; mitogenic for fibroblast, endothelial and smooth muscle cells; stimulates production of MMPs, fibronectin, and HA; stimulates angiogenesis and wound contraction; remodeling; inhibits platelet aggregation; regulates integrin expression
Fibroblast growth factor (FGF)	Macrophages, mast cells, T lymphocytes, endothelial cells, fibroblasts, and many tissues	Chemotactic for fibroblasts,; mitogenic for fibroblast and keratinocytes; stimulates keratinocytes migration, angiogenesis, fam wound contraction and matrix deposition
Keratinocyte growth factor (KGF)	Fibroblasts	Stimulates keratinocyte migration, proliferation, and differentiation

In an ideal situation, the inflammatory response should be concluded, termed resolution, after the elimination of the injurious stimuli and restoration of the damaged tissue. Resolution involves neutralization of inflammatory mediators; restoration of normal vascular permeability; cessation of leukocyte infiltration; and removal of fluid, protein, leukocytes, and foreign agents from the site.

1.4.2 Chronic inflammation and tissue fibrosis

As discussed above, acute inflammation is thought to benefit the repair process. However, a persistent inflammatory response, i.e., a chronic inflammation, can frequently occur in many repair situations. Active inflammation of prolonged duration results in tissue destruction and repair proceeding simultaneously, and leads to tissue fibrosis. Chronic inflammation arises from persistent infection, prolonged exposure to potentially toxic agents, or very rarely autoimmunity. In post-operative adhesion formation, sutures or serious tissue damage at the site of incision are the principal contributors promoting adhesion formation. The features of chronic inflammation can be classified as follows: (1) infiltration of mononuclear cells, mainly macrophages but also lymphocytes and plasma cells; (2) Tissue destruction, due to the persistent offending factors; (3) replacement of damaged tissue by connective tissue, accompanied by growth of small blood vessels (Kumar et al., 2005b).

Macrophages are the dominant cells in chronic inflammation. They are part of the mononuclear phagocyte system, and derive from the bone marrow (Hume, 2006). In addition, tissue-resident macrophages also play an important role in local inflammatory response (Mosser and Edwards, 2008). As we discussed before, macrophages start to appear at the wound sites within 48h of insult and become the

predominant cell type. They can be activated by a variety of factors, including cytokines (e.g., IFN-γ and TNF-α), bacterial endotoxins and other chemical mediators (Mosser and Edwards, 2008). The activated macrophage can not only function as a phagocyte, but also produce several inflammatory factors (Lingen, 2001; Mosser and Edwards, 2008; Huybrechts-Godin et al., 1985), including IL-1, TNF-α, FGF, and MMPs. These mediators play an essential role in body defence and tissue remodelling. However, over a long period they can also induce the tissue destruction that is one of the hallmarks of chronic inflammation.

Another hallmark of chronic inflammation is granulomatous inflammation (Adams, 1976). This is a consequence of failed attempts to eliminate foreign bodies and particles, such as bacteria, toxic materials and suture fragments. It is a distinctive pattern of chronic inflammation reactions characterized by focal accumulations of activated macrophages, which often develops an epithelial-like (epithelioid) appearance. It leads to the formation of granuloma, a microscopic aggregation of macrophages that are transformed into epithelium-like cells surrounded by a collar of mononuclear leukocytes, principally lymphocytes (Williams and Williams, 1983). These epithelioid cells can fuse to form giant cells, which can be found in the periphery or centre of granulomas (Figure 1.7). Granulomas can be divided into two types by their different pathogeneses. One type are called foreign body granulomas and caused by inert foreign bodies, such as talc, sutures or other fibres. These materials are too large to be phagocytosed by a single macrophage, but do not incite any specific inflammatory or immune response. Therefore, the epithelioid or giant cells are formed with the purpose of simply encompassing the foreign body. The other granuloma type is called immune granuloma and is caused by insoluble particles, typically microbes. These particles are capable of inciting a cell-mediated immune response. In these responses, macrophages engulf these foreign particles and present them to respective T lymphocytes. T lymphocytes are activated and start to produce cytokines, such as IL-12 and IFN-γ. IL-12 can activate other T cells to

perpetuate the response, whereas IFN-γ can activate macrophages and transform them into epithelioid cells and multinucleate giant cells. Therefore granulomatous inflammation is seen in a wide variety of diseases, and frequently associated with tissue fibrosis (Woodard et al., 1982; Hartel et al., 2010; Mukhopadhyay and Gal, 2010).

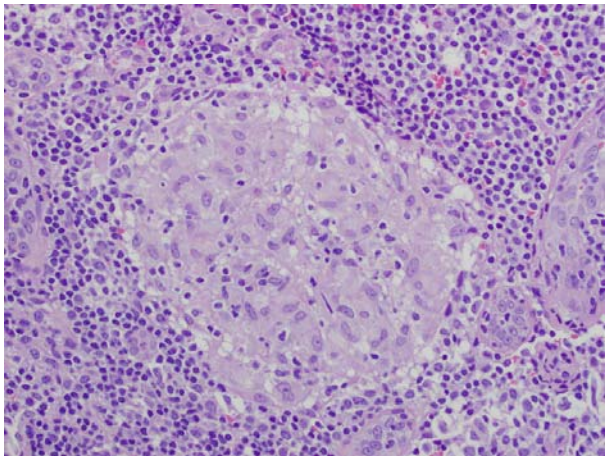

Figure 1.7. Non-necrotizing granuloma in a lymph node (20x objective lens). Figure taken from Mutley Smith (Wikimedia Commons)

1.4.3 Inflammatory cytokines and post-operative adhesion

As discussed above, production of cytokines is one of the key characteristics of the inflammatory response. They can mediate and regulate inflammatory responses in various aspects, including cell infiltration, ECM remodelling and angiogenesis. However, persistent production of cytokines can cause a sustained inflammatory response, which will lead to tissue fibrosis. The role of cytokines involved in post-operative adhesion has been widely studied. For example, serum levels of IL-1 and TNF-α are found to correlate with peritoneal adhesion grades in patients following major abdominal surgery (Saba et al., 1998). In addition, a pilot study of peritoneal fluid obtained from patients following laparoscopy has demonstrated that IL-1, IL-6 and TNF-α concentrations in the fluid are dramatically increased in the initial 48 h. High concentrations of IL-1 and IL-6, but not TNF-α, are associated with significant adhesion formation (Cheong et al., 2002). Furthermore, levels of TGF-β1

are also raised in peritoneal scar tissue compared to normal peritoneal tissue (Chegini et al., 1994). An overview of cytokine effects in post-operative adhesion formation is presented in Table 1.5. The most common cytokines studied in post-operative adhesion are IL-1 and TNF-α and TGF-β. Therefore, in this thesis, the effects of cytokines on adhesion formation will focus on these three cytokines.

Table 1.5. Overview of current literature regarding cytokine orchestration in postoperative adhesion formation. Table adapted from (Cahill and Redmond, 2008)

Cytokine	Species (*in vitro/in vivo*)	Experimental model	Effect on adhesion formation	Referrence
HGF	Rat (both)	Cecal abrasion	Local HGF gene transfer enhance PMC migration and prevent postoperative peritoneal adhesions	(Liu et al., 2006)
IFN-γ, HGF	Mouse (both)	cecal cauterization	Diminishing IFN-γ production can prevent adhesions by regulating PAI-1 and tPA, which is enhanced by HGF	(Kosaka et al., 2008)
IL-1, TNF-α	Human (*in vivo*)	Adhesion samples	Serum levels of IL-1 and TNF-α correlate with peritoneal adhesion grades in humans after major abdominal surgery	(Saba et al., 1998)
IL-1, TNF-α and IL-6	Human (*in vitro*)	Peritoneal fluid samples	Adhesion associated with IL-6 and IL-1	(Cheong et al., 2002)
IL-10, IL-4	Mouse (*in vivo*)	Peritoneal injury	Attenuated by IL-10 but not IL-4	(Holschneider et al., 1999)
IL-1β, IFN-γ, TGF-β1, TNF-α, GM-CSF	Human (*in vitro*)	Peritoneal fluid samples	Only IFN-γand TGF-β1 associated with adhesion, not others	(Chegini et al., 1999)
IL-6	Rat (*in vivo*)	Cecal abrasion with C_2H_5OH	Exacerbated by IL-6, attenuated by monoclonal Ab to IL-6	(Saba et al., 1996)
TGF	Mouse (*in vivo*)	Serosal abraision and apposition	Attenuated by combined TGF-β1 and TGF-β2 mAb, exacerbated by exogenous addition of TGF-β3	(Gorvy et al., 2005)
TGF-β	Rat	Cecal abraision	TGF-β mRNA increased by trauma and expressed higher in injured tissue that healed	(Freeman et al.,

	(*in vivo*)		with adhesion	2003)
TGF-β	Rat (*in vivo*)	Uterine horn abraision	Exacerbated by TGF-β with increased inflammatory cells and fibroblast	(Williams et al., 1992)
MMP-9, TIMP-1	Human (*in vitro*)	Peritoneal fluid samples	Adhesion associated with reduced MMP-9 but elevated MMP-9/TIMP-1 ratio	(Cheong et al., 2003)
TGF-β	Human (*in vitro*)	Biopsy samples	TGF-β protein is higher in scar tissue than normal tissue	(Hobson et al., 2003)
TGF-β1	Rat (*in vivo*)	Cecal ligation and puncture	Peritonitis upregulates TGF-β1 expression	(Ghellai et al., 2000)
TNF-α	Rat (*in vivo*)	Cecal abraision or small bowel resection	Identify TNF-α as a good biological marker for adhesion formation	(Kaidi et al., 1995a)
TNF-α, IL-1	Rat (*in vivo*)	Cecal abraision	Adhesion formation attenuated by mAbs to IL-1 and IL-1/TNF-α	(Kaidi et al., 1995b)
TNF-α, MMP	Rat (*in vivo*)	Peritoneal wounding	No effect of MMP & TACE inhibition, TNF-α may not be adhesiogenic	(Mirastschijski et al., 2005)
VEGF	Mouse (*in vivo*)	Peritoneal injury	Adhesions attenuated by antiserum and monoclonal antibody	(Saltzman et al., 1996; Cahill et al., 2006)
VEGF	Mouse (*in vivo*)	Lap. Uterine horn model	Exacerbated by overexpression of VEGF	(Molinas et al., 2003)
MCP-1	Mouse (*in vivo*)	Peritoneal injury	Adhesions significantly attenuated by anti-MCP-1 Abs	(Zeyneloglu et al., 1998)

Abbreviation: HGF: Hepatocyte growth factor; IFN-γ: Interferon-gamma; IL: Interleukin; TNF-α: Tumour necrosis factor-alpha; TGF-β: Transforming growth factor-beta; GM-CSF: Granulocyte macrophage colony stimulating factor; MMP: Matrix metalloproteinase; TIMP: Tissue inhibitor of metalloproteinase; VEGF: Vascular endothelial growth factor; MCP: Monocyte chemotactic protein.

1.4.3.1 Interleukin-1 family and signalling networks

The principal function of IL-1 is to mediate the host inflammatory response to infections and other stimuli due to its ubiquitous and pleiotropic role in the human body. The IL-1 family includes two members, IL-1α and IL-1β (Clark et al., 1986; Furutani et al., 1986). They share less than 30% amino acid homology in the same species. However, closer relations of the individual IL-1 forms are found between species. Thus, about 88% homology is found between human and mouse IL-1β, and approximately 70% between the various species of IL-1α. Each of the IL-1 forms is encoded by separate genes located on chromosome 2, which leads to the synthesis of a 33-kDa precursor. The precursor is further processed into a 17-kDa mature protein by serine proteases (particularly elastase and plasmin) and cysteine protease caspase-1 (also called IL-1β-converting enzyme) (Fenton et al., 1987). In the cell, IL-1 is associated with lysosomes rather than endoplasmic reticulum, indicating a nonclassical pathway of IL-1 secretion compared to other secreted proteins (Matsushima et al., 1986). A wide variety of cells are shown to synthesize IL-1 including fibroblasts, macrophages and mesothelial cells. The level of IL-1β mRNA predominates over that of IL-1α, possibly due to a second promoter-like sequence contained in the IL-1β gene but not found in the IL-1α one (Libby et al., 1986). Both IL-1α and IL-1β bind equally to the same receptors and induce the same downstream signalling pathway (Bankers-Fulbright et al., 1996). However, the activities of the forms do demonstrate differences. IL-1β is only active after it has been processed to the mature form, whereas IL-1α is active either as the precursor or as the mature product (Mosley et al., 1987). Cells contain active membrane-associated IL-1 (MA-IL-1), which may account for the immunostimulatory effects of IL-1 in local tissues such as lymph nodes, joints, and skin (Dinarello, 1988; Niki et al., 2004). The evidence suggests that most of the membrane-associated IL-1 is IL-1α, because IL-1β needs to be cleaved and secreted into the body system (Dinarello, 1988; Niki et

al., 2004). Therefore IL-1 can participate in autocrine and paracrine responses locally through MA-IL-1α, as well as inducing IL-1β systemic effects. Another member involved in the IL-1 system is a competitive inhibitor of IL-1, IL-1 receptor antagonist (IL-1ra). IL-1ra is an endogenous inhibitor secreted by the same types of cells (Arend et al., 1998). It can inhibit both IL-1α and IL-1β activity by binding to the cell surface IL-1 receptors. There are two types of cell surface receptors: IL-1 receptor type1 (IL-1R1) and IL-1 receptor type2 (IL-1R2) (Sims et al., 1993). They belong to the toll-like/IL-1 receptor (TIR) superfamily and share a 22% homology (Sims et al., 1988). These two receptors have a key conserved TIR cytoplasmic domain that contains at least 200 amino acids and an extracellular ligand-binding Ig domain. It has been shown that the main functional receptor is IL-1R1, whereas IL-1R2 likely acts as a 'decoy' that competitively inhibits IL-1 binding to IL-1R1 (Stylianou et al., 1992). The main biologic effect of IL-1 is to stimulate cells to produce other inflammatory mediators including surface adhesion molecules, cytokines, growth factors, ECM components and mitogens (Stylianou et al., 1992). IL-1 mediates these effects by triggering several transcriptional pathways in the cells through the binding to the IL-1R1 (Stylianou et al., 1992; O'Neill and Dinarello, 2000) (Figure 1.8). After binding to the extracellular Ig domains of the receptor, the external stimulated signal recruits an adapter protein MyD88 to the TIR domain (Wesche et al., 1997). MyD88 then phosphorylates IL-1 receptor-associated kinase-4 (IRAK4) that in turn phosphorylates IRAK-1. The phosphorylation of IRAK-1 further activates another adapter protein, TNF receptor-associated factors-6 (TRAF6), by ubiquitinating at lysine 63 chains of TRAF6 (Chen, 2005). This also leads to the unbiquitination of TGF-β activated kinase-1 (TAK1) through the assembly of TAK1-TAB complex and K-63 ubiquitinated TRAF6 (Sun et al., 2004). TAK-1 can further induce the NF-κB pathway by activating the IκB kinases (IKKs) (Mercurio et al., 1997). In addition, TAK-1 can also induce activation of mitogen-activated protein kinases (MAPKs), including JNK/p38 pathways, resulting in the activation of

activating protein-1 (AP-1) (Sato et al., 2005). The activation of AP-1, together with the NF-κB pathway, could dominate the production of inflammatory mediators from almost all cell types (Kawai and Akira, 2006).

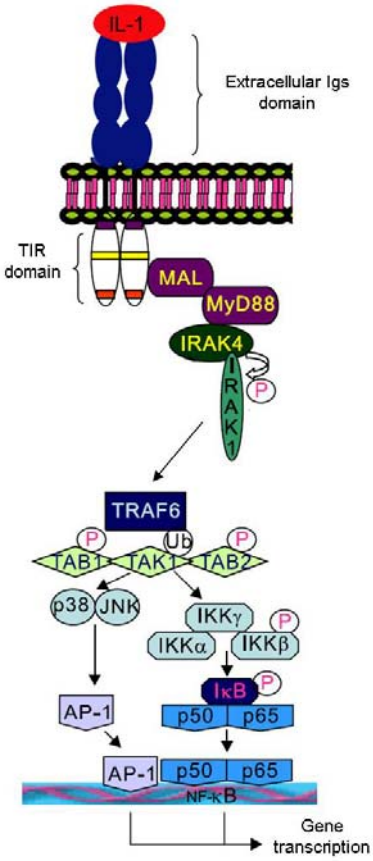

Figure 1.8. IL-1 signalling network. Binding of IL-1 to the IL-R heterodimer induces sequential phosphorylation of serine/threonine kinases that in turn activates NF-κB and AP-1 transcription. Figure adapted from (Krishnan et al., 2007; O'Neill and Dinarello, 2000).

In summary, IL-1 contributes to the inflammatory response both locally and systematically by inducing the production of other inflammatory mediators. The effect of IL-1 can be modulated by its specific endogenous inhibitor IL-1ra, as well as by the regulatory NF-κB and AP-1 transcriptional pathways.

1.4.3.2 TNF-α signalling network

TNF-α is a principal mediator of acute inflammatory responses to infectious microbes and can cause notable systemic inflammation. The major source of TNF-α is activated mononuclear phagocytes. However, various kinds of cells are also found to secrete TNF-α, including antigen-stimulated T cells, NK cells, fibroblasts and mast cells (Wajant et al., 2003). It is primarily produced as a type II transmembrane protein in a stable homotrimer form with an intracellular amino terminus and an extracellular carboxyl terminus (Kriegler et al., 1988). This membrane-integrated form can be futher proteolytically cleavaged by the metalloprotease, TNF alpha converting enzyme (TACE), and is secreted as a soluble homotrimeric cytokine that tends to dissociate at concentrations below the nanomolar range (Black et al., 1997). Both the membrane-integrated and soluble TNF-α exert their functions via interaction with their membrane receptor, TNF receptor (TNF-R).

Two receptors have been identified, TNF-R1 (CD120a, 55kD) and TNF-R2 (CD120b, 75kD) (Locksley et al., 2001). TNF-R1 mediates the inflammatory response in the majority of cells, whereas the effect of TNF-R2 is more focused to the lymphoid system. The main physiologic function of TNF-α is to promote the recruitment of inflammatory cells to sites of infection or injury (Locksley et al., 2001), by inducing adhesion molecule expression on endothelial cells and stimulating production of chemokines. In addition, large amounts of TNF-α can be produced and enter into circulation during chronic inflammation, causing systemic clinical and pathologic abnormalities (e. g, fever, cachexia, and sepsis) (Locksley et al., 2001). Furthermore, TNF-α is also engaged in tissue regeneration. For example, studies have shown an impaired hepatocyte DNA synthesis in TNF-R1-defecient animals after partial hepatectomy, indicating an essential role of TNF-α signalling involved in liver regeneration (Yamada et al., 1997). In contrast, TNF signalling is also a potent factor causing liver destruction in TNF-α-induced acute hepatotoxicity

(Bradham et al., 1998). Therefore, insight into the signalling pathways induced by TNF-α is critical in understanding of the role of TNF in body systems. TNF-α is first recognized as a potent cytotoxic factor due to its capacity to induce cell death (Schulze-Osthoff et al., 1992; Hsu et al., 1995). However, TNF-induced cell death seems to have only a minor role compared to its function in the regulation of inflammatory processes through NF-κB, AP-1, and p38-MAPK pathway.

In vivo, the NF-κB pathway is found to be activated in preference to the death-inducing pathway by TNF-α (Wajant et al., 2000; Tanaka et al., 1999). The activation of TNF-receptor results in the recruitment of the TNF-receptor type 1 associated death domain-containing adaptor protein (TRADD) which in turn interacts with TRAF-2 and receptor-interacting protein-1 (RIP-1), leading the activation of the NF-κB pathway. A summary of the TNF-induced NF-κB pathway is showed in Figure 1.9A. Alternatively, TRAF-2 and RIP-1 are also shown to activate AP-1 (Reinhard et al., 1997) and p38-MAPK pathways (Yuasa et al., 1998), respectively. The AP-1 proteins are well known in the prevention of apoptosis by signalling in cellular proliferation, differentiation and induction (Shaulian and Karin, 2002). In addition, it has been shown that TNF-α can induce cytokine expression in murine embryonic fibroblasts, including IL-1 and IL-6, by activating the p38-MAPK pathway. The study also demonstrated that depletion of Mitogen-activated protein kinase kinase 3 (MKK3) can significantly reduce cytokine production (Wysk et al., 1999). A summary of TNF-induced AP-1 and p38-MAPK pathway is presented in Figure 1.9B

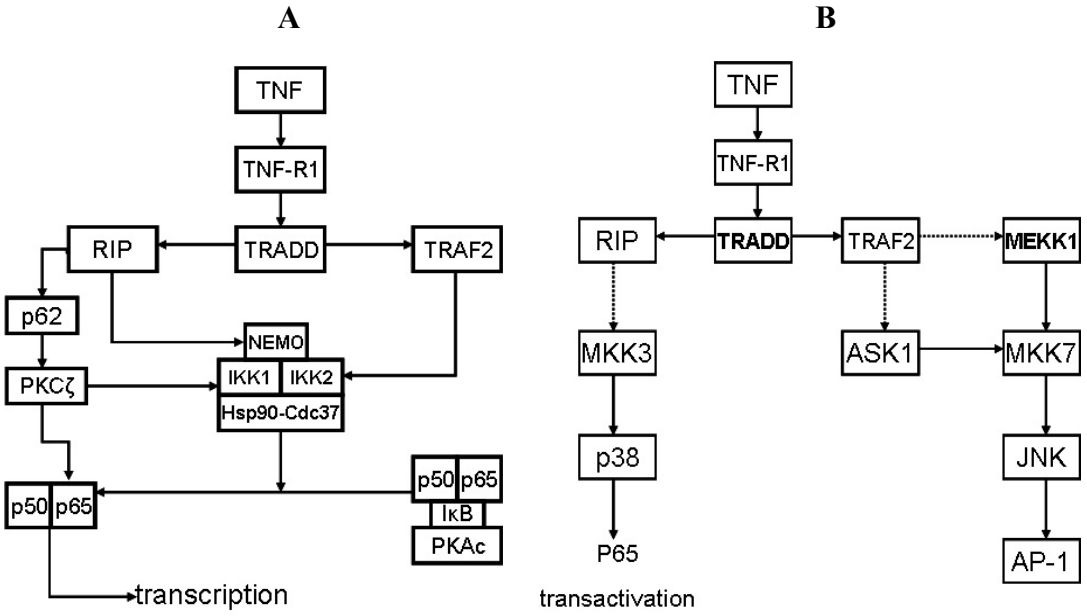

Figure 1.9. TNF-α signalling network. A: TNF-α induced NF-κB activation. B: TNF-α induced activation of p38–MAPK and JNK. The poorly defined connection between RIP and MKK3, TRAF2 and ASK1, TRAF2 and MEKK1 are indicated by a dotted line. Figure adapted from (Wajant et al., 2003).

In summary, the function of TNF is not limited to actions as a pro-apoptotic and inflammatory cytokine. It also acts in tissue repair through its anti-apoptotic signalling pathway. Therefore, the tissue type, cellular context, timing and duration of TNF action are important to define in determining the role of TNF in diseases.

1.4.3.3 TGF-β function and signalling network

TGF-β is another multi-functional cytokine known to be involved in tissue repair. In the immune system, TGF-β can act as an anti-inflammatory factor by inhibiting the proliferation and activation of lymphocytes and other leukocytes (Moustakas et al., 2002). However, abnormal TGF-β expression is found to be associated with many fibrotic diseases including scar and post-operative adhesion. The TGF-β superfamily contains a range of proteins which also include inhibins, activin, and bone morphogenetic protein (Massague, 1998). TGF-β is part of this large family and

exists as three isoforms: TGF-β1, TGF-β2, and TGF-β3 (Massague, 1998). These three isoforms share 60-80% homology but are encoded by different genes. They are synthesized as latent precursors which contain latent TGF-β binding proteins (LTBP). The activation of these precursors requires the removal of the LTBP extracellularly via proteolytic cleavage. Many factors are shown to mediate this process, including plasmin, thrombin, MMP-2, MMP-9, that are also important mediators induced in tissue repair (Annes et al., 2003). Thus, increased TGF-β activation can be expected during any healing process, indicating an important role of TGF-β in tissue repair. TGF-β induces the cellular response by binding to a transmembrane receptor composed of a heteromeric complex of serine/threonine kinases. These receptors are named TGF-β type receptors (TGF-βR) consisting of TGF-βR-I, -II, and III (Roberts, 1999). TGF-β1 is the major effective member in many situations, since it is the predominant one expressed by a number of cells. TGF-β1 is a homodimeric protein that can be produced by antigen-stimulated T cells, LPS-activated monouclear phagocytes, platelets, and many other cell types. The main signalling pathway induced by TGF-β1 is the Smad pathway (Attisano and Wrana, 2002). It has been shown that TGF-β1 can bind to TGF-βR-II, which in turn forms a complex with TGF-βR-I. The external signal from TGF-β1 is transferred through the Smad family. In the presence of TGF-β ligand, the TGF-βR-I can phosphorylate the Smad 2 and 3, which in turn bind a common mediator Smad 4. The complex of Smad 2/3 and Smad 4 translocates into the nucleus and induces suppression and activation of various genes (Klass et al., 2009) (Figure 1.10).

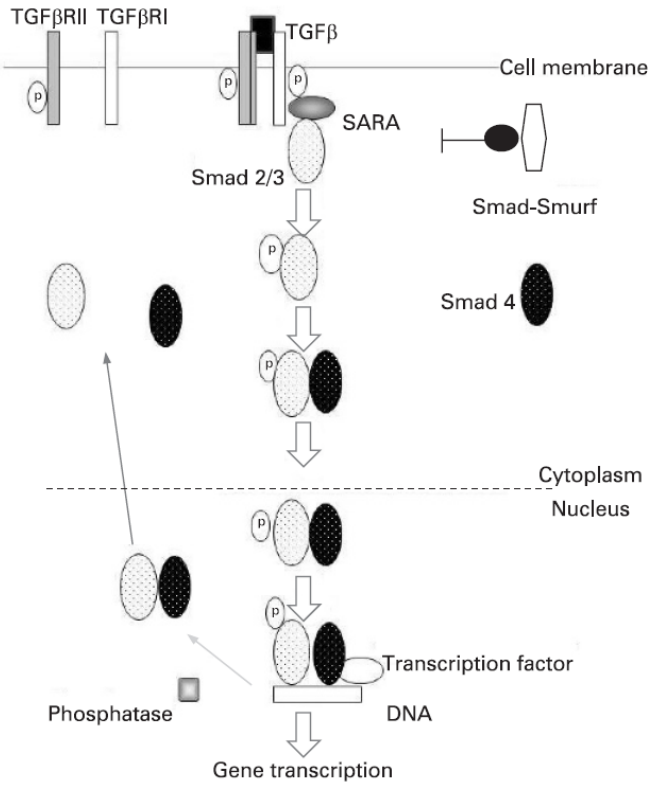

Figure 1.10. TGF-β1–Smad pathway. The ligand (black) binds to the receptors. Active receptors phosphorylate Smad 2/3 (white with black spots), which can be presented to the receptor by accessory proteins such as Smad anchor for receptor activation (SARA) (grey). Phosphorylated Smad 2/3 can form complexes with Smad4 (black with white spots). This complex can translocate into the nucleus and regulate gene transcription. A phosphatase (grey square) can remove the phosphorylation of Smad 2/3. Smad 2/3 and Smad 4 can translocate back into the cytoplasm. A complex of Smad7–Smurf can terminate signalling by preventing the phosphorylation of Smad 2/3 or causing the degradation of the active receptors. Adapted from (Klass et al., 2009).

In addition, TGF-β1 can also signal through non-Smad pathways (Derynck and Zhang, 2003). The activation of these non-Smad pathways is also elicited by the binding of TGF-βR-I and TGF-βR-II receptors. Recent data have shown that the MAPK pathway is activated by TGF-β1 and mediated by Ras (Derynck and Zhang, 2003; Lee et al., 2007) (Figure 1.11). The TGF-β ligand can assemble a Shc/Grb2/Sos complex associated with TGF-βR-I, and then initiate Ras activation. Ras activation can lead to the activation of Erk 1/2 MAP kinase mediated by MEK 1/2. In addition, TGF-β can also induce activation of p38 and JNK MAP kinases

(Figure 1.11) (Bakin et al., 2002; Yu et al., 2002). It has been shown that TGF-β can activate TAK1 by TRAF6 associated with the receptor complex. TAK1 is required for TGF-β-induced p38 and JNK MAPK activation by activating MKK 3/6 or MKK4 respectively (Santibanez, 2006; Alcorn et al., 2008). Other non-Smad signalling pathways induced by TGF-β1 include the activation of Rho-like GTPase (Cho and Yoo, 2007) and PI3 kinase/Akt signaling pathways (Bakin et al., 2000; Yeh et al., 2008). As the involvement of these two signalling pathways in tissue fibrosis is limited, the detail of their activation by TGF-β1 will not be discussed further in this thesis.

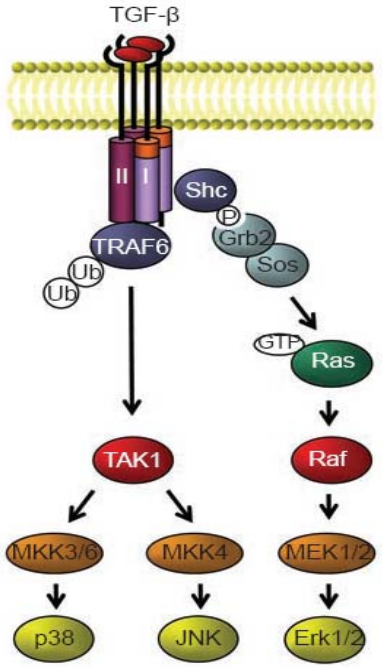

Figure 1.11. TGF-β activates p38-MAPK and JNK-MAPK signalling. through the activation of TAK1 by ubiquitin ligase TRAF6 associated with TGF-β receptor, and Erk MAP kinase signalling through recruitment and phosphorylation of Shc by the TβRI receptor. Figure adapted from (Xu et al., 2009).

As discussed above, TGF-β is a key mediator in tissue fibrosis. It has been shown that Smad signalling contributes to the induction of profibrotic genes such as type I collagen and CTGF in fibroblasts (Verrecchia et al., 2001; Holmes et al., 2001). Smad3 activation is generally required for TGF-β-induced gene expression in

fibroblasts. In contrast, TGF-β is shown to inhibit the activity of MMPs in certain situations (Varga and Jimenez, 1986; Overall et al., 1989). Additionally, TGF-β-induced p38 MAPK and ras/MEK/ERK pathways also contribute to the production of profibrotic genes in various cell types (Chen et al., 2002; Stratton et al., 2002; Sato et al., 2002). As described earlier (section 1.3.2), TGF-β1 plays an important role in the EMT process, mediated by the Smad signalling pathway (Xu et al., 2009). Ectopic adenoviral overexpression of Smad 2/3 with Smad 4 in NMuMG cells is found to induce EMT independently without TGF-β binding (Piek et al., 1999; Valcourt et al., 2005). Overexpression of negative forms of Smad 2/3 significantly blocks TGF-β induced EMT in cell systems (Valcourt et al., 2005). The downstream signal transducers, including the Snail family, the ZEB family, and the basic helix-loop-helix (bHLH) family, are shown to mediate the Smad-dependent EMT process, down-regulating epithelial markers and upregulating mesenchymal ones (Xu et al., 2009). In summary, TGF-β is a key cytokine involved in tissue repair. However, aberrant TGF-β expression is also implicated in scarring and other fibrotic diseases. A deeper understanding of TGF-β effects in post-operative adhesion may lead to the development of novel treatments for fibrotic disease.

1.4.4 Anti-inflammatory effect of glucocorticoid on tissue fibrosis

As previously discussed, tissue fibrosis is mainly caused by chronic inflammation. Anti-inflammatory steroids have long been used as a treatment for inflammatory diseases and disorders. In this context the most important and widely used steroids are glucocorticoids (GC), which are proven to counteract many inflammatory responses (Liberman et al., 2009). GCs are synthesized within the adrenal cortex from cholesterol through a series of reactions (Balsalobre et al., 2000). The major active GC steroid in humans is cortisol. After its synthesis and secretion by the adrenal gland, it travels to sites of action via the circulation. However, local

modulation of cortisol can also be found during inflammatory events. It has been shown that proinflammatory cytokines can regulate the level of 11β-hydroxysteroid dehydrogenase (11β-HSD) expression, involved in local interconversion of cortisol and cortisone (Davani et al., 2000; Quinkler et al., 2001; Rae et al., 2004a). 11β-HSD consists of two isoforms, 11β-HSD1 and 11β-HSD2, encoded by two separate genes sharing only 14% homology (Draper and Stewart, 2005). 11β-HSD1 is the key enzyme converting local cortisone (inactive) into cortisol, whereas 11β-HSD2 catalyzes the opposite reaction (Figure 1.12) (Seckl and Walker, 2001). It has been shown that pro-inflammatory cytokines, such as IL-1α (Rae et al., 2004a; Fegan et al., 2008), can stimulate 11β-HSD1 mRNA expression as well as its enzyme activity, with little if any, change in 11β-HSD2 levels. Therefore, local re-synthesis of cortisol arising from inactive cortisone is tightly regulated by 11β-HSD and inflammatory cytokines. Cortisol is a lipophilic molecule which can cross the cellular lipid bilayer and enters into the cytoplasm by free diffusion (De Bosscher et al., 2003). It then binds to the specific glucocorticoid receptor (GR), a transcription factor that translocates on binding of its ligand into the nucleus and thereafter regulates gene transcription. GR is present in the cytoplasm in an inactive form combined with co-chaperone molecules, such as heat shock protein (hsp) (Pratt and Toft, 1997). The binding of GC allows the GR complex to translocate into the nucleus and bind to specific DNA sequences (De Bosscher et al., 2003). These sequences, called GC-response elements (GRE) are encoded in genes positively regulated by GC, whereas negative GRE (nGRE) are found in genes negatively regulated by GC. GR can also modulate gene transcription by interacting with other transcription factors, including NF-κB, AP-1, signal transduction activator of transcription (STAT) etc. Therefore, GCs can modulate inflammatory response by both dynamic transactivation and transrepression effects.

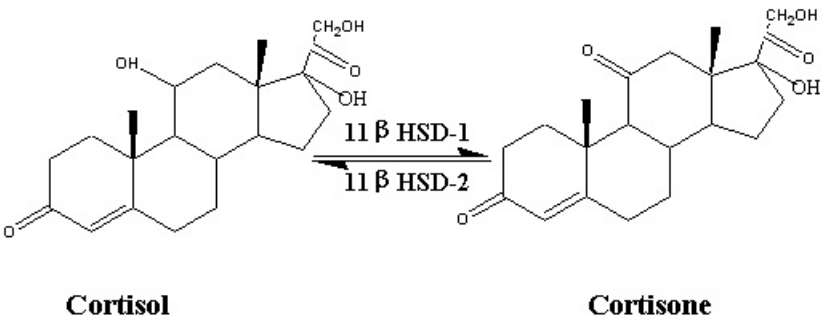

Cortisol **Cortisone**

Figure 1.12. Reactions catalysed by 11βHSD-1 and -2.

As discussed above, negative modulation of the inflammatory response can be achieved by GC-induced transrepression. Binding of GRs to specific nGREs on the DNA can caused direct transcriptional repression of target genes. The function of the nGRE is to guide GR to bind as a monomer (Heck et al., 1994; Radoja et al., 2000). However, the majority of inflammatory genes do not contain nGRE. Therefore, the anti-inflammatory effect of GCs is mainly dependent on the interplay with the other two main transcriptional pathways, NF-κB and AP-1 (Herrlich and Gottlicher, 2002). Evidence indicates that GR suppresses NF-κB through physical association with NF-κB proteins, including RelA and p65 *in vitro* (Ray and Prefontaine, 1994; Caldenhoven et al., 1995; Scheinman et al., 1995b). *In vitro* studies have successfully shown an interaction between endogenous p65 and GR, by using IL-1β and dexamethasone (DEX) co-treatment of A549 cells (Adcock et al., 1999). It has been shown that similar mechanisms are involved in AP-1 transrepression (Cippitelli et al., 1995; Schule et al., 1990; Jonat et al., 1990). However, these mechanisms are strictly dependent on cell type, promoter, and receptor. Alternatively, GC-dependent repression of the NF-κB pathway has been proposed to be triggered by upregulation of IκBα, the cytoplasmic inhibitor of NF-κB (Scheinman et al., 1995a; Auphan et al., 1995). Although the mechanism is not totally understood, transcriptional regulation of the IκBα promoter by GCs has been demonstrated in several studies (Auphan et al., 1995; Heck et al., 1997). Additionally, GR is found to bind certain coactivator molecules which are also required by other transcriptional factors. These coactivators

are characterized by an intrinsic histone acetyltransferase activity (Wolffe et al., 1997) which can promote gene activation by providing a more relaxed chromatin environment. These coactivators are also implicated in bridging p65, AP-1 to the factors of their respective transcription pathways (Kamei et al., 1996; Gerritsen et al., 1997; Sheppard et al., 1999; Vanden Berghe et al., 1999). Hence, GR-induced repression can be due to a territorial subdivision of GR from other transcriptional factors for a limited amount of coactivators (e.g. CBP, p300, and steroid receptor coactivator-1) (Doucas et al., 1999; Lin et al., 2003). Lastly, it has been shown that chromatin modification and remodelling can also contribute to GR-induced repression, since GR can bind to these related coactivators (Yoshinaga et al., 1992; Ostlund Farrants et al., 1997; Fletcher et al., 2000; Belikov et al., 2000).

Although the molecular mechanisms underlying GC-mediated anti-inflammatory response are far from understood, it is accepted that GC activity is based on interference with other transcription factor actions. GC is shown to regulate cytokine receptor expression in inflammatory response. For example, GC can inhibit IL-2 and IL-12 receptor expression. On the other hand, induced IL-6, GM-CSF and IL-7 receptor expression are found after GC treatment of various cell types (Liberman et al., 2007). GC is also capable of regulating cytokine induced transcription by interfering with intra-cellular signalling pathways. Furthermore, GC can regulate inflammatory cell development and maturation. For example, GC can promote a Th2 cellular inflammatory response by inhibition of Th1 cytokines (IL-2 and IFN-γ) and stimulation of Th2 cytokines (IL-4 and IL-10) (Ramirez et al., 1996; Visser et al., 1998b). In addition, GC treatment during the process of monocyte differentiation, results in a marked augmentation of macrophage capacity for phagocytosis of apoptotic cells (Giles et al., 2001). Therefore, the anti-inflammatory effect of GC can contribute to the resolution of tissue fibrosis, through an orchestration of effects.

1.5 ECM remodelling and tissue fibrosis

The previous section discussed the mechanism of normal tissue repair and the pathology of tissue fibrosis. In both processes, the deposition of ECM is critical. The ECM can be secreted locally, assembling into a network in the spaces around cells (Frantz et al., 2010). The ECM serves several functions. For example, it helps maintain water and minerals content of soft tissues. It can also function as a reservoir for growth factors controlling cell proliferation and is also involved in cell-cell interactions (Frantz et al., 2010).

The ECM is made up of three main groups of macromolecules (Jarvelainen et al., 2009; Schaefer and Schaefer, 2010), namely, (1) fibrous structural proteins, including collagens, elastins and fibronectin; (2) adhesive glycoproteins, such as cadherins and integrins; (3) proteoglycans and hyaluronic acid. These factors contribute to the formation of two main general types of ECM structures i.e., interstitial matrix (Jarvelainen et al., 2009) and basement membrance (BM) (Sanes, 2003). The former is present in spaces between epithelial, endothelial, and smooth muscle cells and in connective tissue; whereas the BMs are normally associated with the cell surface. Although these two structures occur at different sites, their components are quite similar. These ECM components are introduced in the following section.

1.5.1 Collagen

Collagens are the most important component providing the ECM framework in the human body. They are composed of a triple helix of three polypeptide alpha chains, each chain having a gly-x-y repeating sequence. The structure of the triple helix is stabilized by numerous hydrogen bonds. Currently, 27 different types of collagen are

found, encoded by 41 genes dispersed on at least 14 chromosomes (Myllyharju and Kivirikko, 2001). The most abundant collagens are the interstitial or fibrillar collagens including types I, II, III, V and XI. In contrast, type IV collagen is non-fibrillar forming sheets instead of fibrils (PH, 2001). Therefore, together with laminin, type IV collagen is the main component of the BM (Sanes, 2003). Besides these, other collagens are found as meshworks and function as anchors in epidermal-dermal junctions, cartilage, and blood vessel walls.

Collagens can be produced by a variety of cells, including fibroblasts, epithelium, mesothelium, hepatocytes and macrophages. Fibrillar collagen is synthesized from procollagen. Procollagen is a precursor molecule derived from preprocollagen which is transcribed from collagen genes. The three procollagen chains are hydroxylated between their proline and lysine residues or lysine glycosylation to form the triple helix. The procollagen is then secreted from the cells and processed by proteases which cleave the propeptides. The mature collagen is the basic unit of the fibrils. They are further oxidised at the specific lysine and hydroxylysine residues. This results in cross-linking between the chains of adjacent collagen molecules, thus changing the soluble collagen macromolecules into insoluble collagen fibrils (Figure 1.13) (Chen and Raghunath, 2009). The main enzyme involved in the cross-linking procedure is called lysyl oxidase (LOX), which we will discuss more in detail in section 1.5.5.

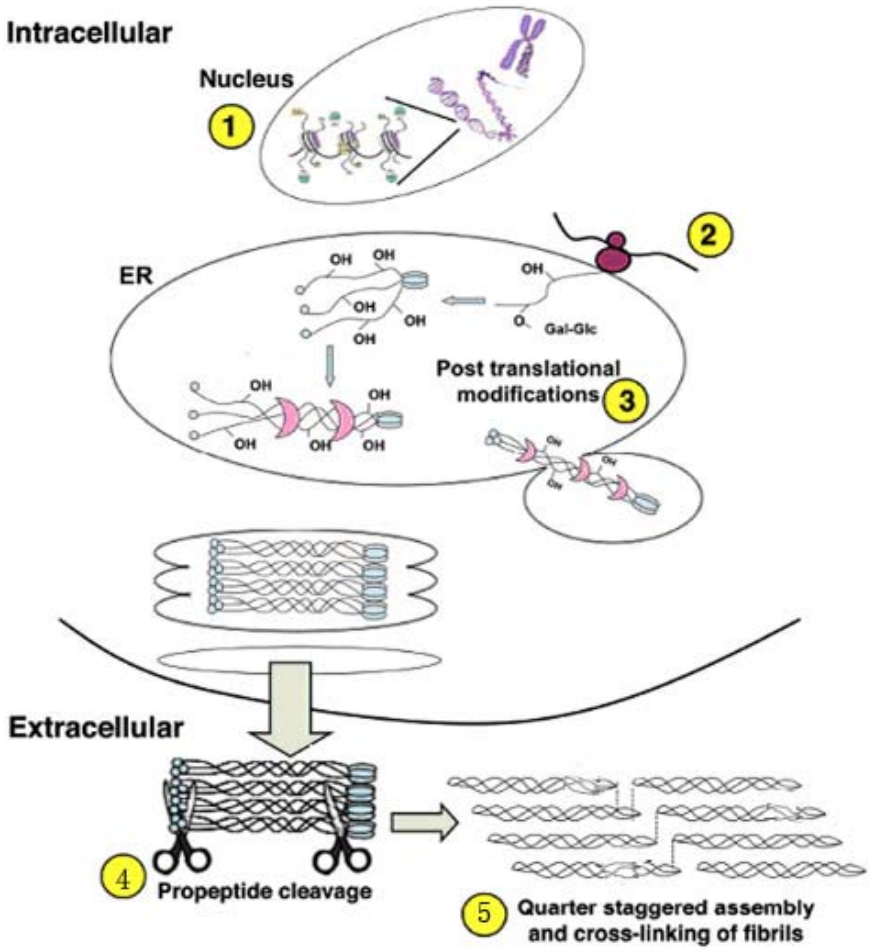

Figure 1.13. Collagen biosynthesis pathways. (1) Epigenetic level: chromatin remodelling and unfolding. (2) Post-transcriptional level: mRNA translation. (3) Post-translational level: Formation of the procollagen triple helix. (4) Post-secretion level: Procollagen proteinases (scissors symbol) cleave propeptides of procollagen molecules at the cell surface (5) Collagen crosslinking: lysyl oxidase (LOX) crosslinks soluble collagen molecules to form fibrils. Figure adapted from (Chen and Raghunath, 2009)

1.5.2 Elastin, Fibrillin, Laminin and Fibronectin

Although ECM mainly consists of collagens, other ECM components include elastin, fibrillin, fibronectin and laminin. Tissues such as blood vessels and skin, which require elasticity for their function, contain elastin fibres. Fibrillin is a 250-kDa secreted glycoprotein forming a peripheral microfibrillar network. Elastic fibres consist of a central core made of elastin, with the microfibrillar network surrounding it (Milewicz et al., 2000).

Fibronectin is another ECM component which can bind to many molecules, including collagen, fibrin, proteoglycans, and cell-surface receptors. It is formed by two glycoprotein chains held together by disulphide bonds. The two forms of fibronectin, tissue fibronectin and plasma fibronectin are translated from two spliced mRNA variants. The tissue fibronectin accounts for the fibrillar aggregates at wound healing sites. The plasma fibronectin binds to fibrin, contributing to the provisional blood clot formation filling the space at the wound sites and serving as a substratum for ECM deposition (Smith et al., 2007).

Laminin is the most abundant glycoprotein in the basement membrane. It is a trimeric protein that contains α-chain, β-chain, and γ-chains; with five, three, and three genetic variants respectively. In the basement membrane, polymers of laminin and collagen type IV form tightly bound networks. It can also provide binding domains for ECM and cell-surface receptors. In addition, it has been shown that laminin can mediate the attachment of cells to connective tissue substrates (Colognato and Yurchenco, 2000).

1.5.3 Cell adhesion molecules

The CAMs (cell adhesion molecules) are classified into four main families: immunoglobulin family CAMs, cadherins, integrins, and selectins (Kumar et al., 2005a). Most are cell membrane-associated receptors, but some can be also found in the cytoplasm. It has been shown that these receptors can bind to various molecules providing interactions between similar cells (homotypic interaction) or different cell types (heterotypic interaction). Immunoglobulin family CAMs can participate in both homotypic and heterotypic cell-to-cell interactions. Selectins are a family of heterotypic CAMs that bind fucosylated carbohydrates, such as mucins. Such binding mediates the attachment of leukocytes to endothelial cells during the inflammatory response. The best studied of the CAMs are the cadherins (Zeisberg and Kalluri, 2004) and integrins (Hynes, 2002; Stupack and Cheresh, 2002), indicating the important roles of these two families in tissue fibrosis. Cadherins are a class of type-1 transmembrane proteins containing almost 90 members (Hazan et al., 2004). They participate in interactions between similar cell types, for example, connecting the plasma membrane of adjacent cells. The cell-to-cell interactions provided by cadherins play a major role in regulating cell proliferation, motility and differentiation. In contrast, integrins (Hynes, 2002; Stupack and Cheresh, 2002) mostly bind to matrix proteins including fibronectin and laminin, mediating adhesion between cells and ECM. All integrins are heterodimeric cell surface proteins composed of two noncovalently linked polypeptide chains, α and β. The family consists of about 30 structurally homologous proteins. The extracellular domains of the heterodimeric chains bind to various ligands, such as ECM glycoproteins, activated complement components, and proteins on the surfaces of other cells. The extracellular ligand signals transfer into the cells through the cytoplasmic domains of the integrins, interacting with cytoskeletal components, including vinculin, talin, actin, α-actinin and tropomyosin. Therefore, integrins play a critical role not only in

cell migration and adhesion formation, but also to regulate cell signalling and cell cycling.

1.5.4 ECM degradation

As discussed above, the inter-relationship between ECM and fibrosis is a complex process regulated by ECM components. Thus, the balance of ECM synthesis and degradation, and the regulation of factors controlling these processes, is critical in regulating tissue repair. Although the ECM components can be degraded by several proteolytic enzymes including neutrophil elastase (Belaaouaj et al., 2000), cathepsin G (Korkmaz et al., 2008), kinins (Cohen et al., 2007) and plasmin (Silverstein et al., 1984), the degradation of collagen and other ECM proteins is mainly mediated by a family of MMPs, which are dependent on zinc ions for their activity (Visse and Nagase, 2003). The MMP family currently has 23 identified members, which share a common 180-residue zinc-protease domain. Various cell types have been shown to secrete MMPs, including macrophages, epithelial and mesothelial cells, and fibroblasts. Their secretion is induced by stimuli including growth factors (PDGF, FGF), cytokines (IL-1, TNF-α), phagocytosis, and physical stress (Werb et al., 1980; Circolo et al., 1991; Goetzl et al., 1996); and is inhibited by TGF-β (Sporn and Roberts, 1992) and steroids (Green and Friedland, 2007). The whole family can be divided into 6 main groups based on their respective substrates: collagenases, gelatinases, stromelysins, matrilysins, membrane-type MMPs, and other MMPs (further detail listed in Table 1.6). Collagenases (including MMP-1,-8,-13) can cleave collagen at a specific site three-quarters of the way from the N-terminus, cutting the triple helix into two unequal fragments to be further digested by other proteinases (Aimes and Quigley, 1995). In contrast, gelatinases (MMP-2,-9) account for the digestion of gelatins, although MMP-2 but not MMP-9 is also shown to digest type I, II, and III collagens (Allan et al., 1995). Stromelysins (MMP-3,-10) have

similar substrates, but the proteolytic efficiency of MMP-3 is higher than that of MMP-10. In addition, MMP-3 also activates a number of proMMPs to generate fully active MMPs (Suzuki et al., 1990). For example, it helps process proMMP-1 to generate the mature MMP-1 enzyme by activating procollagenase. Other important MMPs, such as MMP-7, can process cell surface molecules including pro-TNF-α (Uria and Lopez-Otin, 2000); while MMP-14 is a type I membrane-type MMP playing important role in angiogenesis and cell invasion (Pepper, 2001; Hotary et al., 2002).

Table 1.6. Groups of human MMPs and their respective substrates. Table adapted from (Visse and Nagase, 2003).

MMP (Enzyme)	ECM substrates	Reference
Collagenases		
MMP-1 (Insterstital collagenase; Collagenases-1)	Collagens (type I, II, III, VII, VIII, X, and XI), gelatin, fibronectin, vitronectin, laminin, entactin, tenascin, aggrecan, link protein, myelin basic protein, versican	(Visse and Nagase, 2003; Pilcher et al., 1997)
MMP-8 (Neutrophil collagenase; Collagenases-2)	Collagens (type I, II, and III), aggrecan, fibrinogen	(Visse and Nagase, 2003; Hiller et al., 2000)
MMP-13 (Collagenase-3)	Collagens (type I, II, III, IV, VI, IX, X, and XIV), collagen telopeptides, gelatin, fibronectin, osteonectin, aggrecan, perlecan , large tenascin-C, fibrinogen	(Hiller et al., 2000; Knauper et al., 1997)
Gelatinases		
MMP-2 (Gelatinase A)	Collagens (type I, II, III, IV, V, VII, X, and XI), gelatin, elastin, fibronectin, vitronectin, laminin, entactin, tenascin, osteonectin, aggrecan, link protein, galectin-3, versican, decorin, myelin basic protein	(Patterson et al., 2001; Ochieng et al., 1994; Allan et al., 1995)
MMP-9 (Gelatinase B)	Collagens (type IV, V, XI, and XIV), gelatin, elastin, vitronectin, laminin, osteonectin, aggrecan, link protein, galectin-3, versican, decorin, myelin basic protein	(Ochieng et al., 1994; Allan et al., 1995)
Stromelysins		
MMP-3 (Stromelysin 1)	Collagens (type III, IV, V, VII, IX, X, and XI), collagen telopeptides, gelatin, elastin, Fibronectin, vitronectin, laminin, entactin, tenascin, osteonectin,	(Perides et al., 1995; Bini et al., 1996)

	aggrecan, link protein, decorin, myelin basic protein, perlecan, versican15, fibulin, fibrinogen	
MMP-10 (Stromelysin 2)	Collagens (type III, IV, and V), gelatin, elastin, fibronectin, aggrecan, link protein	(Visse and Nagase, 2003)
MMP-11 (Stromelysin 3)	gelatin, fibronectin, collagen type IV,laminin	(Murphy et al., 1993)
Matrilysins		
MMP-7 (Matrilysin 1, Pump-1)	Collagens (type I, and IV), gelatin, elastin, fibronectin, vitronectin, laminin, entactin, tenascin, osteonectin, aggrecan, link protein, decorin, myelin basic protein, fibulin, versican,	(Visse and Nagase, 2003)
MMP-26 (Matrilysin 2)	Collagen type IV, gelatin, fibronectin, vitronectin	(Marchenko et al., 2001; Uria and Lopez-Otin, 2000)
Membrane-type MMPs		
A) Trans-membrane		
MMP-14 (MT1-MMP)	Collagens (type I, II, and III), gelatin, fibronectin, tenascin, vitronectin, laminin, entactin, aggrecan, perlecan, fibrinogen	(Hiller et al., 2000; Ohuchi et al., 1997)
MMP-15 (MT2-MMP)	fibronectin, tenascin, entactin, laminin, aggrecan, perlecan,	(d'Ortho et al., 1997)
MMP-16 (MT3-MMP)	Collagen type III, gelatin, fibronectin, vitronectin, laminin	(Shimada et al., 1999)
MMP-24 (MT5-MMP)	Fibronectin, Gelatin, chondroitin sulphate proteoglycan, dermatan sulphate proteoglycan	(Wang et al., 1999a)
B) Glycosylphosphatidylinositol (GPI)- anchored		
MMP-17 (MT4-MMP)	Gelatin	(Wang et al., 1999b)
MMP-25 (MT6-MMP)	Collagen type IV, gelatin, fibronectin, chondroitin sulphate proteoglycan, dermatan sulphate proteoglycan	(English et al., 2001; Kang et al., 2001)
Others		
MMP-12 (Macrophage elastase)	Collagens (type I, V, and IV), gelatin, elastin, fibronectin, vitronectin, laminin, entactin, osteonectin, aggrecan, myelin basic protein	(Shapiro et al., 1993; Shipley et al., 1996)
MMP-19	Collagen type IV, gelatin, laminin, entactin, large tenascin-C, fibronectin, aggrecan, COMP,fibrinogen, fibrin	(Stracke et al., 2000b; Stracke et al., 2000a)

The main regulation of MMP activities involves another enzyme family, namely the tissue inhibitors of metalloproteinases (TIMPs). TIMPs are specific endogenous inhibitors that bind MMPs in a 1:1 stoichiometric fashion. The family comprises four protease inhibitors: TIMP-1, TIMP-2, TIMP-3, and TIMP-4 (Brew et al., 2000). They have N- and C-terminal domains of 125 and 65 amino acids respectively, with each containing three conserved disulphide bonds. The N-terminal domain serves as a separate domain and is capable itself of inhibiting MMPs (Murphy et al., 1991). So far, TIMPs are shown to inhibit all MMPs, except that TIMP-1 fails to inhibit MT1-MMPS (MMP-14) (Will et al., 1996). Although some other proteins have been reported as MMP inhibitors, including tissue factor pathway inhibitor-2 (Herman et al., 2001) and chlorotoxin (Deshane et al., 2003), the mechanisms underlying their MMP inhibition are not known.

In summary, the ECM is a complex structure consisting of several components. It is well recognized that the ECM is not only a scaffold for cells, but that it can also have biologic activity to regulate cell function and structure. The degradation of the ECM, regulated by MMPs and TIMPs, is critical during tissue repair and tissue fibrosis. However, the importance of ECM synthesis should be also emphasized, because it is the actual balance between ECM synthesis and ECM degradation that leads to tissue repair or tissue fibrosis. Hereby, in this thesis, we focus our studies of ECM synthesis principally on collagen which is the most important ECM component involved in tissue repair. The role of lysyl oxidase, a specific enzyme accounting for collagen cross-linking, will be the subject of further investigation in this thesis.

1.5.5 The role of lysyl oxidase (LOX)

LOX is a secreted, copper-dependent amine oxidase first demonstrated in 1968 (Pinnell and Martin, 1968). To date, a further four different LOX-like (LOXL)

proteins have been described including LOXL1, LOXL2, LOXL3, and LOXL4 (Csiszar, 2001). These proteins contain a consensus N-terminal signal peptide domain followed by a variable sequence region, and share a similar catalytic C-domain region to that of LOX. LOX is first translated as an N-glycosylated, 50-kDa pro-protein (proLOX), which has two consensus sites for posttranslational N-glycosylation (Trackman et al., 1992). The proLOX is then secreted into the extracellular space in a catalytically quiescent form. The proLOX is activated after proteolytic cleavage between Gly 162 and Asp 163 (rat LOX sequence) by extracellular proteases, mainly procollagen C-proteinase, to form a 30-kDa mature LOX protein (Panchenko et al., 1996). The same procollagen N- and C-proteinase is needed to process the procollagen species into the mature collagens, by removing the N- and C-terminal propeptide domains on each of their three α chain polypeptides (Siegel, 1974). Combined with the findings that purified LOX can only act on mature collagen substrates rather than procollagen precursors, it is noteworthy that the formation of crosslinked collagen is based on a highly integrated mechanism. Additionally, it has been shown that the proteolytic process is reduced in the absent of cellular fibronectin (Fogelgren et al., 2005). Furthermore, several proteolytic activators of proLOX have been found, including tolloid proteinases, mTLD, mTLL-1, AND mTLL-2, in the absence of other proteins. Thus, the proteolytic activation of proLOX is also mediated by these simple factors (Uzel et al., 2001).

The LOX-catalyzed reaction belongs to the oxidation-reduction category. It requires two essential cofactors for its catalytic function: one being a tightly bound copper ion and the other a unique, covalently integrated organic cofactor identified as lysine tyrosylquinone (LTQ) (Wang et al., 1996). LTQ is formed between specific tyrosine and specific lysine residues (Figure 1.14). It plays a critical cofactor role as a transient electron sink in the catalytic mechanism of LOX action.

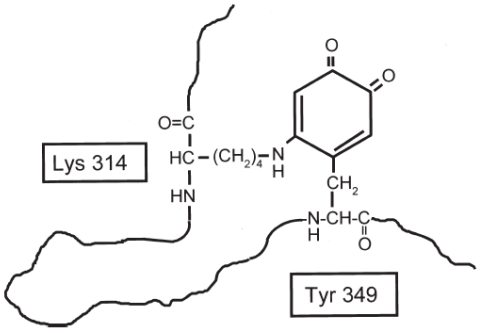

Figure 1.14. The lysyl tyrosine quinone (LTQ) cofactor of LOX. Figure adapted from (Lucero and Kagan, 2006)

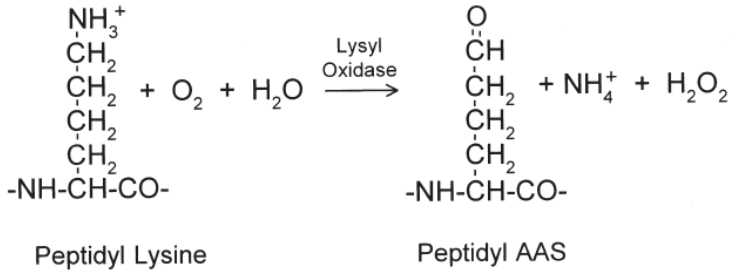

Figure 1.15. Stoichiometry of the LOX-catalyzed reaction. Figure adapted from (Lucero and Kagan, 2006)

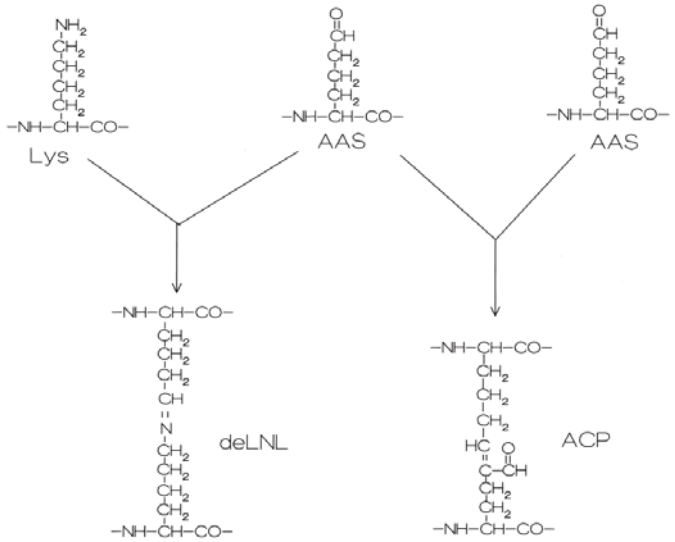

Figure 1.16. Spontaneous formation of the dehydrolysinonorleucine (deLNL) and aldol condensation product (ACP) crosslinkages from peptidyl AAS and lysine residues. Figure adapted from (Lucero and Kagan, 2006)

The main function of LOX is to convert the δ-amino group of peptidyl lysine to the aldehyde residue (Lucero and Kagan, 2006) (Figure 1.15). The generation of the

aldehyde dramatically changes the microenviroment at the site of oxidation, introducing a potentially electrophilic carbonyl in place of the original unreactive methylene carbon of the lysine residue. Thus, the aldehyde can bind to a neighbouring δ-amino group of an unmodified lysine to form the dehydrolysinonorleucine (deLNL). Similarly, two aldehydes of different lysine residues can react to form the aldol condensation product (ACP) (Lucero and Kagan, 2006) (Figure1.16). Both the deLNL and ACP can lead to the crosslinking of collagens and elastins, converting these soluble ECM proteins into insoluble fibres. The substrates of LOX are thought to be limited to the soluble precursors and immature fibrillar forms of elastins and collagens. However, it has been shown that purified LOX can readily oxidize many other basic globular proteins with PI ≥ 8.0 including H1 histone, as well as some non-peptidyl amine substrates including n-butylamine and 1,5-diaminopentane (Kagan et al., 1984). Thus, the catalytic ability of LOX is mainly but not exclusively on collagens and elastin. Mature LOX is found in the extracellular compartments of many tissues including skin, aorta, heart, lung, liver, and cartilage (Trackman et al., 1990; Kagan et al., 1986; Hayashi et al., 2004). Furthermore, the presence of the mature active LOX has been demonstrated within the nuclei of vascular smooth muscle cells (VSMCs) and fibroblasts by confocal immunomicroscopy and by western immunoblot analyses of nuclear extracts (Nellaiappan et al., 2000). The mechanism might well involve specific cellular uptake, since nuclear entry was not inhibited by beta-aminoproprionitrile (BAPN, a chemical inhibitor for LOX) nor competed against by adding 29-kDa carbonic anhydrase. It has been shown that LOX can oxidize histone H1 which has abundant lysine residues (Kagan et al., 1983), as well as histone H2 (Giampuzzi et al., 2003). Since histone H1 plays an important role in electrostatically interacting both with the DNA bridge linking consecutive nucleosomes and with DNA wound around the nucleosome core (Fan et al., 2005; Hizume et al., 2005), oxidation by LOX of histone could disrupt these electrostatic bonds. Therefore, the presence of LOX in the

nucleus might play a role in changing cellular phenotypes by re-organizing the nuclear chromatin.

In addition to its catalytic role in ECM formation, other important functions of LOX have recently been identified. It has been shown that LOX can act as a potent chemoattractant for many cell types. For example, purified 32-kDa LOX was found to increase the migration ability of human peripheral blood mononuclear cells over the control group by 240% (Lazarus et al., 1995). Another study revealed that VSMCs were also chemotactically responsive to a LOX-dependent chemotaxis (Li et al., 2000). Further investigation discovered that the chemotactic response was not due to the reaction of LOX with secreted proteins but to the H_2O_2 product of the LOX-catalyzed reaction. It has been shown that intracellular H_2O_2 can enhance stress fibre formation and focal adhesion assembly, thereby causing the induction of the chemotactic response; since the response was not found if the LOX enzyme was inactivated or catalase was added into the culture system (Li et al., 2000). These studies have been extended to others involving tumour metastasis, since LOX mRNA was found to be upregulated in invasive breast cancer cells (Kirschmann et al., 2002). Reports from the same group found that a LOX-dependent chemotactic response can facilitate the invasion of the breast cancer cells, which is also elicited by the H_2O_2 product of LOX acting on unidentified substrates (Payne et al., 2005). Similar studies have found that an elevated level of LOX under hypoxic conditions is essential for the hypoxia-induced metastatic response of several cancers including head and neck tumours (Erler et al., 2006). A further report noted that hypoxia-induced LOX is critical for pre-metastatic niche formation (Erler et al., 2009). More importantly, Studies (Higgins et al., 2007) found that LOX was involved in hypoxia-promoted fibrogenesis associated with chronic renal disease. The inhibition of LOX and LOXL2 was shown to reduce the hypoxia-induced cell migration *in vitro* and decrease renal fibrogenesis *in vivo*. Similarly, the inhibition of LOX by BANP

appeared to minimize liver fibrosis following bile duct ligation in an experimental animal model (Andrew et al., 2007). These observations point towards a general role that LOX might have in tissue fibrotic diseases, by promoting cell motility and ECM deposition.

1.6 Project background

Post-operative adhesion in the abdominal cavity is a common complication after abdominal surgery. Despite huge progress in surgical techniques in recent decades, the incidence rate of post-operative adhesion has improved very little. Currently, the common strategies used to prevent adhesion are the application of anti-inflammatory agents such as colloids (dextran) and crystalloid solutions (Ringer lactate or saline), or physical barrier including carboxymethyl cellulose and polyethyleneoxide. Although there have been developments in adhesion prevention, none have been demonstrated to produce significant benefit. Since peritoneal fibrosis and its associated ECM remodelling process are critical in the development of post-operative adhesion, further investigation of the pathophysiology of peritoneal fibrosis is undoubtedly required to improve patient outcome.

Homeostasis of the abdominal cavity is maintained by the mesothelium. Many studies have shown a critical role of mesothelium in the development of adhesion following by surgery. Most of these studies are focused on its role in fibrinolysis and re-epithelialization. This thesis examines the role of mesothelium in ECM remodeling, and especially in collagen deposition. A hypothesis is proposed that mesothelial cells can produce lysyl oxidase (LOX), a key mediator in promotion of collagen deposition during the healing process. Thus, inhibition of LOX activity of mesothelial cells could pave the way to minimize post-operative adhesion. The inflammatory response is also involved as a key process in wound healing. A further

hypothesis is that the function of mesothelial cells is regulated by the inflammatory response; particularly inflammatory cytokines. Thus, experiments will be designed to investigate the effect of these inflammatory cytokines on the mesothelial cells. Cell phenotype change, LOX expression, as well as other ECM-adhesion related genes will be used as potential investigable targets.

In addition, ovarian repair presents a scar-free healing model existing alreadt in the adult body. In humans, the ovary is regularly subjected to ovulation-associated injury that heals without fibrosis. The human ovary is covered by a thin layer of ovarian surface epithelial (OSE) cells, which arises in the embryo from the same lateral plate mesoderm as the peritoneal mesothelial cells (PMC). They share many common characteristics and equivalent homeostatic functions (Ross et al., 1998). During ovulation, a local induction of high levels of ovarian steroids occurs (Andersen, 1991; Andersen and Hornnes, 1994; Rae et al., 2004a). Steroids involved in anti-inflammatory processes, such as progesterone and cortisol, are synthesised and secreted into the follicular fluid and peritoneal fluid during ovulation. Therefore, the unique scar-free healing of ovary is hypothesised to be a consequence of the production of the elevated local anti-inflammatory steroids. We propose that the application of anti-inflammatory steroids, such as cortisol or progesterone, might help to minimize the occurrence of post-operative adhesion.

This thesis aims to answer the overarching hypothesis:

'Regulation of extracellular matrix remodeling helps prevent peritoneal fibrosis' by addressing the following sub-questions:

1. What is the role of LOX in peritoneal fibrosis?
2. What is the role of mesothelial cells in peritoneal fibrosis in response to inflammatory cytokines?
3. What is the anti-inflammatory effect of cortisol in the regulation of peritoneal fibrosis?

Chapter 2

Materials and Methods

2.1 Primary cell culture

2.1.1 Primary Peritoneal Mesothelial Cells (PMC) and Ovarian Surface Epithelial (OSE) cell culture

Normal PMC and OSE cells were collected from patients undergoing surgery for benign gynaecological conditions; such as fibroids, heavy menstruation and pelvic pain; with local ethics committee approval (under Local Regulatory Ethics Committee approval LREC 04-51103-36) and informed consent. Exclusion criteria included current malignancy, gynaecological inflammatory states (such as current pelvic inflammatory disease or endometriosis) and use of gonadotrophin-releasing hormone agonists or antagonists. Following recruitment, PMC and OSE were collected by gently brushing the respective organs (Table 2.1) early in the surgical procedure using a Tao cytobrush (Cook Medical, Limerick, Ireland) at laparoscopy. The early stage collection reduced contamination with blood and stromal cells. In addition, handling of the ovaries was minimized by the surgeon to prevent loss of the OSE layer during surgery. The collecting instrument was rinsed in 15ml pre-warmed HOSE1 (Table 2.2) medium to dislodge the cells that were then transported to the laboratory at room temperature.

Table 2.1. Sites for PMC and OSE sample collection

Cell type	Sample description	Collective Sites
PMC	PA	Peritoneal abdominal wall
	PB	Peritoneal side of body of uterus
OSE	HR	Right ovarian cortex
	HL	Left ovarian cortex

Table 2.2. Components of HOSE1 Medium. *: MCDB 105 (Sigma-Aldrich Inc, Poole, UK) was established at pH 7.3 by titrating with 5 M sodium hydroxide. Medium199 (GIBCO, Invitrogen Ltd, Paisley, UK), Pen/Strep (Sigma), L-glutamine (GIBCO).

Additive	Quantity	Supplier
Medium 199:MCDB 105*	1:1 (v/v)	Gibco
Fetal Bovine Serum (FBS)	15% (v/v)	Sigma-Aldrich
L-glutamine	2mmol/l	Sigma-Aldrich
Penicillin	50IU/ml	Sigma-Aldrich
Streptomycin	50μg/ml	Sigma-Aldrich

The primary cells were cultured in HOSEI medium as previously described (Hillier et al., 1998). Briefly, the medium was aspirated and transferred to a $75cm^2$ tissue culture flasks (Corning, Sigma). Flasks were inspected using phase-contrast microscopy to confirm presence of cell "flakes", and then incubated for up to two months in a humidified atmosphere of 5% CO_2, 95% air at 37°C. The flasks were inspected a week later and HOSE1 medium was changed weekly until confluency reached. Normally, cells reached confluency after 4 to 6 weeks of culture. Cell purity was confirmed by phase-contrast microscopy. Confirmation of the purity of mesothelial cultures were checked by staining with several mesothelial markers including cytokeratins 5, 6, 7, 8 and 17 (Fegan et al., 2008). After reaching confluency, the culture medium was removed and cells were washed twice with Dulbecco's phosphate-buffered saline (DPBS, Sigma) and enzymatically isolated by incubating in 5ml 0.05% trypsin/EDTA solution (GIBCO) at 37^oC for 5min. Then the same amount of HOSE1 medium was added to neutralize the trypsin solution. The whole cell solution was transferred into a 15ml centrifuge tube (Corning). After centrifugation at 800 g for 5min, cells were pelleted and the supernatant was discarded. Cells were re-suspended in HOSE1 medium and the cell number was counted using a haemocytometer. Cell viability was assessed with trypan blue (Sigma) staining exclusion. Cell suspensions were then taken forward for experimentation or a further passage. The passage number for primary cells was limited to no more than 3. The outcome of primary cell culture is that 60% of the

total PMC cultures were discarded due to lack of cell growth or fibroblast contamination (Fegan, 2009). Therefore, the experimental repeats conducted in this thesis are limited by the number of viable samples.

2.1.2 Separation of peripheral blood mononuclear cells (PBMC) from Buffy Coat (BC) and PBMC culture

The protocol used in this thesis was adopted from a previous publication (Repnik et al., 2003). Combined Ficoll-Percoll density gradients were used for the separation. The buffy coat samples were generously provided by the Scottish National Blood Transfusion Service. The samples were normally generated from 240ml whole blood taken from healthy people within the previous 24 h. All the materials used throughout the procedure were sterile and endotoxin-free. The detailed procedures included:

(1). PBMC Isolation

The concentrated BC (around 60ml) was diluted with calcium- and magnesium-free PBS (Sigma) up to 200ml (normally twice volume of PBS added to the BC). 12ml Ficoll (GE Healthcare Bio-Sciences AB UK Ltd, Buckinghamshire, UK) into 50ml Falcon centrifuge tubes (BD Biosciences, Oxford, UK). The number of tubes depended on the final volume of the diluted BC. The diluted BC solution was carefully transferred into the tube (25ml per tube), overlaying the Ficoll on the top. The gradients were then centrifuged at 950 g for 15 min with the brake off (Sigma 6K15 centrifuge). The PBMC were collected at the interface between the Ficoll and the plasma-medium layers with a pasteur pipette. Cells were transferred from two tubes into one new tube and resuspended with addition of PBS to a final volume of 45 ml. Then this tube was centrifuged at 350 g for 7 min. The supernatant was discarded carefully and cells were resuspended in PBS. Cells from two tubes were

combined into another new tube with adding PBS to a final volume of 45 ml. Tubes were centrifuged again at 350 g for 7 min. Supernatant was again discarded and the cells from two tubes combined by adding pre-warmed Iscove's Modified Dulbecco's medium (IMDM, GIBCO) to a final volume of 25ml. Cells were counted in a standard haemocytometer and resuspended at a concentration of 40–60 $x10^6$ cells/ml in IMDM medium to give a final volume which is a multiple of 3 (i.e. 3/6/9/12/. . . ml).

(2). Separation of monocytes from lymphocytes

PBMC suspension (3ml, containing 120–180 x 10^6 cells) was carefully laid onto 10 ml of hyper-osmotic Percoll (GE Healthcare) solution (48% Percoll, 41.5% deionized water, 10% 1.6M NaCl) in each centrifuge tube so that the interface between the layers was preserved. The tubes were centrifuged at 580 g for 15 min (brake off). Cells at the interface were collected with a Pasteur pipette, excluding the last 4 ml. Cells from up to three tubes were combined with adding IMDM medium to a final volume of 45ml. Tubes were centrifuged at 350 g for 7 min. Supernatant was discarded and resuspended the cells in 3ml IMDM medium. This suspension is later referred to as a monocyte-enriched suspension.

(3). Separation of monocytes from platelets and dead cells

In each centrifuge tube, 10ml iso-osmotic Percoll solution (41.5%Percoll, 48.5% deionized water, 10% 1.5M NaCl) was overlaid with 3ml of the monocyte-enriched suspension (up to 200 $X10^6$ cells). Tubes were centrifuged at 350 g for 15 min (brake off). The supernatant was discarded using a Pasteur pipette, or alternatively, saved for analysis of its composition. The sediment was resuspended in <1ml of IMDM medium (avoiding tube wall 'wash-off') and transferred into a new centrifuge tube. IMDM medium was added to a final volume of 45ml. Tubes were centrifuged at 350g for 7 min. After the supernatant was discarded, cells were resuspended in 5ml

of culture medium. A cell count was conducted, mixing 20µl of the cell suspension with 180µl trypan blue solution.

(4). Culture of monocytes

Separated PBMC were resuspended at a concentration of $1x10^6$ cells/ml and seeded into 12 well-plates ($1x10^6$cells/well) with pre-warmed IMDM medium. Plates were incubated for 1 hour at 37°C to allow monocytes to adhere to the plate. Swirling the plates gently the supernatant was removed into waste. Fresh IMDM medium (1 ml) was added to each well to remove any unattached cells. The adherent PBMC were cultured in IMDM medium including 10% FBS and 20ng/ml Macrophage colony-stimulating factor (M-CSF) (R&D Systems Inc, Abingdon, UK) for 6-7 days, allowing the PBMC to mature into macrophages. Medium was changed at day 3 and replenished appropriately.

2.1.3 Culture of mesothelial cell line

The mesothelial cell line MeT-5A (ATCC-CRL-9444) was purchased from American Type Culture Collection (ATCC). It is derived from mesothelial cells isolated from pleural fluids obtained from non-cancerous individuals. The cells were transfected with the pRSV-T plasmid (an SV40 ori-construct containing the SV40 early region and the Rous sarcoma virus long terminal repeat) and cloned. Cells originating from ATCC were cultured in the recommended complete medium of Medium 199 containing 10% FBS, 3.3nM epidermal growth factor (EGF) (R&D), 400nM hydrocortisone (Sigma), 20mM HEPES (Sigma), 1% 100X Insulin-Transferrin-Selenium A (GIBCO), and 0.1% trace elements B (Media Tech

Inc, Manassas, USA). Cells were passaged and cultured in adapted medium with IMDM medium plus 10% FBS and 2mmol/l L-glutamine.

2.2 Experimental treatment on cells

2.2.1 Treatment on PMC and MeT-5A cells

For cytokines treatment, primary cells suspensions were adjusted to $3x10^5$ viable cells per well of 6-well culture plates (Corning) for mRNA studies or $1.5\ x10^5$ viable cells per well of a 12-well plate (Corning) for ELISA. After establishment of a cell monolayer (24 h), the culture medium was replaced with HOSE2 medium, serum-free HOSE1 containing 0.01% bovine albumin serum (BSA, Sigma) instead of FBS, for 24 h. Cells were then exposed to the treatments of interest (cytokines, cytokine antagonists, steroids, etc) in HOSE2 medium. Incubation times and concentrations applied are denoted in the relevant Chapters. In all experimental sets, untreated cells were used as the control.

For treatments with multi-wall carbon nanotubes (NT, provided by Matthew Boyles, University of Cambridge) PMC cell suspensions were adjusted to $1.5\ x10^5$ viable cells per well of 12-well plates. Prior to experimental treatment, NT were dispersed by suspending in 0.5% BSA and placed in an ultra-sonic water bath as previously described (Poland et al., 2008). NT solutions were further diluted in HOSE1 medium to achieve the required concentration. PMC were treated with different doses of NT solutions for 48h after the establishment of the cell monolayer.

2.2.2 Treatment on MeT-5A cells

MeT-5A cells suspensions were adjusted to $5x10^5$ viable cells per well of 6-well culture plates for mRNA studies. After establishment of a cell monolayer (24 h), the culture medium was replaced with serum-free IMDM medium containing 0.01% BSA for 24 h. Cells were then exposed to the agents of interest. Incubation times and treatment conditions applied are denoted in the relevant Chapters. In all experimental sets, untreated cells were used as the control.

2.2.3 Treatment on macrophages

Separated PBMC were plated at $1x10^6$ per well of 12-well culture plates as described above (Chapter 2.1.2). After 7 days, the culture medium were replaced with fresh IMDM medium containing 10% FBS for 24 h. NT were diluted to appropriate concentrations as shown above (section 2.2.1). Macrophages were exposed to the NT solution for 48 h.

2.2.4 Sample harvest

For mRNA studies, the cell monolayers of 6-well plates were washed twice with 1ml DPBS after experimental treatments. Homogenization of cells was achieved by cell lysis using 0.35ml guanidine thiocyanate-containing buffer (RLT lysis buffer, Qiagen, UK) supplemented with 0.01% β-mercaptoethanol (Sigma). The resultant cell lysate was transferred to autoclaved eppendorf tubes (Eppendorf UK Limited, Cambridge, UK) and stored at -80°C for further experiments.

For ELISA, PMC culture-conditioned medium from each well were collected in eppendorf tubes and stored at -20°C, while cells were lysed by repeated freezing and

thawing in 1ml serum-free medium. The cell lysates were kept in -20°C for further use. For macrophages, only culture-conditioned media were collected and stored at -20°C until analysis.

2.3 mRNA studies

2.3.1 RNA extraction

RNA was extracted from cultured cells using the RNEasy Mini-kit (Qiagen). This kit allows the purification of RNA longer than 200nt and is based on the selective binding properties of a silica-gel membrane. Cell lysates were removed from storage and thawed in a waterbath at 37°C. 70% ethanol (350µl) was added to the lysate and mixed by pipetting. The sample was applied to a RNEasy mini column, placed inside a centrifuge tube then centrifuged at 10,000rpm for 15 seconds (MIKRO 200, Hettick Zentritugen, DJB Labcare Ltd, Buckinghamshire, UK). The flow-through was discarded. 350µl RW1 buffer (Qiagen) was added to the column followed by centrifuging the tube for 15 seconds at 10000rpm. After the flow-through was discarded, on-column DNase digestion was performed. 10µl DNase I stock solution (Qiagen) was added to 70µl DNase buffer (Qiagen) per sample and mixed by gently flicking the tube. The DNase mix was pipetted directly onto the membrane of the RNEasy column and left at room temperature for 15 minutes. A further 350µl RW1 wash buffer was added and the tube was centrifuged for 15 seconds at 10000 rpm. The flow-through was discarded. 500µl RPE elution buffer (Qiagen) was added to the column, centrifuged for 15 seconds at 10000 rpm and flow-through discarded. A further 500µl RPE elution buffer was added to the column, centrifuged for 2 minutes

at 10000 rpm, and the flow-through discarded. The column was transferred to a new tube and centrifuged for 1 min at full speed to dry the column. The column was once again transferred to a new tube and 20-30µl RNase-free water pipetted directly on to the membrane. The tube was centrifuged for 1 min at 10000 rpm. The eluate was removed from the tube and passed through the column once more as described to obtain a higher RNA concentration. RNA was stored at -80°C.

2.3.2 RNA quantification and quality assay

Purified RNA was quantified using a Nanodrop spectrophotometer (ND-1000, Thermo Scientific, Essex, UK). RNA (1.5µl) was loaded onto an optical fibre to measure the ultraviolet (UV) absorbance from the light passing through the sample. The RNA concentration was measured at 260 nm. To ascertain the purity of RNA, two absorbance ratios were also assessed: the 260/280 and 260/230 ratios to evaluate protein and genomic contamination respectively. Purified RNA samples were used further only when ratios of 260/280 were above 2.0, which indicated minimal protein contamination.

2.3.3 Reverse-Transcriptase PCR

RNA was reverse-transcribed by using the high capacity cDNA Reverse Transcriptase kit (Applied Biosystems, Warrington, UK). RNA was reverse transcribed to cDNA in a 10µl reaction mixture consisted of: 1µl 10X RT buffer, 1µl 10X RT Random Primer, 0.5µl (1U/µl) RNase Inhibitors, 0.4µl (4 mM) 25X dNTP mix, 0.5µl (2.5U/µl) MultiScribeTM Reverse Transcriptase, 200ng RNA sample, and adding RNase-free H_2O up to 10µl. Reaction mixes were thoroughly vortexed and briefly centrifuged in a microcentrifuge to ensure all contents were in the bottom of the tube. Tubes were then put in a thermal cycler (G-Storm, Surrey, UK) and samples

incubated at 25°C for 10 min, 37°C for 120 min, then 85°C for 5 min. Two negative controls were also included, an “RT-negative” containing no multiscribe RTase and a “RT-water” containing nuclease-free water in place of RNA. The resulting cDNA was stored at -20°C.

2.3.4 Quantitative Real-Time PCR (Taqman)

Quantitative Real-Time PCR (QRT-PCR) measures the level of a gene-specific sequence of cDNA generated in a reverse-transcriptase PCR reaction, and thus provides a measure of RNA expression in a tissue. It was carried out using the Taqman system and ABI Prism 7900HT sequence detection system (Applied Biosystems). The underlying mechanism is based on the production of a fluorescent signal during the amplification of the PCR product. Forward and reverse primers are designed for the target DNA sequence and the probe is annealing to this target sequence between the primers. Two labels are contained in the probe, a reporter label at the 5’ end (FAM; 6-carboxyfluoroscein) and a quencher at the 3’ end (TAMRA; 6-carboxytetramethylrhodamine). A higher melting point is designed for the probe compared to the primers. When intact, the quencher suppresses the fluorescence of the reporter. The probe anneals to the cDNA during the polymerisation step while amplification occurs. The probe is cleaved during the amplification step by AmpliTaq Gold (contained within Taqman Universal PCR Master Mix, Applied Biosystems) and the reporter and quencher are separated. Fluorescence can now be detected. The amount of fluorescence is directly proportional to the amount of PCR product, as non-specific amplification does not cause fluorescence. The whole process is represented diagrammatically in Figure 2.1. 18S ribosomal RNA detection is used as an internal control in this system. The 18S probe also has a reporter (VIC)

which emits fluorescence at a different wavelength to the FAM reporter on the gene of interest probe. Quantification is relative to 18S as its levels remain relatively constant in cells. Data are acquired when PCR amplification is in the exponential phase. The data are in the form of the cycle number where the fluorescence of the reporter dye rises above a threshold, this value is the threshold cycle, C_T.

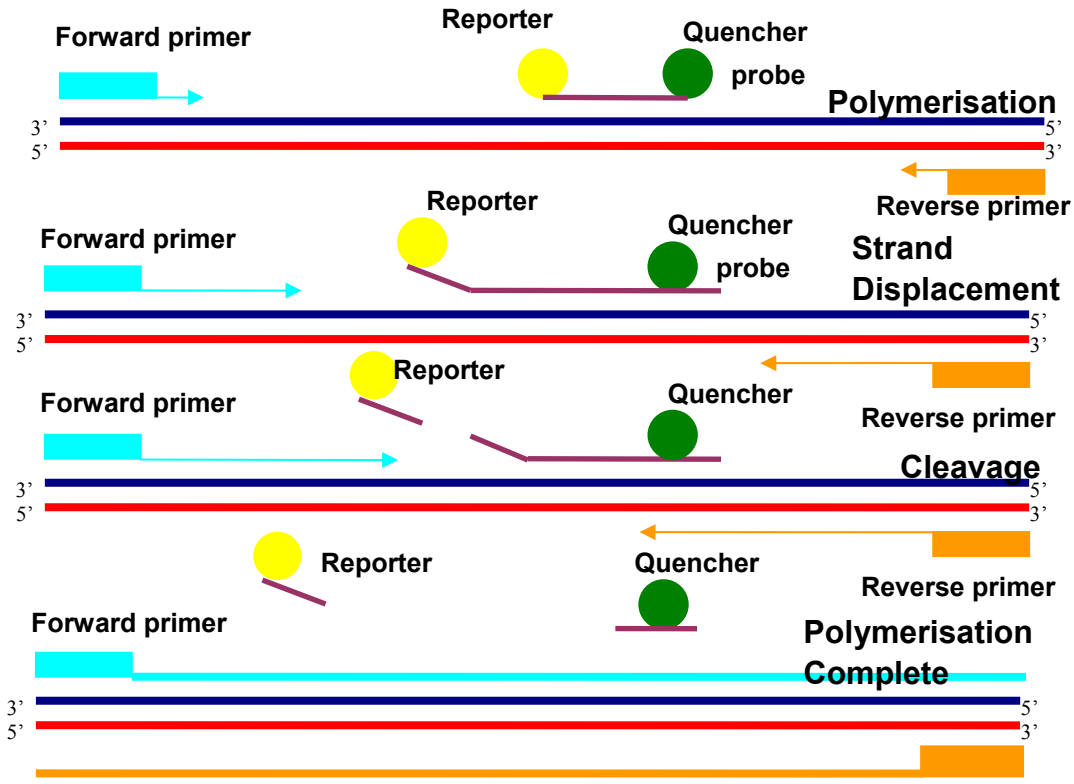

Figure 2.1. Diagrammatic representation of Taqman QRT-PCR. Adapted from Taqman PCR Reagent Kit Protocol (Applied Biosystems).

2.3.4.1 QRT-PCR procedure

Taqman primers and probes were either designed in-house using ProberFinder software (Universal Probe Library), or purchased from Assay on Demand (Applied Biosystems). Details of primers and probes used are given in the Table 2.3. Primers designed in-house were manufactured by Genosys Biotechnologies (Cambridge, UK)

and diluted to 100μM in nuclease-free water (Sigma). The designed primers had previously been validated in the lab before use. Assay on Demand primer/probe sets were used directly as they are provided pre-optimized at a final concentration of 900nM primer and 250μM probe. Pro-collagen-I primers were gifted by Dr. Moira Nicol (University of Edinburgh). Integrin alpha 5 and TGF-β1 primers were gifted by Dr. Sarah McDonald (University of Edinburgh).

Table 2.3. Gene list for QRT-PCR primers and probes.

Gene	Primers	Probe
Lysyl oxidase	Assay on Demand	Assay on Demand
MMP 9	Assay on Demand	Assay on Demand
ACTB	Assay on Demand	Assay on Demand
Fibronectin	Left: 5' ctggccgaaaatacattgtaaa 3'	probe #32 (Universal Probe Library , cat. no. 04687680001)
	Right: 5' ccacagtcgggtcaggag 3'	
Integrin alpha 5	Left: 5' ggaagaacatgtcctccttatacaat 3'	probe #46 (Universal Probe Library , cat. no. 04687680001)
	Right: 5' gcagctacagaaaatccgaaa 3'	
E-cadherin	Left: 5'cccgggacaacgtttattac 3'	probe #35 (Universal Probe Library , cat. no. 04687680001)
	Right: 5'gctggctcaagtcaaagtcc 3'	
TGF-β1	Left: 5' CACAGGAGACATCAGGAG AAGAAA 3'	5'FAM-TTCCAAATTTTAC CTGCCAAACTGCA ACAA-TAM 3′
	Right: 5' ACACTGTCTGCTGTGA TAAAATCCAT 3'	
Pro-collagen-I	Left: 5'CAAGAGGAAGGCCAAG TCGAGG 3'	5'FAM-CCTCAGGT ACCATGACCGAGA CGTGTGGAAACC-TAM 3′
	Right: 5'CGTTGTCGCAGACGCAGAT 3'	

For Assay on Demand primer/probe sets, reaction mixtures containing TaqMan Universal PCR Master Mix (Applied Biosystems) and specific Assay on Demand were made in a final volume of 34μl per sample consisting of: 17μl 2X Universal Taqman mastermix (1X), 0.51μl ribosomal 18S primers and probe (50nM), 1.7μl

20X of the Assay-on-Demand primers and probe mixture of the target genes (1X), 2.72µl cDNA sample, and 12.07µl nuclease-free H_2O.

For in-house designed primers, reaction mixtures containing TaqMan Universal PCR Master Mix and specific forward and reverse primers and probe were also made in a final volume of 34µl per sample consisting of: 17µl 2X universal Taqman mastermix (1X), 0.51µl ribosomal 18S primers and probe (50nM), 0.07µl 100µM primer forward (200nM), 0.07µl 100µM primer reverse (200nM), 0.34µl 10µM probe (100nM), 2.72µl cDNA sample, and 13.29µl nuclease-free H_2O.

All samples were run in triplicate on a 384-well ABI Prism 7900 sequence detection system (Applied Biosystems). For each 34µl sample mixture, 10µl aliquots were pipetted into three separate wells of a 384-well plate. The RT-negative and RT-water controls were included, alongside a "no template" control (NTC, 2.72µl nuclease-free H_2O instead of cDNA) were used as negative controls in each run, while a placental cDNA sample was used as a positive control. Taqman reactions were carried out in the ABI Prism 7900 Sequence Detector following the default protocol (Table 2.4):

Table 2.4. Taqman amplification default protocol.

Cycles	Description
1 Cycle	50^{o}C for 2min for the activation of UNG [UNG prevents re-amplification of carry-over PCR products by removing any uracil incorporated into amplicons
1 Cycle	95^{o}C for 10 min (Taq Polymerase activation)
40 Cycles	-Denaturation at 95^{o}C for 15 sec -Annealing and extension at 60^{o}C for 1 min

2.3.4.2 Data analysis

Data output was in the form of a "C_T" value; the number of PCR cycles required before there is sufficient cDNA amplification to be detected. A C_T value was given for both the gene of interest and 18S. These data were transferred to a Microsoft Excel spreadsheet for analysis. The C_T values were used to calculate the abundance of the mRNA of each sample. Firstly, the difference between the C_T of the target and the internal control was calculated (dC_T). As each sample was run in triplicate, the mean dC_T was ascertained. Then, the mean dC_T of the control was subtracted from the mean dC_T of each sample (ddC_T) to relate all the samples to control, while the mean dC_T of the placenta was used instead of the control when all the samples were expressed relative to placenta. Finally, the relative copy number was determined by the formula $2^{-(ddCT)}$. The results of $2^{-(ddCT)}$ are referred to the fold change of je particular target gene group compared to the control group or placenta. An example spreadsheet is shown in Figure 2.2.

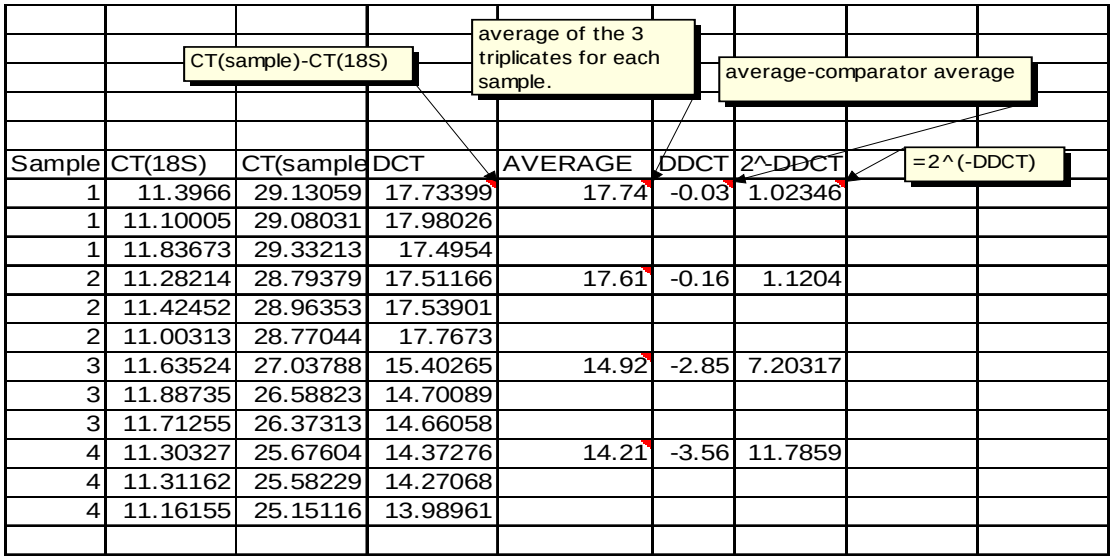

Sample	CT(18S)	CT(sample	DCT	AVERAGE	DDCT	2^-DDCT
1	11.3966	29.13059	17.73399	17.74	-0.03	1.02346
1	11.10005	29.08031	17.98026			
1	11.83673	29.33213	17.4954			
2	11.28214	28.79379	17.51166	17.61	-0.16	1.1204
2	11.42452	28.96353	17.53901			
2	11.00313	28.77044	17.7673			
3	11.63524	27.03788	15.40265	14.92	-2.85	7.20317
3	11.88735	26.58823	14.70089			
3	11.71255	26.37313	14.66058			
4	11.30327	25.67604	14.37276	14.21	-3.56	11.7859
4	11.31162	25.58229	14.27068			
4	11.16155	25.15116	13.98961			

Figure 2.2. Example Microsoft Excel Spreadsheet showing Taqman data analysis

2.3.5 RT2 ProfilerTM PCR Array

2.3.5.1 Sample preparation

For the PCR array, RNA samples were collected and quantified as detailed earlier (Chapter 2.3.1, 2.3.2). To obtain the best results from the PCR array, all RNA samples were selected by the following criteria: i) A260:A230 ratio should be greater than 1.7, ii) A260:A280 ratio should be 1.8 to 2.0, iii) concentration determination by A260 should be greater than 40µg/ml total RNA; iv) No RNA degradation (checked by ribosomal RNA band integrity). RNA 1.5 µg from each sample was used to make cDNA using a RT^2 First Strand Kit (SABiosciences, Qiagen, Crawley, Sussex, UK). RNA samples were first mixed with 2µl GE (5 x gDNA Elimination Buffer) and nuclease-free H_2O added up to 10µl. The mix was incubated at 42^oC for 5 min and chilled on ice immediately for at least 1 min. Then, 10µl RT cocktail that included 4µl BC3 (5 X RT Buffer3), 1µl P2 (Primer & External Control Mix), 2µl RE3 (RT Enzyme Mix 3), and 3µl Nuclease free water; was added to each 10µl RNA mixture. The synthetic reaction mixture was incubated at 42^oC for exactly 15 min, and the reaction was immediately stopped by heating at 95^oC for 5 min. Finally, 91µl of nuclease-free H_2O was added to each 20µl of reaction mixture. The cDNA was stored at -20^oC for later use. An optional RT^2 RNA Quality Control PCR Array (SABiosciences) was used to test the quality of the cDNA samples.

2.3.5.2 Performing Real-Time PCR

i) For RT^2 RNA Quality Control PCR Array

The content of the RT^2 RNA Quality Control PCR Array (SABiosciences) is showed in Table 2.5. Three cocktails for each sample were prepared for respective rows on the plate. 25µl of each cocktail was added to each well (Table 2.6).

Table 2.5. Content of RT^2 RNA Quality Control PCR Array

ROW	Symbol	UniGene	GeneBank	Description
A	ATCB	Hs.520640	NM_001101	Actin, beta
B	HPRT1	Hs.412707	NM_000194	Hypoxanthine phosphoribosyltransferase 1
C	RTC	N/A	N/A	Reverse Transcription Control
D	PPC	N/A	N/A	Positive PCR Control (with template)
E	GDC	N/A	N/A	Genomic DNA Contamination control
F	NRT	N/A	N/A	No Reverse Transcription Control
G	PPC	N/A	N/A	Positive PCR Control (without template)
H	NTC	N/A	N/A	No Template Control

Table 2.6. Reagent mixtures to add to RT^2 RNA Quality Control PCR Array

Cocktail NO	Rows on the 96-well plate	Reagent mixture
Cocktail 1	Rows A through E	- 75µl 2 X SuperArray PCR master mix - 6µl Diluted first strand cDNA synthesis reaction - 69µl nuclease-free water
Cocktail 2	Rows G and H	- 45µl 2 X SuperArray PCR master mix - 45µl nuclease-free water
Cocktail 3	Rows F	- 1µl of a 1:100 dilution of original input total RNA - 24µl 1 X SuperArray PCR master mix

ii) For RT^2 Profiler^{TM} PCR Array (PAHS-013A: Human Extracellular Matrix and Adhesion Molecules)

The PCR array was conducted using the RT^2 ECM-Adhesion PCR Array (Gene list will be shown in Chapter 4.6). The experimental cocktail was prepared as follows: 1350µl 2X SABiosciences RT^2 qPCR master mix, 102µl diluted first strand cDNA synthesis reaction, and 1248µl nuclease-free water. This experimental cocktail (25µl) was added to each well.

iii) For both PCR arrays, a two-step cycling program was used on the ABI Prism 7900HT sequence detection system by detecting the fluorescent signal released from SYBR-green (Table 2.7)

Table 2.7. Amplification protocol for super array.

Cycles	Description
1 Cycle	95°C for 10 min
40 Cycles	- Denaturation at 95°C for 15 sec - Annealing and extension at 60°C for 1 min
1 Cycle for disassociation	- 95°C for 15 sec - 60°C for 15 sec - 95°C for 15 sec

2.3.5.3 Data analysis

Data from each PCR array were input into the respective Excel-based RT^2 RNA QC PCR Array Data Analysis template or RT^2 Profiler PCR Array Data Analysis Template v3.3 (http://www.sabiosciences.com/pcrarraydataanalysis.php).

2.4 ELISA

IL-1α and TNF-α contents of conditioned-culture media and cell lysates from primary PMC and primary macrophages were determined using the DuoSet® ELISA Development System (R&D). Firstly, a capture antibody was diluted into respective working concentration in PBS (Sigma) without carrier protein. Diluted capture antibody (100µl) was added to each well to coat a 96-well Costar EIA plate (R&D) and left overnight at room temperature. The plate was sealed with a ELISA plate sealer (R&D). The plate was then washed three times with wash buffer (0.05% Tween® 20 in PBS, Sigma) and dried by blotting on clean paper towels. The plate was blocked by adding 300µl of reagent diluent (1% BSA in PBS, pH 7.2-7.4) to each well for a minimum of 1 h at room temperature. When the block reagent was washed off as noted above, sample (100µl) or standard were added to each well in duplicate. The plate was sealed and incubated for 2 h at room temperature. After 2 h, samples and standards were washed off as detailed above. Detection antibody (100µl)

diluted in reagent diluent was added to each well. The plate was incubated for another 2h at room temperature. Repeated washes were carried as noted above. A working dilution of streptavidin-HRP (100µl) was added to each well and incubated for 20 minutes at room temperature. The plate was placed in a dark area to avoid direct light and washed after 20 minutes incubation. Substrate solution (100µl, a 1:1 mixture of H_2O_2 and tetramethylbenzidine, R&D) was added to each well and incubated for a further 20 min at room temperature in the dark. Then, stop solution (50µl, 2N H_2SO_4, R&D) was added to each well. The optical density of each well was immediately determined using a microplate reader (Max microplate reader, Thermo) with the wavelength set at 450 nm.

For data analysis, the average of duplicate readings for each standard and sample were subtracted from the average zero standard optical density. A standard curve was generated for each set of samples assayed by using software (Softmax Pro V5) capable of generating a four-parameter logistic curve-fit. Sample concentrations were calculated using their OD value corresponding to the generated standard curve.

2.5 Immunohistochemistry

Immunohistochemistry, an experimental method to allow investigation of the presence or absence of a protein *in situ* in tissue, is based on the antigen-antibody complex that naturally occurs in living organisms. Primary antibodies, specifically raised to recognize the target protein (antigen), are reacted with the tissue *in situ*. Then, a secondary antibody, raised against the immunoglobulin of the species in which the primary antibody was produced, is added to bind the primary antibody. The secondary antibody is usually labelled with biotin that allows the recognition and amplification of the signal with avidin-biotin complex (ABC) conjugated to

horseradish peroxidise (HRP). Finally, a substrate that specifically interacts with HRP is added allowing visualisation (colourimetric reaction) of the signal.

For colourimetric inmmunohistochemistry, sections were dewaxed in xylene, following by rehydration in serial dilutions of ethanol (100%, 95%, and 70%) and double deionised water (dH_2O). Then, sections were boiled in pressure cooker (20 minutes) with pre-heated 0.1M Na citrate buffer pH 6.0 (42.02g citric acid, made up to 2l) for antigen retrieval. The sections were then cooled for a further 20 min under running tap H_2O. Sequential steps of blocking endogenous peroxidase (3% H_2O_2 in dH_2O (v/v); Sigma), avidin and biotin additions (Vector; Peterborough, UK) were then carried out for 30 min, 15 min, and 15 min respectively. Each step was followed by two washes with tris-buffered saline (TBS: 100ml 0.5M Tris-HCl, 8.5g NaCl, made up to 1L). Afterwards, sections were submitted to blocking with non-immune normal goat serum (NGS; Sigma) diluted in PBS (1:5 v/v) containing 5% (w/v) BSA (Sigma) for 20 min. Then the sections were incubated overnight with a rabbit polyclonal antibody raised against a synthetic peptide of human LOX (EDTSCDYGYHRRFA; a kind gift from Dr. Janine T. Erler, Institute of Cancer Research, London, UK). The antibody had been proved to work for both human and mouse tissue (Erler et al., 2006). A one in fifty dilution of this LOX antibody was used for the staining. Negative antibody staining controls incubated with matched concentratons of unconjugated normal rabbit IgG fraction (Dako, Birmingham, UK) were routinely included. Sequential incubations with goat-anti-rabbit biotinylated secondary antibody (Dako) and RTU-ABC elite kit (avidin-biotin complex; HRP conjugated; Vector) were conducted for 30 min each. Between steps sections were washed three times with TBS supplemented with 0.05% Tween 20 (v/v) (TBST). Sections were subsequently incubated with HRP-conjugated diaminobenzidine (DAB; Vector) chromagen for 5 min followed by haematoxylin counterstaining. Finally, slides were dehydrated in serial ethanol dilutions (70-100%) and xylene and mounted

with a cover glass (VWR, UK) in an aqueous medium. The immunostained sections were visualized with an Olympus Provis microscope.

2.6 LOX enzyme activity assay

To test the LOX enzyme activity of the conditioned cell culture medium, a fluorometric-based assay was adapted in our lab from the published work of Prof. Philip Trackman (Palamakumbura and Trackman, 2002). The assay to detect LOX activity in medium is based on measuring released H_2O_2 from the oxidation process using the Amplex red (N-Acety1-3,7-dihydroxyphenoxazine) fluorometric reaction. Generally LOX present in the medium can effectively oxidise a simple amine substrate, 1,5-diaminopentane. The reaction generates H_2O_2, which in turn oxidises Amplex red. The oxidation of Amplex red is facilitated by the addition of horseradish peroxidase. It produces resorufin with a fluorescent excitation maximum at 563 nm and an emission maximum at 587 nm. Meanwhile, parallel assays were prepared with 500μM BAPN to completely inhibit the activity of LOX. The differences in emission between the raw samples and the BAPN-treated ones are used as a fluorescence increase recorded either in a discontinuous end-point reading or as a continuous reading. The enzyme activity therefore is presented by the relative fluorescence increase. It has been demonstrated that this assay allows the detection the activity of LOX as low as 20ng/ml (Palamakumbura and Trackman, 2002).

To evaluate LOX production, PMC cell suspensions were adjusted to $1x10^5$ viable cells per well of 24-well culture plates (Corning). After 24 h, the cells were washed with phenol red/serum-free medium consisted of phenol-red free medium 199 (GIBCO), 0.01% BSA, 2mmol/l L-glutamine, 50IU/ml penicillin and 50μg/ml streptomycin. Cells were serum-starved for a further 24 h in the phenol red/serum-free medium. Phenol red was excluded as it interfered with the emission

intensity, due to fluorescence quenching. The cells were then treated in the following groups for 96 h with phenol red-free medium: (1) Control, (2) cortisol (F, 10^{-6} M, Sigma), (3) IL-1α (0.5ng/ml, R&D), (4) IL-1α + F. After 96 hours, whole media were collected for the assay. For the activity assay, reaction solutions were prepared in a final volume of 1ml at pH 8.2 containing 1.2M urea (Sigma), 0.05M sodium borate (Sigma), 1unit/ml horseradish peroxides (Sigma), 10μM Amplex red (Invitrogen), 10mM 1,5-diaminopentane dihydrochloride (Sigma), and 200μl of sample. A parallel set of negative controls was set up by adding 500μM BAPN in the solutions. Solutions were mixed by vortexing, and aliquoted into a 96-well Fluoronunc™ black solid plate (nunc, Thermo) at 200μl per well. One set of triplicates for each sample and another set of triplicates with BAPN were set up in the plate. Fluorescence readings were obtained at 0 h using a BMG FLUO star plate reader (BMG LABTECH, Aylesbury, Germany) at a specified range of excitation (570 nm) and emission (590 nm). The plate was then incubated at 37°C with protection from light. Fluorescence readings were taken again at 1 h and 2 h time points.

For the fluorescence increase calculation, subtractions were taken by both 1 h and 2 h record from the 0 h record. The average of the triplicates was taken to present each sample and negative control. The difference of the fluorescence increase between the sample and the negative controls gave the enzyme activity for each sample. This calculation gave a relative activity determination for LOX.

2.7 In vitro wound healing assay

For an *in vitro* scratch assay, 1.5 x 10^5 PMC were seeded into 12-well plates (Corning) and incubated at 37 °C. Cells were allowed to grow to form a confluent monolayer, when culture medium was removed and replaced with serum-free

HOSE2 medium for 24h. To investigate the effect of cytokines on cell motility, cells were pre-treated in following groups for 48h: (1) Control, (2) BAPN (500μM), (3) IL-1α (0.5ng/ml)+TGFβ-1 (2ng/ml, R&D), (4) IL-1α +TGF-β1+BAPN. Before scratching, 500μM fresh BAPN solution was added to groups 2 and 4 again to completely suppress LOX enzyme activity. A wound in the centre of the well was made by scratching the monolayer gently using a 1 ml pipette tip. Wound widths were recorded at 0 h and 16 h by measuring the width across the wound area between the wound edges on a pixel scale. The cell migration distance was calculated by subtracting the wound width at 16 h from the width in the corresponding wound area at the 0 h time point. Usually quadruplicate replicates were employed for each treatment group due to the limited number of cells available from any individual patient.

2.8 In vitro cell-ECM adhesion assay

The *in vitro* adhesion assay carried out in this thesis was based on a previous description (Odero-Marah et al., 2003). The ability of cells to adhere to the ECM was achieved using fibronectin-coated plates. 12-well plates were pre-coated with fibronectin (Sigma) at a final concentration of 10μg/ml, and 400μl per well of fibronectin solution was added to make a surface coverage at 1μg/cm^2. Plates were incubated in a 37 ^{o}C incubator for 1 h to allow the completion of coating and solution then removed. The plates were air-dried in the fume hood, and then used for adhesion assays or kept at 4^{o}C for later use. To investigate the effect of cytokines on cell-ECM adhesion, PMC were serum-starved in HOSE2 medium for 24 h, and then pre-treated in groups for 48 h as follows: (1) Control, (2) BAPN (500μM), (3) IL-1α (0.5ng/ml)+TGFβ-1 (2ng/ml), (4) IL-1α+TGF-β1+BAPN. Then, the condition medium from each treatment were collected, fresh BAPN (500μM) was added again to the condition medium from group (2) and (4). Cells were harvested by

trypinisation and counted using a haemocytometer. A final number of 2 x 10^5 cells were added into each fibronectin-coated well with 1ml of corresponding condition medium. Plates were incubated in 37 ^oC incubator for 1h to allow the cells adhere to fibronectin. Non-adherent cells were removed by washing three times with warm HOSE2 medium. Adhered cells were detached by trypsinisation (1ml/well) and cell counts were carried out with a haemocytometer. Duplicate wells were set up for each treatment group.

2.9 In vivo animal work.

All animal experiments were performed with Home Office Approval under a project license issued to Professor Ken Donaldson. The animal work was done with the kind assistance of Dr. Craig Poland.

Initially a preliminary BAPN dose trial was carried out to determine the optimum dose of BAPN to use in further experiments. 8-week-old female C57/Bl6 mice (Harlan, UK) were randomly assigned to 6 treatment groups: Vehicle (saline), 0.1, 0.2, 0.5, 1 and 2g/kg BAPN, experiment was done in triplicate for each treatment group. Mice were injected directly into the peritoneal cavity (I.P. injection) daily for a period of 2 weeks. From this trial it was concluded that 1g/kg would be the most appropriate dose to use in further experiments as analysis of the ovaries, diaphragms and peritoneal fluid from the different BAPN treatment groups showed no clear differences to the control group; however, the highest evaluated dose (2g/kg) appeared to make the mice lethargic.

Following on from this, 24 mice were randomly assigned to 8 treatment groups as follows: Vehicle (Saline), BAPN (1g/kg), dexamethasone (DEX) (Sigma, 1mg/kg), multi-walls nanotubes (NT) (20µg/ml, which equated to 10µg/mouse, provided by

Matthew Boyles, University of Cambridge), NT+BAPN, NT+DEX, BAPN+DEX and NT+BAPN+DEX. Each treatment was done in triplicate. Prior to experimental treatment, NT were dispersed by suspending in 0.5% BSA (Sigma) and placed in an ultrasonic water bath, as previously described (Poland et al., 2008). On day 1 of the experiment, mice were injected intraperitoneally within their treatment groups. Injection volumes were as follows: 0.5ml NT, 0.5ml vehicle, 250µl BAPN and 250µl DEX. NT and vehicle injections were given only once, whereas BAPN and DEX injections were given daily for a period of 7 days. The diaphragms were carefully dissected from the mice and fixed overnight in methacarn (60% methanol, 30% chloroform, 10% glacial acetic acid) for histological analysis.

Sections were stained with H&E, and collagen in the tissue was stained with picrosirius red. Pictures of each section were taken by Olympus BH-2 microscope. The whole fibrotic lesion area (granuloma) and collagens contained in these areas were quantified by Imagine Analysis (Image-Pro 4.0). Briefly, the whole fibrotic lesion was highlighted in the picture, the total pixels contain in the highlighted area were counted and recalculated into landmeasure (mm^2). The area of collagen staining was calculated in the same way. Quantification data was presented by using the area of lesion and collagens over the length of respective diaphragm section.

2.10 Statistical analysis

All data from each experimental set were combined and presented as means and standard errors (±sem). Numbers of replicate experiments are denoted by the number (n) of independent replicates and are given in figure legends and text. Basic statistical analysis was performed using one-way analysis of variance with the GraphPad Prism 5.0 software (GraphPad Software Inc., San Diego, USA). Repeated-measures-one-way ANOVA and Turkey post test were run for multiple comparisons between parametric samples (cell line) , whereas repeated-measures-

nonparametric Friedman test and Dunn's multiple comparison test were done for group comparisons between nonparametric samples (primary samples). Two-tailed paired Student t-tests were performed for single parametric test. Wilcoxon matched-paired tests were performed for single nonparametric test. A p value <0.05 was taken as statistically significant in robust data sets.

Chapter 3

In vivo peritoneal fibrosis model

3.1 Introduction

Several animal models have been developed to investigate the formation of peritoneal adhesions and fibrosis in the peritoneum. For example, Sulaiman and colleagues have successfully induced peritoneal adhesion by injuring the surface of the caecum and adjacent abdominal wall (Sulaiman et al., 2000). Hung and associates induced peritoneal fibrosis in a rat model by introducing *Staphylococcus aureus* into the peritoneal cavity using microcarriers (Hung et al., 2001). Other studies induced peritoneal adhesion as a consequence of direct injury by suturing or electrocoagulation (Kucukozkan et al., 2004; Reed et al., 2008; Wallwiener et al., 2010).

A recent study by Poland and colleagues proposed a new model to investigate peritoneal fibrosis in the peritoneal cavity (Poland et al., 2008). They induced tissue fibrosis on the peritoneal side of the diaphragm by direct intraperitoneal (i.p) injection of mice with long multi-walled nanotubes (NT). Carbon nanotubes (CNT) are a new type of nanomaterial that has been developed as a novel structural material. They are graphite cylinders that vary in size but are usually a few nanometers in diameter, with their length ranging from a few micrometers to millimeters. NTs are CNTs which are made up of more than one graphite cylinder whereas a single cylinder is referred to as a single-walled nanotube (SWNT) (Figure 3.1). Such structures give nanotubes properties that are highly desirable in many industrial products (Maynard, 2007), especially in target drug delivery systems (Zhang et al., 2011).

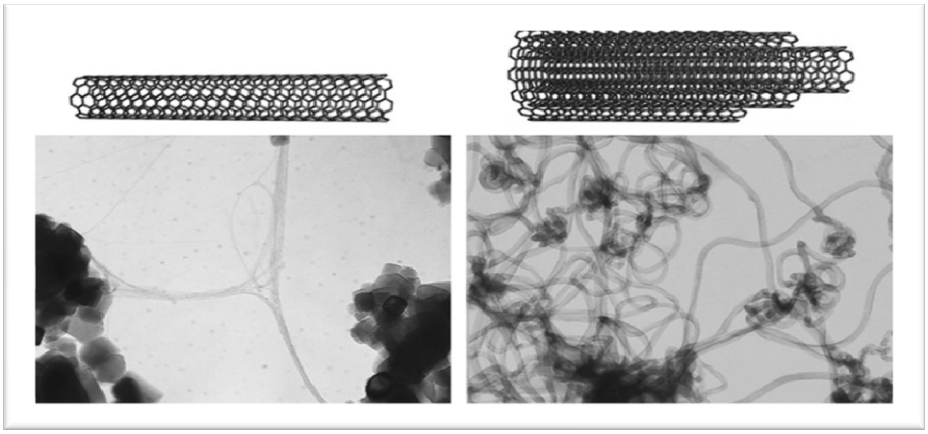

Figure 3.1. Representative molecular images and transmission electron micrographs of SWNT (left) and NT (right). Figure adapted from (Donaldson et al., 2006).

The pathology of the NT-induced fibrosis on the diaphragm is due to the chronic inflammation caused by the injection of long forms of NTs. It occurs most probably as a consequence of the failure of macrophages, the inflammatory cells usually responsible for clearing infection or infectious agents, to completely phagocytose the NT, as illustrated in Figure 3.2 (Poland et al., 2008; Kostarelos, 2008). It has been shown that such frustrated phagocytosis can induce significantly more TNF-α and reactive oxygen species production from macrophages (Brown, 2007). This initiates a chronic inflammation, as indicated by elevated levels of total protein, polymorphonuclear leukocytes (PMN) and foreign body giant cells (FBGCs) presenting in the lavage fluid from NT-treated mice. It results in the formation of granulomas on the mesothelial side of the diaphragm. The granulomas are formed by aggregates of cells containing NT fibres, most likely macrophages and FBGCs, with massive deposition of collagen.

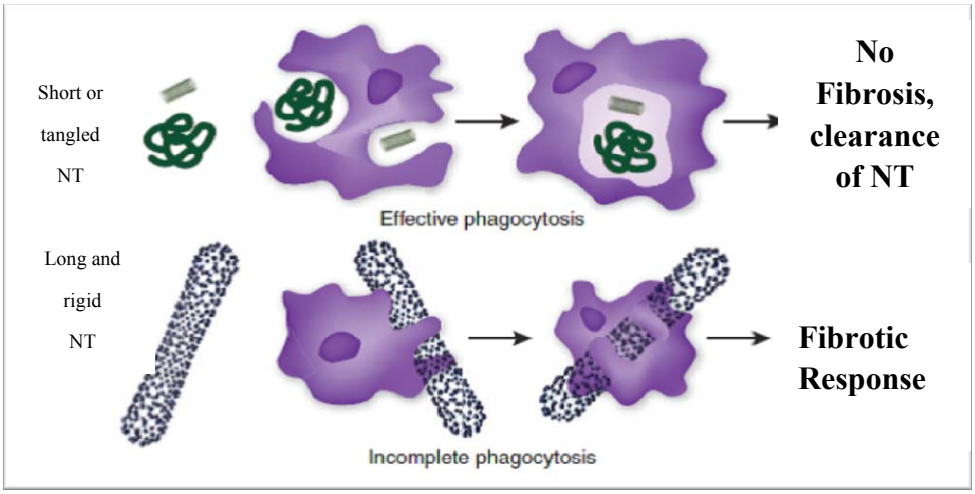

Figure 3.2. Response of Macrophages to Long NTs. Diagrammatic representation of the response of macrophages to NTs as demonstrated by Poland *et al* (Poland et al., 2008), summarising the fact that macrophages are able to cope with short or tangled NT as these can be efficiently taken up by the macrophage cells and degraded, resulting in resolution of the inflammatory response and no fibrosis or granuloma formation. This should be compared to the reaction to long NT that cannot be effectively taken up and phagocytosed by the macrophages resulting in a chronic inflammatory response, which leads to granuloma formation and fibrosis. Figure adapted from (Kostarelos, 2008).

This *in vivo* model was used to investigate the role of LOX and anti-inflammatory factors in pathologic peritoneal fibrosis caused by NT. Obviously there are a few differences between NT-induced fibrosis and postoperative adhesion; one causes hyperplasia whereas the other causes adhesion. Furthermore, surgery may sometimes cause much more serious damage to the peritoneal architecture than a NT injection. However, adhesions are widely regarded as a form of fibrosis, and they share common features. Both are caused by external irritation and undergo a chronic inflammation at particular sites. A previous study showed that suturing is a principal reason for peritoneal adhesion (Hubbard et al., 1967). The pathology is thought to be quite similar to the failed digestion of NT. In addition, both are formed on the peritoneal mesothelium. I therefore believe that the NT-induced adhesion model is both convenient and appropriate for the study of tissue fibrosis in the abdominal cavity.

3.2 Material and Methods

To investigate the effect of BAPN and DEX on NT-induced peritoneal fibrosis, 24 mice were divided into 8 groups as shown in section 2.9: Vehicle (Saline), BAPN (1g/kg), dexamethasone (DEX) (Sigma, 1mg/kg), multi-walls nanotubes (NT) (20µg/ml, which equated to 10µg/mouse), NT+BAPN, NT+DEX, BAPN+DEX and NT+BAPN+DEX. Pathologic fibrosis was induced on the peritoneal side of the diaphragm by i.p injection of 0.5ml of carbon nanotubes. Daily injections with 250µl BAPN or 250µl DEX were given for 7 days, and diaphragm sections were sampled for further investigation.

To investigate the effect of NT on macrophages, buffy coat samples were obtained from Scottish National Blood Transfusion Service. The profile of the individual donated samples used for these studies is presented in Table 3.1

Table 3.1 Profile of buffy coat donator

Donation No/ LOT	ABO	Volume (ml)	Collection Data
G101 610 897 847 1	A+	62	14/07/10
G101 610 771 680 H	A+	67	20/07/10
G101 610 767 668 J	O+	60	22/07/10
G101 610 766 797 H	O+	63	05/08/10

3.3 Results

3.3.1 Carbon nanotubes induction of peritoneal fibrosis within mouse abdominal cavity

Seven days after i.p injection of carbon nanotubes, diaphragms of experimental mice were sampled and sectioned as indicated in Figure 3.3A. The complete section comprised two main parts: the muscle-rich costal parts on both sides and the collagen-rich tendon parts in the middle, linking the muscle-rich parts. These were stained with picrosirius red to indicate the distribution of collagen deposition. In control diaphragm sections, both the pleural and peritoneal sides were covered by a thin layer of mesothelium with an underlying collagen-rich basement membrane (Figure 3.3B). In contrast, diaphragm sections of NT-treated mice showed extensive granuloma lesions on the peritoneal side with massive collagen deposition, whereas the mesothlium on the pleural side was normal in all cases (Figure 3.3C). The inset image also show NT contained within a granuloma.

Immunohistochemistry was used to locate LOX protein in the control and fibrotic tissue (Figure 3.4). In the control group, a weak staining of LOX was distributed inside the muscle area, and also in the peritoneal mesothelial cells on the edge of the diaphragm (Figure 3.4 A, C, E). In the NT-treated group weak LOX staining was also found in the muscle. However, intensive staining was found along the edge of the fibrotic lesion, with gradual reduction from the edge to the inside areas (Figure 3.4 B, D, F). Furthermore, in higher magnification images, larger cells and bigger nuclei were found in the NT-treated group, which are hallmarks of granuloma tissue (Figure 3.4 G, H). LOX staining was found to locate in both the cytoplasm and intercellular space. However, the granuloma tissue which contained the NT fibres had no observable LOX staining (Figure 3.4 D, H).

A

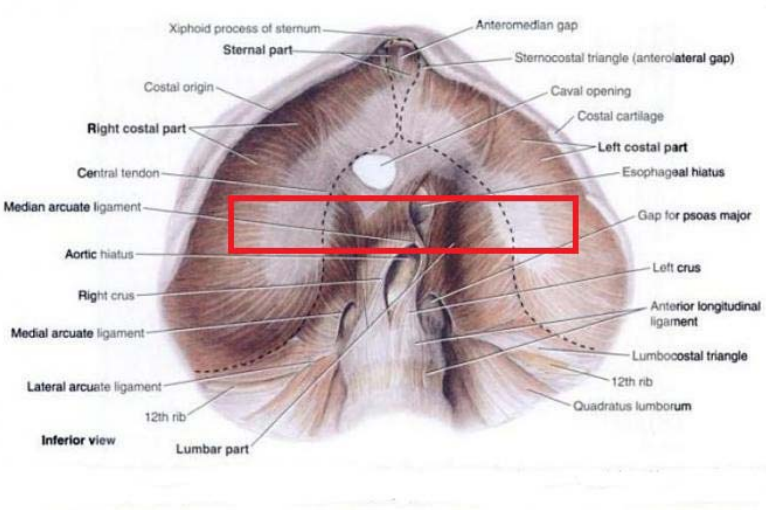

B

C

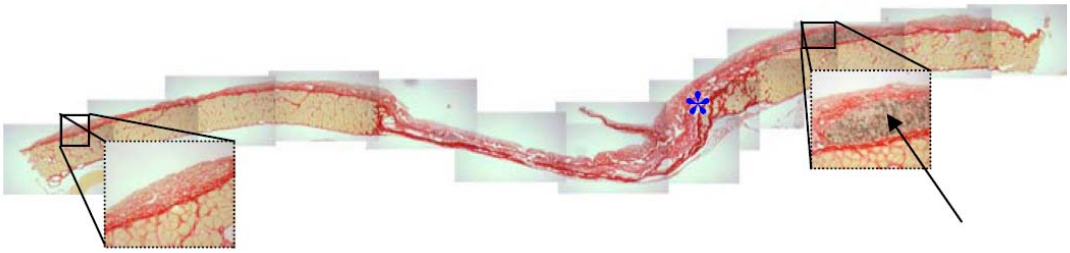

Figure 3.3. *In vivo* peritoneal fibrosis model. A: Abdominal surface of a diaphragm and its attachment. The fleshy sternal, costal and lumbar origins of the diaphragm attach centrally to the trefoil-shaped central tendon, the aponeurotic insertion of the diaphragmatic muscle fibres. The red box indicates the sampling site. B: Histology section of control mouse diaphragm stained with picrosirius red. Insert pictures indicate the abdominal surface of the diaphragm. C: Histology section of NT-treated mouse diaphragm stained with picrosirius red. Insert pictures indicate the abdominal surface of diaphragm. ***:** Widespread collagen staining observed as the red staining. Arrow: NT fibres deposits within a granuloma.

Figure 3.4. NT-treated mice exhibit upregulated LOX expression in diaphragm. Immunohistochemistry staining for LOX using rabbit anti-LOX (1:50 dilution) performed on diaphragm sections. (A, C, E) Control group X4, X20, X40. (B) NT group X4. (D, F) NT group X20. (G, H) NT group X40. Negative control for NT group can be found in appendix 1.

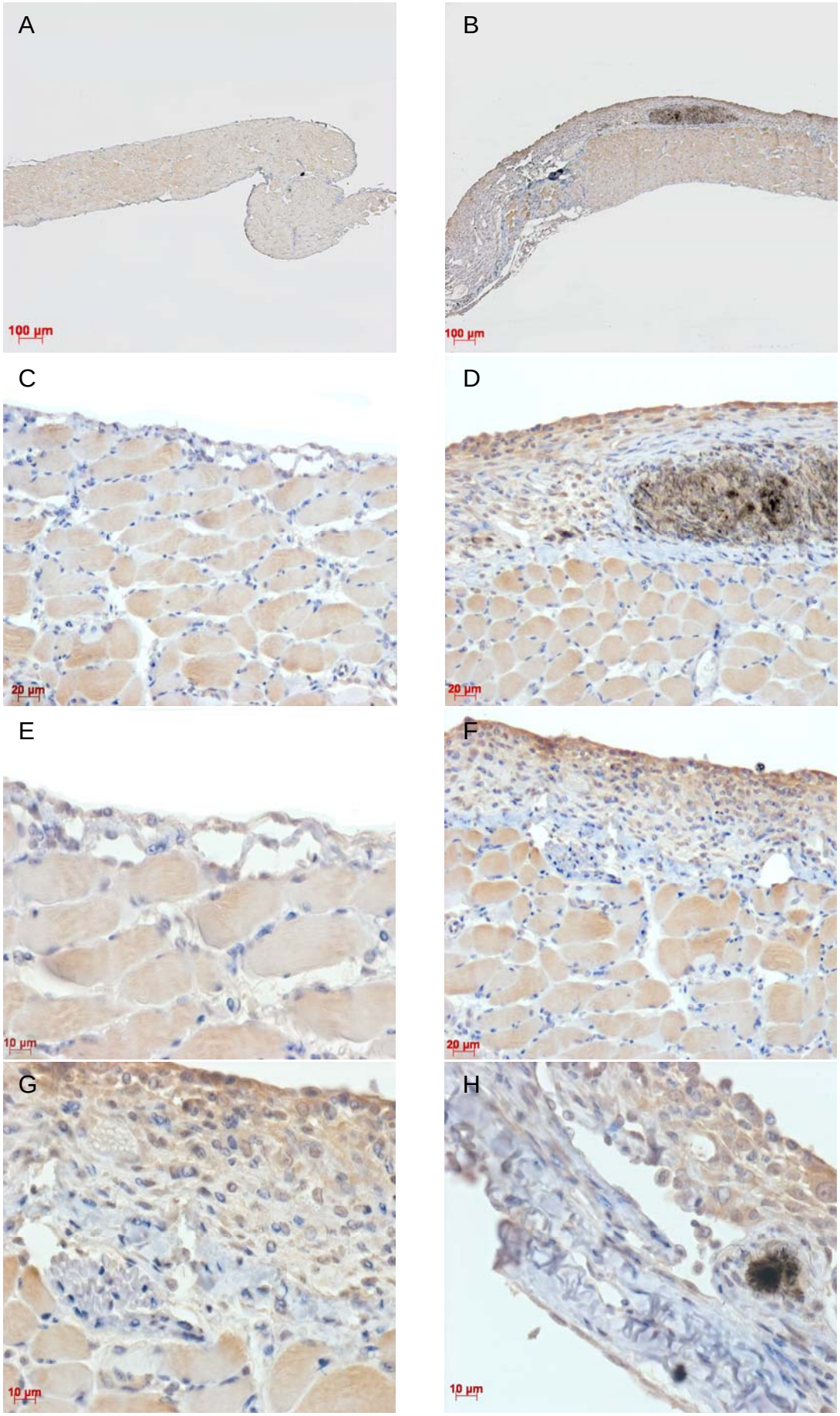
A
100 µm
B
100 µm
C
20 µm
D
20 µm
E
10 µm
F
20 µm
G
10 µm
H
10 µm

3.3.2 Effects of β-aminoproprionitrile and dexamethasone on the inhibition of peritoneal fibrosis

As shown above, NTs induced fibrosis on the peritoneal side of the diaphragm and this was associated with an elevated LOX expression. Daily injection of LOX activity inhibitor (β-aminoproprionitrile, BAPN) and dexamethasone (DEX) was conducted as attempts to resolve the pathologic fibrosis *in vivo*.

Representative whole diaphragm sections from five groups of treatment are shown in Figure 3.5 (A: control, B: NT, C: NT+BAPN, D: NT+DEX, E: NT+BAPN+DEX), with inset images taken at a higher magnification to highlight the peritoneal mesothelium and the tendon link in the middle. No granulomas were seen on the diaphragms of the control group (Figure 3.5A), as well as those treated with BAPN, DEX and BAPN+DEX in the absence of NT (Appecdix 2). Sections of the NT-treated group showed dramatic granuloma formation on the peritoneal side, with widespread collagen staining (Figure 3.5B).

Importantly there was a dramatic reduction of fibrotic tissue formation in the NT+BAPN, NT+DEX and NT+BAPN+DEX groups, as well as a visual reduction of collagen staining (Figure 3.5C, D and E). We used software to quantify the formation of such fibrotic granuloma tissue and the percentage of collagen (one section per group). The data indicated that granuloma formation was significantly reduced in the treatment groups compared to the NT group ($p<0.05$) (Figure 3.6A), with a 75% reduction in granuloma formation in the NT+BAPN+DEX group, The quantification of collagen staining also showed significant reductions of collagen deposition in these three groups compared to the NT group ($p<0.01$) (Figure 3.6B), with an 90% reduction in collagen staining found in the NT+BAPN group.

Figure 3.5. Histology sections of mouse diaphragm stained with picrosirius red. Diaphrams were recovered from mice following 7 days treatment of the following groups: A: Control, animal treated with 0.5ml saline on day 1 and daily 200µl i.p. injections of saline for 7 days. B: animal treated with 0.5ml NT (20µg/ml) on day 1 and daily 200µl i.p. injections of saline for 7 days, or C: daily 200µl i.p. injections of BAPN (1g/kg) for 7 days, or D: daily 200µl i.p. injections of DEX (1mg/kg) for 7 days, or E: daily 200µl i.p. injections of BAPN+DEX for 7 days. No granulomas seen in control group (A). Extensive granuloma formation on peritoneal side of diaphragms of the NT-treated group with widespread collagen staining (B). Granuloma formation, but much reduced, also seen in NT+BAPN, NT+DEX, NT+DEX+BAPN diaphragms (C, D, and E, insert pictures).

A: Control

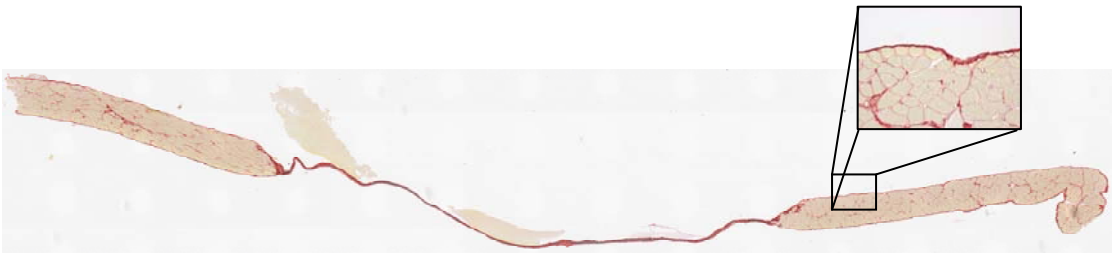

B: NT

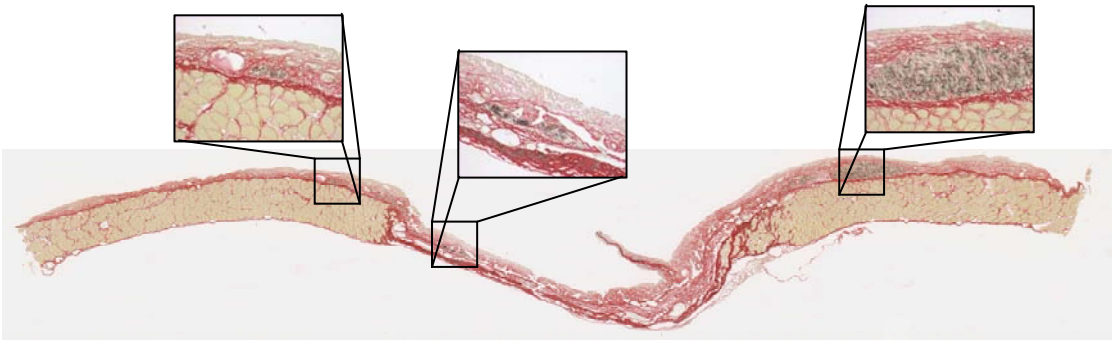

C: NT+BAPN

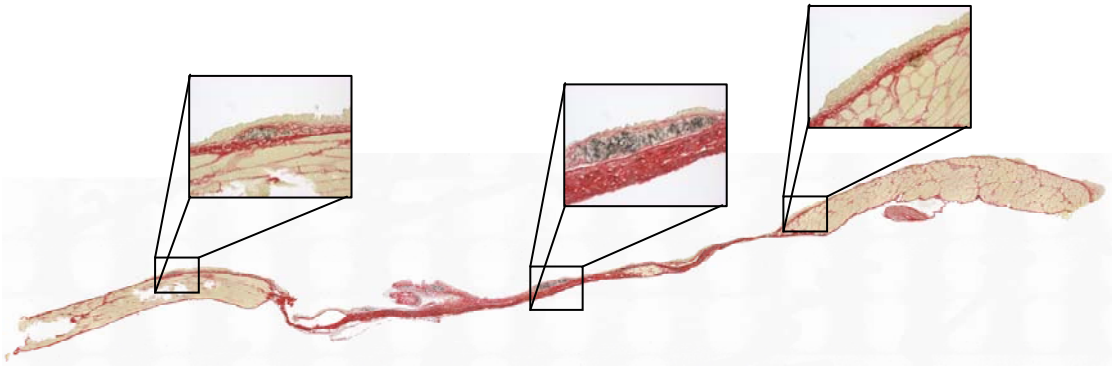

D: NT+DEX

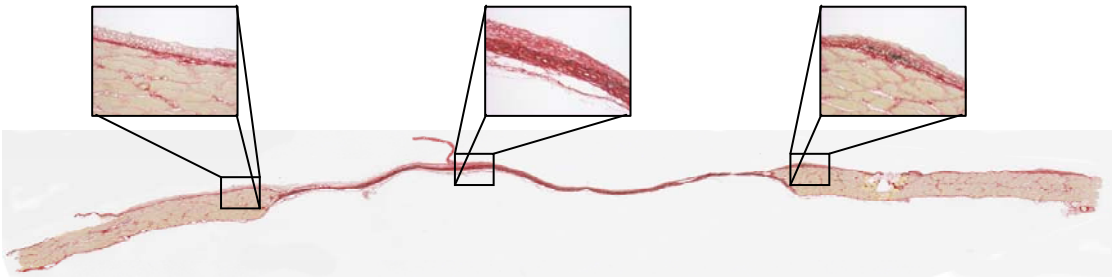

E: NT+DEX+BAPN

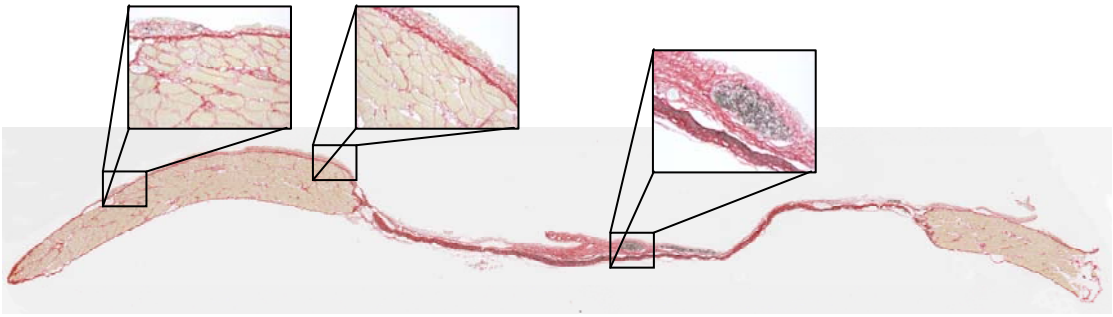

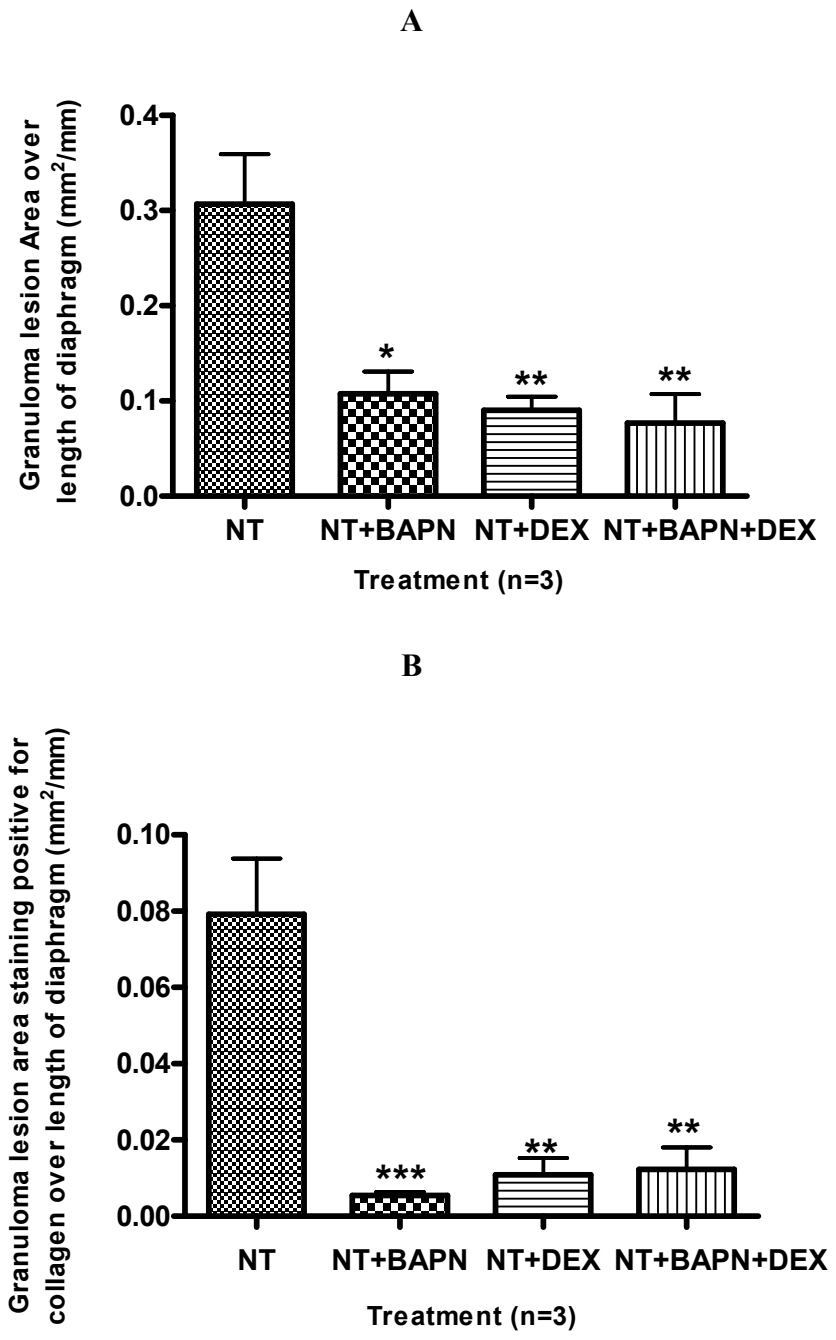

Figure 3.6. Quantification of the effect of NT and anti-fibrotic treatment on diaphragms after 7 days. A: Quantification of granuloma formation on the peritoneal side of diaphragm from NT, NT+BAPN, NT+DEX, NT+BANP+DEX groups. (n=3), *: $p<0.05$, **: $p<0.01$ compared to the NT group. B: Quantification of the amount of collagen staining within the granuloma lesions. (n=3). Statistical analysis was undertaken by one-way ANOVA. Bars represent mean±S.E.M. **: $p<0.01$, ***: $p<0.001$ compared to the NT group.

3.3.3 Effect of nanotubes on human peripheral blood mononuclear cell-derived macrophages

To investigate the effect of NT on macrophages, peripheral blood mononuclear cells (PBMC) were separated from buffy coat samples obtained from healthy donors. As described in section 2.1.2, an adapted ficoll-percoll density gradient separation protocol was used. This method allowed PBMC separation from buffy coat with high purity and minimal lymphocyte contamination (Figure 3.7A, B). PBMC were further enriched by adhering cells to culture plates, followed by several washing steps. After 6 days of culture with serum and M-CSF, PBMC matured into macrophages (Figure 3.7C, D), indicated by the increased size of the cells, a rounded regular nucleus in the centre, and developing cytoplasm vacuolation.

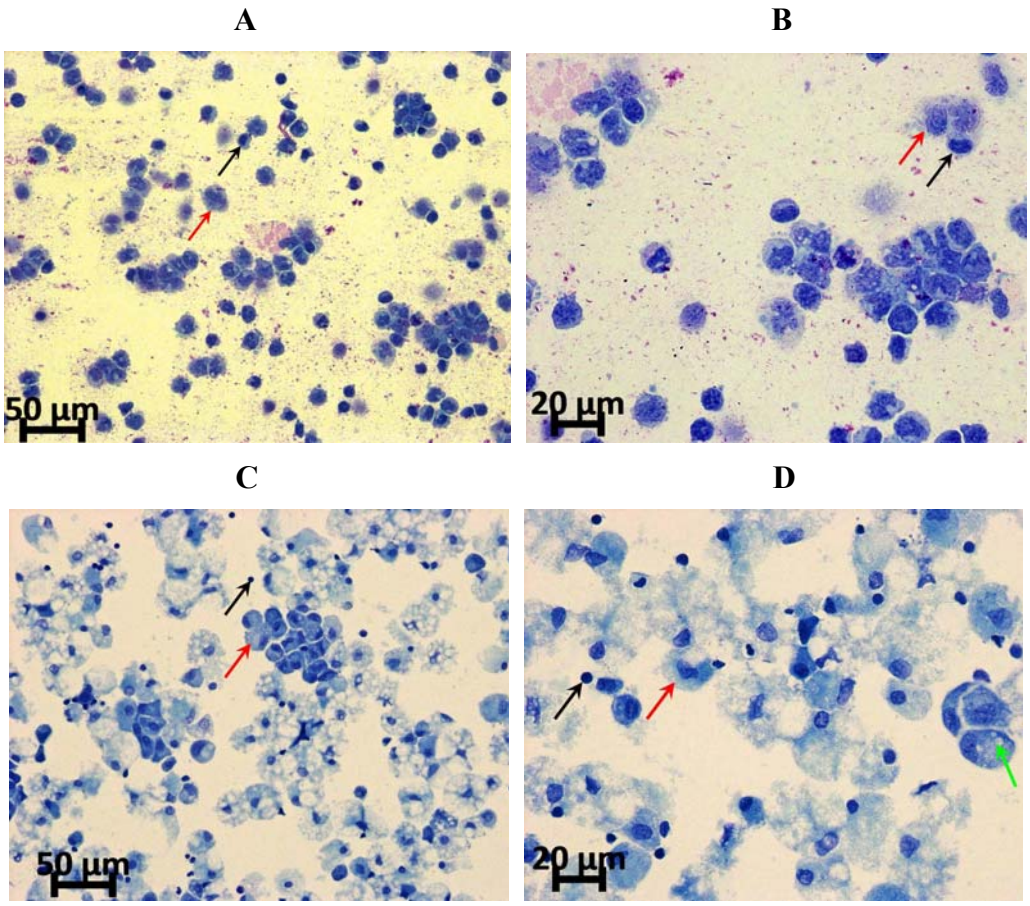

Figure 3.7. A, B: Population of PBMC separated from buffy coat stained with haematoxylin at X20 magnification (A) and X40 magnification (B) (Red arrow: monocyte; black arrow: lymphocyte). C,D: A population of matured macrophages after 6 days culture at X20 magnification (C) and X40 magnification (D) (Red arrow: monocyte; black arrow: lymphocyte; green arrow: cytoplasm vacuolation).

LOX mRNA level was first measured in cultured macrophages (Figure 3.8). The result showed that LOX mRNA levels were extremely low in matured macrophages, while a dramatically higher level (10,000-fold) was found in peritoneal mesothelial cells.

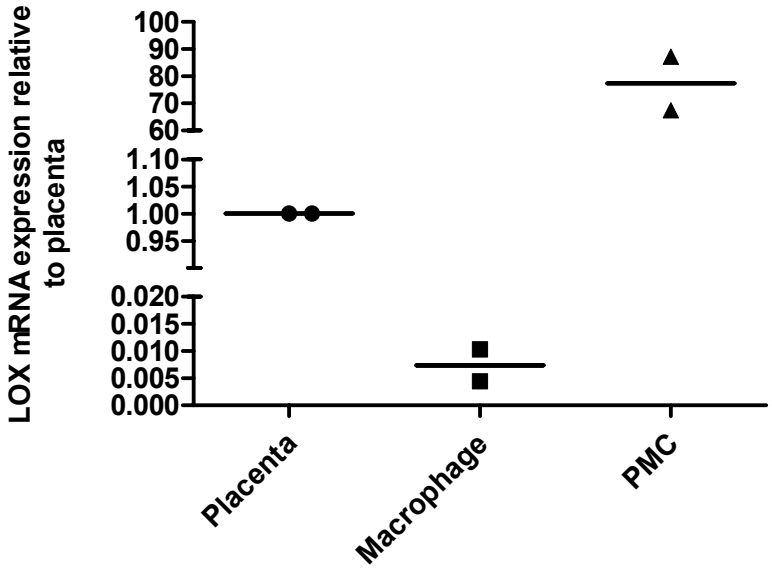

Figure 3.8. Quantitative RT-PCR comparing LOX mRNA expression in matured macrophages and peritoneal mesothelial cells (PMC). Values are relative to placenta (n=2 donors).

Macrophages were then exposed to NT across a range of doses (0, 5, 15, and 30μg/ml) for 48h. TNF-α and IL-1α contents of the culture media were evaluated by ELISA. The data showed a dose-dependent increase of TNF-α released from NT-treated macrophages, with 30μg/ml NT significantly increasing TNF-α levels in the culture medium (Figure 3.9A, 810±405pg/ml compared to 7.8±4pg/ml in the control). In contrast, IL-1α levels remained low in all treatment groups and was not significantly increased by NT over the dose range used (Figure 3.9B).

A

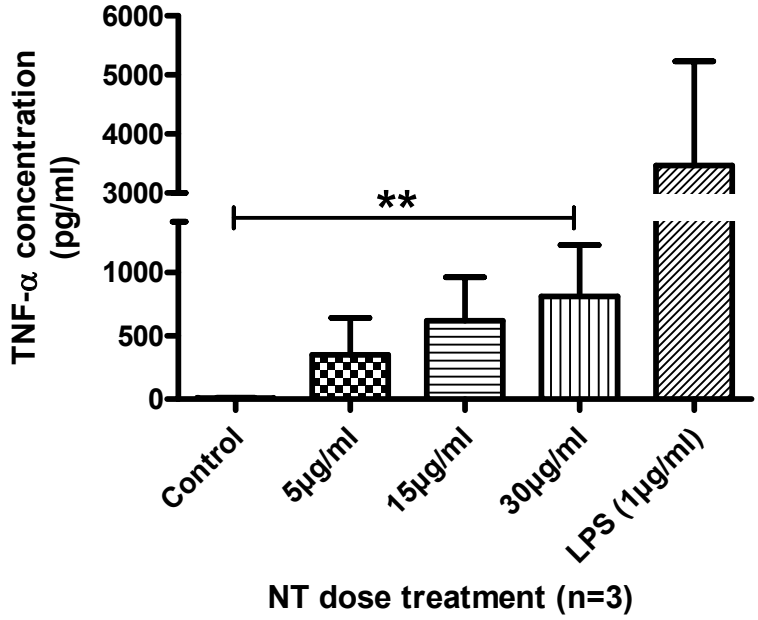

B

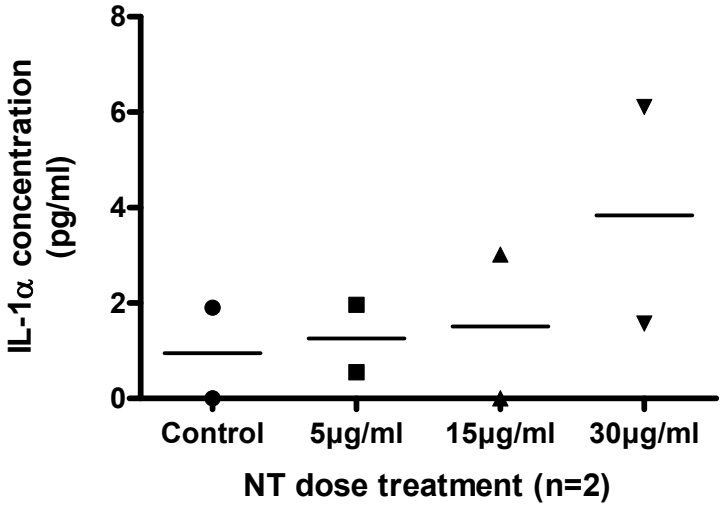

Figure 3.9. Cytokine production from NT-treated macrophages. A: TNF-α released by human macrophages after 48h treatment with carbon NTs at 0, 5, 15, and 30µg/ml. Treatment with 1µg/ml LPS (48h) was used as a positive control for these experiments. Statistical analysis was done by repeated-measures-nonparametric Friedman test; group comparisons were done by Dunn's multiple comparison test (n=3 donors). Data represent the mean±S.E.M. **: $p<0.01$. B: IL-1α release by human macrophages after 48h treatment with carbon NTs at 0, 5, 15, and 30µg/ml. Insufficient replicates (n=2 donors) did not allow statistical analysis.

Since the *in vivo* studies showed that DEX treatment could minimize the formation of granuloma tissue, we further tested whether DEX treatment could suppress TNF-α production from NT-treated macrophages. The results showed that the addition of DEX reduced the level of TNF-α released from NT-treated macrophages (Figure 3.10). However, no statistical analysis was possible due to insufficient independent repeats (n=2).

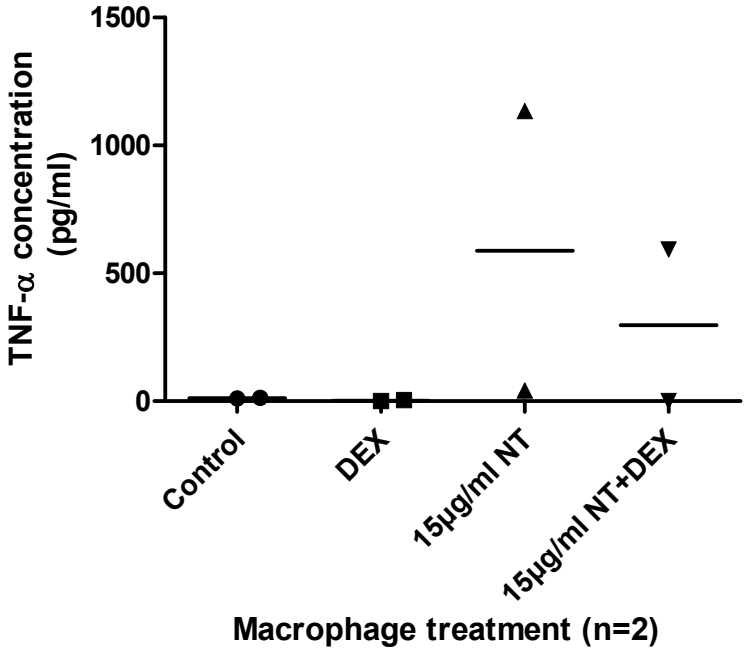

Figure 3.10. TNF-α release by human macrophages after 48h treatment with DEX (1µM), carbon NTs (15µg/ml), and NT+DEX. Insufficient replicates (n=2donors) did not allow statistical analysis.

3.4 Discussion

By using the protocols previously published (Poland et al., 2008), we established an *in vivo* peritoneal fibrosis model using C57/BL6 mice. Injection of multi-wall nanotubes (NT) into the abdominal cavity notably induced fibrotic lesions on the peritoneal side of diaphragms. The lesions exhibited features of granulomatous tissue, comprised of aggregates of cells containing NT fibres, most likely foreign body giant

cells (FBGCs), and associated deposition of collagen. As noted in the Introduction, such pathologic changes induced by NT could arise from a frustrated phagocytosis when macrophages tried to eliminate the NT particles. This leads to increased numbers of FBGCs presenting in the peritoneal fluid, with significant PMN and protein exudation (Poland et al., 2008). Peritoneal fluid moves in response to pressures generated by the diaphragm (Yao et al., 2003). Such a mechanism aids peritoneal clearance by drainage into lymphatic lacunae that lie beneath gaps (stomata) in the mesothelium lining the undersurface of the diaphragm (Nakatani et al., 1996). Therefore, the peritoneal side of the diaphragm becomes a perfect bed to house either NT particles or the FBGCs presented in the fluid. The deposition of NTs or FBGC can further breakdown the normal construction of the diaphragm and replace the mesothelium with granulomas. In addition, milky spots in omentum can be another possible way of the self-clearance of NTs in peritoneal cavity. Therefore, omentum could be another important site to investigate such peritoneal fibrosis induced by NTs. Due to the extremely long half life for the NT particles (He et al., 2010), it can be expected that more severe fibrotic damage can be seen over longer periods. The experiment shown in this chapter ended at day 7 after the injection of NT. Another experiment, which continued for 14 days after NT injection, revealed significant adhesions forming between the diaphragm and the liver (F Gardiner & C Harlow, unpublished results). It indicates a potential of these granuloma lesions to develop into fibrotic adhesion.

LOX protein was localized to the edge of the granuloma lesions, and the staining was much more intense than on the normal mesothelium overlying the peritoneal side of the diaphragm. A gradation of LOX staining was found from the edge of granulomas to the inner part. This suggested a completed collagen deposition process had occurred in the older granuloma tissue, while an ongoing process was occurring at the newly forming edge of the granuloma lesions. Additionally, we showed that there

was no apparent LOX staining in the granuloma tissue (or FBGCs) wrapping the NT fibres. Thus, combined with the finding that LOX mRNA was highly expressed in PMC but not in macrophages, the data were suggestive that such collagen deposition might be mediated by PMC-derived LOX presented in the peritoneal fluid, while FBGCs were not essential for this process since they did not express LOX.

The results also showed a potential method to minimize peritoneal fibrosis by inhibiting LOX activity. By daily injection of BAPN (an irreversible chemical inhibitor of LOX activity), significant reduction of collagen deposition was found which was associated with a reduction of the size of the granuloma lesion. DEX was also shown to suppress the formation of granulomas and collagen deposition. Unfortunately, there was no significant additive effect when using the combined treatment of BAPN plus DEX. DEX has long been used as a treatment for inflammatory diseases. The application of DEX to prevent post-operative adhesion has been shown in many studies (Binda and Koninckx, 2009; Kucukozkan et al., 2004; Letowska-Andrzejewicz et al., 2011), which indicates an anti-adhesion effect of DEX. Interestingly, inhibition of LOX showed a similar pattern of reduction in fibrotic tissue as DEX. It suggests an alternative method to prevent post-operative adhesion by suppressing collagen crosslinking, which can further reduce collagen deposition. It may be of particular clinical relevance in situations where glucocorticoids are contra-indicated. Inhibition of LOX by BAPN has been used in many studies related to cancer metastasis (Erler et al., 2009; Erler et al., 2006). There has been no obvious side-effect seen in any of these studies. We also demonstrated that i.p injections of BAPN can be used at doses up to 1 g/kg. However, 2 g/kg injection of BAPN appeared to make the mice lethargic. Thus, BAPN may be an effective clinical treatment at doses associated with no, or at least minimal, side effects.

Because macrophages are essential components in our *in vivo* fibrosis model, our studies also focused on macrophage responses to NT particles. The results firstly showed that LOX was principally expressed by PMC, and not by macrophages. Therefore, we hypothesized that macrophages could induce LOX expression by producing inflammatory cytokines in response to NT. It has been shown that carbon NTs can induce TNF-α release from macrophages, as well as production of reactive oxygen species (ROS) (Brown, 2007). The underlying mechanism might involve the activation of the proinflammatory transcription factor NF-κB by ROS, a second messenger regulating such transcription processes. Our studies confirmed this by demonstrating a dose-dependent increase in TNF-α released by macrophages in response to NT. The impact of NT on macrophages varies considerably, as shown previously (Brown, 2007), suggesting that variable effects of NT could occur in individuals. In contrast, another important cytokine, IL-1α, was not secreted by macrophages in response to NT treatment. However, the most commonly secreted form of IL-1 is IL-1β, while IL-1α is largely retained in the cytoplasm in a precursor form. Thus, the level of IL-1β in the medium remains to be tested. Furthermore, addition of DEX into the medium suppressed the production of TNF-α from NT-treated macrophages, possibly due to suppression of the NF-κB pathway caused by DEX binding to glucocorticoids receptors (van der Laan and Meijer, 2008). Therefore, DEX may help to minimize granuloma lesions by reducing TNF-α release from macrophages.

In summary, our *in vivo* model had been shown to be a simple and suitable model to study peritoneal fibrosis. Quantification can be made on a section of the diaphragm allowing the study to be more objective and reliable. However, since measurements were only conducted on one section from each group, a series of sections cut from the same sample would have been preferable so that the mean value of all sections can be used to minimize variation between sections. We confirmed a key role of

LOX in peritoneal fibrosis. Inhibition of LOX could reduce collagen deposition, further minimizing the formation of granuloma lesions. In addition, application of DEX was also shown to prevent fibrosis in this model, possibly through the suppression of TNF-α production from macrophages exposed to NT. However, LOX was mainly found expressed in PMC and not macrophages. Therefore, the interplay between PMC and the inflammatory response remains another key relationship to be studied.

Chapter 4
Role of peritoneal mesothelial cells in peritoneal fibrosis

4.1 Introduction

As shown in Chapter 3, LOX was highly expressed in peritoneal mesothelial cells (PMC) whereas macrophages had reduced expression of LOX compared to PMC. The research focus of this thesis was therefore shifted from macrophages to PMC. Although a large body of work has looked at the role of PMC in peritoneal repair, the interaction between PMC and inflammation and their roles in extracellular matrix (ECM) remodeling require further investigation. From previous studies, we knew that an elevated accumulation of several cytokines was found in the peritoneal fluid after surgery, particularly TNF-α, IL-1 and TGF-β (see section 1.4.3). The concentrations of these three cytokines were found to vary in the peritoneal fluid after surgery. For example, after 48h, the concentration of IL-1 increased significantly to around 20pg/ml in patients who had adhesion reformation; whereas, in those who had no adhesion reformation, the concentrations of IL-1 remained relatively low (around 4pg/ml) (Cheong et al., 2002). Similarly TNF-α was 700pg/ml in the adhesion reformation group compared to 200pg/ml in the no adhesion reformation group (Cheong et al., 2002). In addition, the concentration of TGF-β1 in the peritoneal fluid after surgery (2861±347pg/ml) was significantly higher compared to that before the surgery (1229±157pg/ml) (Cheong et al., 2003). Therefore, the interaction between PMC and these three cytokines may be critical to an understanding of the pathology of post-operative adhesion formation. In Chapter 3, we showed that macrophages could produce TNF-α but not IL-1α when exposed to nanotubes. However, TNF-α has also been shown to induce IL-1 production from other cells, such as murine embryo fibroblasts (Wysk et al., 1999). It suggested that TNF-α could be the initial inflammatory cytokine at the site of nanotube deposits in our *in vivo* model, followed by the production of either IL-1 or TGF-β. Therefore, in this Chapter, interactions between PMC and these three cytokines were tested *in vitro*,

to better understand the role of PMC and the inflammatory response in post-operative adhesion.

4.2 Materials and methods

Investigation of the role of PMC in peritoneal fibrosis was assessed using primary PMC monolayers as described in Chapter 2. Treatments of several inflammatory cytokines were conducted on PMC monolayers for 48h in serum-free medium. RNA was extracted from the experimental groups, and quantitative real-time PCR was used to evaluate gene expression in the groups. ELISA was performed on cell lyasates and conditioned medium as described in section 2.4. *In vitro* wound healing assay and cell-ECM adhesion assay were performed as described in section 2.7 and 2.8 respectively. The basic clinical profile of patients involved with the respective assays performed on each are presented in Table 4.1.

Table 4.1. Clinical profile of patients used for respective assays

Patient Code	Age	Cycle day	Surgery	Reason for surgery	Study
6848	54	NA	TAH & BSO	Fibroids & HMB	mRNA
7672	47	19	TAH	HMB	mRNA
7638	23	25	Diag Lapscpy	HMB	mRNA
6832	51	19	STAH & BSO	HMB	mRNA
7641	38	11	TAH	HMB	mRNA
7548	31	5	Lap Ster	NA	mRNA
3028	29	19	Diag Lapscpy	RIF Pain	mRNA
7539	40	27	TAH	HMB & Pain	mRNA

7532	27	4	Diag Lapscpy	LIF pain	mRNA
Patient Code	**Age**	**Cycle day**	**Surgery**	**Reason for surgery**	**Study**
7538	21	NA	Diag Lapscpy	Pelvic pain	mRNA
7607	45	17	Diag Lapscpy	RIF pain & IMB	mRNA
5621	44	8	TAH	HMB & Fibroids	mRNA, healing assay
7531	37	27	Diag Lapscpy	HMB & Pain	mRNA, healing assay
7613	48	26	STAH	Erratic Menstrual Cycle	mRNA, Adhesion assay
6316	43	24	TAH & RSO	HMB & Pain	Healing assay
7541	33	7	Lap Ster	Unwanted Fertility	Healing assay Adhesion assay
5636	34	NA	TAH	morbid fear of pregnancy	Adhesion assay
7638	23	25	Diag Lapscpy	HMB & Endometriosis	Adhesion assay
6832	51	19	STAH & BSO	HMB	ELISA
7672	47	19	TAH	HMB	ELISA
7686	43	16	Laparoscopy	HMB	ELISA
7715	46	45	TAH & BSO	HMB	ELISA
5678	38	4	Diag Lapscpy Hysteroscopy	HMB	ELISA
7741	37	NA	TAH	No cycle constant bleeding	ELISA

Abbreviation: TAH = total abdominal hysterectomy, BSO = bilateral salpingo-oophorectomy, HMB= heavy menstrual bleeding, Diag Lapscpy = diagnostic laparoscopy, Lap Ster = laparoscopic sterilisation, NA = not applicable, RIF = right Iliac Fossa, LIF = left Iliac Fossa, STAH = subtotal abdominal hysterectomy, IMB = irregular menstrual bleeding, RSO = right salpingo-oophorectomy

4.3 Results

4.3.1 Regulation of LOX mRNA expression in peritoneal mesothelial cells by inflammatory cytokines.

In order to mimic the inflammatory response caused by frustrated phagocytosis of macrophages, PMC were treated with TNF-α (10ng/ml) for 48h. LOX was up-regulated nearly 3-fold in the TNF-α-treated group compared to control, although this increase did not quite reach statistical significance (Figure 4.1, p=0.076).

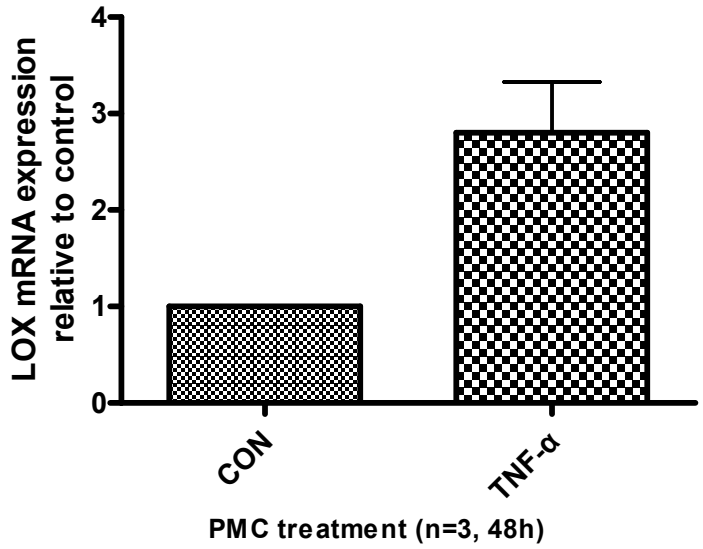

Figure 4.1. Quantitative RT-PCR for LOX mRNA expression in PMC. PMC cells were treated with 10ng/ml TNF-α for 48h. Statistical analysis was conducted by paired t-test (n=3 donors). Bars represent mean (±S.E.M.) values relative to untreated control.

In addition to TNF-α, other cytokines were also tested in our cell culture system, including IL-1α, IL-4, IL-6, IL-8, IL-10, and TGF-β1. Treatments of PMC were conducted for 48h at a concentration of 0.5ng/ml for all the interleukin factors and 2ng/ml for TGF-β1. IL-1α, IL-4 and TGF-β1 were found to significantly increase LOX expression in PMC (Figure 4.2, 2.9±0.18-fold, 2.1±0.08-fold and 2.6±0.05-fold

respectively), whereas the other cytokines had no significantly effect on LOX mRNA. Combined with the outcome from TNF-α treatment, these results indicated that IL-1α was likely the most effective cytokine inducing LOX expression during peritoneal fibrosis, since it induced a 3-fold increase of LOX at 0.5ng/ml, whereas the fold changes induced by TNF-α and TGF-β1, even at a much higher concentration, are less than that induced by IL-1α.

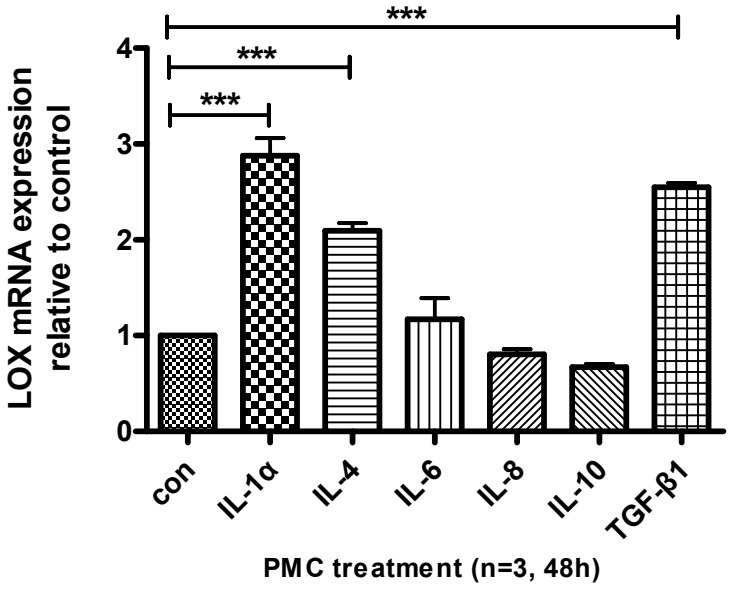

Figure 4.2. Quantitative RT-PCR for LOX mRNA expression in PMC. PMC were treated with IL-1α, IL-4, IL-6, IL-8, IL-10 (0.5ng/ml), and TGF-β1 (2ng/ml) for 48h. Statistical analysis was conducted by repeated-measures-paired-one-way ANOVA (n=3 donors). Bars represent mean (±S.E.M.) values relative to untreated control, ***: $p<0.001$.

TNF-α and IL-1α are believed to induce common signalling networks, whereas TGF-β1 has been shown to signal through a separate pathway. Therefore, we asked whether there was any synergistic effect between TNF-α and TGF-β1, or IL-1α and TGF-β1. To investigate this, PMC were treated with TNF-α and TGF-β1 alone, or in the combination, at the same concentration used above. The result showed that LOX was significantly upregulated by TNF-α alone or the combination of TNF-α and TGF-β1 (Figure 4.3, 2.6±0.52-fold and 3.0±0.20-fold respectively), whereas TGF-β1

alone appeared to increase LOX expression but not significantly (Figure 4.3, 2.1±0.39-fold).

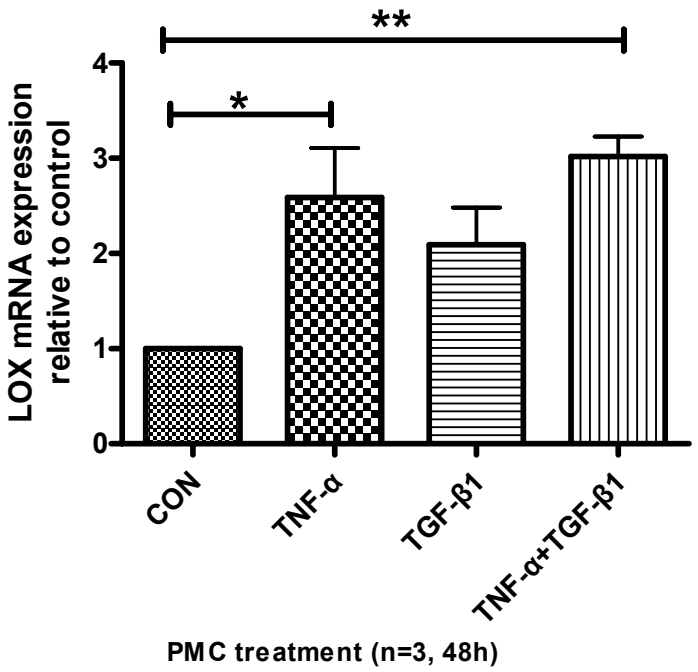

Figure 4.3. Quantitative RT-PCR for LOX mRNA expression in PMC. PMC were treated with TNF-α (10ng/ml) and TGF-β1 (2ng/ml) alone, or in combination: TNF-α+TGF-β1 for 48h. Statistical analysis was conducted by repeated-measures-paired-one-way ANOVA (n=3 donors). Bars represent mean (±S.E.M.) values relative to untreated control, *: $p<0.05$, **: $p<0.01$.

A similar study was carried out by treating PMC with IL-1α and TGF-β1 alone, or in combination. We found that LOX was up-regulated significantly in the IL-1α-treated group compared to control (Figure 4.4, 3.9±0.63-fold). TGF-β1 induced LOX expression in PMC by 2.5±0.67-fold, but this was not significant. There was an additive effect of IL-1α plus TGF-β1 in the up-regulation of LOX (6.4±1.3-fold); this was significant compared to control or TGF-β1 treatments, but not that of IL-1α. Interesting, the combined effect of IL-1α and TGF-β1 was dramatically stronger than that of TNF-α and TGF-β1 (6.4-fold change compared to a 3.0-fold change).

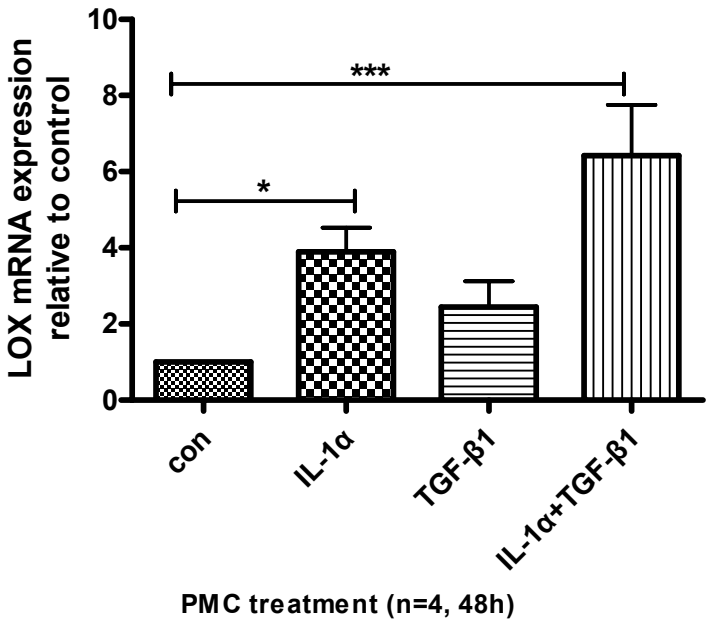

Figure 4.4. Quantitative RT-PCR for LOX mRNA expression in PMC. PMC were treated with IL-1α (0.5ng/ml) and TGF-β1 (2ng/ml) alone, or in combination for 48h. Statistical analysis was conducted by repeated-measures-paired-one-way ANOVA (n=4 donors). Bars represent mean (±S.E.M.) values relative to untreated control, *: $p<0.05$, ***: $p<0.001$.

To test the effect of inflammatory cytokines on gene transcription in more detail, we asked whether IL-1α and/or TGF-β1 would affect procollagen I expression in PMC. Procollagen I mRNA was up-regulated by TGF-β1 in PMC compared to control (Figure 4.5, 3.6±0.95-fold), while IL-1α treatment had only a modest effect (1.7±0.14-fold increase). There appeared an additive effect of combined IL-1α and TGF-β1 treatments of PMC (4.8±1.03-fold), but this was not significant compared to IL-1α or TGF-β1 alone.

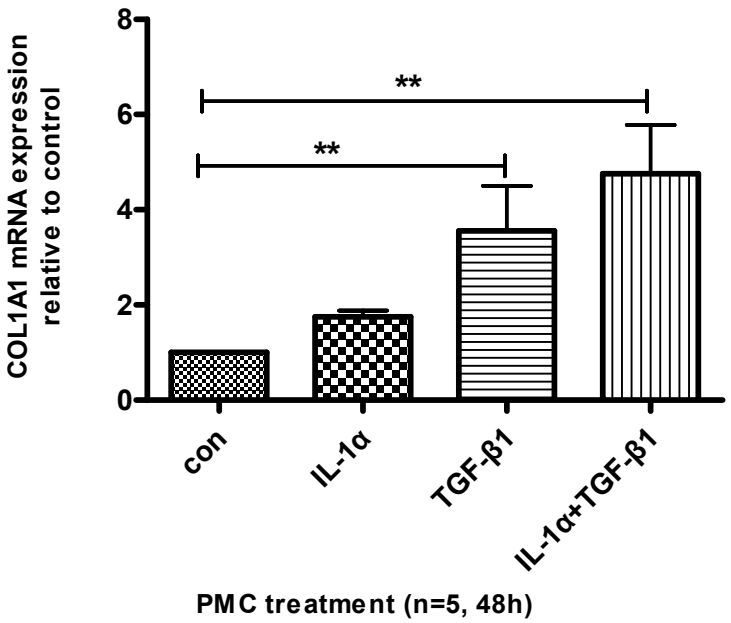

Figure 4.5. Quantitative RT-PCR for COL1A1 mRNA expression in PMC. PMC were treated with IL-1α (0.5ng/ml) and TGF-β1 (2ng/ml) alone, or in combination for 48h. Statistical analysis was conducted by repeated-measures-paired-one-way ANOVA (n=5 donors). Bars represent mean (±S.E.M.) values relative to untreated control, **: $p<0.01$.

These results showed that LOX and procollagen-I expression were regulated by IL-1α and TGF-β1 separately. This suggests that both IL-1α and TGF-β1 are required for promoting collagen deposition during tissue fibrosis. Given that IL-1 shares common signalling pathways with TNF-α, we believe that the combination of IL-1α and TGF-β1 treatments provided a suitable model to mimic the inflammatory response *in vivo* during peritoneal adhesion formation.

4.3.2 Inflammation-induced epithelial-mesenchymal transition of peritoneal mesothelial cells

4.3.2.1 IL-1α and TGF-β1 treatment induces cell morphology change

As we showed above, in order to mimic the inflammatory environment in wound healing, we treated the cells with IL-1α and TGF-β1 for 48h. Under control conditions confluent PMC formed a monolayer of flat polygonal, polarized cells exhibiting typical cobblestone morphology. The cells were connected to each other by tight cell junctions and covered the whole submatrix without any visible intercellular clefts (Figure 4.6A). Treatment of the PMC with IL-1α for 48h resulted in a cell morphologic change, which included loss of cell-cell contacts and an exposure of submatrix. The cells were less rounded in shape and showed a complete disorganization with a loss of cellular polarization (Figure 4.6B). A similar loss of intercellular junctions was found in the TGF-β1-treated PMC. In addition, cells were scattered and adopted a spindle-shaped fibroblastic phenotype (Figure 4.6C), characteristic of an epithelial-mesenchymal transition (EMT). The synergistic effect of IL-1α and TGF-β1 on morphology was even more exaggerated compared with that of each cytokine alone. It was characterized by a more intensive exposure of the submatrix and cell scattering (Figure 4.6D).

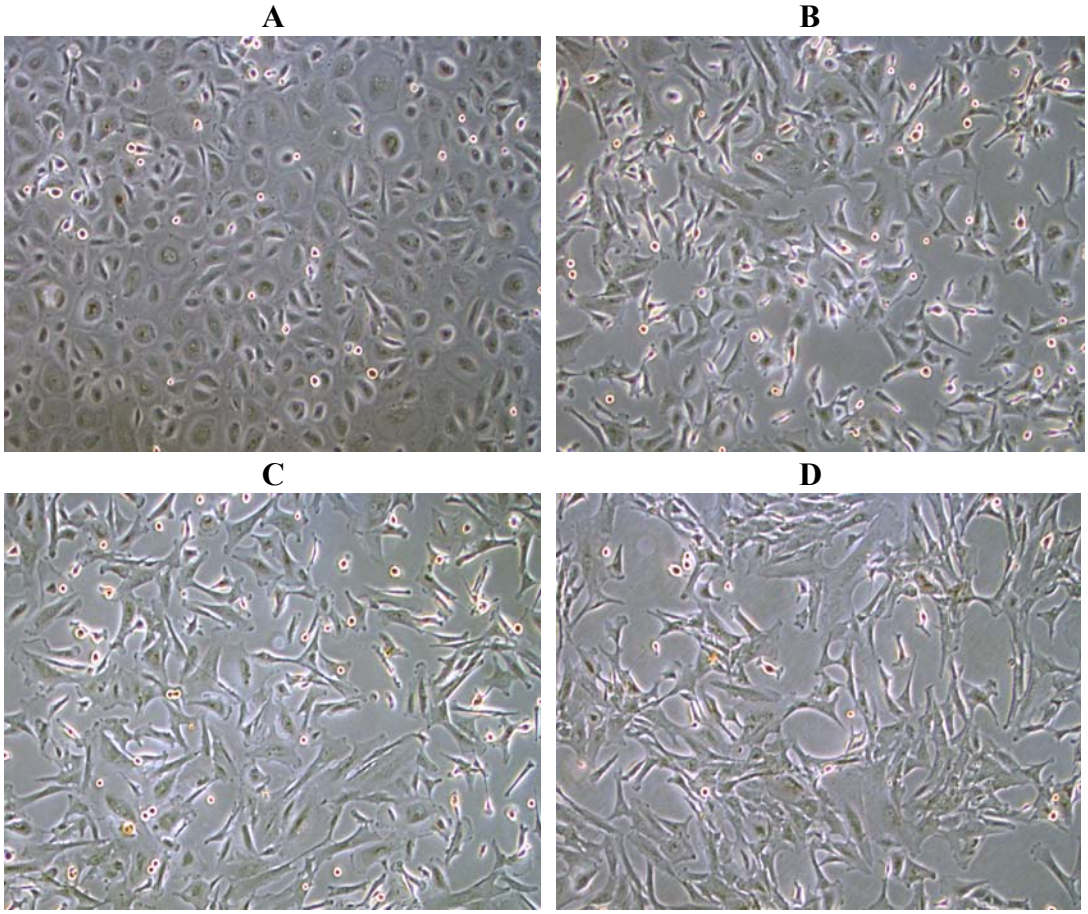

Figure 4.6. Pro-inflammatory factors promote phenotype changes in PMC monolayer. Cells were treated in 6-well plates for 48h in the following groups: A. Control, B. IL-1α (0.5ng/ml), C. TGF-β1 (2ng/ml), D. IL-1α + TGF-β1.

To further confirm the EMT process, E-cadherin and fibronectin mRNA expression in the treated PMC was measured by qRT-PCR. Downregulation of E-cadherin and upregulation of fibronectin are considered as key hallmarks of the EMT process. In the treated PMC (Figure 4.7A), both IL-1α (5-fold) and TGF-β1 (6-fold) were shown to downregulate E-cadherin expression significantly compared to control. A further reduction was found in response to IL-1α and TGF-β1 treatment combined (30-fold compared to control). On the other hand, expression of fibronectin was upregulated by both IL-1α (7-fold) and TGF-β1 (11-fold) in PMC (Figure 4.7B). A further upregulation was found in response to IL-1α and TGF-β1 treatment combined (28-fold compared to control).

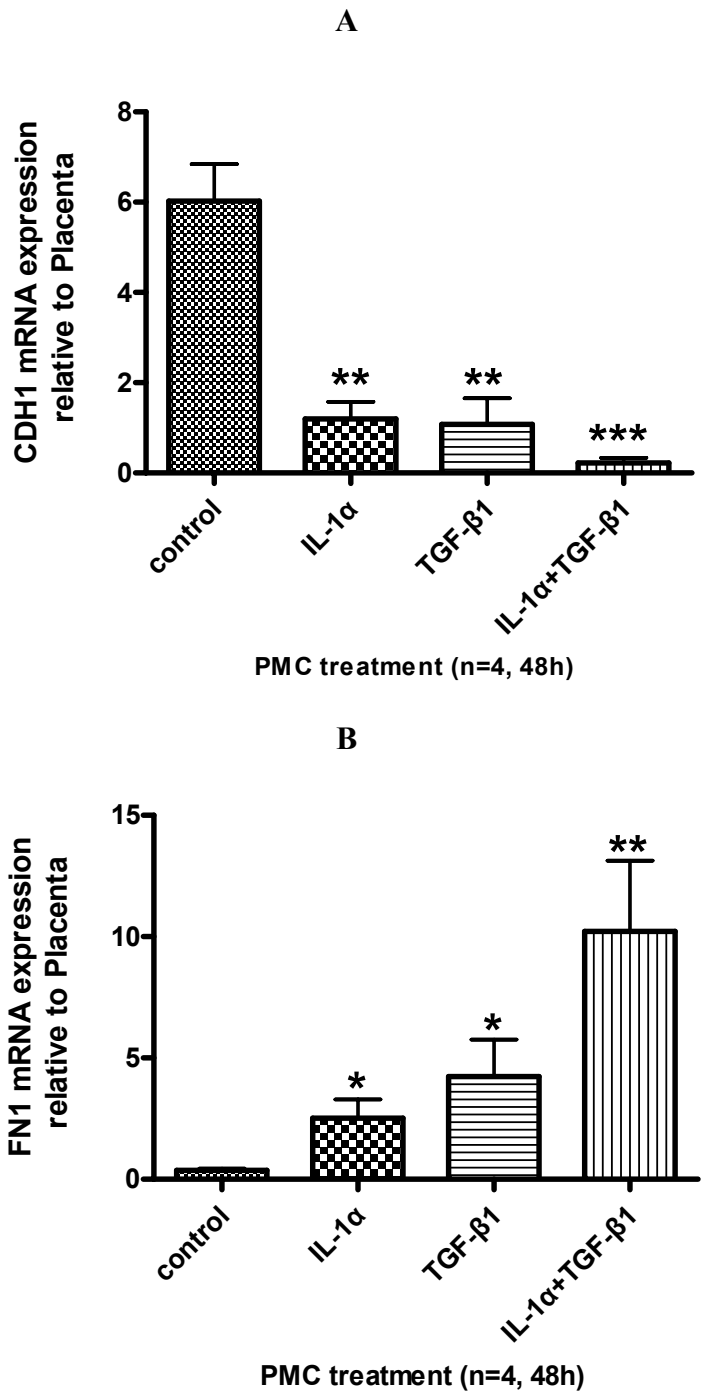

Figure 4.7. EMT process changes E-cadherin and Fibronectin expression in PMC. A: Quantitative RT-PCR for CDH1 (E-cadherin) mRNA expression in PMC. B: Quantitative RT-PCR for FN1 (Fibronectin) mRNA expression in PMC. PMC were treated with IL-1α (0.5ng/ml) and TGF-β1 (2ng/ml) alone, or in combination for 48h. Statistical analysis was conducted by repeated-measures-nonparametric Friedman test and Dunn's multiple comparison test (n=4 donors). Bars represent mean (±S.E.M.) values relative to placenta, *: $p<0.05$, **: $p<0.01$, ***: $p<0.001$ compared to control.

4.3.2.2 EMT-promoted cell migration

We questioned whether the EMT process would promote cell migration. Cell motility is considered to have an important role in wound healing, as it could affect cell infiltration and cell aggregation at the wound site. In our study, we performed an *in vitro* wound healing assay to investigate the effect of IL-1α and TGF-β1 on PMC migration. We observed an almost complete closure of the wound after 16 h in the IL-1α+TGF-β1 treated group, while the control group still had a large gap in the central area (Figure 4.8A). Because LOX has been shown to be essential for hypoxia-induced cancer metastasis, indicating a role of LOX in promoting cancer cell migration, we hypothesized that the up-regulation of LOX by pro-inflammatory factors on PMC could also contribute to such enhanced cell motility. In order to confirm this, PMC were pretreated with BAPN alone or in combination with IL-1α+TGF-β1 to completely inhibit LOX activity. BAPN-treated PMC showed a similar rate of wound closure to the control group, while the rate of wound closure in the IL-1α+TGF-β1+BAPN group was also no different compared to the IL-1α+TGF-β1 group. We quantified the cell migration by measuring the distance between the edges of the wound (Figure 4.8B). The results indicated that cell migration was promoted by IL-1α and TGF-β1 treatment, whereas inhibition of LOX did not seem to be critically involved in this process.

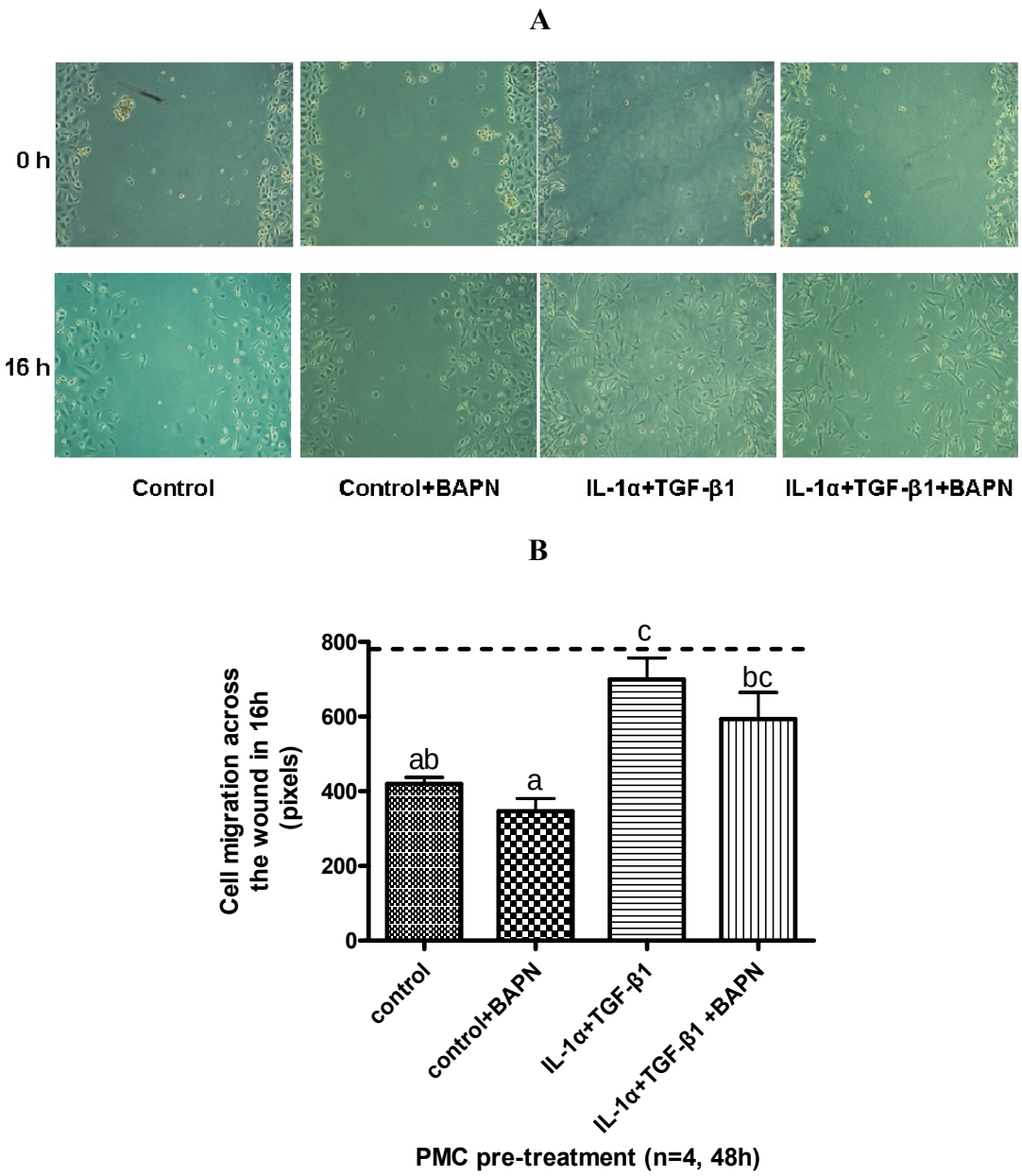

Figure 4.8: *In vitro* wound healing assay. PMC were treated with a combination of IL-1α (0.5ng/ml) and TGF-β1 (2ng/ml) in the presence or absence of BAPN (500μM). A: Photomicrograph of PMC 0 and 16 h after wounding. The top panel shows the initial wound in each group; the bottom panel is the wound after 16h. B: Quantification of the effect of IL-1α+TGF-β1 on PMC migration in wound healing assay. Broken line indicates the initial wound width. Statistical analysis was conducted by repeated-measures-paired-one-way ANOVA, values with no superscript letter in common are statistically different from each other (n=4 donors). Bars represent mean (±S.E.M.) values of each group, $p<0.05$.

4.3.2.3 EMT enhances Cell-ECM adhesion

We then examined whether EMT also enhanced the adherence of PMC to ECM substances. We first demonstrated that expression of integrin α5, an important fibronectin receptor, was induced by IL-1α (2-fold) and TGF-β1 (2.4-fold) in PMC. Moreover, IL-1α+TGF-β1 treatment significantly upregulated the expression of integrin α5 in PMC (Figure 4.9, 3-fold). Later on, PMC were pre-treated with IL-1α+TGF-β1 for 48h, and then seeded on to fibronectin-coated 12-well plates. After 1 h incubation, unattached PMC were washed off, and photomicrographs of each treatment groups were taken. More PMC were found to attach to fibronectin in the IL-1α+TGF-β1-treated group compared to the control (Figure 4.10A). The effect of LOX on cell-ECM adhesion was also tested by adding BAPN during pretreatment. However, there was no effect of BAPN on cell-ECM adhesion in either the control group or the IL-1α+TGF-β1-treated group (Figure 4.10A). To quantify cell adhesion, cell counts were performed on the attached cells after trypsinisation. The results indicated that EMT-transformed PMC could more efficiently adhere to the ECM component than normal PMC, while inhibition of LOX activity had no effect on reducing cell adherence (Figure 4.10B).

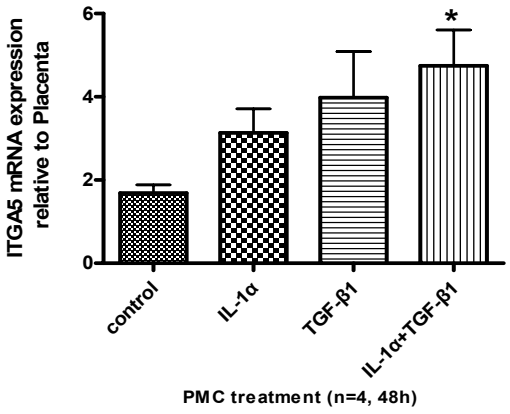

Figure 4.9. Quantitative RT-PCR for ITGA5 (Integrin α5) mRNA expression in PMC. PMC were treated with IL-1α (0.5ng/ml) and TGF-β1 (2ng/ml) alone, or in combination for 48h. Statistical analysis was conducted by repeated-measures-nonparametric Friedman test (n=4 donors). Bars represent mean (±S.E.M.) values relative to placenta, *: $p<0.05$ compared to control.

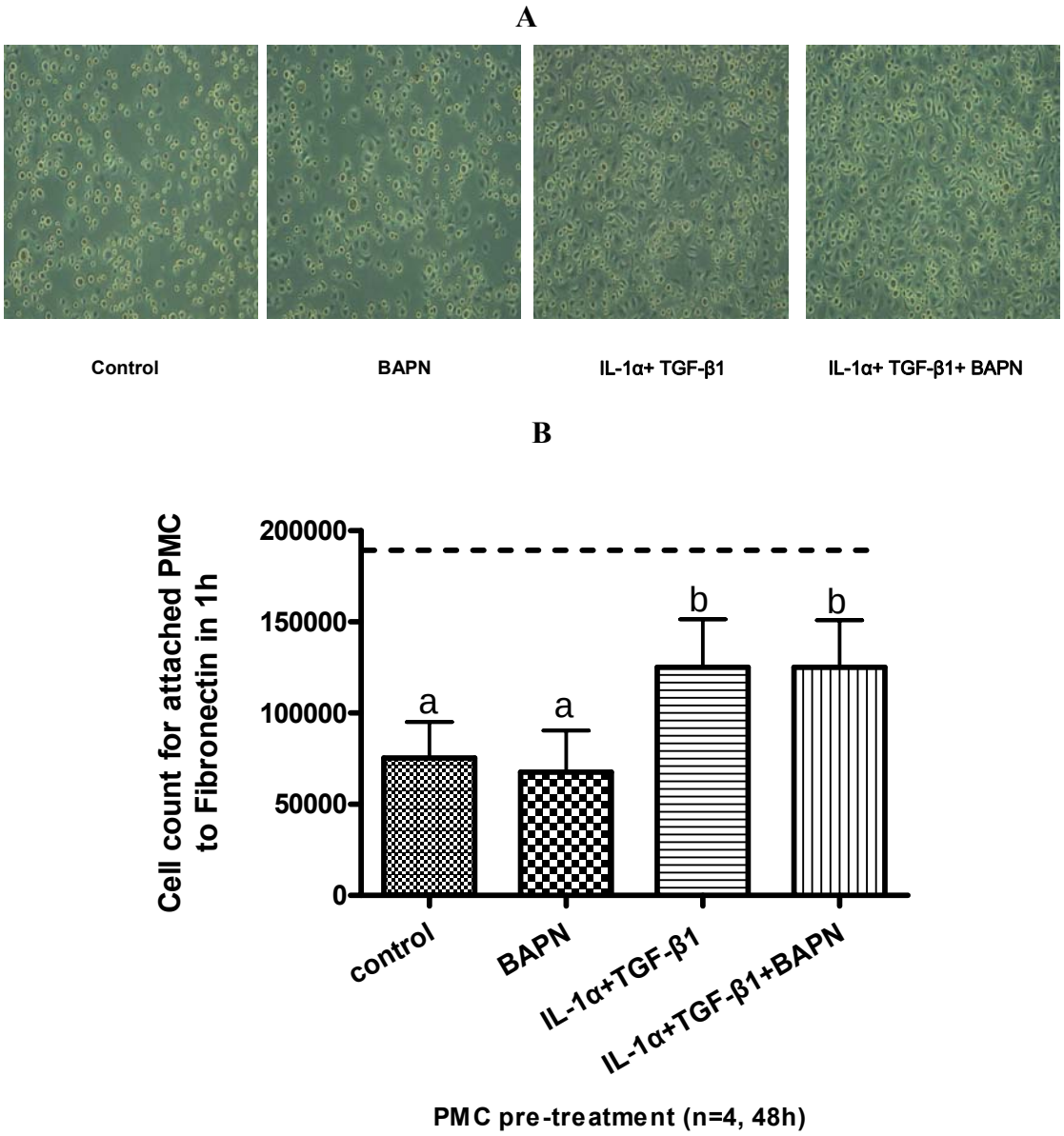

Figure 4.10. ***In vitro*** **Cell-ECM adhesion assay.** PMC were treated with a combination of IL-1α (0.5ng/ml) and TGF-β1 (2ng/ml) in the presence or absence of BAPN (500μM). A: Photomicrograph of *in vitro* cell-ECM adhesion assay on PMC. From left to right: control, BAPN, IL-1α+TGF-β1, IL-1α+TGF-β1+BAPN. B: Quantification of the effect of IL-1α+TGF-β1 on PMC-ECM adhesion *in vitro.* Broken line indicates the initial cell number added. Statistical analysis was conducted by repeated-measures-paired-one-way ANOVA, values with no superscript letter in common are statistically different from each other (n=4 donors). Bars represent mean (±S.E.M.) values of each group, $p<0.05$.

4.3.3 Cytokine production from peritoneal mesothelial cells

4.3.3.1 IL-1α production from nanotube (NT)-treated PMC

As shown above, IL-1α is likely the most potent cytokine to induce LOX expression in PMC. However, previous results showed that it was TNF-α rather than IL-1α that was secreted by NT-treated macrophages. The origin of IL-1α required further investigation. As the main cell type to maintain homeostasis within the abdominal cavity, PMC can produce many cytokines in response to stress, inflammation or other stimuli. Therefore, we first investigated IL-1α production from PMC in response to NT. PMC were treated with increasing doses of NT (0, 5, 10, and 20μg/ml). Levels of IL-1α were measured in the culture medium after 48h. IL-1α production was undetectable in untreated cells and the production of IL-1α in response to NT was not dose dependent (Figure 4.11). However, due to a limitation of sample, only one independent experiment was done on the PMC.

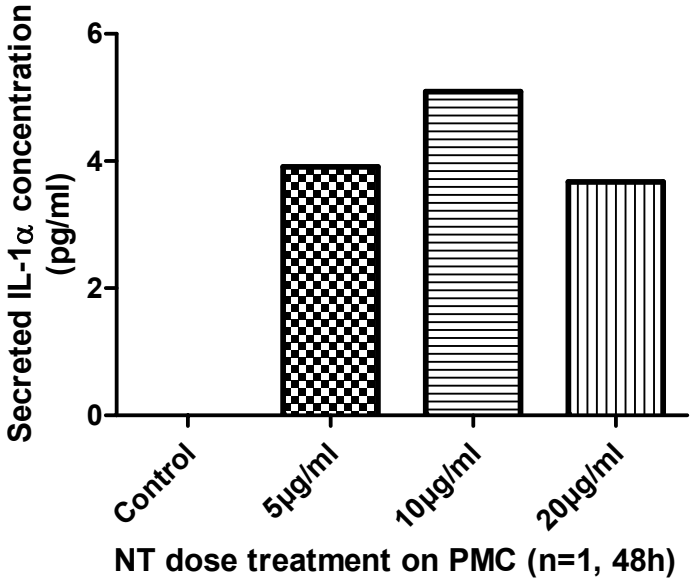

Figure 4.11. Secreted IL-1α production of PMC in response to NT treatment for 48h. Insufficient independent replicates (n=1 donor) did not allow statistical analysis.

4.3.3.2 IL-1α production from cytokines-treated PMC

Since TNF-α production was induced *in vitro* from NT-treated macrophages and TNF-α was shown to induce other cytokines expression in an autocrine fashion, we questioned whether such elevated TNF-α could contribute to a local IL-1α secretion from PMC. Therefore, PMC were treated with increasing doses of TNF-α (0, 5, 10, 20, 50, and 100ng/ml). IL-1α secretion was evaluated in condition medium by ELISA after 24h of treatment. However, TNF-α did not induce IL-1α secretion to a biologically relevant level, as the highest concentration detected was 5pg/ml in the 50ng/ml TNF-α-treated group (Figure 4.12). This suggested that TNF-α alone was not able to stimulate PMC to secrete IL-1α. Due to a limitation of sample, only one independent experiment was done on the PMC.

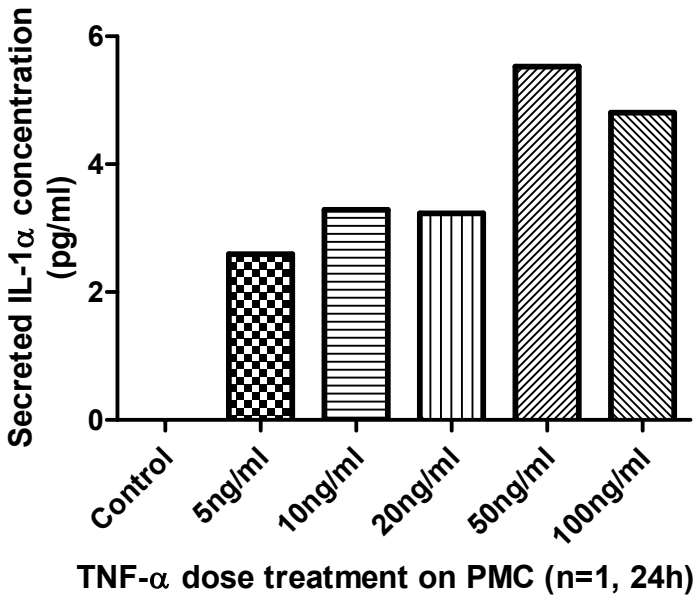

Figure 4.12. Secreted IL-1α production of PMC in response to TNF-α treatment for 24h. Insufficient independent replicates (n=1 donor) did not allow statistical analysis.

Cytokine orchestration is quite common in chronic inflammation due to the redundancy of these inflammatory factors. The combined effect of various cytokines can provide a much more effective stimulation of target cells. In the case of our *in*

vivo model, TGF-β1 could be another critical cytokine promoting peritoneal fibrosis, as dramatic tissue remodelling has been reported in the diaphragm. Therefore, IL-1α production was tested in PMC treated with TNF-α and TGF-β1 alone, or in combination. The results showed that neither TNF-α nor TGF-β1 alone caused a significant elevation of IL-1α secretion compared with control (Figure 4.13A, 14.9±1.09pg/ml and 9.3±1.17pg/ml respectively). However, TNF-α and TGF-β1 had a significant synergistic effect increasing IL-1α secretion to 64.7±16.55pg/ml.

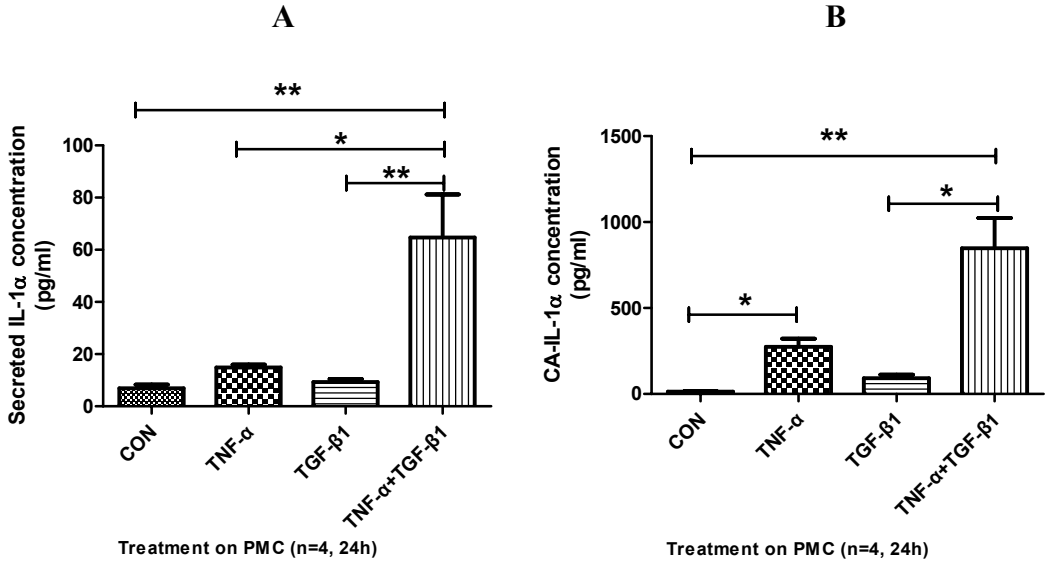

Figure 4.13. ELISA of IL-1α production from PMC treated with TNF-α (10ng/ml), TGF-β1 (2ng/ml), and TNF-α+TGF-β1 for 24h. A: Secreted IL-1α concentration in the culture medium. Statistical analysis was conducted by repeated-measures-paired-one-way ANOVA (n=4). Bars represent mean (±S.E.M.) values of each group, *: $p<0.05$, **: $p<0.01$. B: cell-associated IL-1α (CA-IL-1α) concentration in the cell lysate. Statistical analysis was conducted by repeated-measures-noparametric Friedman test, group comparisons were done by Dunn's multiple comparison test (n=4 donors). Bars represent mean (±S.E.M.) values of each group, *: $p<0.05$, **: $p<0.01$.

As discussed in section 1.4.3.1, IL-1α can be active as both secreted protein and membrane-associated protein. Thus, we tested the cell-associated IL-1α (CA-IL-1α) production of PMC from the same TNF-α- and TGF-β1-treated cells. The same ELISA kit was used to measure the level of IL-1α in the cell lysate (CA-IL-1α). The data showed that both TNF-α and TNF-α+ TGF-β1 treatments significantly increased

CA-IL-1α protein within the PMC (Figure 4.13B). In addition, the level of CA-IL-1α found within the cell was much higher than the amount of secreted IL-1α. TNF-α induced CA-IL-1α up to 274.7±47.23pg/ml (Figure 4.13B) compared to the secreted level of IL-1α (14.9±1.09pg/ml). TGF-β1 also induced the production of CA-IL-1α (Figure 4.12B, 91.64±21.94pg/ml), while only 9.3±1.17 pg/ml was found for the secreted form. In the TNF-α+TGF-β1-treated group, a similar synergistic effect was found for the secreted form, but at a much higher level (848.1±176.3pg/ml compared to 64.7±16.55pg/ml). Overall, between 10- and 20-fold higher IL-1α levels were found to be as the cell-associated form compared to the secreted form. In summary, TNF-α and TGF-β1 can induce the production of CA-IL-1α within the PMC on their own, while neither of them was able to dramatically increase the level of secreted IL-α. However, the synergistic action of TNF-α+TGF-β1 was found not only to be a much more potent inducer of CA-IL-1α expression, but also of its secreted form recovered in the conditioned medium.

4.3.4 Suppression of the TNF-α signalling pathway by inhibition of IL-1.

As discussed in section 1.4.3.1, CA-IL-1α has equal biological activity, which can be transferred to the cell membrane and mediate local inflammatory responses. Therefore, we hypothesized that the elevated CA-IL-1α level observed above could also contribute to the inflammatory response. To confirm this hypothesis, MeT-5A cells (a PMC cell line) were treated with TNF-α (10ng/ml) and TGF-β1 (10ng/ml) in the presence or absence of the IL-1 receptor antagonist (IL-1ra, 100ng/ml). Treatments of IL-1α (2ng/ml) plus or minus IL-1ra (100ng/ml) on MeT-5A cells were used as a positive control in the experiment. MeT-5A cells were used due to a shortage of primary PMC cells from sample collections. The result is shown in Figure 4.14A. IL-1α, TNF-α and TGF-β1 all induced LOX expression significantly (6-fold, 4-fold and 12-fold respectively compared to the control group). The addition

of IL-1ra suppressed the effects of IL-1α and TNF-α significantly (70% and 56% respectively) whereas there was no suppression of TGF-β1-treatment. A similar effect was confirmed in one PMC sample as shown in Figure 4.14B.

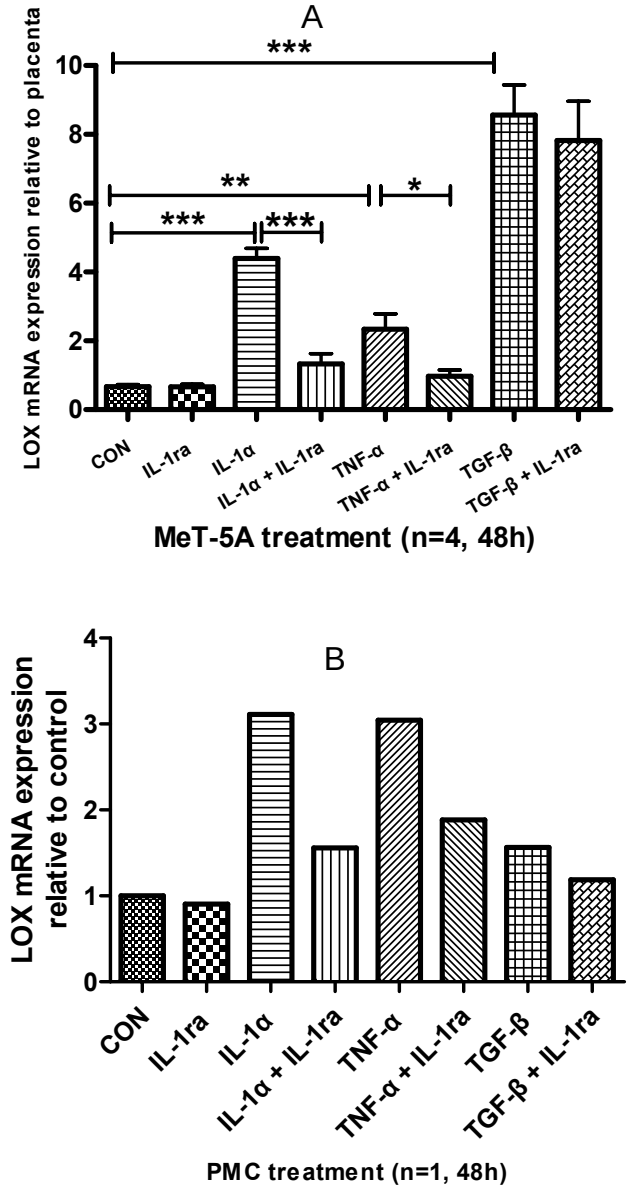

Figure 4.14. Quantitative RT-PCR for LOX mRNA expression in MeT-5A cells and PMC. A. MeT-5A cells were treated with IL-1α (2ng/ml), TNF-α (10ng/ml) and TGF-β1 (10ng/ml) in the presence or absence of IL-1ra (100ng/ml) for 48h. Statistical analysis was conducted by one-way ANOVA (n=4), Bars represent mean (±S.E.M.) values relative to placenta, *: $p<0.05$, **: $p<0.01$, ***: $p<0.001$. B. PMC were treated with IL-1α (0.5ng/ml), TNF-α (10ng/ml) and TGF-β1 (2ng/ml) in the presence or absence of IL-1ra (25ng/ml) for 48h. Value relative to control. Insufficient independent replicates (n=1 donor) did not allow statistical analysis.

4.4 Discussion

In Chapter 3, we demonstrated that LOX played an important role in the formation of peritoneal fibrosis by regulating collagen deposition. In addition, we further confirmed that PMC express high levels of LOX mRNA, while macrophages have little LOX expression. Therefore PMC, as an important cell type to maintain homeostasis of the abdominal cavity, can also be pro-fibrotic by producing LOX in response to inflammatory stimuli. In this Chapter, we have demonstrated that LOX mRNA can be induced by several cytokines, including IL-1α, IL-4, TNF-α and TGF-β1. However, only IL-1α (0.5ng/ml) was shown to be the most potent inducer of LOX expression. In contrast, the effects of TNF-α and TGF-β1 were weaker than that of IL-1α, even when used at much higher concentrations than IL-1α (TNF-α: 10ng/ml, TGF-β1: 2ng/ml, compared to IL-1α: 0.5ng/ml). IL-4 is considered as a pro-fibrotic mediator in fibroblasts, being twice as effective as TGF-β (Fertin et al., 1991). It also functions as an important mediator that can activate macrophages, differentiating them into wound-healing macrophages (Loke et al., 2007). However, IL-4 has also been considered as an anti-inflammatory cytokine. For example, IL-4 was shown to increase 3β-HSD activity in ovarian surface epithelial (OSE) cells, resulting in an intracrine generation of progesterone (Papacleovoulou et al., 2009). Furthermore, IL-4 was shown to suppress IL-1α-induced cyclooxygenase-2 mRNA expression, an important inflammatory-related factor (Kurumbail et al., 1996), in OSE cells (Papacleovoulou, 2009). Given the similarity between PMC and OSE cells, IL-4 might also exert anti-inflammatory effects on PMC. Thus, the effect of IL-4 in peritoneal fibrosis could be conflicting. Since previous studies have not shown an association between IL-4 and postoperative adhesion, the effect of IL-4 was not investigated further in this thesis.

Cytokine orchestration is quite common during the inflammatory process due to their redundancy and pleiotropic function. Synergistic effects of different cytokines could co-regulate target genes expression. TNF-α and IL-1α have long been suggested to share common signalling pathways through NF-κB and AP-1 pathways (see section 1.4.3.1 and 1.4.3.2), while TGF-β1 has been shown to regulate gene expression through Ras and Smad signaling (see section 1.4.3.3). Therefore, possible synergistic effects of TGF-β1 with TNF-α or IL-1α were tested on PMC. No combined effect of TNF-α+TGF-β1 was found on LOX expression, whereas an additive up regulation was found in response to IL-1α+TGF-β1. Therefore, in this case, cross-talk between different signalling pathways did not appear to cause significant changes in IL-1α-induced LOX expression in PMC. It further confirmed that IL-1 could be the most potent cytokine to induce LOX expression in PMC during inflammation. In contrast, expression of procollagen-I mRNA in PMC was mainly induced by TGF-β1, IL-1α being less effective. Again, no combined effect of IL-1α+TGF-β1 was found compared to the TGF-β1 alone group. Previous studies had shown that overexpression of procollagen-I was involved in many fibrotic diseases (Kaimori et al., 2007; Bergeron et al., 2003). These results suggest a crucial role of TGF-β1 in collagen production from PMC. Since procollagen-I is the precursor of mature collagen I, the main substrate for LOX enzyme, it indicated that IL-1α and TGF-β1 were both needed for collagen deposition during peritoneal fibrosis.

In contrast, TNF-α appeared less involved in this pathologic progression, since it did not exert a dramatic effect even at levels of 10ng/ml, which is far higher than physiological levels. However, the combination of TNF-α+TGF-β1 stimulated secreted IL-1α production from PMC. More interestingly, TNF-α alone and TNF-α+TGF-β1 can stimulate the production of the cell-associated form of IL-1α within PMC to a level dramatically higher than the secreted level. Due to the unique way that IL-1α is processed and secreted (section 1.4.3.1), the cell-associated IL-1α

could be the IL-1α precursor with biological activity. In contrast, the secreted form of IL-1α detected in the culture medium could be either the mature IL-1α or IL-1α precursors released from dead cells, since TNF-α and TGF-β1 can induce cell death through cell necrosis or cell apoptosis. It has been demonstrated in previous studies that TNF-α can induce IL-1 expression in fibroblasts, which requires the participation of mitogen-activated protein kinase kinase 3 (MKK3) (Wysk et al., 1999). On the other hand, TGF-β1 has also been shown to activate MKK3/6 through TAK1 (Xu et al., 2009). Therefore, the synergistic effect of TNF-α and TGF-β1 on IL-1α production could be due to a co-activation of MKK3 in PMC.

IL-1α precursors can exert their biological activity as a cell surface-bound protein (membrane-associated IL-1, MA-IL-1). Although there was no evidence that all the cell-associated IL-1α detected in cell lysate was membrane-associated, we assume that such elevation of IL-1α is a natural response of cells to create a local inflammatory environment rather than causing a systemic inflammation. In addition, we hypothesized that TNF-α signalling might be partially mediated by MA-IL-1. To confirm the concept, we showed that inhibition of IL-1 action with IL-1ra can suppress TNF-α induced LOX expression but that not of TGF-β1 in MeT-5A cells. Meanwhile, IL-1α was not detected in the medium from TNF-α-treated MeT-5A cells. However, since the IL-1β content of the culture medium has not been evaluated, TNF-α may exert its effect by increasing IL-1β production. However, MeT-5A cells do not represent primary cells in several aspects. For example, TGF-β1 induces EMT in PMC but not in Met-5A. Therefore, the same experiment needs to be carefully confirmed in PMC. In addition, the expression of MA-IL-1α needs to be confirmed by flow cytometric analysis and its bioactivity also requires further investigation.

From the findings above, we assume that TNF-α could be an initial signal released at the first stage of peritoneal fibrosis in our *in vivo model*. Such inflammatory effect

may be kept locally to avoid the induction of persisted systemic inflammation. However, if such a response existed long term in combination with other cytokines such as TGF-β1, systemic inflammation can be induced by elevating other key secreted inflammatory mediators such as IL-1, leading to tissue fibrosis. Support for this mechanism is that overexpression of TNF-α in the rat peritoneum leads to a transient pathological change to the peritoneum, including dramatic angiogenesis together with collagen deposition, whereas overexpression of IL-1β induced a persisting vasculogenesis with submesothelial fibrosis (Margetts et al., 2002). In addition, overexpression of IL-1β has been demonstrated to lead to progressive fibrosis in the lung (Kolb et al., 2001), while overexpression of TNF-α leads only to a mild fibrosis (Sime et al., 1998).

In contrast, TGF-β1 signalling was shown to be an essential complement for IL-1 with respect to fibrosis progression. Therefore, the combination of TGF-β1 and IL-1 is an ideal model to reproduce the complex inflammatory environment and profibrotic stimuli present during peritoneal fibrosis. This model has also been used in other studies of peritoneal dialysis-induced peritonitis (Strippoli et al., 2008; Yanez-Mo et al., 2003). As discussed above, in addition to regulating PMC gene expression at the transcriptional level, IL-1α and TGF-β1 caused phenotypic changes of PMC both on their own and in combination. TGF-β1 is a well known inducer of epithelial-mesenchymal transition (EMT). In the current study, IL-1α also appeared to induce EMT-like changes in PMC. Both IL-1α and TGF-β1 caused downregulation of E-cadherin and upregulation of fibronectin mRNA levels in PMC, hallmarks of the EMT process. Furthermore, the combination of these two cytokines provoked a further change in cell morphology, which was more intensive than any of the effects on their own. An additive effect of IL-1α and TGF-β1 treatment on E-cadherin reduction and fibronectin upregulation was also found. The same treatment has also been used to induce EMT on PMC (Strippoli et al., 2008;

Yanez-Mo et al., 2003), confirming that EMT is an important process involved in peritoneal fibrosis. It can disrupt intercellular junctions and increase mesenchymal features in the PMC. Eventually PMC are transformed into fibroblast-like cells with increased motility, cell-ECM adhesion ability, and fibrogenic features. A series of interlinked activation processes of IL-1α and TGF-β1 might account for such dynamic cell behaviors. For example, TGF-β is shown to activate Rho-like GTPase including Rho, Rac and Cdc42 which are key regulators involved in cell migration (Vicente-Manzanares et al., 2005; Xu et al., 2009). During EMT, TGF-β induces RhoA expression, which directly increases cell contractility (Cho and Yoo, 2007; Pellegrin and Mellor, 2007). Activation of RhoA was also shown to regulate mDia1 promoting actin polymerization, which controls protrusion of the cells during migration (Vicente-Manzanares et al., 2005). On the other hand, EMT is associated with an increased cell-ECM adherence, which might be associated with the upregulation of several integrins molecular. We showed that integrin-α5 was upregulated by both IL-1α and TGF-β1. Integrin-α5β1 is a well know receptor binding to fibronectin (Morgan et al., 2009). Therefore, the enhanced adherence we found in the cell-ECM adhesion assay could be due to the increased integrin-α5 level. In addition, expression of integrin-α5β1 was also associated with RhoA-mediated contractility and random cell migration (Danen et al., 2005; White et al., 2007). Furthermore, the upregulation and activation of integrins were shown to induce the autophosphorylation of focal adhesion kinase (FAK) (Mitra and Schlaepfer, 2006) which further regulated adhesion turnover and membrane protrusion during cell migration (Huveneers and Danen, 2009).

In previous studies, LOX had also been shown to regulate cell motility and cell-ECM adhesion in cancer cells (Payne et al., 2005) and vascular smooth muscle cells (Li et al., 2000). The underlying mechanism involved the activation of FAK and Src kinase, two key proteins involved in cell adhesion formation and turnover. It has been shown

that the H_2O_2 product of amine oxidation by LOX is critical in promoting such a response. H_2O_2 has long been known to cause changes in cell adhesion and motility (Sellak et al., 1994; Mahabeleshwar and Kundu, 2003). Removal of H_2O_2 by catalase suppressed cell migration and cell-ECM adhesion in both invasive cancer cell lines and vascular smooth muscle cells (Payne et al., 2005; Li et al., 2000). Hence, the effect of LOX on cell motility and adhesion ability was also tested in our *in vitro* model. However, inhibition of LOX was not found to suppress the IL-1α+TGF-β1-induced rise of cell-ECM adhesion or cell motility. One explanation could be that the FAK and Src kinase were already activated by the upregulation of integrins. The signal induced by H_2O_2 is not the key mechanism to promote cell adhesion or migration in our model.

In summary, this Chapter shows that the combination of IL-1α and TGF-β1 can be a suitable *in vitro* model to mimic the inflammatory response during peritoneal fibrosis. Treatment of PMC with IL-1α+TGF-β1 induced the expression of LOX and pro-collagen I which are involved in the progression of fibrosis. However, due to a limitation in numbers of viable samples, a single dose and time were chosen for the experiment. The lack of dose treatments and time-points may cause misleading conclusions when comparing effects of different cytokines. In addition, up-regulation of procollagen needs to be confirmed at the protein level when more viable samples are obtained; however, a longer period of treatment seems to be required to obtain a detectable level of procollagen protein in the medium (Clarke et al., 2010). IL-1α+TGF-β1 treatment caused EMT of PMC. These transformed cells have enhanced cell motility and are more adherent to fibronectin. These findings provide a likely explanation for the centripetal cell migration and incorporation of free-floating mesothelial cells that are widely accepted mechanisms for peritoneal repair. Moreover, results showed an IL-1-mediated autocrine signaling network of PMC in response to TNF-α, which could be a likely mechanism to regulate the switch between local and systemic inflammation.

Chapter 5

Anti-inflammatory effects of glucocorticoids on peritoneal mesothelial cells and ovarian surface epithelial cells

5.1 Introduction

In humans, not all injured tissue is healed with associated scarring. One example is the repair of ovary after each ovulatory cycle. The human ovary is covered with a thin layer of ovarian surface epithelium that separates the ovary from other organs within the lower abdominal cavity. Ovarian surface epithelial (OSE) cells are regularly subjected to ovulation-associated injury which is comparable to an inflammatory reaction (Espey, 1994). Such an inflammatory reaction can cause serious proteolytic damage to the ovarian surface (Murdoch et al., 2001). However, despite the dramatic structural damage to the surface of the ovary and underlying connective tissue caused by ovulation, the ovary always heals without residual scarring. Such remarkable postovulatory repair helps maintain the function of ovary, ensuring adhesions do not form with associated structures such as the Fallopian tube, and prepares for the next ovulation. Therefore, it suggests that there might be a unique mechanism in the ovary to repair this natural damage without scarring. Understanding of this mechanism might inform treatments to avoid other fibrotic conditions, including post-operative adhesions. PMC and OSE cells share many common characteristics. Both form an inconspicuous monolayer of squamous-to-cuboidal mesothelium that lies on a basement matrix. They arise in the embryo from the lateral plate mesoderm (Michailova and Usunoff, 2006) and share equivalent homeostatic functions (Ross et al., 1998). However, despite these common origins, there are also some significant differences between them. PMC are dominated by microvilli on the surface to increase the mesothelial surface area (Dobbie, 1990). These may influence absorption or secretion across the cell surface and play a role in the trapping of secreted proteins or glycoproteins. In contrast, OSE does not have microvilli. Additionally, monthly ovulation causes the release of the oocyte from the ovarian cortex. This process is always accompanied by an elevated local production of ovarian steroids. For example, the preovulatory follicle and

corpus luteum, the major sites of ovarian hormone production, can produce estrogen (Hillier et al., 1994) and progesterone (Rekawiecki et al., 2008), respectively. Such natural processes associated with ovulation create a steroid-rich environment around the ovary that is different from the environment within the abdominal cavity. Although OSE cells are unlikely to be a site of *de novo* steroid biosythesis (Rae and Hillier, 2005; Rae et al., 2004b), they can be involved in further steroid metabolism through expression of steroid dehydrogenases/reductases (SDR) which convert circulating bioinert steroids into bioactive forms (Okamura et al., 2003; Rae and Hillier, 2005). Many steroids circulate as bioinert precursor forms. They differ with respect to the redox state of important hydroxyl moieties, which determine the ability of these steroids to bind and activate their cognate receptors. For example, it has been shown that OSE cells can convert bioinert cortisone into bioactive cortisol by expressing 11βHSD-1 as discussed in section 1.4.4. Moreover, IL-1α was shown to induce time- and dose-dependent enhancement of 11βHSD-1 enzymic activity in OSE cells, whereas no changes were found in 11βHSD-2 expression that converts cortisol back to cortisone (Rae et al., 2004b). Therefore, the inflammatory response enhances the ability of OSE cells to produce anti-inflammatory steroid. Although the PMC exhibit similar characteristics to OSE cells in their transcriptional level activities with respect to local cortisol conversion, the actual 11βHSD-1 enzyme activity of OSE cells is much higher than that of PMC in both its normal quiescent phenotype and in response to IL-1α (Fegan et al., 2008). Given the finding that there is commonly 3-10 times more cortisone than cortisol in the local ovarian environment (Kushnir et al., 2009), it suggests that OSE might be more effective than PMC to create a local elevated level of cortisol based on such abundant supply of inactive cortisone.

It has been shown that both cortisol and progesterone can act as anti-inflammatory steroids. The anti-inflammatory mechanism underlying cortisol action was discussed

in section 1.4.4. Progesterone shares a similar mode of action with cortisol, which includes binding to its cognate receptor (progesterone receptor, PR) and ligand-activated suppression of inflammation; however, its effect is less potent than cortisol (van der Burg and van der Saag, 1996). Receptors for both progesterone and cortisol (PR and GR) are expressed by PMC (Fegan et al., 2008) and OSE cells (Li et al., 2003). In addition, IL-1 was shown to upregulate GR but not PR in OSE cells (Rae et al., 2004a), which could further enhance the action of cortisol. Therefore, the local production of these steroids provides an anti-inflammatory environment around the ovary after ovulation that could help to minimize the inflammatory response and maintain tissue homeostasis. In contrast, the peritoneum has no such protective mechanism to counteract the inflammatory response caused by surgery, hence exposing it to adhesion formation.

We hypothesized that scar-free healing of the ovary is a consequence of the anti-inflammatory steroid environment created by ovulation. Cortisol is considered as an important anti-inflammatory factor, which can be elevated in the ovary compared with the circulation due to enhanced local 11βHSD-1 enzyme activity (Fegan et al., 2008). The understanding of such a mechanism may assist in finding ways to prevent post-operative adhesions.

5.2 Materials and Methods

Investigation of the effect of cortisol (F) on PMC and OSE cells was assessed using primary PMC and OSE monolayers as described in Chapter 2. Treatments of several inflammatory cytokines were conducted on cell monolayers for 24 h or 48 h in serum-free medium. RNA was extracted from the experimental groups, and quantitative real-time PCR was used to evaluate gene expression in the treatment groups. ELISA was performed on cell lyasates and conditional medium as described

in section 2.4. Extracellular LOX activity was tested in the conditional medium by fluorometric-based assay (section 2.6). The basic clinical profile of patients involved with the respective assays performed on each are presented in Table 5.1.

Table 5.1. Clinical profile of patients used for respective assays

Patient Code	Age	Cycle day	Surgery	Reason for surgery	Study
6848	54	NA	TAH & BSO	Fibroids & HMB	mRNA
7672	47	19	TAH	HMB	mRNA
7539	40	27	TAH	HMB & Pain	mRNA
7532	27	4	Diag Lapscpy	LIF pain	mRNA
7538	21	NA	Diag Lapscpy	Pelvic pain	mRNA
7541	33	7	Lap Ster	Unwanted Fertility	mRNA
6321	26	22	Diag Lapscpy	RIF Pain	mRNA
7559	43	4	TAH	HMB	mRNA
7613	48	26	STAH	Erratic Menstrual Cycle	mRNA,
6814	44	4	TAH	HMB	mRNA, LOX activity assay
7607	45	17	Diag Lapscpy	RIF pain & IMB	mRNA, LOX activity assay
7618	49	27	TAH & BSO	Urinary Symptoms, Cycle & Bleeding Erratic since Zoladex	LOX activity assay
6392	42	NA	Diag Lapscpy	Dysmen & Pain	LOX activity assay
7593	51	13	TAH & BSO	Fibroid Uterus & HMB	LOX activity assay
7686	43	16	Laparoscopy	HMB	ELISA
7715	46	45	TAH & BSO	HMB	ELISA
5678	38	4	DiagLapscpy Hysteroscopy	HMB	ELISA
7741	37	NA	TAH	No cycle constant bleeding	ELISA

Abbreviation: TAH = total abdominal hysterectomy, BSO = bilateral salpingo-oophorectomy, HMB= heavy menstrual bleeding, Diag Lapscpy = diagnostic laparoscopy, Lap Ster = laparoscopic sterilisation, NA = not applicable, RIF = right Iliac Fossa, LIF = left Iliac Fossa, STAH = subtotal abdominal hysterectomy, IMB = irregular menstrual bleeding.

5.3 Results

5.3.1 Effect of glucocorticoid on lysyl oxidase mRNA expression in peritoneal mesothelial cells and ovarian surface epithelial cells

To investigate how cortisol may contribute to the scar-free healing, we treated OSE cells with IL-1α and TGF-β1 in the presence and absence of cortisol. Induction of LOX mRNA by IL-1α alone or the combination of IL-1α plus TGF-β1 was confirmed in OSE cells (Figure 5.1A, 3.2±0.31-fold and 4.7±0.5-fold respectively), but not by TGF-β1 (Figure 5.1A, 1.9±0.28-fold). Cortisol alone had no significant effect on LOX expression in OSE cells. However, in the presence of cortisol, the IL-1α induced-rise in LOX expression was significantly suppressed up to 50% compared to the IL-1α treatment group (Figure 5.1A, 1.7±0.08-fold compared to 3.2±0.31-fold). There was no significant suppression when cortisol was added to the TGF-β1 group or the IL-1α+TGF-β1 group. In PMC, LOX mRNA expression was significantly increased by IL-1α alone or the combination of IL-1α plus TGF-β1 (Figure 5.1B, 2.6±0.14-fold and 5.2±0.5-fold, respectively), but not by TGF-β1 alone (Figure 5.1B, 2.1±0.34-fold). Cortisol alone had no significant effect on LOX expression in PMC. A slight suppression of cortisol was seen in the IL-1α treatment group (1.7±0.34-fold compared to 2.6±0.14-fold); however, the addition of cortisol had no significant suppressive effect in any group.

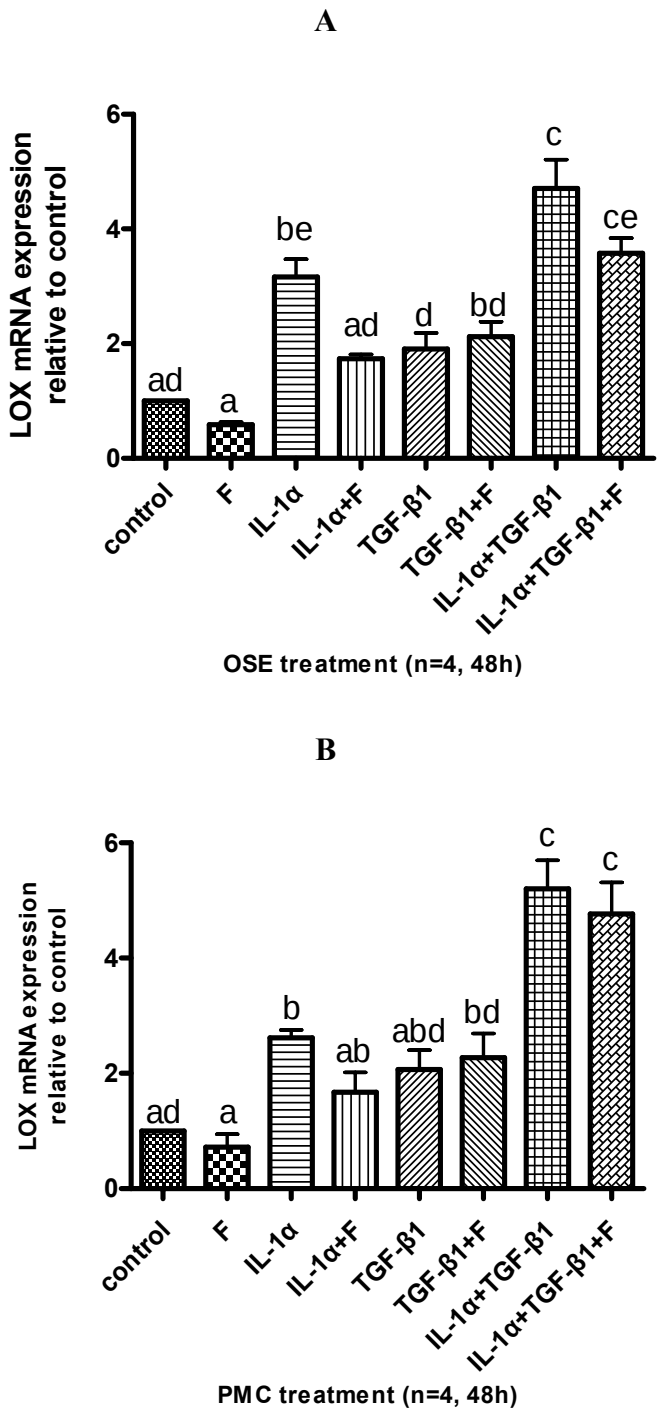

Figure 5.1. Quantitative RT-PCR for LOX mRNA expression in OSE cells and PMC. A: OSE cells were treated for 48h by IL-1α (0.5ng/ml) and TGF-β1 (2ng/ml), or the combination of IL-1α+TGF-β1, in the presence or absence of cortisol (F, 1μM). B: PMC were treated for 48h by IL-1α (0.5ng/ml) and TGF-β1 (2ng/ml), or the combination of IL-1α+TGF-β1, in the presence or absence of cortisol (F, 1μM). Statistical analysis was conducted by repeated-measures-paired-one-way ANOVA; bars represent mean (±S.E.M.) values relative to untreated control. Values with no common superscript letter are statistically different from each other ($P<0.05$).

5.3.2 Effect of glucocorticoid on lysyl oxidase enzyme activity of peritoneal mesothelial cells and ovarian surface epithelial cells

In the previous chapter, we showed that IL-1α increased LOX mRNA levels in both PMC and OSE cells, while cortisol only significantly suppressed its increase in OSE cells. Since the presence of mRNAs might not always signify the synthesis of functional proteins, we evaluated LOX activity secreted by PMC and OSE cells into their culture media, using our adaptation of a previously developed fluorimetric assay. LOX enzyme activity of PMC and OSE cells was tested in response to IL-1α plus or minus cortisol. The relative activity changes for secreted LOX of PMC and OSE cells are shown in Figure 5.2. The results showed significant fluorescence increases after IL-1α treatment for both PMC and OSE cells, indicating increased LOX activity in the culture media. Cortisol alone had no significant effect on LOX activity in either PMC or OSE cells. In the presence of cortisol, the IL-1α-induced rise of LOX activity was suppressed significantly in OSE cells. However, cortisol had only a slight suppressive effect in PMC that was not significant. These findings further confirmed previous mRNA results at the protein level.

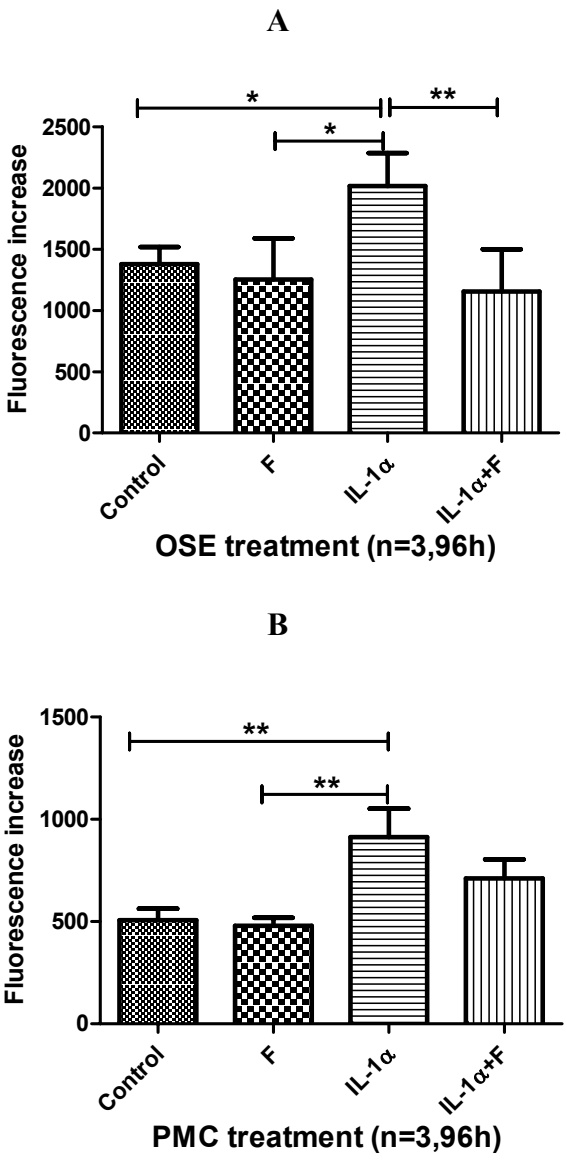

Figure 5.2. Effect of IL-1α and Cortisol (F) on LOX enzyme activity of OSE cells and PMC. A: OSE cells were treated by IL-1α (0.5ng/ml) in the presence or absence of cortisol (F, 1μM) for 96h. B: PMC were treated by IL-1α (0.5ng/ml) in the presence or absence of cortisol (F, 1μM) for 96h. Statistical analysis was conducted by repeated-measures-paired-one-way ANOVA; bars represent mean (±S.E.M.) values. *: $p<0.05$, **: $p<0.01$.

5.3.3 Effect of glucocorticoid on IL-1α production of peritoneal mesothelial cells.

In section 4.4.2, we showed that the synergistic effect of TNF-α plus TGF-β1 induced IL-1α secretion from PMC, as well as a large amount of the cell-associated

form of IL-1α (CA-IL-1α). Thus, we were interested in whether the anti-inflammatory effect of cortisol treatment could prevent such a response. PMC were treated with TNF-α and TGF-β1 alone or in combination, in the presence or absence of cortisol. IL-1α production was assayed in the conditioned medium and cell lysates. As already shown previously (Figure 4.12), neither TNF-α nor TGF-β1 alone caused a significant elevation of secreted IL-1α in the medium (Figure 4.13A, 16.31±1.03pg/ml and 9.96±0.82pg/ml respectively compared to control: 7.47±1.24pg/ml), while the synergistic effect of TNF-α plus TGF-β1 significantly induced IL-1α secretion to a concentration of 50.57±14.06pg/ml. Addition of cortisol significantly suppressed the synergistic effect and reduced the level of secreted IL-1α down to 19.81±1.66pg/ml (Figure 5.3A). On the other hand, TNF-α alone and TNF-α+TGF-β1 also induced elevated levels of CA-IL-1α (Figure 5.3B, 315.2±62.91pg/ml and 659.7±90.4pg/ml respectively compared to control: 15.48±2.24pg/ml). Addition of cortisol significantly suppressed these elevations (Figure 5.3B, 97.28±30.8pg/ml in the TNF-α+cortisol group, and 395.4±59.12pg/ml in the TNF-α+TGF-β1+cortisol group, respectively).

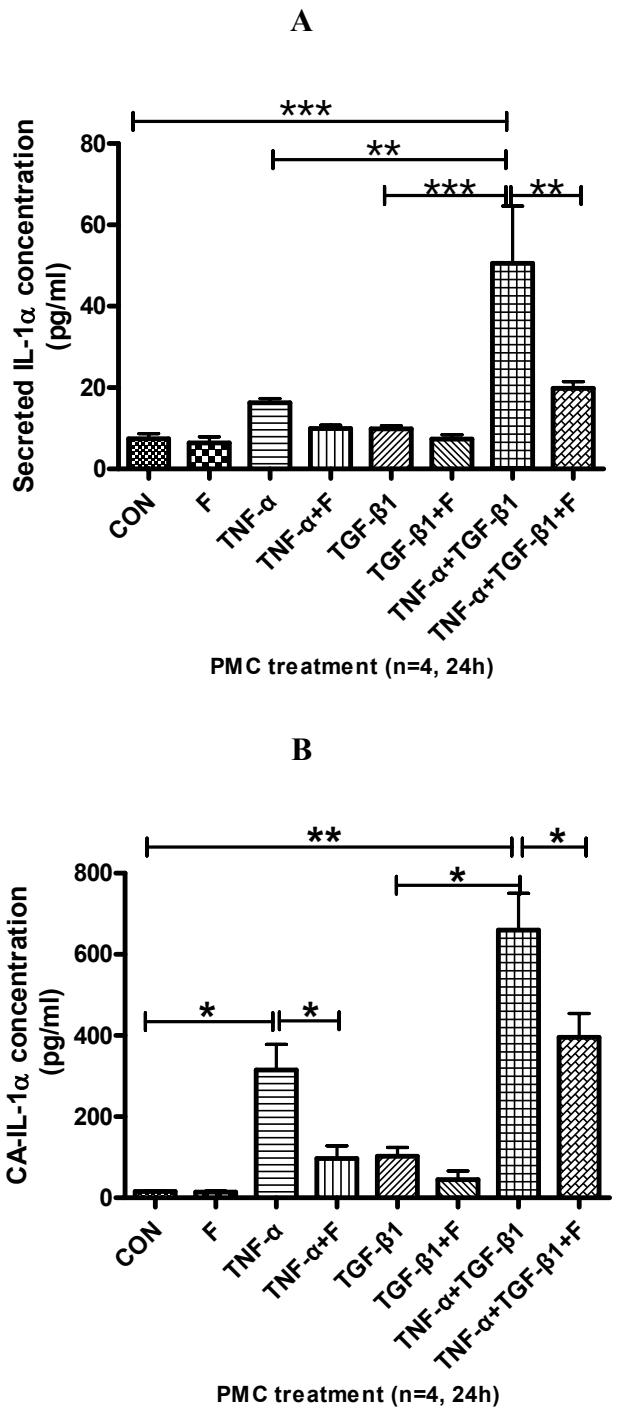

Figure 5.3. A: Secreted IL-1α levels in the culture media of control and treated PMC. B: CA-IL-1α concentration in the cell lysates of PMC. PMC were treated with TNF-α (10ng/ml) and TGF-β1 (2ng/ml) alone or the combination, in the presence or absence of cortisol (F, 1μM) for 24h. Statistical analysis was by repeated-measures-nonparametric Friedman test; group comparisons were by Dunn's multiple comparison test; bars represent mean (±S.E.M.) values. *: $p<0.05$, **: $p<0.01$. ***: $p<0.001$.

As shown earlier (Figure 4.13), TNF-α-induced LOX expression in PMC might be mediated by IL-1. Therefore, we hypothesized that cortisol might suppress TNF-α-induced LOX expression by its anti-inflammatory signalling and the suppression of IL-1α production. To investigate this, PMC were treated with TNF-α and TGF-β1 alone or in combination, in the presence or absence of cortisol. LOX mRNA levels were measured by Q-RTPCR. TNF-α and TNF-α+TGF-β1 treatments significantly stimulated LOX mRNA expression in PMC compared to the control group (Figure 5.4, 2.6±0.52-fold and 3.0±0.21-fold, respectively), but not by TGF-β1 (2.1±0.39-fold). The addition of cortisol inhibited the effect of TNF-α and the synergistic effect of TNF-α plus TGF-β1; however, no significant differences were found between the respective treatment groups (Figure 5.4, TNF-α vs TNF-α+F: 2.6±0.52-fold vs 1.5±0.30-fold, TNF-α+TGF-β1 vs TNF-α+TGF-β1+F: 3.0±0.21-fold vs 2.1±0.24-fold).

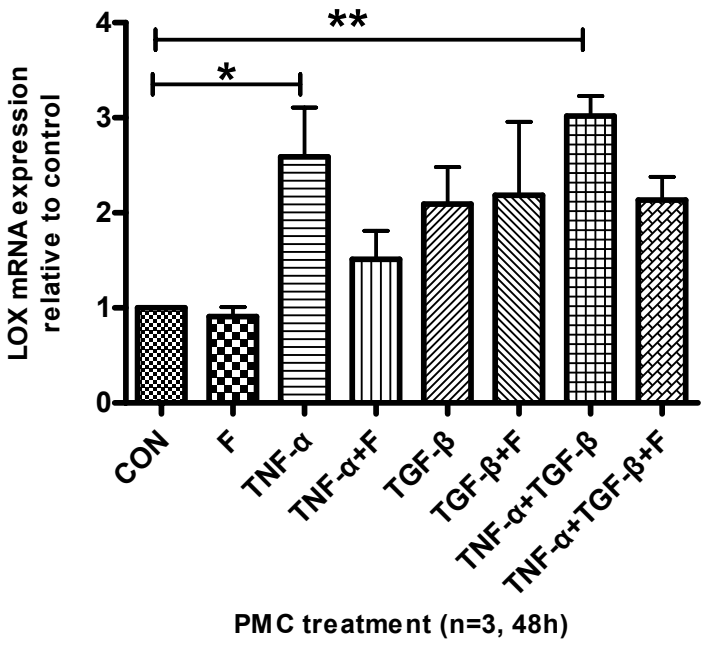

Figure 5.4. Quantitative RT-PCR for LOX mRNA expression in PMC. PMC were treated by TNF-α (10ng/ml) and TGF-β1 (2ng/ml), or in combination (TNF-α+TGF-β1), in the presence or absence of cortisol (F, 1μM) for 48h. Statistical analysis was conducted by repeated-measures-paired-one-way ANOVA; bars represent mean (±S.E.M.) values relative to untreated control. *: $p<0.05$, **: $p<0.01$.

5.4 Discussion

In this Chapter, a comparison between PMC and OSE cells was undertaken to address the mechanism of ovarian scar-free healing and whether OSE have an intrinsic mechanism that prevents scarring in response to inflammatory and fibrotic stimuli. First, we showed that cortisol can suppress the IL-1α-induced rise of LOX expression in OSE cells. In contrast, cortisol suppression of IL-1α levels was less in PMC compared to OSE cells (35% reduction in PMC compared to 50% in OSE cells), indicating that PMC might be less sensitive in responding to cortisol compared to OSE cells. Such a difference was confirmed by the LOX activity assay. It showed that extra-cellular LOX activity was increased in both PMC and OSE cells by IL-1α treatment. Addition of cortisol significantly reduced the elevation in LOX activity in OSE cells (43% reduction), but not in PMC (22% reduction). The difference between PMC and OSE responses might due to a different level of glucocorticoid receptor (GR) expression in the two cell types. Fegan (Fegan, 2009) showed a higher level of GR mRNA was expressed in OSE cells compared to PMC, and although this difference was not statistically significant, suggesting a greater OSE sensitivity to cortisol thereby increasing the anti-inflammatory effect. In the meantime, no quantification has been made for the expression of GR protein. Thus, it remains to be established whether OSE cells have a higher GR protein content than PMC. As discussed above, OSE cells have higher 11-oxoreductase activity compared to PMC, that can be enhanced by the inflammatory response (Fegan et al., 2008). This might help the ovary to convert circulating cortisone into cortisol locally during the ovulatory process, providing a local anti-inflammatory steroid environment that the peritoneum lacks. Such mechanisms would explain how the ovary could minimize ovulation-induced inflammation and prevent adhesion formation.

Cortisol was unable to significantly suppress IL-1α-induced LOX expression in PMC; however, the results indicate that cortisol could still aid peritoneal repair by suppressing the levels of secreted IL-1α and CA-IL-1α. We further showed that cortisol suppressed the TNF-α-induced rise of LOX expression. Although the effect was not statistically significant, it was likely more effective than that on the suppression with IL-1α (43% reduction with TNF-α compared to 35% reduction on IL-1α). The anti-inflammatory effect of cortisol is mainly dependent on the interplay with two main transcriptional pathways, NF-κB and AP-1 (Herrlich and Gottlicher, 2002), which can be induced by many cytokines. Cortisol inhibits the activation of NF-κB by upregulation of IκBα (Scheinman et al., 1995a; Auphan et al., 1995). This mechanism can contribute to the suppressive effect of cortisol on IL-1 and TNF-α signalling. However, other mechanisms including protein-protein interaction or transrepression are plausible. In addition, TNF-α induces IL-1 expression via p38 MAP kinase signalling by activating MKK3 (Wysk et al., 1999), which is also a downstream factor activated by TGF-β (Santibanez, 2006; Alcorn et al., 2008). The most likely mechanism for cortisol to interfere with the MAPK pathway involves the induction of MAPK phosphatase 1 (MKP-1) (Lasa et al., 2002; King et al., 2009). MKP-1 is a dual specificity phosphatase that targets p38 and thereby inhibits its kinase activity. This might explain the downregulation of CA-IL-1α by cortisol addition to both the TNF-α and TGF-β1 treatment groups. Through direct interplay with the TNF-α signalling network, cortisol might also suppress TNF-α effects by reducing the production of IL-1α within the cell. Thus, cortisol suppresses TNF-α mediated effects more effectively than the suppression of IL-1α. In contrast, no effect of cortisol has been reported on TGF-β1 signalling. TGF-β1 has been shown to regulate gene transcription mainly through Ras-ERK and Smad pathways (Derynck and Zhang, 2003; Lee et al., 2007). Therefore, cortisol seems unable to interact with the TGF-β1 signalling pathway, which suggests that other small molecules, including retinoids, might be involved in inhibiting the effect of TGF-β1 (Yang et al., 2008).

In summary, PMC and OSE cells have differences in their biological functions despite arising from the same lateral plate mesoderm and sharing many common features. The ovary is subjected to a regular cycle of injury and repair, whereas the peritoneum is present in a more stable environment which is less prone to natural injury. The monthly regeneration of OSE cells might also be associated with their capacity to maintain some features with higher regenerative potential. However, that hypothesis needs further exploration. In addition, the ovary appears to maintain a compensatory anti-inflammatory environment, which minimizes the formation of fibrosis. In contrast, the peritoneum lacks a similar mechanism to protect it from iatrogenic sporadic injury, such as surgery. Thus, the inflammatory response can be more persistent and severe which thus permits fibrosis and adhesion formation. Application of anti-inflammatory steroids on PMC only partly suppresses pro-inflammatory signalling and has no effect on TGF-β action. Therefore, the successful use of steroid treatments to routinely prevent post-operative adhesion remains an elusive target and warrants further investigation.

Chapter 6

PCR-based microarray study of inflammation- and fibrosis-induced extracellular matrix and adhesion related gene expression in peritoneal mesothelial cells.

6.1 Introduction

As discussed in Chapter 1, peritoneal repair is a complex process including phases of coagulation, infiltration of inflammatory cells, cell proliferation, extracellular matrix (ECM) deposition and remodelling, commonly with overlap between the phases (Hubbard et al., 1967). The data in previous chapters indicate an important role of PMC in the development of fibrotic tissue, including collagen deposition. In addition, it also revealed that PMC undergo an epithelial-mesenchymal transition (EMT) in response to an inflammatory stimulus, the combination of IL-1α and TGF-β1. These transformed cells have enhanced cell motility and are more adherent to fibronectin. Although these findings provide a likely mechanism for the centripetal cell migration (Whitaker and Papadimitriou, 1985; Mutsaers et al., 2000) and incorporation of free-floating mesothelial cells (Watters and Buck, 1973; Whitaker and Papadimitriou, 1985) that are important for peritoneal repair, the underlying mechanism at the molecular level remaining unknown. To date, the only well-established pathologic mechanism of post-operative adhesion involves the formation of the fibrin layer and the regulation of peritoneal fibrinolytic capacity (Holmdahl et al., 1996). However, the contributions of collagen deposition and ECM remodelling to peritoneal repair are not well understood.

Herein, we employed a real-time PCR-based microarray that allowed genomic analysis of ECM-adhesion-related gene expression of PMC in response to two main inflammatory factors, IL-1 and TGF-β. As presented earlier, IL-1α and TGF-β1 regulate gene expression in PMC using independent signalling pathways. Therefore, microarrays were conducted to compare untreated PMC to IL-1-treated or TGF-β1-treated PMC. These data provide insight into the molecular response of PMC during peritoneal repair, helping to identify other key pro-fibrotic factors

involved in the development of peritoneal fibrosis which may further cause post-operative adhesion.

6.2 Materials and methods

To address other potential targets in the development of post-operative adhesion, a PCR-based microarray set on ECM-adhesion related gene was selected. Patient samples treated by IL-1α and TGF-β1 from previous experiment were carefully chose. Preparation of cDNA was conducted by using the cDNA synthesis kit from the microarray set (section 2.3.5.1). The quality of synthesized cDNA samples was tested by the RT^2 RNA Quality Control PCR Array (section 2.3.5.2). The eligible cDNA samples were used for the microarray (section 2.3.5.2). To validate the microarray, RT-PCR was performed to verify that the observed changes in gene expression level. Using the same samples used for microarray analysis or other samples with the same treatments, gene-specific PCR was performed on a selection (*n*=7) of the genes modulated by IL-1α or TGF-β1. The basic clinical profile of patients involved with the respective assays performed on each are presented in Table 6.1.

Table 6.1. Clinical profile of patients used for respective assays

Patient Code	Age	Cycle day	Surgery	Reason for surgery	Study
7607	45	17	Diag Lapscpy	RIF pain & IMB	Microarray, validation
7613	48	26	STAH	Erratic Menstrual Cycle	Microarray, validation
7641	38	11	TAH	HMB	Microarray, validation
7548	31	5	Lap Ster	NA	Microarray, validation
5621	44	8	TAH	HMB & Fibroids	validation
3028	29	19	Diag Lapscpy	RIF Pain	validation
7531	37	27	Diag Lapscpy	HMB & Pain	validation
6814	44	4	TAH	HMB	validation

Abbreviation: TAH = total abdominal hysterectomy, HMB= heavy menstrual bleeding, Diag Lapscpy = diagnostic laparoscopy, Lap Ster = laparoscopic sterilisation, NA = not applicable, RIF = right Iliac Fossa, STAH = subtotal abdominal hysterectomy.

6.3 Results

6.3.1 A comparison of IL-1α and TGF-β1 effects on PMC by PCR Microarray

Table 6.2. Gene expression of PMC in response to IL-1α (0.5ng/ml) and TGF-β1 (2ng/ml) treatment for 48h. The values are fold up- (positive values) or down- (negative values) regulation of gene expression in response to treatment compared to untreated cells. Two-fold or greater differences are highlighted (up-regulated in red, down-regulated in blue). Differences that are statistically significant have P values highlighted in red. n=4 samples per treatment

Ref Seq	Symbol	Description	IL-1α Effect	P Value	TGF-β1 Effect	P Value
NM_006988	ADAMTS1	ADAM metallopeptidase with thrombospondin type 1 motif, 1	-1.12	0.6011	-4.12	0.0256
NM_139028	ADAMTS13	ADAM metallopeptidase with thrombospondin type 1 motif, 13	-1.26	0.3715	1.68	0.1595
NM_007037	ADAMTS8	ADAM metallopeptidase with thrombospondin type 1 motif, 8	1.28	0.5612	-1.21	0.6707
NM_000610	CD44	CD44 molecule (Indian blood group)	1.90	0.2690	1.87	0.3400
NM_004360	CDH1	Cadherin 1, type 1, E-cadherin (epithelial)	-7.84	0.0020	-24.97	0.0030
NM_001843	CNTN1	Contactin 1	-1.53	0.5229	1.39	0.5852
NM_080629	COL11A1	Collagen, type XI, alpha 1	-1.56	0.7012	-1.24	0.8480
NM_004370	COL12A1	Collagen, type XII, alpha 1	-1.20	0.6134	-1.01	0.9757
NM_021110	COL14A1	Collagen, type XIV, alpha 1 (undulin)	-4.25	0.0030	-1.92	0.3324
NM_001855	COL15A1	Collagen, type XV, alpha 1	-1.03	0.9599	-2.31	0.1258
NM_001856	COL16A1	Collagen, type XVI, alpha 1	4.31	0.0446	5.29	0.0454
NM_000088	COL1A1	Collagen, type I, alpha 1	1.96	0.0916	6.77	0.0010
NM_001846	COL4A2	Collagen, type IV, alpha 2	1.24	0.4717	3.96	0.0028
NM_000093	COL5A1	Collagen, type V, alpha 1	1.30	0.2851	2.19	0.0353
NM_001848	COL6A1	Collagen, type VI, alpha 1	1.07	0.8835	3.69	0.0295
NM_001849	COL6A2	Collagen, type VI, alpha 2	1.08	0.8237	1.29	0.5571
NM_000094	COL7A1	Collagen, type VII, alpha 1 (epidermolysis bullosa, dystrophic, dominant and recessive)	7.48	0.0457	22.04	0.0139
NM_001850	COL8A1	Collagen, type VIII, alpha 1	-1.84	0.0858	5.12	0.0362
NM_004385	VCAN	Versican	1.80	0.2063	13.57	0.0023
NM_001901	CTGF	Connective tissue growth factor	-2.06	0.0974	2.21	0.0267
NM_001903	CTNNA1	Catenin (cadherin-associated protein), alpha 1, 102kDa	-1.16	0.3706	-1.31	0.0647
NM_001904	CTNNB1	Catenin (cadherin-associated protein), beta 1, 88kDa	1.06	0.6315	-1.01	0.9314

Ref Seq	Symbol	Description	IL-1α Effect	P Value	TGF-β1 Effect	P Value
NM_001331	CTNND1	Catenin (cadherin-associated protein), delta 1	1.25	0.1221	1.36	0.1231
NM_001332	CTNND2	Catenin (cadherin-associated protein), delta 2 (neural plakophilin-related arm-repeat protein)	-5.65	0.0317	1.33	0.7402
NM_004425	ECM1	Extracellular matrix protein 1	1.70	0.0500	2.13	0.0129
NM_002026	FN1	Fibronectin 1	5.10	0.0058	18.86	0.0004
NM_001523	HAS1	Hyaluronan synthase 1	1.23	0.6363	1.78	0.2734
NM_000201	ICAM1	Intercellular adhesion molecule 1 (CD54), human rhinovirus receptor	1.31	0.1379	1.85	0.0053
NM_181501	ITGA1	Integrin, alpha 1	4.82	0.0154	1.44	0.4216
NM_002203	ITGA2	Integrin, alpha 2 (CD49B, alpha 2 subunit of VLA-2 receptor)	2.03	0.0972	5.53	0.0093
NM_002204	ITGA3	Integrin, alpha 3 (antigen CD49C, alpha 3 subunit of VLA-3 receptor)	-1.92	0.2602	1.25	0.5022
NM_000885	ITGA4	Integrin, alpha 4 (antigen CD49D, alpha 4 subunit of VLA-4 receptor)	-1.47	0.5041	5.29	0.0966
NM_002205	ITGA5	Integrin, alpha 5 (fibronectin receptor, alpha polypeptide)	2.29	0.0374	4.27	0.0048
NM_000210	ITGA6	Integrin, alpha 6	-2.31	0.0028	1.08	0.6795
NM_002206	ITGA7	Integrin, alpha 7	-1.32	0.4871	2.33	0.0222
NM_003638	ITGA8	Integrin, alpha 8	-1.21	0.3085	1.21	0.6208
NM_002209	ITGAL	Integrin, alpha L (antigen CD11A (p180), lymphocyte function-associated antigen 1; alpha polypeptide)	1.54	0.5964	1.23	0.5997
NM_000632	ITGAM	Integrin, alpha M (complement component 3 receptor 3 subunit)	1.36	0.4506	1.35	0.3214
NM_002210	ITGAV	Integrin, alpha V (vitronectin receptor, alpha polypeptide, antigen CD51)	1.32	0.3799	1.78	0.0673
NM_002211	ITGB1	Integrin, beta 1 (fibronectin receptor, beta polypeptide, antigen CD29 includes MDF2, MSK12)	1.71	0.0022	1.64	0.0596
NM_000211	ITGB2	Integrin, beta 2 (complement component 3 receptor 3 and 4 subunit)	4.41	0.0445	-1.11	0.8287
NM_000212	ITGB3	Integrin, beta 3 (platelet glycoprotein IIIa, antigen CD61)	2.50	0.0016	6.96	0.0006
NM_000213	ITGB4	Integrin, beta 4	-5.66	0.0404	-1.69	0.4185
NM_002213	ITGB5	Integrin, beta 5	-1.35	0.1418	1.68	0.0037
NM_000216	KAL1	Kallmann syndrome 1 sequence	-1.16	0.2634	-1.04	0.7891
NM_005559	LAMA1	Laminin, alpha 1	-2.88	0.0111	-2.36	0.0417

Ref Seq	Symbol	Description	IL-1α Effect	P Value	TGF-β1 Effect	P Value
NM_000426	LAMA2	Laminin, alpha 2 (merosin, congenital muscular dystrophy)	-1.07	0.8996	-3.17	0.1099
NM_000227	LAMA3	Laminin, alpha 3	-3.19	0.0014	-5.31	0.0092
NM_002291	LAMB1	Laminin, beta 1	-1.05	0.8314	1.12	0.5147
NM_000228	LAMB3	Laminin, beta 3	4.15	0.0203	1.22	0.7551
NM_002293	LAMC1	Laminin, gamma 1 (formerly LAMB2)	-1.07	0.8099	1.15	0.4630
NM_002421	MMP1	Matrix metallopeptidase 1 (interstitial collagenase)	4.64	0.0092	1.33	0.5187
NM_002425	MMP10	Matrix metallopeptidase 10 (stromelysin 2)	1.88	0.3267	2.78	0.2674
NM_005940	MMP11	Matrix metallopeptidase 11 (stromelysin 3)	-1.49	0.0187	1.14	0.1675
NM_002426	MMP12	Matrix metallopeptidase 12 (macrophage elastase)	13.91	0.0291	2.00	0.4401
NM_002427	MMP13	Matrix metallopeptidase 13 (collagenase 3)	35.73	0.0217	4.94	0.2466
NM_004995	MMP14	Matrix metallopeptidase 14 (membrane-inserted)	1.28	0.2139	3.09	0.0141
NM_002428	MMP15	Matrix metallopeptidase 15 (membrane-inserted)	-1.91	0.0576	-1.39	0.3123
NM_005941	MMP16	Matrix metallopeptidase 16 (membrane-inserted)	-1.11	0.8321	3.79	0.0200
NM_004530	MMP2	Matrix metallopeptidase 2 (gelatinase A, 72kDa gelatinase, 72kDa type IV collagenase)	1.25	0.4174	1.87	0.0977
NM_002422	MMP3	Matrix metallopeptidase 3 (stromelysin 1, progelatinase)	4.21	0.0062	3.69	0.1004
NM_002423	MMP7	Matrix metallopeptidase 7 (matrilysin, uterine)	1.14	0.8929	-2.42	0.3231
NM_002424	MMP8	Matrix metallopeptidase 8 (neutrophil collagenase)	20.95	0.0002	1.42	0.6494
NM_004994	MMP9	Matrix metallopeptidase 9 (gelatinase B, 92kDa gelatinase, 92kDa type IV collagenase)	17.82	0.0124	11.74	0.0163
NM_000615	NCAM1	Neural cell adhesion molecule 1	-2.00	0.0077	1.11	0.6969
NM_000442	PECAM1	Platelet/endothelial cell adhesion molecule (CD31 antigen)	1.77	0.1250	-1.13	0.7728
NM_000450	SELE	Selectin E (endothelial adhesion molecule 1)	1.15	0.7367	1.27	0.5401
NM_000655	SELL	Selectin L (lymphocyte adhesion molecule 1)	1.50	0.3829	-1.48	0.4084
NM_003005	SELP	Selectin P (granule membrane protein 140kDa, antigen CD62)	-1.13	0.7645	-1.90	0.1507
NM_003919	SGCE	Sarcoglycan, epsilon	-1.10	0.5713	-1.20	0.5489
NM_003118	SPARC	Secreted protein, acidic, cysteine-rich (osteonectin)	-1.52	0.1419	-1.04	0.8009

Ref Seq	Symbol	Description	IL-1α Effect	P Value	TGF-β1 Effect	P Value
NM_003119	SPG7	Spastic paraplegia 7, paraplegin (pure and complicated autosomal recessive)	-1.13	0.4013	1.12	0.5336
NM_000582	SPP1	Secreted phosphoprotein 1 (osteopontin, bone sialoprotein I, early T-lymphocyte activation 1)	-2.31	0.1333	2.38	0.2076
NM_000358	TGFBI	Transforming growth factor, beta-induced, 68kDa	2.88	0.0025	12.04	0.0020
NM_003246	THBS1	Thrombospondin 1	2.54	0.2395	35.14	0.0045
NM_003247	THBS2	Thrombospondin 2	-1.06	0.8511	2.85	0.0109
NM_007112	THBS3	Thrombospondin 3	-1.59	0.1120	2.07	0.0229
NM_003254	TIMP1	TIMP metallopeptidase inhibitor 1	1.31	0.0497	1.15	0.6037
NM_003255	TIMP2	TIMP metallopeptidase inhibitor 2	-1.22	0.2837	1.66	0.0416
NM_000362	TIMP3	TIMP metallopeptidase inhibitor 3 (Sorsby fundus dystrophy, pseudoinflammatory)	1.79	0.0428	1.54	0.1604
NM_003278	CLEC3B	C-type lectin domain family 3, member B	-1.14	0.7771	-1.03	0.9466
NM_002160	TNC	Tenascin C (hexabrachion)	4.82	0.0416	5.39	0.0408
NM_001078	VCAM1	Vascular cell adhesion molecule 1	-1.51	0.2700	-6.90	0.0342
NM_000638	VTN	Vitronectin	-1.36	0.5494	-5.09	0.0252
NM_004048	B2M	Beta-2-microglobulin	-1.20	0.1240	-2.30	0.0126
NM_000194	HPRT1	Hypoxanthine phosphoribosyltransferase 1 (Lesch-Nyhan syndrome)	1.04	0.8691	-1.19	0.7160
NM_012423	RPL13A	Ribosomal protein L13a	-1.30	0.0133	-1.58	0.0920
NM_002046	GAPDH	Glyceraldehyde-3-phosphate dehydrogenase	1.75	0.0008	1.06	0.7344
NM_001101	ACTB	Actin, beta	-1.16	0.4649	1.32	0.1824

The arrays revealed that some genes were regulated by both IL-1α and TGF-β1, whereas others were independently regulated by IL-1α or TGF-β1. Genes that were upregulated by both IL-1α and TGF-β1 were COL16A1, COL7A1, FN1, ITGA5, ITGB3, MMP9, TGFB1, and TNC. Genes that were downregulated by both IL-1α and TGF-β1 were CDH1, LAMA1 and LAMA3. IL-1α upregulated several genes on its own, including ITGA1, ITGB2, LAMB3, MMP1, MMP3, MMP8, MMP12 and MMP13; while COL14A1, CTNND2, ITGA6, ITGB4 and NCAM1 were downregulated by IL-1α alone. TGF-β1 upregulated several genes on its own, including COL1A1, COL4A2, COL5A1, COL6A1, COL8A1, VCAN, CTGF, ECM1,

ITGA2, ITGA7, MMP14, MMP16, THBS1, THBS2 and THBS3; while ADAMTS1, VCAM1, VTN, and B2M were downregulated by TGF-β1 treatment.

To validate the microarray, RT-PCR was performed to confirm the observed changes in gene expression level. Using the same samples used for microarray analysis, together with other samples, gene-specific PCR was performed on a selection (n=7) of the genes modulated by IL-1α or TGF-β1. This analysis confirmed the reliability of the microarray data: all the genes tested showed the same significant predicted shifts in expression (Table 6.3).

Table 6.3. Subset of genes randomly selected and validated by quantitative real-time PCR on PMC samples subjected to microarray analysis. Statistical analysis was by paired t-test or nonparametric Wilcoxon-matched-pairs test, mean fold change ±S.E.M. ns, not significant, *p<0.05, **p<0.01 compared to untreated cells.

Ref Seq	Symbol	Repeats (n)	IL-1α Effect		TGF-β1 Effect	
			Array	qRT-PCR	Array	qRT-PCR
NM_004360	CDH1	n=4	**-7.84**	**-5.03±1.60***	**-24.97**	**-5.60±3.02***
NM_000088	COL1A1	n=5	**1.96**	**1.67±0.46***	**6.77**	**2.83±0.45****
NM_002026	FN1	n=6	**5.10**	**6.30±2.29***	**18.86**	**11.56±3.89***
NM_002205	ITGA5	n=6	**2.29**	**1.77±0.32***	**4.27**	**2.54±0.48***
NM_004994	MMP9	n=6	**17.82**	**23.82±9.87***	**11.74**	**14.90±6.45***
NM_000358	TGFBI	n=6	**2.88**	**1.64±0.15****	**12.04**	**2.63±0.38****
NM_001101	ACTB	n=6	**-1.16**	**-1.05±0.12^{ns}**	**1.32**	**-1.03±0.16^{ns}**

6.3 Discussion

The microarray results confirm the involvement of IL-1α and TGF-β1 in the activation or inhibition of a wide range of different genes, involved in tissue repair and fibrosis. This may help us to better understand the underlying mechanism of tissue repair that is unique to PMC. To interpret these findings more clearly, the genes regulated by IL-1α and TGF-β1 will be discussed by organizing them into five

groups namely a collagen group, a laminin group, an integrin group, a MMP group and others.

The collagen family is the most important component in the progression of adhesion or fibrosis. They are formed by the triple helical three α chains that are composed of repeating peptide triplets of glycine-X-Y (X,Y can be any amino acid). However, different members of the collagen family may also include non-collagenous (non-gly-X-Y) regions flanked in each α chain. These regions contain recognizable spots found in other matrix molecules, which can direct collagen incorporation into the matrix (Gordon and Hahn, 2010). Therefore, the functions of collagens can be variable. It depends on the proper assembly of the supramolecular structure that directs incorporation into the matrix. The current data showed that TGF-β1 but not IL-1α induced the expression of most of the collagen family members, including collagens I, IV, V, VI and VIII. Collagens I and V are fibrillar collagens that contain a perfect gly-X-Y triplet structure. They can be assembled into heterotrimers with type V collagen molecules buried within the fibril and type I collagen molecules presented along the fibril surface (Birk, 2001). Type V collagen is also shown to nucleate fibrils of type I collagen and regulate the fibril diameter (Wenstrup et al., 2006; Birk et al., 1990). Collagens IV, VI and VIII are shown to be network-forming collagens. Type IV is a basement membrane collagen which forms a three-dimensional structure from a chicken wire-like two-dimensional structure (Khoshnoodi et al., 2008). Collagen VI is a ubiquitous extracellular matrix protein that is present in the stroma. It also forms a microfibrillar network in close association with the basement membrane of most tissues (Lampe and Bushby, 2005). Collagen VIII can make a hexagonal lattice. It is expressed by many cells, particularly endothelial cells. Therefore, collagen VIII is an important component of vascular wall (Plenz et al., 2003). In summary, our data showed that TGF-β1 can induce collagen deposition by promoting fibril assembly and network collagen

formation. In the array, both IL-1α and TGF-β1 were shown to induce collagen VII and XVI expression in PMC. Both of these are non-fibrillar types of collagen which associate with other fibrils. The role of collagen VII is crucial to the attachment complex that rivets the epidermis to the dermis (Aumailley et al., 2006; Bruckner-Tuderman, 2009). As the major component of anchoring fibrils, collagen VII has been shown to be localized to the lamina densa of the epithelial basement membrane by binding to anchoring filaments at one end, while the other end can interact with derma by merging into the banded collagen fibrils of the dermis. Therefore, the production of collagen VII may contribute to adhesion formation by anchoring into the peritoneal tissue on opposite sides of the adhesion. Collagen XVI is primarily localized to basement membrane or junctions between tissues (Ratzinger et al., 2010). Evidence has shown that collagen XVI is a preferred substrate for the formation and maturation of focal contacts of myofibroblasts, promoting more stable and longer adhesion of myofibroblasts to the matrix (Ratzinger et al., 2010). Thus, the induction of collagen VII by IL-1α and TGF-β1 observed in the present study may promote tissue adhesion, while the upregulation of collagen XVI may enhance the adherence of myofibroblasts in the inflammatory areas. Interesting, the results also showed that IL-1α downregulated collagen XIV expression in PMC. Collagen XIV is also a non-fibrillar type of collagen binding to the surface of other fibrillar collagens. It functions as a fibril diameter regulator by preventing the fusion of fibrils into larger complexes (Ansorge et al., 2009). Therefore, IL-1α might also contribute to the formation of larger fibril bundles by suppressing collagen XIV expression in PMC.

Laminins are also important components of the basement membrane together with collagens. The production of laminins by PMC will contribute to the reconstruction of basement membrane while they are also critical for the adherence of PMC to the newly forming basement membrane matrix (Tzu and Marinkovich, 2008). In the

array, both IL-1α and TGF-β1 downregulated laminin α1 and α3 expression in PMC. These comprise the two main alpha chains that combine with other β and γ chains to form the trimeric assembled laminin proteins. In contrast, laminin β3 was upregulated in PMC by IL-1α. To date, the only known role of laminin β3 is its involvement in the formation of laminin-332 that functions as a component of the hemidesmosome-anchoring filament complex (Tzu and Marinkovich, 2008). It helps to bridge the cell surface with the dermis. However, such function is based on the ability of C-terminal G domains of the α3 chain to bind to the cell surface integrins (α6β4, α3β1), while the N-terminal can connect to collagen VII to provide anchorage to the dermis (Tzu and Marinkovich, 2008; Suzuki et al., 2005). Therefore, the upregulation of laminin β3 is difficult to interpret in light of the downregulation of laminin α3. In summary, the effects of IL-1α and TGF-β1 may delay the repair of the basement at the injured sites by impeding the production of laminin protein. In addition, it may also prevent the cell-basement matrix attachment by preventing the hemidesmosome-anchoring filament complex formation.

As discussed above, integrins are important for the adherence of cells to the ECM and cell motility. In this study, integrin α1 and α2 were upregulated by IL-1α and TGF-β1, respectively. Both integrin α1 and α2 can form heterodimers with integrin β1 (integrin α1β1 and α2β1) to function as collagen receptors which mediate cell binding to collagen (Humphries et al., 2006). Meanwhile, integrin α5 was upregulated by both IL-1α and TGF-β1 in the array. It can form heterodimers with integrin β1 (integrin α5β1) to function as the main fibronectin receptor mediating cell binding to fibronectin (Humphries et al., 2006). In addition, we showed that integrin β3 was upregulated by both IL-1α and TGF-β1. It also forms heterodimers with integrin αV and αIIb (integrin αVβ3 and αIIbβ3) to function as another fibronectin receptor mediating cell binding to fibronectin (Xiong et al., 2002). Integrin α5β1 and αVβ3 are also involved in the activation of RhoA and Rac1, respectively. They can

regulate the balance between RhoA and Rac1, and thus promote cell migration and control the direction of cell movement (Danen et al., 2005; White et al., 2007). These findings were partially confirmed in the wound-healing and cell-ECM adhesion assays. Integrin α7 was upregulated in PMC by TGF-β1. It can form heterodimers with integrin β1 (integrin α7β1) to function as a laminin receptor mediating cell binding to laminin-111 and to a mixture of laminin-211 and -221 but not to laminin-332 (Yao et al., 1996). In contrast, IL-1α was shown to suppress integrin α6 and β4 expression in the array. Both integrin α6β1 and α6β4 play a role in the adherence of cells to laminin (Lee et al., 1992; Sonnenberg et al., 1990), including laminin-332. Integrin α6β4 is widely expressed in most epithelial tissues and contributes to the formation of hemidesmomes with laminin-332 (Soung et al., 2011; Borradori and Sonnenberg, 1999). A defect in integrin α6β4 leads to a skin blistering condition (Ashton et al., 2001). Integrin α7β1 is mainly expressed on the surface of skeletal myoblasts and myofibres. A lack of integrin α7β1 is associated with congenital muscular dystrophies. Therefore, integrin α7β1 is not as essential as integrin α6β1 and α6β4 with respect to the role of PMC during peritoneal repair. Lastly, IL-1α upregulated integrin β2 expression in PMC. Integrin β2 can form heterodimers with integrins αL, αM, αX and αD to function as leukocyte-specific receptors mediating leukocyte binding to cells by recognizing ICAM-1 on the target cells (Wang and Springer, 1998; Shimaoka et al., 2003). It is mainly expressed on leukocytes. Therefore, integrin β2 expression in PMC may be low, but its function is not clear. In general, IL-1α and TGF-β1 induced the expression of several integrin family members, which facilitate the adherence of PMC to ECM substrates including collagen and fibronectin. This enhanced cell adhesion could also promote cell motility by activating Rho-GTPases. Interesting, IL-1α was shown to impede cell attachment to the basement membrane by suppressing the expression of integrin α6 and β4. Meanwhile, IL-1α reduced production of laminin from PMC that further inhibits the repair of basement membrane. This might explain the origin of

free-floating mesothelial cells in the peritoneal cavity found in other studies, due to lower adherence to the basement membrane and its delayed repair.

The MMPs were regulated independently by IL-1α and TGF-β1 in PMC. IL-1α upregulated MMP1, MMP3, MMP8, MMP12 and MMP13. As discussed above (section 1.5.4), MMP1, MMP8 and MMP13 belong to a collagenase subgroup which preferentially cleave collagen. MMP3 is a stromelysin able to digest a wide range of substrates including collagens, laminins, fibronectin, etc. It also activates other MMPs including MMP-1, MMP-7, and MMP-9. MMP12 is mainly produced by macrophages as a macrophage elastase. It has also been shown that MMP12 is a potent proinflammatory molecule associated with lung fibrosis (Qu et al., 2009; Madala et al., 2010; Garbacki et al., 2009). The role of MMP12 produced by PMC in peritoneal fibrosis, however, requires further investigation. Both IL-1α and TGF-β1 upregulated MMP9 expression in PMC. MMP9 is mainly a gelatinase, but it can also degrade collagens IV and V. It is a secreted product of activated monocytes (Opdenakker et al., 2001) and a major component of the tertiary granules of human neutrophils (Cowland and Borregaard, 1999). Elevated MMP9 is found during the wound-healing process in a variety of tissues. Its role may be in promoting cell locomotion in the wound matrix, remodelling of the granulation tissue matrix and angiogenesis in ischemic tissue (Muhs et al., 2003; Heissig et al., 2010). In addition to MMP9, TGF-β1 also upregulated MMP14 and MMP16 expression in PMC. Both are membrane-inserted MMPs. It has been shown that MMP14 and MMP16 can operate in an autonomous fashion to drive fibrin-invasive activity of fibroblasts (Hotary et al., 2002). In addition, MMP14 also exerts pericellualr collagenolytic activity supporting the tissue-invasive phenotype of fibroblast on collagen substrate, whereas MMP16 is not necessary for such cell behaviour (Sabeh et al., 2009). Therefore, the upregulation of MMP14 and 16 by TGF-β1 can facilitate the invasion of EMT-transformed PMC into fibrin-rich clots covering injury sites or other

pro-fibrotic tissue further promoting the progression of fibrosis. In general, IL-1α induced variant expression of MMPs in PMC, a response for the degradation and remodelling of the ECM. In contrast, TGF-β1 had little effect on the expression of secreted MMPs except for MMP9. However, membrane-inserted MMPs (MMP14, 16) were upregulated only by TGF-β1, which might contribute to the invasion of PMC into the repairing tissue.

Fibronectin 1 (FN1), another important component of ECM, was upregulated by both IL-1α and TGF-β1. In addition, both IL-1α and TGF-β1 were likely to induce an autocrine production of TGF-β1 from PMC by upregulating TGFBI transcription. Such a self-induced autocrine mechanism might account for a persistent and excessive tissue remodelling. In contrast, both IL-1α and TGF-β1 induced tenascin C expression in PMC, a well known anti-adhesive ECM component. Tenascin C is an extracellular matrix glycoprotein. It provides weak substrate adhesion with the formation of focal adhesion and loss of actin-containing stress fibres, which is also called an intermediate state of adhesiveness (Murphy-Ullrich, 2001). This state allows cell shape changes and motility but prevents apoptosis and differentiation. In addition, tenascin C also antagonizes the pro-adhesive effects of collagens, fibronectin and laminins (Hsia and Schwarzbauer, 2005). However, our *in vitro* adhesion assay confirmed an enhanced adherence of PMC to fibronectin. Thus, in this case, the elevation of tenascin C might be insufficient to prevent adherence of PMC to other ECM substrates.

As a hallmark of the EMT process, E-cadherin had been shown to be downregulated by both IL-1α and TGF-β1 previously. IL-1α was also shown to suppress CTNND2 expression in the array. CTNND2 can directly bind to the unique juxtamembrane domain in E-cadherin to support the stability of E-cadherin-based adherent junctions, that help to maintain epithelial tissue integrity (Lu, 2010). The role of CTNND2 in

cancer pathogenesis has been widely studied (Zhang et al., 2010; Wang et al., 2009), but its role in peritoneal fibrosis is still unclear. IL-1α also suppressed neural cell adhesion molecule 1 (NCAM1) expression in PMC. NCAM1 is a homophilic binding glycoprotein that has been studied in neurons (Stoenica et al., 2006) and renal interstitial cells (Markovic-Lipkovski et al., 2007). NCAM has been implicated as having a role in cell–cell adhesion, neurite outgrowth and learning and memory.

TGF-β1 treatment alone upregulated some other important genes in PMC, including versican, CTGF, EMC1 and thrombospondins (TSP) 1,2 & 3. Versican is a large extracellular matrix proteoglycan present in many tissues. It is a basic structural molecule to create loose and hydrated matrices during events including tissue repair (Wight, 2002). It also regulates ECM assembly and expansion, cell adhesion and survival, cell proliferation and cell migration (Wight, 2002). Due to these varied functions, the induction of versican in PMC by TGF-β1 may apparently contribute to peritoneal repair. CTGF is a well-known downstream factor in TGF-β1-induced tissue remodelling. A recent paper has demonstrated a cooperative interaction between CTGF and TGF-β signalling to induce fibrosis and adhesion between organs in the abdominal cavity (Wang et al., 2011). ECM1 has a key interaction with perlecan, a major heparin sulphate proteoglycan of basement membrane, that allows ECM1 to function as a biological glue to help regulate basement membrane and collagen fibril assembly, and growth factor binding in dermis (Chan, 2004). However, the role of ECM1 in peritoneal fibrosis remains unclear. TSP 1, 2 and 3 are multifunctional secreted glycoproteins with anti-angiogenic properties. As the most common type, TSP 1 is secreted by a variety of cell types including endothelial and epithelial cells, fibroblasts and smooth muscle cells (Kazerounian et al., 2008). TSP-1 has been shown to inhibit angiogenesis and activate the latent form of platelet-derived TGF-β1 (Fitchev et al., 2010; Ahamed et al., 2009; Simantov and Silverstein, 2003). Therefore, the upregulation of TSP 1, 2 and 3 by TGF-β1 may

have an anti-angiogenic role and augment the autocrine circuit of TGF-β1 production.

In the array, TGF-β1 also suppressed the expression of ADAMTS1, VCAM1 and VTN. ADAMTS1 encodes the ADAMTS 1 (a disintegrin and metalloproteinase with thrombospondin motifs 1) protein, which is a secreted zinc metalloprotease with an ancillary domain containing one or more thrombospondin type 1 repeats. It has been shown that ADAMTS-1 plays a role in anti-angiogenesis (Vazquez et al., 1999) and degradation of aggrecan including the cleaving of versican (Rodriguez-Manzaneque et al., 2002; Kuno et al., 2000). Knockdown of ADAMTS1 in mice can induce growth retardation, malformation of adipose tissue, decreased fertility with changes in histology of uterus and ovaries, and renal lesions mimicking obstructive nephropathy (Shindo et al., 2000; Thai and Iruela-Arispe, 2002; Yokoyama et al., 2002), indicating a possible role of ADAMTS1 in ECM remodelling. VCAM1 encodes the key adhesion molecule expressed by endothelial cells to mediate leucocyte attachment to blood vessels during inflammation (Barreiro et al., 2002). Therefore, the downregulation of VCAM1 by TGF-β1 in PMC could prevent the adherence of leucocytes to the transformed PMC. VTN encodes vitronectin that is an abundant plasma protein regulating coagulation, fibrinolysis, complement activation, as well as cell adhesion (Hess et al., 1995). It has been shown that vitronectin can bind to type 1 plasminogen activator inhibitor (PAI-1) and stabilize PAI-1 in its active form (Mayasundari et al., 2004; Lawrence et al., 1997). In addition, vitronectin is also shown to bind fibrin during coagulation (Podor et al., 2002). Furthermore, vitronectin can contribute to the fusion of macrophages into foreign body giant cells (McNally and Anderson, 2011; McNally et al., 2008). Therefore, vitronectin may play an essential role in modulation of hemostasis and fibrinolysis during tissue repair. The suppression of vitronectin by TGF-β1 in PMC may facilitate fibrinolysis in the area of cell invasion.

A summary of the possible underlying mechanisms of post-operative adhesion are shown in Figures 6.1 and 6.2. Our results showed that IL-1 can cause cell detachment from basement membrane by suppressing integrin α6β4. Meanwhile, IL-1α and TGF-β1 were shown to cause EMT in PMC which further broke down the intercellular junction by reducing E-cadherin expression on cell membrane (Figure 6.1A). EMT-transformed cells had enhanced cell motility and were more adherent to ECM components. In addition, TGF-β1 could facilitate the invasion of transformed PMC into ECM by inducing membrane-inserted MMP 14 and 16 (Figure 6.1B). These suggest a likely mechanism of the origin of free-floating PMC and their invasion into repairing tissue. Moreover, IL-1α is mainly involved in the disruption of tissue homeostasis by inducing MMPs production. In contrast, TGF-β1 is involved in the reconstruction of damaged tissue by inducing the production of collagens and other ECM-related proteins, but not laminins (Figure 6.2). Thus, the balance between IL-1 and TGF-β effects is crucial for the remodeling of ECM. However, both IL-1α and TGF-β1 are able to upregulate some key pro-fibrotic factors in adhesion formation such as collagen VII and fibronectin, which might account for irreversible adhesion formation. This mechanism can be further enhanced by an autocrine circuit of TGF-β1 action in PMC induced by IL-1α and TGF-β1 (Figure 6.2).

In this Chapter, we discussed some possible underlying mechanisms involved in peritoneal repair based on the microarray results. Since the results only reflect the regulation at the mRNA level, other studies looking at the same genes in other cell types are referenced to help us understand the consequences of these changes. Therefore, some concepts need further confirmation, while the roles of a number of genes in peritoneal repair are not yet clear.

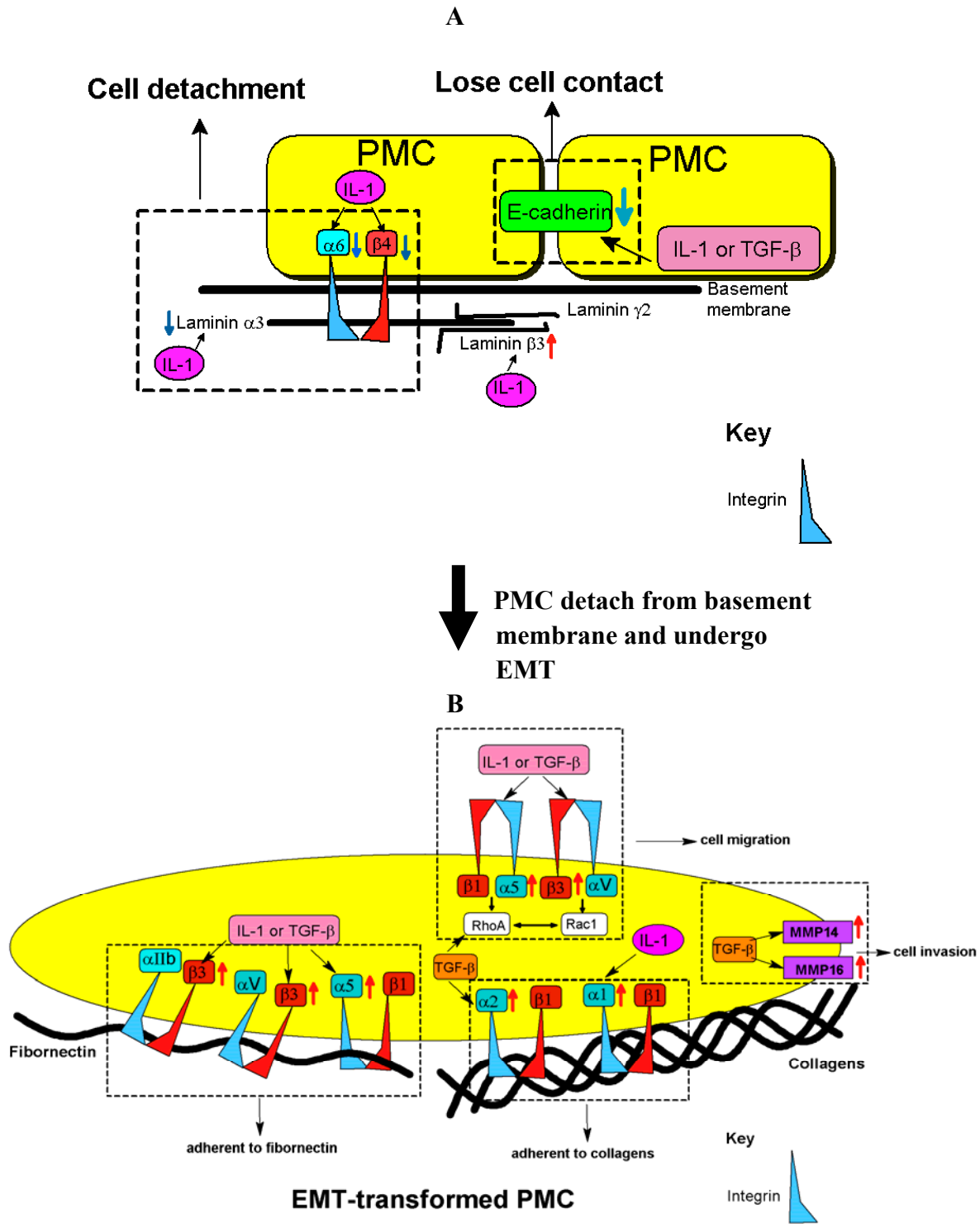

Figure 6.1. Underlying mechanism for recruiting PMC to repairing tissue during peritoneal healing. A: Origin of free-floating PMC by reducing cell-cell contact and cell-basement attachment. B: recruitment of EMT-transformed PMC to ECM tissue by enhanced cell invasion, as well as enhanced cell migration and cell-ECM adherence

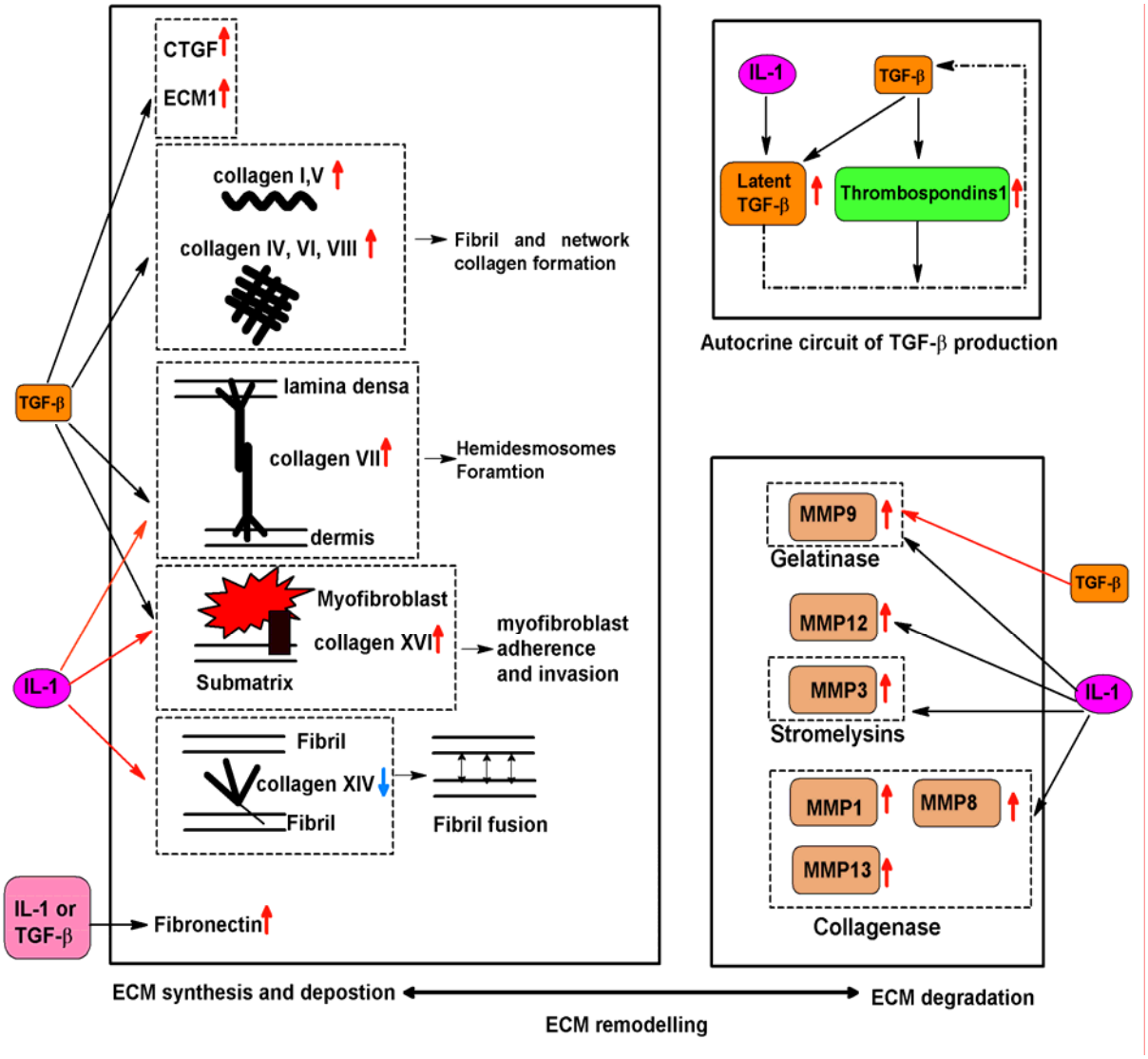

Figure 6.2. Regulation of ECM remodelling by EMT-transformed PMC and autocrine circuit of TGF-β production.

Chapter 7

General Discussion and Future work

7.1 Major findings of the thesis

The work presented in this thesis has provided new insights into both the physiological and pathological roles of peritoneal mesothelial cells (PMC) in the progression of post-operative peritoneal adhesion.

First, *in vivo* peritoneal fibrosis was induced by i.p injection of carbon nanotubes (NT), which adopted from the published work of Poland et al (Poland et al., 2008). We found that lysyl oxidase (LOX), a critical enzyme for collagen crosslinking, played an important role in the development of peritoneal fibrosis. In our *in vivo* fibrosis model, inhibition of LOX activity reduced collagen deposition, which further minimized the granuloma lesions on the peritoneal side of diaphragm. Subsequent studies confirmed PMC as a major source of LOX in the abdominal cavity; and the expression of LOX can be regulated by several inflammatory cytokines, including IL-1, IL-4, TNF-α, and TGF-β. Upregulation of LOX by IL-1 was confirmed at both mRNA and protein levels, whereas the effects of other cytokines were found not as potent as IL-1. In contrast, collagen expression in PMC was induced by TGF-β, but not by IL-1. These data provide a likely fundamental mechanism for collagen deposition which needs the presence of both IL-1 and TGF-β. Therefore, the combination of IL-1 and TGF-β was used to mimic the complicated inflammatory environment during peritoneal fibrosis. Results showed that, in the presence of IL-1 and TGF-β, PMC underwent a dramatic cell morphologic change, in terms of an epithelial-mesenchymal-transition (EMT). These EMT-transformed PMC had enhanced cell motility and were more adherent to ECM component (fibronectin) compared to normal PMC.

A real-time quantitative PCR-based microarray was used for genomic analysis of ECM-adhesion-related PMC genes in response to IL-1 and TGF-β treatments. The

results showed that IL-1 was more involved in regulating ECM degradation by inducing expression of matrix metalloproteinase (MMP) genes, including MMP 1, 3, 8, 9, and 13. In contrast, TGF-β mainly affected genes involved in ECM deposition, including collagens (collagens I, IV, V, VI, VIII) and other ECM components (Versican, ECM1). However, both cytokines were shown to regulate some key genes involved in the development of adhesion, including COL16A1, COL7A1, FN1, and ITGA5. In addition, the combination of IL-1 and TGF-β was shown to induce an autocrine circuit of TGF-β production from PMC by increasing TGFB1 and THBS1 expression (Figure 6.2). Furthermore, IL-1 reduced ITGA4 and ITGB6 expression affecting adherence of PMC to basement membrane; while TGF-β increased MMP14 and MMP16 expression, which could facilitate invasion of EMT-transformed PMC to the site of tissue repair.

Inflammatory cytokines were strongly associated with these studies. We first identified that NT-treated macrophages can release TNF-α, but not IL-1α. Meanwhile, results also showed that the cell-associated form of IL-1α (CA-IL-1α) was produced by PMC in response to TNF-α. Moreover, the combination of TNF-α and TGF-β1 synergistically induced both secreted IL-1α and CA-IL-1α expression from PMC. In addition, TNF-α-induced LOX expression in PMC was inhibited by the addition of the IL-1 receptor antagonist (IL-1ra). This is suggestive that TNF-α signalling network could be partially mediated by the elevation of IL-1.

In the thesis, we also showed that application of dexamethasone (DEX) reduced NT-induced fibrosis on mouse diaphragms. Our *in vitro* results showed that DEX can suppress TNF-α production from NT-treated macrophages. In addition, addition of cortisol reduced IL-1-induced LOX production from ovarian surface epithelial (OSE) cells. A similar suppression of cortisol had been observed on PMC, but this was not as effective as that on OSE cells. Furthermore, cortisol suppressed both secreted

IL-1α and CA-IL-1α production from PMC in response to TNF-α and TNF-α+TGF-β treatments. However, no interaction between cortisol and TGF-β was found in either PMC or OSE cells.

7.2 Prospective pathology of peritoneal repair and peritoneal adhesion.

The unique mechanism of peritoneal repair is the incorporation of free-floating PMC into the regenerating mesothelium, to reconstitute an intact mesothelial monolayer (Foley-Comer et al., 2002). However, how these cells become detached from the basement membrane and appear on regenerating peritoneum still requires further investigation. Our result showed that, these free-floating PMC could be a consequence of downregulation of integrin α6β4 expression induced by IL-1. Since integrin α6β4 plays an important role in the adherence of cells to laminin (Lee et al., 1992; Sonnenberg et al., 1990), reduction of integrin α6β4 could lead to the dissociation of PMC from the basement membrane. Moreover, our results showed that PMC underwent EMT in response to inflammatory stimuli, which broke down the intercellular junction by reducing E-cadherin expression on cell membrane. This process may further disrupt the mesothelial monolayer and result in more free-floating PMC (Figure 6.1A). In addition, the results showed that EMT-transformed cells had enhanced cell motility and were more adherent to ECM components. Therefore, EMT can promote the centripetal migration of PMC from the wound edge, as well as the reattachment of free-floating PMC to the regenerating peritoneum covered with ECM components, including collagen, fibronectin and fibrin. In the meantime, TGF-β was shown to induce the MMP 14 and MMP 16 expression on the cell membrane, which may promote the invasion of PMC into the underlying connective tissue or the fibrin clot (Figure 6.1B). This could explain the presence of cells with epithelial-like characteristics in the subserosal layer of biopsies

from various pathological conditions (Bolen et al., 1986; Bolen et al., 1987; Davila and Crouch, 1993; Dobbie, 1990).

Furthermore, these EMT-transformed cells can contribute to the peritoneum repair by producing several ECM components, including collagens, fibronectin, versican, and tenascin C. As we discussed previously, collagen crosslinking and deposition can be enhanced by the increased PMC-derived LOX expression in response to IL-1. Fibril and network collagen growth can be promoted by the production of collagens I, IV, V, VI, and VIII; while fibril fusion can be enhanced by reduction of collagen XIV. The increasing level of collagen XVI may further recruit more EMT-transformed PMC and myofibroblast into the injured areas. Meanwhile, the upregulation of collagen VII could promote hemidesmosome formation which could eventually lead to adhesions forming between the wounded area and the opposing mesothelium. Moreover, CTGF and ECM1 were also found produced by the transformed cells, which synergistically promote EMC synthesis and deposition together with TGF-β. Therefore, EMT-transformed PMC not only reconstitute the mesothelium monolayer by cell proliferation, they also contribute to the repair process by increasing ECM deposition (Figure 6.2). Interestingly, laminin α3 expression was reduced in the EMT-transformed cells, indicating a possible delayed repair of the damaged basement membrane (Figure 6.1A).

Although these transformed PMC can promote ECM synthesis and deposition, our results also showed they played an important role in ECM degradation. EMT-transformed PMC was shown to secrete various MMPs in response to IL-1. These MMPs, including collagenase and gelatinase, are highly involved in the degradation of ECM components, especially for collagen, fibronectin and fibrin (Figure 6.2). Therefore, EMT-transformed PMC are able to initiate both ECM deposition and degradation within the injured tissue or the fibrin clot. During a

normal peritoneal repair, the balance of such ECM remodelling mechanism of PMC might be well controlled, leading to tissue repair without any fibrosis. However, as is well known, serious surgical damage can cause a chronic inflammation in the abdominal cavity, causing a persisted activation of inflammatory factors and a significant delay in fibrinolysis (Holmdahl et al., 1996). Therefore, chronic inflammation may cause a persisting EMT process on normal PMC, which facilitates more EMT-transformed PMC recruitment into the fibrin clot. The delayed fibrinolysis can further provide a platform for PMC to deposit ECM components, which makes the fibrin clot become a precursor for an adhesion. In addition, the fibrin tissue might also provide a barrier for the infiltrated PMC, separating these cells from outside inflammatory stimuli, including IL-1 and TGF-β. However, our results indicated an autocrine circuit of TGF-β production of PMC (Figure 6.2). Therefore, after infiltration into the fibrin, the IL-1-induced ECM degradation might become weaker, whereas the TGF-β-induced ECM deposition can persist by its own autocrine feedback circuit. The balance of the ECM remodelling will shift to the synthesis and deposition site, eventually leading to adhesion formation replacing the fibrin.

7.3 Anti-inflammatory steroid treatments for peritoneal adhesion.

In the thesis, we already showed that anti-inflammatory steroid (DEX) can reduce peritoneal fibrosis induced by carbon nanotubes. The underlying mechanism involved a suppression of DEX on the NT-induced TNF-α production from macrophages. As we discussed previously, anti-inflammatory steroid environment seemed to play an important role in ovary scar-free repair. Results showed that cortisol can significantly suppress IL-1-induced LOX rise in OSE cells, while its effect on PMC was similar albeit less effective. It suggested a more sensitive responding model might present in OSE cells compared to PMC. However, cortisol

was shown to reduce both secreted IL-1α and CA-IL-1α production from PMC in response to TNF-α and TGF-β. Since both types of IL-1α have biological activity, the suppression of cortisol not only reduced secreted IL-1α levels to avoid a systemic inflammation, but also minimized any local inflammatory response by reducing CA-IL-1α levels. Interestingly, cortisol alone had no interaction with TGF-β signalling pathways. Therefore, the application of DEX or cortisol treatment may not be able to prevent TGF-β-induced ECM deposition effectively.

7.4 Future work

In this thesis, I tried to draw a picture of the pathology of peritoneal repair and peritoneal adhesion, aiming to find potential therapeutic methods to treat post-operative adhesion. However, most of the data presented in the chapters are restricted to the gene level. Functional studies for particular genes are needed to confirm the conclusions. Single dose and time-point may not represent the real effects of selected cytokines. Quantification on a single section for each diaphragm sample could also generate inconsistent results for further experiments. Therefore, some of the conclusions still need further consolidation and investigation. The mechanism for MMP-mediated PMC invasion needs to be confirmed by *in vitro* cell invasion assays used in other studies (Hotary et al., 2002; Sabeh et al., 2009). An *in vitro* adhesion model could be developed by seeding EMT-transformed PMC onto fibrin clots. ECM remodelling within the fibrin can then be examined by immunohistochemistry. Localization of infiltrating cells into the fibrin clot or pre-adhesion sites can be putatively identified by immunohistochemistry, staining with a specific PMC marker, such as HBME-1 (Foley-Comer et al., 2002). Meanwhile, blocking of membrane-associated MMPs can be conducted to inhibit cell invasion and prevent adhesion formation in animal models. Collagens involved in adhesion formation, especially collagen VII, can be indentified by specific antibody

for individual collagen member. Moreover, signalling pathways regulating the autocrine production circuit of TGF-β1 require confirmation and more detailed investigation. In addition, we also showed a possible manner for the PMC to manipulate local inflammation and systemic inflammation by secreted IL-1α and CA- IL-1α. However, levels of IL-1β secreted by PMC were not investigated in the studies. The actually amount of membrane-associated IL-1α (MA-IL-1α) derived from CA-IL-1α still requires determination. Flow cytometric and bioactivity analysis described in other studies can be used to identify the level of MA-IL-1α present in PMC (Niki et al., 2004).

The underlying mechanism elucidated above indicated that the treatment of post-operative adhesion might not be simply by inhibiting any single factor. Instead, a combined treatment is more likely to aid the healing process before control is lost. First, application of an anti-inflammatory steroid, such as DEX, should help to suppress any excess inflammatory response. In addition, the suppression of inflammation may further facilitate fibrinolysis by preventing inflammation-induced plasminogen activator inhibitor expression (see section 1.3.3). Secondly, specific inhibition of MMP 14 and 16 activities may prevent EMT-transformed PMC or myofibroblasts infiltrating into the fibrin clot and promoting adhesion formation. Lastly, inhibition of LOX activity can be used to prevent collagen deposition and to minimize further adhesion formation. Alternatively, selective suppression of TGF-β1 action could also help to prevent excess ECM deposition.

In summary, the work in this thesis provides an underlying mechanism for peritoneal repair and peritoneal adhesion. The concepts of the thesis also offer some therapeutic ideas to prevent post-operative adhesion.

Reference

ADAMS, D. O. 1976. The granulomatous inflammatory response. A review. *Am J Pathol,* 84**,** 164-92.

ADCOCK, I. M., NASUHARA, Y., STEVENS, D. A. & BARNES, P. J. 1999. Ligand-induced differentiation of glucocorticoid receptor (GR) trans-repression and transactivation: preferential targetting of NF-kappaB and lack of I-kappaB involvement. *Br J Pharmacol,* 127**,** 1003-11.

AFIFY, A. M., AL-KHAFAJI, B. M., PAULINO, A. F. & DAVILA, R. M. 2002. Diagnostic use of muscle markers in the cytologic evaluation of serous fluids. *Appl Immunohistochem Mol Morphol,* 10**,** 178-82.

AHAMED, J., JANCZAK, C. A., WITTKOWSKI, K. M. & COLLER, B. S. 2009. In vitro and in vivo evidence that thrombospondin-1 (TSP-1) contributes to stirring- and shear-dependent activation of platelet-derived TGF-beta1. *PLoS One,* 4**,** e6608.

AHMAD, G., DUFFY, J. M., FARQUHAR, C., VAIL, A., VANDEKERCKHOVE, P., WATSON, A. & WISEMAN, D. 2008. Barrier agents for adhesion prevention after gynaecological surgery. *Cochrane Database Syst Rev***,** CD000475.

AIMES, R. T. & QUIGLEY, J. P. 1995. Matrix metalloproteinase-2 is an interstitial collagenase. Inhibitor-free enzyme catalyzes the cleavage of collagen fibrils and soluble native type I collagen generating the specific 3/4- and 1/4-length fragments. *J Biol Chem,* 270**,** 5872-6.

ALCORN, J. F., GUALA, A. S., VAN DER VELDEN, J., MCELHINNEY, B., IRVIN, C. G., DAVIS, R. J. & JANSSEN-HEININGER, Y. M. 2008. Jun N-terminal kinase 1 regulates epithelial-to-mesenchymal transition induced by TGF-beta1. *J Cell Sci,* 121**,** 1036-45.

ALLAN, J. A., DOCHERTY, A. J., BARKER, P. J., HUSKISSON, N. S., REYNOLDS, J. J. & MURPHY, G. 1995. Binding of gelatinases A and B to type-I collagen and other matrix components. *Biochem J,* 309 (Pt 1)**,** 299-306.

ANDERSEN, C. Y. 1991. Concentrations of free oestradiol and progesterone in human preovulatory follicular fluid. *Hum Reprod,* 6**,** 359-64.

ANDERSEN, C. Y. & HORNNES, P. 1994. Intrafollicular concentrations of free cortisol close to follicular rupture. *Hum Reprod,* 9**,** 1944-9.

ANDREW, Y. W., JIA-JI, H., MARGARET, E. M., ROSALYN, D., KEITH, S. F., KATALIN, C., PAUL, A. J., EMMA, E. F. & REBECCA, W. 2007. Lysyl Oxidase Inhibition Reduces Rat Liver Fibrosis After Bile Duct Ligation [abstract]. *Gastroenterology,* 132**,** A827.

ANDREWS, P. M. & PORTER, K. R. 1973. The ultrastructural morphology and possible functional significance of mesothelial microvilli. *Anat Rec,* 177**,** 409-26.

ANNES, J. P., MUNGER, J. S. & RIFKIN, D. B. 2003. Making sense of latent TGFbeta activation. *J Cell Sci,* 116**,** 217-24.

ANSORGE, H. L., MENG, X., ZHANG, G., VEIT, G., SUN, M., KLEMENT, J. F., BEASON, D. P., SOSLOWSKY, L. J., KOCH, M. & BIRK, D. E. 2009. Type XIV Collagen Regulates

Fibrillogenesis: PREMATURE COLLAGEN FIBRIL GROWTH AND TISSUE DYSFUNCTION IN NULL MICE. *J Biol Chem,* 284**,** 8427-38.

ANTONY, V. B., GODBEY, S. W., KUNKEL, S. L., HOTT, J. W., HARTMAN, D. L., BURDICK, M. D. & STRIETER, R. M. 1993. Recruitment of inflammatory cells to the pleural space. Chemotactic cytokines, IL-8, and monocyte chemotactic peptide-1 in human pleural fluids. *J Immunol,* 151**,** 7216-23.

ANTONY, V. B., HOTT, J. W., KUNKEL, S. L., GODBEY, S. W., BURDICK, M. D. & STRIETER, R. M. 1995. Pleural mesothelial cell expression of C-C (monocyte chemotactic peptide) and C-X-C (interleukin 8) chemokines. *Am J Respir Cell Mol Biol,* 12**,** 581-8.

AREND, W. P., MALYAK, M., GUTHRIDGE, C. J. & GABAY, C. 1998. Interleukin-1 receptor antagonist: role in biology. *Annu Rev Immunol,* 16**,** 27-55.

ASHTON, G. H., SORELLI, P., MELLERIO, J. E., KEANE, F. M., EADY, R. A. & MCGRATH, J. A. 2001. Alpha 6 beta 4 integrin abnormalities in junctional epidermolysis bullosa with pyloric atresia. *Br J Dermatol,* 144**,** 408-14.

ATTISANO, L. & WRANA, J. L. 2002. Signal transduction by the TGF-beta superfamily. *Science,* 296**,** 1646-7.

AUMAILLEY, M., HAS, C., TUNGGAL, L. & BRUCKNER-TUDERMAN, L. 2006. Molecular basis of inherited skin-blistering disorders, and therapeutic implications. *Expert Rev Mol Med,* 8**,** 1-21.

AUPHAN, N., DIDONATO, J. A., ROSETTE, C., HELMBERG, A. & KARIN, M. 1995. Immunosuppression by glucocorticoids: inhibition of NF-kappa B activity through induction of I kappa B synthesis. *Science,* 270**,** 286-90.

BAER, A. N. & GREEN, F. A. 1993. Cyclooxygenase activity of cultured human mesothelial cells. *Prostaglandins,* 46**,** 37-49.

BAKIN, A. V., RINEHART, C., TOMLINSON, A. K. & ARTEAGA, C. L. 2002. p38 mitogen-activated protein kinase is required for TGFbeta-mediated fibroblastic transdifferentiation and cell migration. *J Cell Sci,* 115**,** 3193-206.

BAKIN, A. V., TOMLINSON, A. K., BHOWMICK, N. A., MOSES, H. L. & ARTEAGA, C. L. 2000. Phosphatidylinositol 3-kinase function is required for transforming growth factor beta-mediated epithelial to mesenchymal transition and cell migration. *J Biol Chem,* 275**,** 36803-10.

BALSALOBRE, A., BROWN, S. A., MARCACCI, L., TRONCHE, F., KELLENDONK, C., REICHARDT, H. M., SCHUTZ, G. & SCHIBLER, U. 2000. Resetting of circadian time in peripheral tissues by glucocorticoid signaling. *Science,* 289**,** 2344-7.

BANKERS-FULBRIGHT, J. L., KALLI, K. R. & MCKEAN, D. J. 1996. Interleukin-1 signal transduction. *Life Sci,* 59**,** 61-83.

BARADI, A. F. & CAMPBELL, W. G., JR. 1974. Exudative peritonitis induced in mice by bovine serum albumin. *Arch Pathol,* 97**,** 2-12.

BARADI, A. F. & HOPE, J. 1964. Observations on Ultrastructure of Rabbit Mesothelium. *Exp Cell Res,* 34**,** 33-44.

BARADI, A. F. & RAO, S. N. 1976. A scanning electron microscope study of mouse peritoneal mesothelium. *Tissue Cell,* 8**,** 159-62.

BARREIRO, O., YANEZ-MO, M., SERRADOR, J. M., MONTOYA, M. C., VICENTE-MANZANARES, M., TEJEDOR, R., FURTHMAYR, H. & SANCHEZ-MADRID, F. 2002. Dynamic interaction of VCAM-1 and ICAM-1 with moesin and ezrin in a novel endothelial docking structure for adherent leukocytes. *J Cell Biol,* 157**,** 1233-45.

BEAVIS, J., HARWOOD, J. L., COLES, G. A. & WILLIAMS, J. D. 1994. Synthesis of phospholipids by human peritoneal mesothelial cells. *Perit Dial Int,* 14**,** 348-55.

BECK, D. E., OPELKA, F. G., BAILEY, H. R., RAUH, S. M. & PASHOS, C. L. 1999. Incidence of small-bowel obstruction and adhesiolysis after open colorectal and general surgery. *Dis Colon Rectum,* 42**,** 241-8.

BELAAOUAJ, A., KIM, K. S. & SHAPIRO, S. D. 2000. Degradation of outer membrane protein A in Escherichia coli killing by neutrophil elastase. *Science,* 289**,** 1185-8.

BELIKOV, S., GELIUS, B., ALMOUZNI, G. & WRANGE, O. 2000. Hormone activation induces nucleosome positioning in vivo. *EMBO J,* 19**,** 1023-33.

BELPERIO, J. A., DY, M., BURDICK, M. D., XUE, Y. Y., LI, K., ELIAS, J. A. & KEANE, M. P. 2002. Interaction of IL-13 and C10 in the pathogenesis of bleomycin-induced pulmonary fibrosis. *Am J Respir Cell Mol Biol,* 27**,** 419-27.

BERGERON, C., PAGE, N., BARBEAU, B. & CHAKIR, J. 2003. Interleukin-4 promotes airway remodeling in asthma: regulation of procollagen I (alpha1) gene by interleukin-4. *Chest,* 123**,** 424S.

BETJES, M. G., TUK, C. W., STRUIJK, D. G., KREDIET, R. T., ARISZ, L., HART, M. & BEELEN, R. H. 1993. Interleukin-8 production by human peritoneal mesothelial cells in response to tumor necrosis factor-alpha, interleukin-1, and medium conditioned by macrophages cocultured with Staphylococcus epidermidis. *J Infect Dis,* 168**,** 1202-10.

BINDA, M. M. & KONINCKX, P. R. 2009. Prevention of adhesion formation in a laparoscopic mouse model should combine local treatment with peritoneal cavity conditioning. *Hum Reprod,* 24**,** 1473-9.

BINI, A., ITOH, Y., KUDRYK, B. J. & NAGASE, H. 1996. Degradation of cross-linked fibrin by matrix metalloproteinase 3 (stromelysin 1): hydrolysis of the gamma Gly 404-Ala 405 peptide bond. *Biochemistry,* 35**,** 13056-63.

BIRK, D. E. 2001. Type V collagen: heterotypic type I/V collagen interactions in the regulation of fibril assembly. *Micron,* 32**,** 223-37.

BIRK, D. E., FITCH, J. M., BABIARZ, J. P., DOANE, K. J. & LINSENMAYER, T. F. 1990. Collagen fibrillogenesis in vitro: interaction of types I and V collagen regulates fibril diameter. *J Cell Sci,* 95 (Pt 4)**,** 649-57.

BLACK, R. A., RAUCH, C. T., KOZLOSKY, C. J., PESCHON, J. J., SLACK, J. L., WOLFSON, M. F., CASTNER, B. J., STOCKING, K. L., REDDY, P., SRINIVASAN, S., NELSON, N., BOIANI, N., SCHOOLEY, K. A., GERHART, M., DAVIS, R., FITZNER, J. N., JOHNSON, R. S., PAXTON, R. J., MARCH, C. J. & CERRETTI, D. P. 1997. A metalloproteinase disintegrin that releases tumour-necrosis factor-alpha from cells. *Nature,* 385**,** 729-33.

BLEASE, K., JAKUBZICK, C., WESTWICK, J., LUKACS, N., KUNKEL, S. L. & HOGABOAM, C. M. 2001. Therapeutic effect of IL-13 immunoneutralization during chronic experimental fungal asthma. *J Immunol,* 166**,** 5219-24.

BLOMBACK, B., HESSEL, B., HOGG, D. & THERKILDSEN, L. 1978. A two-step fibrinogen--fibrin transition in blood coagulation. *Nature,* 275**,** 501-5.

BLOTNICK, S., PEOPLES, G. E., FREEMAN, M. R., EBERLEIN, T. J. & KLAGSBRUN, M. 1994. T lymphocytes synthesize and export heparin-binding epidermal growth factor-like growth factor and basic fibroblast growth factor, mitogens for vascular cells and fibroblasts: differential production and release by CD4+ and CD8+ T cells. *Proc Natl Acad Sci U S A,* 91**,** 2890-94.

BOLEN, J. W., HAMMAR, S. P. & MCNUTT, M. A. 1986. Reactive and neoplastic serosal tissue. A light-microscopic, ultrastructural, and immunocytochemical study. *Am J Surg Pathol,* 10**,** 34-47.

BOLEN, J. W., HAMMAR, S. P. & MCNUTT, M. A. 1987. Serosal tissue: reactive tissue as a model for understanding mesotheliomas. *Ultrastruct Pathol,* 11**,** 251-62.

BORRADORI, L. & SONNENBERG, A. 1999. Structure and function of hemidesmosomes: more than simple adhesion complexes. *J Invest Dermatol,* 112**,** 411-8.

BOTTLES, K. D., LASZIK, Z., MORRISSEY, J. H. & KINASEWITZ, G. T. 1997. Tissue factor expression in mesothelial cells: induction both in vivo and in vitro. *Am J Respir Cell Mol Biol,* 17**,** 164-72.

BOYLAN, A. M., RUEGG, C., KIM, K. J., HEBERT, C. A., HOEFFEL, J. M., PYTELA, R., SHEPPARD, D., GOLDSTEIN, I. M. & BROADDUS, V. C. 1992. Evidence of a role for mesothelial cell-derived interleukin 8 in the pathogenesis of asbestos-induced pleurisy in rabbits. *J Clin Invest,* 89**,** 1257-67.

BRADHAM, C. A., PLUMPE, J., MANNS, M. P., BRENNER, D. A. & TRAUTWEIN, C. 1998. Mechanisms of hepatic toxicity. I. TNF-induced liver injury. *Am J Physiol,* 275**,** G387-92.

BREW, K., DINAKARPANDIAN, D. & NAGASE, H. 2000. Tissue inhibitors of metalloproteinases: evolution, structure and function. *Biochim Biophys Acta,* 1477**,** 267-83.

BROWN, D. M., KINLOCH , IAN A, BANGERT, U, WINDLE, ALAN, WALTER, D M, WALKER, G S, SCOTCHFORD, C A, DONALDSON, KEN AND STONE, VICKI 2007. An in vitro study of the potential of carbon nanotubes and nanofibres to induce inflammatory mediators and frustrated phagocytosis. *Carbon,* 45**,** 1743-1756.

BRUCKNER-TUDERMAN, L. 2009. Can type VII collagen injections cure dystrophic epidermolysis bullosa? *Mol Ther,* 17**,** 6-7.

BRUGGMANN, D., TCHARTCHIAN, G., WALLWIENER, M., MUNSTEDT, K., TINNEBERG, H. R. & HACKETHAL, A. 2010. Intra-abdominal adhesions: definition, origin, significance in surgical practice, and treatment options. *Dtsch Arztebl Int,* 107**,** 769-75.

BUCK, M., HOUGLUM, K. & CHOJKIER, M. 1996. Tumor necrosis factor-alpha inhibits collagen alpha1(I) gene expression and wound healing in a murine model of cachexia. *Am J Pathol,* 149**,** 195-204.

CAHILL, R. A. & REDMOND, H. P. 2008. Cytokine orchestration in post-operative peritoneal adhesion formation. *World J Gastroenterol,* 14**,** 4861-6.

CAHILL, R. A., WANG, J. H., SOOHKAI, S. & REDMOND, H. P. 2006. Mast cells facilitate local VEGF release as an early event in the pathogenesis of postoperative peritoneal adhesions. *Surgery,* 140**,** 108-12.

CALDENHOVEN, E., LIDEN, J., WISSINK, S., VAN DE STOLPE, A., RAAIJMAKERS, J., KOENDERMAN, L., OKRET, S., GUSTAFSSON, J. A. & VAN DER SAAG, P. T. 1995. Negative cross-talk between RelA and the glucocorticoid receptor: a possible mechanism for the antiinflammatory action of glucocorticoids. *Mol Endocrinol,* 9**,** 401-12.

CAMPBELL, J. H., EFENDY, J. L., HAN, C., GIRJES, A. A. & CAMPBELL, G. R. 2000. Haemopoietic origin of myofibroblasts formed in the peritoneal cavity in response to a foreign body. *J Vasc Res,* 37**,** 364-71.

CANNISTRA, S. A., OTTENSMEIER, C., TIDY, J. & DEFRANZO, B. 1994. Vascular cell adhesion molecule-1 expressed by peritoneal mesothelium partly mediates the binding of activated human T lymphocytes. *Exp Hematol,* 22**,** 996-1002.

CHAN, I. 2004. The role of extracellular matrix protein 1 in human skin. *Clin Exp Dermatol,* 29**,** 52-6.

CHEEVER, A. W., WILLIAMS, M. E., WYNN, T. A., FINKELMAN, F. D., SEDER, R. A., COX, T. M., HIENY, S., CASPAR, P. & SHER, A. 1994. Anti-IL-4 treatment of Schistosoma mansoni-infected mice inhibits development of T cells and non-B, non-T cells expressing Th2 cytokines while decreasing egg-induced hepatic fibrosis. *J Immunol,* 153**,** 753-9.

CHEGINI, N., GOLD, L. I., WILLIAMS, R. S. & MASTERSON, B. J. 1994. Localization of transforming growth factor beta isoforms TGF-beta 1, TGF-beta 2, and TGF-beta 3 in surgically induced pelvic adhesions in the rat. *Obstet Gynecol,* 83**,** 449-54.

CHEGINI, N., RONG, H., BENNETT, B. & STONE, I. K. 1999. Peritoneal fluid cytokine and eicosanoid levels and their relation to the incidence of peritoneal adhesion. *J Soc Gynecol Investig,* 6**,** 153-7.

CHEN, C. Z. & RAGHUNATH, M. 2009. Focus on collagen: in vitro systems to study fibrogenesis and antifibrosis state of the art. *Fibrogenesis Tissue Repair,* 2**,** 7.

CHEN, J. Y., CHIU, J. H., CHEN, H. L., CHEN, T. W., YANG, W. C. & YANG, A. H. 2000. Human peritoneal mesothelial cells produce nitric oxide: induction by cytokines. *Perit Dial Int,* 20**,** 772-7.

CHEN, Y., BLOM, I. E., SA, S., GOLDSCHMEDING, R., ABRAHAM, D. J. & LEASK, A. 2002. CTGF expression in mesangial cells: involvement of SMADs, MAP kinase, and PKC. *Kidney Int,* 62**,** 1149-59.

CHEN, Z. J. 2005. Ubiquitin signalling in the NF-kappaB pathway. *Nat Cell Biol,* 7**,** 758-65.

CHEONG, Y. C., LAIRD, S. M., LI, T. C., SHELTON, J. B., LEDGER, W. L. & COOKE, I. D. 2001. Peritoneal healing and adhesion formation/reformation. *Hum Reprod Update,* 7**,** 556-66.

CHEONG, Y. C., LAIRD, S. M., SHELTON, J. B., LEDGER, W. L., LI, T. C. & COOKE, I. D. 2002. The correlation of adhesions and peritoneal fluid cytokine concentrations: a pilot study. *Hum Reprod,* 17**,** 1039-45.

CHEONG, Y. C., SHELTON, J. B., LAIRD, S. M., LI, T. C., LEDGER, W. L. & COOKE, I. D. 2003. Peritoneal fluid concentrations of matrix metalloproteinase-9, tissue inhibitor of metalloproteinase-1, and transforming growth factor-beta in women with pelvic adhesions. *Fertil Steril,* 79**,** 1168-75.

CHO, H. J. & YOO, J. 2007. Rho activation is required for transforming growth factor-beta-induced epithelial-mesenchymal transition in lens epithelial cells. *Cell Biol Int,* 31**,** 1225-30.

CHOE, N., TANAKA, S. & KAGAN, E. 1998. Asbestos fibers and interleukin-1 upregulate the formation of reactive nitrogen species in rat pleural mesothelial cells. *Am J Respir Cell Mol Biol,* 19**,** 226-36.

CIPPITELLI, M., SICA, A., VIGGIANO, V., YE, J., GHOSH, P., BIRRER, M. J. & YOUNG, H. A. 1995. Negative transcriptional regulation of the interferon-gamma promoter by glucocorticoids and dominant negative mutants of c-Jun. *J Biol Chem,* 270**,** 12548-56.

CIRCOLO, A., WELGUS, H. G., PIERCE, G. F., KRAMER, J. & STRUNK, R. C. 1991. Differential regulation of the expression of proteinases/antiproteinases in fibroblasts. Effects of interleukin-1 and platelet-derived growth factor. *J Biol Chem,* 266**,** 12283-8.

CLARK, B. D., COLLINS, K. L., GANDY, M. S., WEBB, A. C. & AURON, P. E. 1986. Genomic sequence for human prointerleukin 1 beta: possible evolution from a reverse transcribed prointerleukin 1 alpha gene. *Nucleic Acids Res,* 14**,** 7897-914.

CLARK, R. A., FOLKVORD, J. M., HART, C. E., MURRAY, M. J. & MCPHERSON, J. M. 1989. Platelet isoforms of platelet-derived growth factor stimulate fibroblasts to contract collagen matrices. *J Clin Invest,* 84**,** 1036-40.

CLARKE, C., BAGHDADI, H., HOWIE, A. F., MASON, J. I., WALKER, S. W. & BECKETT, G. J. 2010. Selenium supplementation attenuates procollagen-1 and interleukin-8 production in fat-loaded human C3A hepatoblastoma cells treated with TGFbeta1. *Biochim Biophys Acta,* 1800**,** 611-8.

COHEN, P. A., GOWER, A. C., STUCCHI, A. F., LEEMAN, S. E., BECKER, J. M. & REED, K. L. 2007. A neurokinin-1 receptor antagonist that reduces intraabdominal adhesion formation increases peritoneal matrix metalloproteinase activity. *Wound Repair Regen,* 15**,** 800-8.

COLOGNATO, H. & YURCHENCO, P. D. 2000. Form and function: the laminin family of heterotrimers. *Dev Dyn,* 218**,** 213-34.

COTRAN, R. S. & KARNOVSKY, M. J. 1968. Ultrastructural studies on the permeability of the mesothelium to horseradish peroxidase. *J Cell Biol,* 37**,** 123-37.

COULOMB-L'HERMIN, A., AMARA, A., SCHIFF, C., DURAND-GASSELIN, I., FOUSSAT, A., DELAUNAY, T., CHAOUAT, G., CAPRON, F., LEDEE, N., GALANAUD, P., ARENZANA-SEISDEDOS, F. & EMILIE, D. 1999. Stromal cell-derived factor 1 (SDF-1) and antenatal human B cell lymphopoiesis: expression of SDF-1 by mesothelial cells and biliary ductal plate epithelial cells. *Proc Natl Acad Sci U S A,* 96**,** 8585-90.

COWLAND, J. B. & BORREGAARD, N. 1999. The individual regulation of granule protein mRNA levels during neutrophil maturation explains the heterogeneity of neutrophil granules. *J Leukoc Biol,* 66**,** 989-95.

CRONAUER, M. V., STADLMANN, S., KLOCKER, H., ABENDSTEIN, B., EDER, I. E., ROGATSCH, H., ZEIMET, A. G., MARTH, C. & OFFNER, F. A. 1999. Basic fibroblast growth factor synthesis by human peritoneal mesothelial cells: induction by interleukin-1. *Am J Pathol,* 155**,** 1977-84.

CSISZAR, K. 2001. Lysyl oxidases: a novel multifunctional amine oxidase family. *Prog Nucleic Acid Res Mol Biol,* 70**,** 1-32.

CZERNOBILSKY, B., MOLL, R., LEVY, R. & FRANKE, W. W. 1985. Co-expression of cytokeratin and vimentin filaments in mesothelial, granulosa and rete ovarii cells of the human ovary. *Eur J Cell Biol,* 37**,** 175-90.

D'ORTHO, M. P., WILL, H., ATKINSON, S., BUTLER, G., MESSENT, A., GAVRILOVIC, J., SMITH, B., TIMPL, R., ZARDI, L. & MURPHY, G. 1997. Membrane-type matrix metalloproteinases 1 and 2 exhibit broad-spectrum proteolytic capacities comparable to many matrix metalloproteinases. *Eur J Biochem,* 250**,** 751-7.

DANEN, E. H., VAN RHEENEN, J., FRANKEN, W., HUVENEERS, S., SONNEVELD, P., JALINK, K. & SONNENBERG, A. 2005. Integrins control motile strategy through a Rho-cofilin pathway. *J Cell Biol,* 169**,** 515-26.

DANIELS, C. E., WILKES, M. C., EDENS, M., KOTTOM, T. J., MURPHY, S. J., LIMPER, A. H. & LEOF, E. B. 2004. Imatinib mesylate inhibits the profibrogenic activity of TGF-beta and prevents bleomycin-mediated lung fibrosis. *J Clin Invest,* 114**,** 1308-16.

DARBY, I. A. & HEWITSON, T. D. 2007. Fibroblast differentiation in wound healing and fibrosis. *Int Rev Cytol,* 257**,** 143-79.

DAVANI, B., KHAN, A., HULT, M., MARTENSSON, E., OKRET, S., EFENDIC, S., JORNVALL, H. & OPPERMANN, U. C. 2000. Type 1 11beta -hydroxysteroid dehydrogenase mediates glucocorticoid activation and insulin release in pancreatic islets. *J Biol Chem,* 275**,** 34841-4.

DAVILA, R. M. & CROUCH, E. C. 1993. Role of mesothelial and submesothelial stromal cells in matrix remodeling following pleural injury. *Am J Pathol,* 142**,** 547-55.

DE BOSSCHER, K., VANDEN BERGHE, W. & HAEGEMAN, G. 2003. The interplay between the glucocorticoid receptor and nuclear factor-kappaB or activator protein-1: molecular mechanisms for gene repression. *Endocr Rev,* 24**,** 488-522.

DECHERNEY, A. H. & DIZEREGA, G. S. 1997. Clinical problem of intraperitoneal postsurgical adhesion formation following general surgery and the use of adhesion prevention barriers. *Surg Clin North Am,* 77**,** 671-88.

DELAVARY, B. M., VAN DER VEER, W. M., VAN EGMOND, M., NIESSEN, F. B. & BEELEN, R. H. 2011. Macrophages in skin injury and repair. *Immunobiology*.

DEMETRI, G. D., ZENZIE, B. W., RHEINWALD, J. G. & GRIFFIN, J. D. 1989. Expression of colony-stimulating factor genes by normal human mesothelial cells and human malignant mesothelioma cells lines in vitro. *Blood,* 74**,** 940-6.

DERYNCK, R. & ZHANG, Y. E. 2003. Smad-dependent and Smad-independent pathways in TGF-beta family signalling. *Nature,* 425**,** 577-84.

DESHANE, J., GARNER, C. C. & SONTHEIMER, H. 2003. Chlorotoxin inhibits glioma cell invasion via matrix metalloproteinase-2. *J Biol Chem,* 278**,** 4135-44.

DIAZ, R., KIM, J. W., HUI, J. J., LI, Z., SWAIN, G. P., FONG, K. S., CSISZAR, K., RUSSO, P. A., RAND, E. B., FURTH, E. E. & WELLS, R. G. 2008. Evidence for the epithelial to mesenchymal transition in biliary atresia fibrosis. *Hum Pathol,* 39**,** 102-15.

DIJKSTRA, F. R., NIEUWENHUIJZEN, M., REIJNEN, M. M. & VAN GOOR, H. 2000. Recent clinical developments in pathophysiology, epidemiology, diagnosis and treatment of intra-abdominal adhesions. *Scand J Gastroenterol Suppl***,** 52-9.

DINARELLO, C. A. 1988. Interleukin-1. *Ann N Y Acad Sci,* 546**,** 122-32.

DIZEREGA, G. S., COAD, J. & DONNEZ, J. 2007. Clinical evaluation of endometriosis and differential response to surgical therapy with and without application of Oxiplex/AP* adhesion barrier gel. *Fertil Steril,* 87**,** 485-9.

DOBBIE, J. W. 1990. New concepts in molecular biology and ultrastructural pathology of the peritoneum: their significance for peritoneal dialysis. *Am J Kidney Dis,* 15**,** 97-109.

DONALDSON, K., AITKEN, R., TRAN, L., STONE, V., DUFFIN, R., FORREST, G. & ALEXANDER, A. 2006. Carbon nanotubes: a review of their properties in relation to pulmonary toxicology and workplace safety. *Toxicol Sci,* 92**,** 5-22.

DOUCAS, V., TINI, M., EGAN, D. A. & EVANS, R. M. 1999. Modulation of CREB binding protein function by the promyelocytic (PML) oncoprotein suggests a role for nuclear bodies in hormone signaling. *Proc Natl Acad Sci U S A,* 96**,** 2627-32.

DOUCET, C., BROUTY-BOYE, D., POTTIN-CLEMENCEAU, C., CANONICA, G. W., JASMIN, C. & AZZARONE, B. 1998. Interleukin (IL) 4 and IL-13 act on human lung fibroblasts. Implication in asthma. *J Clin Invest,* 101**,** 2129-39.

DOVI, J. V., HE, L. K. & DIPIETRO, L. A. 2003. Accelerated wound closure in neutrophil-depleted mice. *J Leukoc Biol,* 73**,** 448-55.

DRAPER, N. & STEWART, P. M. 2005. 11beta-hydroxysteroid dehydrogenase and the pre-receptor regulation of corticosteroid hormone action. *J Endocrinol,* 186**,** 251-71.

DROLLETTE, C. M. & BADAWY, S. Z. 1992. Pathophysiology of pelvic adhesions. Modern trends in preventing infertility. *J Reprod Med,* 37**,** 107-21; discussion 121-2.

DUFFIELD, J. S., FORBES, S. J., CONSTANDINOU, C. M., CLAY, S., PARTOLINA, M., VUTHOORI, S., WU, S., LANG, R. & IREDALE, J. P. 2005. Selective depletion of macrophages reveals distinct, opposing roles during liver injury and repair. *J Clin Invest,* 115**,** 56-65.

EGOZI, E. I., FERREIRA, A. M., BURNS, A. L., GAMELLI, R. L. & DIPIETRO, L. A. 2003. Mast cells modulate the inflammatory but not the proliferative response in healing wounds. *Wound Repair Regen,* 11**,** 46-54.

ENGLISH, W. R., VELASCO, G., STRACKE, J. O., KNAUPER, V. & MURPHY, G. 2001. Catalytic activities of membrane-type 6 matrix metalloproteinase (MMP25). *FEBS Lett,* 491**,** 137-42.

ERLER, J. T., BENNEWITH, K. L., COX, T. R., LANG, G., BIRD, D., KOONG, A., LE, Q. T. & GIACCIA, A. J. 2009. Hypoxia-induced lysyl oxidase is a critical mediator of bone marrow cell recruitment to form the premetastatic niche. *Cancer Cell,* 15**,** 35-44.

ERLER, J. T., BENNEWITH, K. L., NICOLAU, M., DORNHOFER, N., KONG, C., LE, Q. T., CHI, J. T., JEFFREY, S. S. & GIACCIA, A. J. 2006. Lysyl oxidase is essential for hypoxia-induced metastasis. *Nature,* 440**,** 1222-6.

ESPEY, L. L. 1994. Current status of the hypothesis that mammalian ovulation is comparable to an inflammatory reaction. *Biol Reprod,* 50**,** 233-8.

FALK, P., MA, C., CHEGINI, N. & HOLMDAHL, L. 2000. Differential regulation of mesothelial cell fibrinolysis by transforming growth factor beta 1. *Scand J Clin Lab Invest,* 60**,** 439-47.

FAN, Y., NIKITINA, T., ZHAO, J., FLEURY, T. J., BHATTACHARYYA, R., BOUHASSIRA, E. E., STEIN, A., WOODCOCK, C. L. & SKOULTCHI, A. I. 2005. Histone H1 depletion in mammals alters global chromatin structure but causes specific changes in gene regulation. *Cell,* 123**,** 1199-212.

FAULL, R. J., STANLEY, J. M., FRASER, S., POWER, D. A. & LEAVESLEY, D. I. 2001. HB-EGF is produced in the peritoneal cavity and enhances mesothelial cell adhesion and migration. *Kidney Int,* 59**,** 614-24.

FEDORKO, M. E. & HIRSCH, J. G. 1971. Studies on transport of macromolecules and small particles across mesothelial cells of the mouse omentum. I. Morphologic aspects. *Exp Cell Res,* 69**,** 113-27.

FEGAN, K. S. 2009. *A Study of Inflammatory Signalling in Epithelial Ovarian Cancer and the Normal Human Mesothelium.* Ph.D, University of Edinburgh.

FEGAN, K. S., RAE, M. T., CRITCHLEY, H. O. & HILLIER, S. G. 2008. Anti-inflammatory steroid signalling in the human peritoneum. *J Endocrinol,* 196**,** 369-76.

FENTON, M. J., CLARK, B. D., COLLINS, K. L., WEBB, A. C., RICH, A. & AURON, P. E. 1987. Transcriptional regulation of the human prointerleukin 1 beta gene. *J Immunol,* 138**,** 3972-9.

FERTIN, C., NICOLAS, J. F., GILLERY, P., KALIS, B., BANCHEREAU, J. & MAQUART, F. X. 1991. Interleukin-4 stimulates collagen synthesis by normal and scleroderma fibroblasts in dermal equivalents. *Cell Mol Biol,* 37**,** 823-9.

FITCHEV, P. P., WCISLAK, S. M., LEE, C., BERGH, A., BRENDLER, C. B., STELLMACH, V. M., CRAWFORD, S. E., MAVROUDIS, C. D., CORNWELL, M. L. & DOLL, J. A. 2010. Thrombospondin-1 regulates the normal prostate in vivo through angiogenesis and TGF-beta activation. *Lab Invest,* 90**,** 1078-90.

FLETCHER, T. M., RYU, B. W., BAUMANN, C. T., WARREN, B. S., FRAGOSO, G., JOHN, S. & HAGER, G. L. 2000. Structure and dynamic properties of a glucocorticoid receptor-induced chromatin transition. *Mol Cell Biol,* 20**,** 6466-75.

FOGELGREN, B., POLGAR, N., SZAUTER, K. M., UJFALUDI, Z., LACZKO, R., FONG, K. S. & CSISZAR, K. 2005. Cellular fibronectin binds to lysyl oxidase with high affinity and is critical for its proteolytic activation. *J Biol Chem,* 280**,** 24690-7.

FOLEY-COMER, A. J., HERRICK, S. E., AL-MISHLAB, T., PRELE, C. M., LAURENT, G. J. & MUTSAERS, S. E. 2002. Evidence for incorporation of free-floating mesothelial cells as a mechanism of serosal healing. *J Cell Sci,* 115**,** 1383-9.

FOLLONIER CASTELLA, L., GABBIANI, G., MCCULLOCH, C. A. & HINZ, B. 2010. Regulation of myofibroblast activities: calcium pulls some strings behind the scene. *Exp Cell Res,* 316**,** 2390-401.

FOTEV, Z., WHITAKER, D. & PAPADIMITRIOU, J. M. 1987. Role of macrophages in mesothelial healing. *J Pathol,* 151**,** 209-19.

FOUSSAT, A., BALABANIAN, K., AMARA, A., BOUCHET-DELBOS, L., DURAND-GASSELIN, I., BALEUX, F., COUDERC, J., GALANAUD, P. & EMILIE, D. 2001. Production of stromal cell-derived factor 1 by mesothelial cells and effects of this chemokine on peritoneal B lymphocytes. *Eur J Immunol,* 31**,** 350-9.

FRANTZ, C., STEWART, K. M. & WEAVER, V. M. 2010. The extracellular matrix at a glance. *J Cell Sci,* 123**,** 4195-200.

FREEMAN, M. L., SAED, G. M., ELHAMMADY, E. F. & DIAMOND, M. P. 2003. Expression of transforming growth factor beta isoform mRNA in injured peritoneum that healed with adhesions and without adhesions and in uninjured peritoneum. *Fertil Steril,* 80 Suppl 2**,** 708-13.

FUJINO, S., YOKOYAMA, A., KOHNO, N. & HIWADA, K. 1996. Interleukin 6 is an autocrine growth factor for normal human pleural mesothelial cells. *Am J Respir Cell Mol Biol,* 14**,** 508-15.

FUKATA, H. 1963. Electron Microscopic Study on Normal Rat Peritoneal Mesothelium and Its Changes in Absorption of Particulate Iron Dextran Complex. *Acta Pathol Jpn,* 13**,** 309-25.

FURUTANI, Y., NOTAKE, M., FUKUI, T., OHUE, M., NOMURA, H., YAMADA, M. & NAKAMURA, S. 1986. Complete nucleotide sequence of the gene for human interleukin 1 alpha. *Nucleic Acids Res,* 14**,** 3167-79.

GABRIELSON, E. W., GERWIN, B. I., HARRIS, C. C., ROBERTS, A. B., SPORN, M. B. & LECHNER, J. F. 1988. Stimulation of DNA synthesis in cultured primary human mesothelial cells by specific growth factors. *FASEB J,* 2**,** 2717-21.

GARBACKI, N., DI VALENTIN, E., PIETTE, J., CATALDO, D., CRAHAY, C. & COLIGE, A. 2009. Matrix metalloproteinase 12 silencing: a therapeutic approach to treat pathological lung tissue remodeling? *Pulm Pharmacol Ther,* 22**,** 267-78.

GARY LEE, Y. C., MELKERNEKER, D., THOMPSON, P. J., LIGHT, R. W. & LANE, K. B. 2002. Transforming growth factor beta induces vascular endothelial growth factor elaboration from pleural mesothelial cells in vivo and in vitro. *Am J Respir Crit Care Med,* 165**,** 88-94.

GAUDIO, E., RENDINA, E. A., PANNARALE, L., RICCI, C. & MARINOZZI, G. 1988. Surface morphology of the human pleura. A scanning electron microscopic study. *Chest,* 93**,** 149-53.

GEORAS, S. N., BECK, L. A. & STELLATO, C. 2002. What is eotaxin doing in the pleura? Insights into innate immunity from pleural mesothelial cells. *Am J Respir Cell Mol Biol,* 26**,** 384-7.

GERRITSEN, M. E., WILLIAMS, A. J., NEISH, A. S., MOORE, S., SHI, Y. & COLLINS, T. 1997. CREB-binding protein/p300 are transcriptional coactivators of p65. *Proc Natl Acad Sci U S A,* 94**,** 2927-32.

GHELLAI, A. M., STUCCHI, A. F., CHEGINI, N., MA, C., ANDRY, C. D., KASETA, J. M., BURNS, J. W., SKINNER, K. C. & BECKER, J. M. 2000. Role of transforming growth factor beta-1 in peritonitis-induced adhesions. *J Gastrointest Surg,* 4**,** 316-23.

GIAMPUZZI, M., OLEGGINI, R. & DI DONATO, A. 2003. Demonstration of in vitro interaction between tumor suppressor lysyl oxidase and histones H1 and H2: definition of the regions involved. *Biochim Biophys Acta,* 1647**,** 245-51.

GILES, K. M., ROSS, K., ROSSI, A. G., HOTCHIN, N. A., HASLETT, C. & DRANSFIELD, I. 2001. Glucocorticoid augmentation of macrophage capacity for phagocytosis of apoptotic cells is associated with reduced p130Cas expression, loss of paxillin/pyk2 phosphorylation, and high levels of active Rac. *J Immunol,* 167**,** 976-86.

GOETZL, E. J., BANDA, M. J. & LEPPERT, D. 1996. Matrix metalloproteinases in immunity. *J Immunol,* 156**,** 1-4.

GORDON, M. K. & HAHN, R. A. 2010. Collagens. *Cell Tissue Res,* 339**,** 247-57.

GORVY, D. A., HERRICK, S. E., SHAH, M. & FERGUSON, M. W. 2005. Experimental manipulation of transforming growth factor-beta isoforms significantly affects adhesion formation in a murine surgical model. *Am J Pathol,* 167**,** 1005-19.

GREEN, J. A. & FRIEDLAND, J. S. 2007. Astrocyte-leucocyte interactions and the mechanisms regulating matrix degradation in CNS tuberculosis. *Biochem Soc Trans,* 35**,** 686-8.

GROUP., O. L. S. 1991. Postoperative adhesion development after operative laparoscopy: evaluation at early second-look procedures. Operative Laparoscopy Study Group. *Fertil Steril,* 55**,** 700-4.

HART, J. 2002. Inflammation. 1: Its role in the healing of acute wounds. *J Wound Care,* 11**,** 205-9.

HARTEL, P. H., SHILO, K., KLASSEN-FISCHER, M., NEAFIE, R. C., OZBUDAK, I. H., GALVIN, J. R. & FRANKS, T. J. 2010. Granulomatous reaction to pneumocystis jirovecii: clinicopathologic review of 20 cases. *Am J Surg Pathol,* 34**,** 730-4.

HARVEY, W. & AMLOT, P. L. 1983. Collagen production by human mesothelial cells in vitro. *J Pathol,* 139**,** 337-47.

HASLINGER, B., MANDL-WEBER, S., SELLMAYER, A. & SITTER, T. 2001. Hyaluronan fragments induce the synthesis of MCP-1 and IL-8 in cultured human peritoneal mesothelial cells. *Cell Tissue Res,* 305**,** 79-86.

HAYASHI, K., FONG, K. S., MERCIER, F., BOYD, C. D., CSISZAR, K. & HAYASHI, M. 2004. Comparative immunocytochemical localization of lysyl oxidase (LOX) and the lysyl oxidase-like (LOXL) proteins: changes in the expression of LOXL during development and growth of mouse tissues. *J Mol Histol,* 35**,** 845-55.

HAZAN, R. B., QIAO, R., KEREN, R., BADANO, I. & SUYAMA, K. 2004. Cadherin switch in tumor progression. *Ann N Y Acad Sci,* 1014**,** 155-63.

HE, X., ZHANG, H., MA, Y., BAI, W., ZHANG, Z., LU, K., DING, Y., ZHAO, Y. & CHAI, Z. 2010. Lung deposition and extrapulmonary translocation of nano-ceria after intratracheal instillation. *Nanotechnology,* 21**,** 285103.

HECK, S., BENDER, K., KULLMANN, M., GOTTLICHER, M., HERRLICH, P. & CATO, A. C. 1997. I kappaB alpha-independent downregulation of NF-kappaB activity by glucocorticoid receptor. *EMBO J,* 16**,** 4698-707.

HECK, S., KULLMANN, M., GAST, A., PONTA, H., RAHMSDORF, H. J., HERRLICH, P. & CATO, A. C. 1994. A distinct modulating domain in glucocorticoid receptor monomers in the repression of activity of the transcription factor AP-1. *EMBO J,* 13**,** 4087-95.

HEISSIG, B., NISHIDA, C., TASHIRO, Y., SATO, Y., ISHIHARA, M., OHKI, M., GRITLI, I., ROSENKVIST, J. & HATTORI, K. 2010. Role of neutrophil-derived matrix metalloproteinase-9 in tissue regeneration. *Histol Histopathol,* 25**,** 765-70.

HELDIN, P. & PERTOFT, H. 1993. Synthesis and assembly of the hyaluronan-containing coats around normal human mesothelial cells. *Exp Cell Res,* 208**,** 422-9.

HERMAN, M. P., SUKHOVA, G. K., KISIEL, W., FOSTER, D., KEHRY, M. R., LIBBY, P. & SCHONBECK, U. 2001. Tissue factor pathway inhibitor-2 is a novel inhibitor of matrix metalloproteinases with implications for atherosclerosis. *J Clin Invest,* 107**,** 1117-26.

HERMANS, J. & MCDONAGH, J. 1982. Fibrin: structure and interactions. *Semin Thromb Hemost,* 8**,** 11-24.

HERRICK, S. E. & MUTSAERS, S. E. 2004. Mesothelial progenitor cells and their potential in tissue engineering. *Int J Biochem Cell Biol,* 36**,** 621-42.

HERRLICH, P. & GOTTLICHER, M. 2002. The anti-inflammatory action of glucocorticoid hormones. *Ernst Schering Res Found Workshop***,** 297-304.

HERSHLAG, A., DIAMOND, M. P. & DECHERNEY, A. H. 1991. Adhesiolysis. *Clin Obstet Gynecol,* 34**,** 395-402.

HESS, S., KANSE, S. M., KOST, C. & PREISSNER, K. T. 1995. The versatility of adhesion receptor ligands in haemostasis: morpho-regulatory functions of vitronectin. *Thromb Haemost,* 74**,** 258-65.

HESSELDAHL, H. & LARSEN, J. F. 1969. Ultrastructure of human yolk sac: endoderm, mesenchyme, tubules and mesothelium. *Am J Anat,* 126**,** 315-35.

HIGGINS, D. F., KIMURA, K., BERNHARDT, W. M., SHRIMANKER, N., AKAI, Y., HOHENSTEIN, B., SAITO, Y., JOHNSON, R. S., KRETZLER, M., COHEN, C. D., ECKARDT, K. U., IWANO, M. & HAASE, V. H. 2007. Hypoxia promotes fibrogenesis in vivo via HIF-1 stimulation of epithelial-to-mesenchymal transition. *J Clin Invest,* 117**,** 3810-20.

HILLER, O., LICHTE, A., OBERPICHLER, A., KOCOUREK, A. & TSCHESCHE, H. 2000. Matrix metalloproteinases collagenase-2, macrophage elastase, collagenase-3, and membrane type 1-matrix metalloproteinase impair clotting by degradation of fibrinogen and factor XII. *J Biol Chem,* 275**,** 33008-13.

HILLIER, S. G., ANDERSON, R. A., WILLIAMS, A. R. & TETSUKA, M. 1998. Expression of oestrogen receptor alpha and beta in cultured human ovarian surface epithelial cells. *Mol Hum Reprod,* 4**,** 811-5.

HILLIER, S. G., WHITELAW, P. F. & SMYTH, C. D. 1994. Follicular oestrogen synthesis: the 'two-cell, two-gonadotrophin' model revisited. *Mol Cell Endocrinol,* 100**,** 51-4.

HIZUME, K., YOSHIMURA, S. H. & TAKEYASU, K. 2005. Linker histone H1 per se can induce three-dimensional folding of chromatin fiber. *Biochemistry,* 44**,** 12978-89.

HOBSON, K. G., DEWING, M., HO, H. S., WOLFE, B. M., CHO, K. & GREENHALGH, D. G. 2003. Expression of transforming growth factor beta1 in patients with and without previous abdominal surgery. *Arch Surg,* 138**,** 1249-52.

HOLMDAHL, L., ERIKSSON, E., AL-JABREEN, M. & RISBERG, B. 1996. Fibrinolysis in human peritoneum during operation. *Surgery,* 119**,** 701-5.

HOLMDAHL, L., ERIKSSON, E., ERIKSSON, B. I. & RISBERG, B. 1998. Depression of peritoneal fibrinolysis during operation is a local response to trauma. *Surgery,* 123**,** 539-44.

HOLMDAHL, L. & RISBERG, B. 1997. Adhesions: prevention and complications in general surgery. *Eur J Surg,* 163**,** 169-74.

HOLMES, A., ABRAHAM, D. J., SA, S., SHIWEN, X., BLACK, C. M. & LEASK, A. 2001. CTGF and SMADs, maintenance of scleroderma phenotype is independent of SMAD signaling. *J Biol Chem,* 276**,** 10594-601.

HOLSCHNEIDER, C. H., NEJAD, F. & MONTZ, F. J. 1999. Immunomodulation with interleukin-10 and interleukin-4 compared with ketorolac tromethamine for prevention of postoperative adhesions in a murine model. *Fertil Steril,* 71**,** 67-73.

HOTARY, K. B., YANA, I., SABEH, F., LI, X. Y., HOLMBECK, K., BIRKEDAL-HANSEN, H., ALLEN, E. D., HIRAOKA, N. & WEISS, S. J. 2002. Matrix metalloproteinases (MMPs) regulate fibrin-invasive activity via MT1-MMP-dependent and -independent processes. *J Exp Med,* 195**,** 295-308.

HOTT, J. W., GODBEY, S. W. & ANTONY, V. B. 1994. Mesothelial cell modulation of pleural repair: thrombin stimulated mesothelial cells release prostaglandin E2. *Prostaglandins Leukot Essent Fatty Acids,* 51**,** 329-35.

HSIA, H. C. & SCHWARZBAUER, J. E. 2005. Meet the tenascins: multifunctional and mysterious. *J Biol Chem,* 280**,** 26641-4.

HSU, H., XIONG, J. & GOEDDEL, D. V. 1995. The TNF receptor 1-associated protein TRADD signals cell death and NF-kappa B activation. *Cell,* 81**,** 495-504.

HUBBARD, T. B., JR., KHAN, M. Z., CARAG, V. R., JR., ALBITES, V. E. & HRICKO, G. M. 1967. The pathology of peritoneal repair: its relation to the formation of adhesions. *Ann Surg,* 165**,** 908-16.

HUME, D. A. 2006. The mononuclear phagocyte system. *Curr Opin Immunol,* 18**,** 49-53.

HUMPHRIES, J. D., BYRON, A. & HUMPHRIES, M. J. 2006. Integrin ligands at a glance. *J Cell Sci,* 119**,** 3901-3.

HUNG, K. Y., SHYU, R. S., FANG, C. C., TSAI, C. C., LEE, P. H., TSAI, T. J. & HSIEH, B. S. 2001. Dipyridamole inhibits human peritoneal mesothelial cell proliferation in vitro and attenuates rat peritoneal fibrosis in vivo. *Kidney Int,* 59**,** 2316-24.

HUNT, T. K., HOPF, H. & HUSSAIN, Z. 2000. Physiology of wound healing. *Adv Skin Wound Care,* 13**,** 6-11.

HUVENEERS, S. & DANEN, E. H. 2009. Adhesion signaling - crosstalk between integrins, Src and Rho. *J Cell Sci,* 122**,** 1059-69.

HUYBRECHTS-GODIN, G., PEETERS-JORIS, C. & VAES, G. 1985. Partial characterization of the macrophage factor that stimulates fibroblasts to produce collagenase and to degrade collagen. *Biochim Biophys Acta,* 846**,** 51-4.

HYNES, R. O. 2002. Integrins: bidirectional, allosteric signaling machines. *Cell,* 110**,** 673-87.

IDELL, S., ZWIEB, C., KUMAR, A., KOENIG, K. B. & JOHNSON, A. R. 1992. Pathways of fibrin turnover of human pleural mesothelial cells in vitro. *Am J Respir Cell Mol Biol,* 7**,** 414-26.

JANSSEN, Y. M., MARSH, J. P., ABSHER, M. P., GABRIELSON, E., BORM, P. J., DRISCOLL, K. & MOSSMAN, B. T. 1994. Oxidant stress responses in human pleural mesothelial cells exposed to asbestos. *Am J Respir Crit Care Med,* 149**,** 795-802.

JARVELAINEN, H., SAINIO, A., KOULU, M., WIGHT, T. N. & PENTTINEN, R. 2009. Extracellular matrix molecules: potential targets in pharmacotherapy. *Pharmacol Rev,* 61**,** 198-223.

JAYNE, D. G., PERRY, S. L., MORRISON, E., FARMERY, S. M. & GUILLOU, P. J. 2000. Activated mesothelial cells produce heparin-binding growth factors: implications for tumour metastases. *Br J Cancer,* 82**,** 1233-8.

JONAT, C., RAHMSDORF, H. J., PARK, K. K., CATO, A. C., GEBEL, S., PONTA, H. & HERRLICH, P. 1990. Antitumor promotion and antiinflammation: down-modulation of AP-1 (Fos/Jun) activity by glucocorticoid hormone. *Cell,* 62**,** 1189-204.

JONJIC, N., PERI, G., BERNASCONI, S., SCIACCA, F. L., COLOTTA, F., PELICCI, P., LANFRANCONE, L. & MANTOVANI, A. 1992. Expression of adhesion molecules and chemotactic cytokines in cultured human mesothelial cells. *J Exp Med,* 176**,** 1165-74.

KAGAN, H. M., VACCARO, C. A., BRONSON, R. E., TANG, S. S. & BRODY, J. S. 1986. Ultrastructural immunolocalization of lysyl oxidase in vascular connective tissue. *J Cell Biol,* 103**,** 1121-8.

KAGAN, H. M., WILLIAMS, M. A., CALAMAN, S. D. & BERKOWITZ, E. M. 1983. Histone H1 is a substrate for lysyl oxidase and contains endogenous sodium borotritide-reducible residues. *Biochem Biophys Res Commun,* 115**,** 186-92.

KAGAN, H. M., WILLIAMS, M. A., WILLIAMSON, P. R. & ANDERSON, J. M. 1984. Influence of sequence and charge on the specificity of lysyl oxidase toward protein and synthetic peptide substrates. *J Biol Chem,* 259**,** 11203-7.

KAIDI, A. A., GURCHUMELIDZE, T., NAZZAL, M., FIGERT, P., VANTERPOOL, C. & SILVA, Y. 1995a. Tumor necrosis factor-alpha: a marker for peritoneal adhesion formation. *J Surg Res,* 58**,** 516-8.

KAIDI, A. A., NAZZAL, M., GURCHUMELIDZE, T., ALI, M. A., DAWE, E. J. & SILVA, Y. J. 1995b. Preoperative administration of antibodies against tumor necrosis factor-alpha (TNF-alpha) and interleukin-1 (IL-1) and their impact on peritoneal adhesion formation. *Am Surg,* 61**,** 569-72.

KAIMORI, A., POTTER, J., KAIMORI, J. Y., WANG, C., MEZEY, E. & KOTEISH, A. 2007. Transforming growth factor-beta1 induces an epithelial-to-mesenchymal transition state in mouse hepatocytes in vitro. *J Biol Chem,* 282**,** 22089-101.

KALLURI, R. & NEILSON, E. G. 2003. Epithelial-mesenchymal transition and its implications for fibrosis. *J Clin Invest,* 112**,** 1776-84.

KAMEI, Y., XU, L., HEINZEL, T., TORCHIA, J., KUROKAWA, R., GLOSS, B., LIN, S. C., HEYMAN, R. A., ROSE, D. W., GLASS, C. K. & ROSENFELD, M. G. 1996. A CBP integrator complex mediates transcriptional activation and AP-1 inhibition by nuclear receptors. *Cell,* 85**,** 403-14.

KAMEL, R. M. 2010. Prevention of postoperative peritoneal adhesions. *Eur J Obstet Gynecol Reprod Biol,* 150**,** 111-8.

KANG, T., YI, J., GUO, A., WANG, X., OVERALL, C. M., JIANG, W., ELDE, R., BORREGAARD, N. & PEI, D. 2001. Subcellular distribution and cytokine- and chemokine-regulated secretion of leukolysin/MT6-MMP/MMP-25 in neutrophils. *J Biol Chem,* 276**,** 21960-8.

KATAYAMA, H., YOKOYAMA, A., KOHNO, N., SAKAI, K., HIWADA, K., YAMADA, H. & HIRAI, K. 2002. Production of eosinophilic chemokines by normal pleural mesothelial cells. *Am J Respir Cell Mol Biol,* 26**,** 398-403.

KAWAI, T. & AKIRA, S. 2006. Innate immune recognition of viral infection. *Nat Immunol,* 7**,** 131-7.

KAZEROUNIAN, S., YEE, K. O. & LAWLER, J. 2008. Thrombospondins in cancer. *Cell Mol Life Sci,* 65**,** 700-12.

KEANE, M. P., GOMPERTS, B. N., WEIGT, S., XUE, Y. Y., BURDICK, M. D., NAKAMURA, H., ZISMAN, D. A., ARDEHALI, A., SAGGAR, R., LYNCH, J. P., 3RD, HOGABOAM, C., KUNKEL, S. L., LUKACS, N. W., ROSS, D. J., GRUSBY, M. J., STRIETER, R. M. & BELPERIO, J. A. 2007. IL-13 is pivotal in the fibro-obliterative process of bronchiolitis obliterans syndrome. *J Immunol,* 178**,** 511-9.

KENNEDY, L., LIU, S., SHI-WEN, X., CHEN, Y., EASTWOOD, M., SABETKAR, M., CARTER, D. E., LYONS, K. M., BLACK, C. M., ABRAHAM, D. J. & LEASK, A. 2007. CCN2 is necessary for the function of mouse embryonic fibroblasts. *Exp Cell Res,* 313**,** 952-64.

KHOSHNOODI, J., PEDCHENKO, V. & HUDSON, B. G. 2008. Mammalian collagen IV. *Microsc Res Tech,* 71**,** 357-70.

KING, E. M., HOLDEN, N. S., GONG, W., RIDER, C. F. & NEWTON, R. 2009. Inhibition of NF-kappaB-dependent transcription by MKP-1: transcriptional repression by glucocorticoids occurring via p38 MAPK. *J Biol Chem,* 284**,** 26803-15.

KIRSCHMANN, D. A., SEFTOR, E. A., FONG, S. F., NIEVA, D. R., SULLIVAN, C. M., EDWARDS, E. M., SOMMER, P., CSISZAR, K. & HENDRIX, M. J. 2002. A molecular role for lysyl oxidase in breast cancer invasion. *Cancer Res,* 62**,** 4478-83.

KLASS, B. R., GROBBELAAR, A. O. & ROLFE, K. J. 2009. Transforming growth factor beta1 signalling, wound healing and repair: a multifunctional cytokine with clinical implications for wound repair, a delicate balance. *Postgrad Med J,* 85**,** 9-14.

KLUGE, T. & HOVIG, T. 1967a. The ultrastructure of human and rat pericardium. I. Parietal and visceral mesothelium. *Acta Pathol Microbiol Scand,* 71**,** 529-46.

KLUGE, T. & HOVIG, T. 1967b. The ultrastructure of human and rat pericardium. II. Intercellular spaces and junctions. *Acta Pathol Microbiol Scand,* 71**,** 547-63.

KNAUPER, V., COWELL, S., SMITH, B., LOPEZ-OTIN, C., O'SHEA, M., MORRIS, H., ZARDI, L. & MURPHY, G. 1997. The role of the C-terminal domain of human collagenase-3 (MMP-13) in the activation of procollagenase-3, substrate specificity, and tissue inhibitor of metalloproteinase interaction. *J Biol Chem,* 272**,** 7608-16.

KOLB, M., MARGETTS, P. J., ANTHONY, D. C., PITOSSI, F. & GAULDIE, J. 2001. Transient expression of IL-1beta induces acute lung injury and chronic repair leading to pulmonary fibrosis. *J Clin Invest,* 107**,** 1529-36.

KOLODSICK, J. E., TOEWS, G. B., JAKUBZICK, C., HOGABOAM, C., MOORE, T. A., MCKENZIE, A., WILKE, C. A., CHRISMAN, C. J. & MOORE, B. B. 2004. Protection from fluorescein isothiocyanate-induced fibrosis in IL-13-deficient, but not IL-4-deficient, mice results from impaired collagen synthesis by fibroblasts. *J Immunol,* 172**,** 4068-76.

KORKMAZ, B., MOREAU, T. & GAUTHIER, F. 2008. Neutrophil elastase, proteinase 3 and cathepsin G: physicochemical properties, activity and physiopathological functions. *Biochimie,* 90**,** 227-42.

KOSAKA, H., YOSHIMOTO, T., FUJIMOTO, J. & NAKANISHI, K. 2008. Interferon-gamma is a therapeutic target molecule for prevention of postoperative adhesion formation. *Nat Med,* 14**,** 437-41.

KOSTARELOS, K. 2008. The long and short of carbon nanotube toxicity. *Nat Biotechnol,* 26**,** 774-6.

KRIEGLER, M., PEREZ, C., DEFAY, K., ALBERT, I. & LU, S. D. 1988. A novel form of TNF/cachectin is a cell surface cytotoxic transmembrane protein: ramifications for the complex physiology of TNF. *Cell,* 53**,** 45-53.

KRISHNAN, J., SELVARAJOO, K., TSUCHIYA, M., LEE, G. & CHOI, S. 2007. Toll-like receptor signal transduction. *Exp Mol Med,* 39**,** 421-38.

KUCUKOZKAN, T., ERSOY, B., UYGUR, D. & GUNDOGDU, C. 2004. Prevention of adhesions by sodium chromoglycate, dexamethasone, saline and aprotinin after pelvic surgery. *ANZ J Surg,* 74**,** 1111-5.

KULAR, L., PAKRADOUNI, J., KITABGI, P., LAURENT, M. & MARTINERIE, C. 2011. The CCN family: a new class of inflammation modulators? *Biochimie,* 93**,** 377-88.

KUMAR, R. K., HERBERT, C., YANG, M., KOSKINEN, A. M., MCKENZIE, A. N. & FOSTER, P. S. 2002. Role of interleukin-13 in eosinophil accumulation and airway remodelling in a mouse model of chronic asthma. *Clin Exp Allergy,* 32**,** 1104-11.

KUMAR, V., ABBAS, A. K. & FAUSTO, N. 2005a. Extracellular Matrix(ECM) and Cell-Matrix Interactions. *In:* VINAY KUMAR, A. K. A., NELSON FAUSTO ; WITH ILLUSTRATIONS BY JAMES A. PERKINS. (ed.) *Robbins and Cotran pathologic basis of disease.* Philadelphia, Pa: Elsevier Saunders.

KUMAR, V., ABBAS, A. K., FAUSTO, N., ROBBINS, S. L. S. L.-. & COTRAN, R. S. 2005b. Acute and Chronic Inflammation. *In:* KUMAR, V., ABBAS, A. K., FAUSTO, N., ROBBINS, S. L. S. L.-. & COTRAN, R. S. (eds.) *Robbins and Cotran pathologic basis of disease.*

. Philadelphia, Pa.: Elsevier Saunders.

KUMAR, V., ABBAS, A. K., FAUSTO, N., ROBBINS, S. L. S. L.-. & COTRAN, R. S. 2005c. Tissue Renewal and Repair: Regeneration, Healing, and Fibrosis. *In:* KUMAR, V., ABBAS, A. K., FAUSTO, N., ROBBINS, S. L. S. L.-. & COTRAN, R. S. (eds.) *Robbins and Cotran pathologic basis of disease.*

. Philadelphia, Pa.: Elsevier Saunders.

KUNO, K., OKADA, Y., KAWASHIMA, H., NAKAMURA, H., MIYASAKA, M., OHNO, H. & MATSUSHIMA, K. 2000. ADAMTS-1 cleaves a cartilage proteoglycan, aggrecan. *FEBS Lett,* 478**,** 241-5.

KURUMBAIL, R. G., STEVENS, A. M., GIERSE, J. K., MCDONALD, J. J., STEGEMAN, R. A., PAK, J. Y., GILDEHAUS, D., MIYASHIRO, J. M., PENNING, T. D., SEIBERT, K., ISAKSON, P. C. & STALLINGS, W. C. 1996. Structural basis for selective inhibition of cyclooxygenase-2 by anti-inflammatory agents. *Nature,* 384**,** 644-8.

KUSHNIR, M. M., NAESSEN, T., KIRILOVAS, D., CHAIKA, A., NOSENKO, J., MOGILEVKINA, I., ROCKWOOD, A. L., CARLSTROM, K. & BERGQUIST, J. 2009. Steroid profiles in ovarian follicular fluid from regularly menstruating women and women after ovarian stimulation. *Clin Chem,* 55**,** 519-26.

KUWAHARA, M., VERMA, K., ANDO, T., HEMENWAY, D. R. & KAGAN, E. 1994. Asbestos exposure stimulates pleural mesothelial cells to secrete the fibroblast chemoattractant, fibronectin. *Am J Respir Cell Mol Biol,* 10**,** 167-76.

LAMPE, A. K. & BUSHBY, K. M. 2005. Collagen VI related muscle disorders. *J Med Genet,* 42**,** 673-85.

LANFRANCONE, L., BORASCHI, D., GHIARA, P., FALINI, B., GRIGNANI, F., PERI, G., MANTOVANI, A. & PELICCI, P. G. 1992. Human peritoneal mesothelial cells produce many cytokines (granulocyte colony-stimulating factor [CSF], granulocyte-monocyte-CSF, macrophage-CSF, interleukin-1 [IL-1], and IL-6) and are activated and stimulated to grow by IL-1. *Blood,* 80**,** 2835-42.

LASA, M., ABRAHAM, S. M., BOUCHERON, C., SAKLATVALA, J. & CLARK, A. R. 2002. Dexamethasone causes sustained expression of mitogen-activated protein kinase (MAPK) phosphatase 1 and phosphatase-mediated inhibition of MAPK p38. *Mol Cell Biol,* 22**,** 7802-11.

LAURENT, P., MAGNE, L., DE PALMAS, J., BIGNON, J. & JAURAND, M. C. 1988. Quantitation of elastin in human urine and rat pleural mesothelial cell matrix by a sensitive avidin-biotin ELISA for desmosine. *J Immunol Methods,* 107**,** 1-11.

LAVECK, M. A., SOMERS, A. N., MOORE, L. L., GERWIN, B. I. & LECHNER, J. F. 1988. Dissimilar peptide growth factors can induce normal human mesothelial cell multiplication. *In Vitro Cell Dev Biol,* 24**,** 1077-84.

LAWRENCE, D. A., PALANIAPPAN, S., STEFANSSON, S., OLSON, S. T., FRANCIS-CHMURA, A. M., SHORE, J. D. & GINSBURG, D. 1997. Characterization of the binding of different conformational forms of plasminogen activator inhibitor-1 to vitronectin. Implications for the regulation of pericellular proteolysis. *J Biol Chem,* 272**,** 7676-80.

LAWRENCE, W. T. 1998. Physiology of the acute wound. *Clin Plast Surg,* 25**,** 321-40.

LAZARUS, H. M., CRUIKSHANK, W. W., NARASIMHAN, N., KAGAN, H. M. & CENTER, D. M. 1995. Induction of human monocyte motility by lysyl oxidase. *Matrix Biol,* 14**,** 727-31.

LE, S. J., GONGORA, M., ZHANG, B., GRIMMOND, S., CAMPBELL, G. R., CAMPBELL, J. H. & ROLFE, B. E. 2010. Gene expression profile of the fibrotic response in the peritoneal cavity. *Differentiation,* 79**,** 232-43.

LEAK, L. V. & RAHIL, K. 1978. Permeability of the diaphragmatic mesothelium: the ultrastructural basis for "stomata". *Am J Anat,* 151**,** 557-93.

LEASK, A. 2008. Targeting the TGFbeta, endothelin-1 and CCN2 axis to combat fibrosis in scleroderma. *Cell Signal,* 20**,** 1409-14.

LEASK, A. & ABRAHAM, D. J. 2006. All in the CCN family: essential matricellular signaling modulators emerge from the bunker. *J Cell Sci,* 119**,** 4803-10.

LEAVESLEY, D. I., STANLEY, J. M. & FAULL, R. J. 1999. Epidermal growth factor modifies the expression and function of extracellular matrix adhesion receptors expressed by peritoneal mesothelial cells from patients on CAPD. *Nephrol Dial Transplant,* 14**,** 1208-16.

LEE, C. G., HOMER, R. J., ZHU, Z., LANONE, S., WANG, X., KOTELIANSKY, V., SHIPLEY, J. M., GOTWALS, P., NOBLE, P., CHEN, Q., SENIOR, R. M. & ELIAS, J. A. 2001. Interleukin-13 induces tissue fibrosis by selectively stimulating and activating transforming growth factor beta(1). *J Exp Med,* 194**,** 809-21.

LEE, E. C., LOTZ, M. M., STEELE, G. D., JR. & MERCURIO, A. M. 1992. The integrin alpha 6 beta 4 is a laminin receptor. *J Cell Biol,* 117**,** 671-8.

LEE, M. K., PARDOUX, C., HALL, M. C., LEE, P. S., WARBURTON, D., QING, J., SMITH, S. M. & DERYNCK, R. 2007. TGF-beta activates Erk MAP kinase signalling through direct phosphorylation of ShcA. *EMBO J,* 26**,** 3957-67.

LEIBOVICH, S. J. & ROSS, R. 1975. The role of the macrophage in wound repair. A study with hydrocortisone and antimacrophage serum. *Am J Pathol,* 78**,** 71-100.

LETOWSKA-ANDRZEJEWICZ, K., TORRES, A., TORRES, K., DOBROWOLSKI, P., PIERSIAK, T., MACIEJEWSKI, R., GAWRON, A., STASKIEWICZ, G. & PLEWA, Z. 2011. The use of morphometric and fractal parameters to assess the effects of 5-fluorouracil, interferon and dexamethasone treatment on colonic anastomosis healing: an experimental study in rats. *Folia Histochem Cytobiol,* 49**,** 80-9.

LI, A. J., BALDWIN, R. L. & KARLAN, B. Y. 2003. Estrogen and progesterone receptor subtype expression in normal and malignant ovarian epithelial cell cultures. *Am J Obstet Gynecol,* 189**,** 22-7.

LI, F. K., DAVENPORT, A., ROBSON, R. L., LOETSCHER, P., ROTHLEIN, R., WILLIAMS, J. D. & TOPLEY, N. 1998. Leukocyte migration across human peritoneal mesothelial cells is dependent on directed chemokine secretion and ICAM-1 expression. *Kidney Int,* 54**,** 2170-83.

LI, W., LIU, G., CHOU, I. N. & KAGAN, H. M. 2000. Hydrogen peroxide-mediated, lysyl oxidase-dependent chemotaxis of vascular smooth muscle cells. *J Cell Biochem,* 78**,** 550-7.

LIAKAKOS, T., THOMAKOS, N., FINE, P. M., DERVENIS, C. & YOUNG, R. L. 2001. Peritoneal adhesions: etiology, pathophysiology, and clinical significance. Recent advances in prevention and management. *Dig Surg,* 18**,** 260-73.

LIANG, Y. & SASAKI, K. 2000. Expression of adhesion molecules relevant to leukocyte migration on the microvilli of liver peritoneal mesothelial cells. *Anat Rec,* 258**,** 39-46.

LIAW, Y. S., YU, C. J., SHUN, C. T., LEE, Y. C., KUO, S. H., LUH, K. T. & YANG, P. C. 2001. Expression of integrins in human cultured mesothelial cells: the roles in cell-to-extracellular matrix adhesion and inhibition by RGD-containing peptide. *Respir Med,* 95**,** 221-6.

LIBBY, P., ORDOVAS, J. M., BIRINYI, L. K., AUGER, K. R. & DINARELLO, C. A. 1986. Inducible interleukin-1 gene expression in human vascular smooth muscle cells. *J Clin Invest,* 78**,** 1432-8.

LIBEREK, T., TOPLEY, N., LUTTMANN, W. & WILLIAMS, J. D. 1996. Adherence of neutrophils to human peritoneal mesothelial cells: role of intercellular adhesion molecule-1. *J Am Soc Nephrol,* 7**,** 208-17.

LIBERMAN, A. C., DRUKER, J., GARCIA, F. A., HOLSBOER, F. & ARZT, E. 2009. Intracellular molecular signaling. Basis for specificity to glucocorticoid anti-inflammatory actions. *Ann N Y Acad Sci,* 1153**,** 6-13.

LIBERMAN, A. C., DRUKER, J., PERONE, M. J. & ARZT, E. 2007. Glucocorticoids in the regulation of transcription factors that control cytokine synthesis. *Cytokine Growth Factor Rev,* 18**,** 45-56.

LIN, D. Y., LAI, M. Z., ANN, D. K. & SHIH, H. M. 2003. Promyelocytic leukemia protein (PML) functions as a glucocorticoid receptor co-activator by sequestering Daxx to the PML oncogenic domains (PODs) to enhance its transactivation potential. *J Biol Chem,* 278**,** 15958-65.

LINGEN, M. W. 2001. Role of leukocytes and endothelial cells in the development of angiogenesis in inflammation and wound healing. *Arch Pathol Lab Med,* 125**,** 67-71.

LIU, H. J., WU, C. T., DUAN, H. F., WU, B., LU, Z. Z. & WANG, L. 2006. Adenoviral-mediated gene expression of hepatocyte growth factor prevents postoperative peritoneal adhesion in a rat model. *Surgery,* 140**,** 441-7.

LOCKSLEY, R. M., KILLEEN, N. & LENARDO, M. J. 2001. The TNF and TNF receptor superfamilies: integrating mammalian biology. *Cell,* 104**,** 487-501.

LOKE, P., GALLAGHER, I., NAIR, M. G., ZANG, X., BROMBACHER, F., MOHRS, M., ALLISON, J. P. & ALLEN, J. E. 2007. Alternative activation is an innate response to injury

that requires CD4+ T cells to be sustained during chronic infection. *J Immunol,* 179**,** 3926-36.

LOPEZ-COTARELO, C., SELLHAUS, B., BABA, H. A., MANEGOLD, E., LUKA, J., HANDT, S., MITTERMAYER, C., KLOSTERHALFEN, B. & TIETZE, L. 2000. Expression of heat shock proteins 72/73 in human peritoneal mesothelial cells in vivo and in vitro. *Nephron,* 85**,** 148-55.

LU, Q. 2010. delta-Catenin dysregulation in cancer: interactions with E-cadherin and beyond. *J Pathol,* 222**,** 119-23.

LUCERO, H. A. & KAGAN, H. M. 2006. Lysyl oxidase: an oxidative enzyme and effector of cell function. *Cell Mol Life Sci,* 63**,** 2304-16.

LUIJENDIJK, R. W., DE LANGE, D. C., WAUTERS, C. C., HOP, W. C., DURON, J. J., PAILLER, J. L., CAMPRODON, B. R., HOLMDAHL, L., VAN GELDORP, H. J. & JEEKEL, J. 1996. Foreign material in postoperative adhesions. *Ann Surg,* 223**,** 242-8.

MA, C., TARNUZZER, R. W. & CHEGINI, N. 1999. Expression of matrix metalloproteinases and tissue inhibitor of matrix metalloproteinases in mesothelial cells and their regulation by transforming growth factor-beta1. *Wound Repair Regen,* 7**,** 477-85.

MADALA, S. K., PESCE, J. T., RAMALINGAM, T. R., WILSON, M. S., MINNICOZZI, S., CHEEVER, A. W., THOMPSON, R. W., MENTINK-KANE, M. M. & WYNN, T. A. 2010. Matrix metalloproteinase 12-deficiency augments extracellular matrix degrading metalloproteinases and attenuates IL-13-dependent fibrosis. *J Immunol,* 184**,** 3955-63.

MADISON, L. D., BERGSTROM-PORTER, B., TORRES, A. R. & SHELTON, E. 1979. Regulation of surface topography of mouse peritoneal cells. Formation of microvilli and vesiculated pits on omental mesothelial cells by serum and other proteins. *J Cell Biol,* 82**,** 783-97.

MAHABELESHWAR, G. H. & KUNDU, G. C. 2003. Tyrosine kinase p56lck regulates cell motility and nuclear factor kappaB-mediated secretion of urokinase type plasminogen activator through tyrosine phosphorylation of IkappaBalpha following hypoxia/reoxygenation. *J Biol Chem,* 278**,** 52598-612.

MAIS, V., BRACCO, G. L., LITTA, P., GARGIULO, T. & MELIS, G. B. 2006. Reduction of postoperative adhesions with an auto-crosslinked hyaluronan gel in gynaecological laparoscopic surgery: a blinded, controlled, randomized, multicentre study. *Hum Reprod,* 21**,** 1248-54.

MANDL-WEBER, S., HASLINGER, B. & SITTER, T. 1999. Thrombin upregulates production of plasminogen activator inhibitor type 1 in human peritoneal mesothelial cells. *Perit Dial Int,* 19**,** 319-24.

MARCHENKO, G. N., RATNIKOV, B. I., ROZANOV, D. V., GODZIK, A., DERYUGINA, E. I. & STRONGIN, A. Y. 2001. Characterization of matrix metalloproteinase-26, a novel metalloproteinase widely expressed in cancer cells of epithelial origin. *Biochem J,* 356**,** 705-18.

MARGETTS, P. J., KOLB, M., YU, L., HOFF, C. M., HOLMES, C. J., ANTHONY, D. C. & GAULDIE, J. 2002. Inflammatory cytokines, angiogenesis, and fibrosis in the rat peritoneum. *Am J Pathol,* 160**,** 2285-94.

MARKOVIC-LIPKOVSKI, J., MULLER, C. A., KLEIN, G., FLAD, T., KLATT, T., BLASCHKE, S., WESSELS, J. T. & MULLER, G. A. 2007. Neural cell adhesion molecule expression on renal interstitial cells. *Nephrol Dial Transplant,* 22**,** 1558-66.

MARSHALL, B. C., SANTANA, A., XU, Q. P., PETERSEN, M. J., CAMPBELL, E. J., HOIDAL, J. R. & WELGUS, H. G. 1993. Metalloproteinases and tissue inhibitor of metalloproteinases in mesothelial cells. Cellular differentiation influences expression. *J Clin Invest,* 91**,** 1792-9.

MARTIN, P., D'SOUZA, D., MARTIN, J., GROSE, R., COOPER, L., MAKI, R. & MCKERCHER, S. R. 2003. Wound healing in the PU.1 null mouse--tissue repair is not dependent on inflammatory cells. *Curr Biol,* 13**,** 1122-8.

MASSAGUE, J. 1998. TGF-beta signal transduction. *Annu Rev Biochem,* 67**,** 753-91.

MATSUSHIMA, K., TAGUCHI, M., KOVACS, E. J., YOUNG, H. A. & OPPENHEIM, J. J. 1986. Intracellular localization of human monocyte associated interleukin 1 (IL 1) activity and release of biologically active IL 1 from monocytes by trypsin and plasmin. *J Immunol,* 136**,** 2883-91.

MAYASUNDARI, A., WHITTEMORE, N. A., SERPERSU, E. H. & PETERSON, C. B. 2004. The solution structure of the N-terminal domain of human vitronectin: proximal sites that regulate fibrinolysis and cell migration. *J Biol Chem,* 279**,** 29359-66.

MAYNARD, A. D. 2007. Nanotechnology: the next big thing, or much ado about nothing? *Ann Occup Hyg,* 51**,** 1-12.

MCNALLY, A. K. & ANDERSON, J. M. 2011. Macrophage fusion and multinucleated giant cells of inflammation. *Adv Exp Med Biol,* 713**,** 97-111.

MCNALLY, A. K., JONES, J. A., MACEWAN, S. R., COLTON, E. & ANDERSON, J. M. 2008. Vitronectin is a critical protein adhesion substrate for IL-4-induced foreign body giant cell formation. *J Biomed Mater Res A,* 86**,** 535-43.

MENE, P., POLCI, R. & FESTUCCIA, F. 2003. Mechanisms of repair after kidney injury. *J Nephrol,* 16**,** 186-95.

MENZIES, D. 1993. Postoperative adhesions: their treatment and relevance in clinical practice. *Ann R Coll Surg Engl,* 75**,** 147-53.

MENZIES, D. & ELLIS, H. 1990. Intestinal obstruction from adhesions--how big is the problem? *Ann R Coll Surg Engl,* 72**,** 60-3.

MERCURIO, F., ZHU, H., MURRAY, B. W., SHEVCHENKO, A., BENNETT, B. L., LI, J., YOUNG, D. B., BARBOSA, M., MANN, M., MANNING, A. & RAO, A. 1997. IKK-1 and IKK-2: cytokine-activated IkappaB kinases essential for NF-kappaB activation. *Science,* 278**,** 860-6.

METWALLY, M., WATSON, A., LILFORD, R. & VANDEKERCKHOVE, P. 2006. Fluid and pharmacological agents for adhesion prevention after gynaecological surgery. *Cochrane Database Syst Rev***,** CD001298.

MICHAILOVA, K., WASSILEV, W. & WEDEL, T. 1999. Scanning and transmission electron microscopic study of visceral and parietal peritoneal regions in the rat. *Ann Anat,* 181**,** 253-60.

MICHAILOVA, K. N. & USUNOFF, K. G. 2006. Serosal membranes (pleura, pericardium, peritoneum). Normal structure, development and experimental pathology. *Adv Anat Embryol Cell Biol,* 183**,** i-vii, 1-144, back cover.

MIETTINEN, P. J., EBNER, R., LOPEZ, A. R. & DERYNCK, R. 1994. TGF-beta induced transdifferentiation of mammary epithelial cells to mesenchymal cells: involvement of type I receptors. *J Cell Biol,* 127**,** 2021-36.

MILEWICZ, D. M., URBAN, Z. & BOYD, C. 2000. Genetic disorders of the elastic fiber system. *Matrix Biol,* 19**,** 471-80.

MIRASTSCHIJSKI, U., JOHANNESSON, K., JEPPSSON, B. & AGREN, M. S. 2005. Effect of a matrix metalloproteinase activity and TNF-alpha converting enzyme inhibitor on intra-abdominal adhesions. *Eur Surg Res,* 37**,** 68-75.

MITRA, S. K. & SCHLAEPFER, D. D. 2006. Integrin-regulated FAK-Src signaling in normal and cancer cells. *Curr Opin Cell Biol,* 18**,** 516-23.

MOLINAS, C. R., CAMPO, R., DEWERCHIN, M., ERIKSSON, U., CARMELIET, P. & KONINCKX, P. R. 2003. Role of vascular endothelial growth factor and placental growth factor in basal adhesion formation and in carbon dioxide pneumoperitoneum-enhanced adhesion formation after laparoscopic surgery in transgenic mice. *Fertil Steril,* 80 Suppl 2**,** 803-11.

MOLINAS, C. R. & KONINCKX, P. R. 2000. Hypoxaemia induced by CO(2) or helium pneumoperitoneum is a co-factor in adhesion formation in rabbits. *Hum Reprod,* 15**,** 1758-63.

MOLINAS, C. R., MYNBAEV, O., PAUWELS, A., NOVAK, P. & KONINCKX, P. R. 2001. Peritoneal mesothelial hypoxia during pneumoperitoneum is a cofactor in adhesion formation in a laparoscopic mouse model. *Fertil Steril,* 76**,** 560-7.

MOLLOY, D., MARTIN, M., SPEIRS, A., LOPATA, A., CLARKE, G., MCBAIN, J., NGU, A. & JOHNSTON, I. H. 1987. Performance of patients with a "frozen pelvis" in an in vitro fertilization program. *Fertil Steril,* 47**,** 450-5.

MONK, B. J., BERMAN, M. L. & MONTZ, F. J. 1994. Adhesions after extensive gynecologic surgery: clinical significance, etiology, and prevention. *Am J Obstet Gynecol,* 170**,** 1396-403.

MONTESANO, R. & ORCI, L. 1988. Transforming growth factor beta stimulates collagen-matrix contraction by fibroblasts: implications for wound healing. *Proc Natl Acad Sci U S A,* 85**,** 4894-7.

MORGAN, M. R., BYRON, A., HUMPHRIES, M. J. & BASS, M. D. 2009. Giving off mixed signals--distinct functions of alpha5beta1 and alphavbeta3 integrins in regulating cell behaviour. *IUBMB Life,* 61**,** 731-8.

MORI, T., KAWARA, S., SHINOZAKI, M., HAYASHI, N., KAKINUMA, T., IGARASHI, A., TAKIGAWA, M., NAKANISHI, T. & TAKEHARA, K. 1999. Role and interaction of connective tissue growth factor with transforming growth factor-beta in persistent fibrosis: A mouse fibrosis model. *J Cell Physiol,* 181**,** 153-9.

MOSLEY, B., URDAL, D. L., PRICKETT, K. S., LARSEN, A., COSMAN, D., CONLON, P. J., GILLIS, S. & DOWER, S. K. 1987. The interleukin-1 receptor binds the human interleukin-1 alpha precursor but not the interleukin-1 beta precursor. *J Biol Chem,* 262**,** 2941-4.

MOSSER, D. M. & EDWARDS, J. P. 2008. Exploring the full spectrum of macrophage activation. *Nat Rev Immunol,* 8**,** 958-69.

MOUSTAKAS, A., PARDALI, K., GAAL, A. & HELDIN, C. H. 2002. Mechanisms of TGF-beta signaling in regulation of cell growth and differentiation. *Immunol Lett,* 82**,** 85-91.

MUHS, B. E., PLITAS, G., DELGADO, Y., IANUS, I., SHAW, J. P., ADELMAN, M. A., LAMPARELLO, P., SHAMAMIAN, P. & GAGNE, P. 2003. Temporal expression and activation of matrix metalloproteinases-2, -9, and membrane type 1-matrix metalloproteinase following acute hindlimb ischemia. *J Surg Res,* 111**,** 8-15.

MUKHOPADHYAY, S. & GAL, A. A. 2010. Granulomatous lung disease: an approach to the differential diagnosis. *Arch Pathol Lab Med,* 134**,** 667-90.

MURDOCH, W. J., TOWNSEND, R. S. & MCDONNEL, A. C. 2001. Ovulation-induced DNA damage in ovarian surface epithelial cells of ewes: prospective regulatory mechanisms of repair/survival and apoptosis. *Biol Reprod,* 65**,** 1417-24.

MURPHY-ULLRICH, J. E. 2001. The de-adhesive activity of matricellular proteins: is intermediate cell adhesion an adaptive state? *J Clin Invest,* 107**,** 785-90.

MURPHY, G., HOUBRECHTS, A., COCKETT, M. I., WILLIAMSON, R. A., O'SHEA, M. & DOCHERTY, A. J. 1991. The N-terminal domain of tissue inhibitor of metalloproteinases retains metalloproteinase inhibitory activity. *Biochemistry,* 30**,** 8097-102.

MURPHY, G., SEGAIN, J. P., O'SHEA, M., COCKETT, M., IOANNOU, C., LEFEBVRE, O., CHAMBON, P. & BASSET, P. 1993. The 28-kDa N-terminal domain of mouse stromelysin-3 has the general properties of a weak metalloproteinase. *J Biol Chem,* 268**,** 15435-41.

MUTSAERS, S. E. 2002. Mesothelial cells: their structure, function and role in serosal repair. *Respirology,* 7**,** 171-91.

MUTSAERS, S. E., MCANULTY, R. J., LAURENT, G. J., VERSNEL, M. A., WHITAKER, D. & PAPADIMITRIOU, J. M. 1997. Cytokine regulation of mesothelial cell proliferation in vitro and in vivo. *Eur J Cell Biol,* 72**,** 24-9.

MUTSAERS, S. E., WHITAKER, D. & PAPADIMITRIOU, J. M. 2000. Mesothelial regeneration is not dependent on subserosal cells. *J Pathol,* 190**,** 86-92.

MUTSAERS, S. E., WHITAKER, D. & PAPADIMITRIOU, J. M. 2002. Stimulation of mesothelial cell proliferation by exudate macrophages enhances serosal wound healing in a murine model. *Am J Pathol,* 160**,** 681-92.

MYLLYHARJU, J. & KIVIRIKKO, K. I. 2001. Collagens and collagen-related diseases. *Ann Med,* 33**,** 7-21.

NAGASE, H. & WOESSNER, J. F., JR. 1999. Matrix metalloproteinases. *J Biol Chem,* 274**,** 21491-4.

NAKATANI, T., OHTANI, O. & TANAKA, S. 1996. Lymphatic stomata in the murine diaphragmatic peritoneum: the timing of their appearance and a map of their distribution. *Anat Rec,* 244**,** 529-39.

NASREEN, N., HARTMAN, D. L., MOHAMMED, K. A. & ANTONY, V. B. 1998. Talc-induced expression of C-C and C-X-C chemokines and intercellular adhesion molecule-1 in mesothelial cells. *Am J Respir Crit Care Med,* 158**,** 971-8.

NASREEN, N., MOHAMMED, K. A., HARDWICK, J., VAN HORN, R. D., SANDERS, K. L., DOERSCHUK, C. M., HOTT, J. W. & ANTONY, V. B. 2001. Polar production of interleukin-8 by mesothelial cells promotes the transmesothelial migration of neutrophils: role of intercellular adhesion molecule-1. *J Infect Dis,* 183**,** 1638-45.

NELLAIAPPAN, K., RISITANO, A., LIU, G., NICKLAS, G. & KAGAN, H. M. 2000. Fully processed lysyl oxidase catalyst translocates from the extracellular space into nuclei of aortic smooth-muscle cells. *J Cell Biochem,* 79**,** 576-82.

NIKI, Y., YAMADA, H., KIKUCHI, T., TOYAMA, Y., MATSUMOTO, H., FUJIKAWA, K. & TADA, N. 2004. Membrane-associated IL-1 contributes to chronic synovitis and cartilage destruction in human IL-1 alpha transgenic mice. *J Immunol,* 172**,** 577-84.

O'KANE, S. 2002. Wound remodelling and scarring. *J Wound Care,* 11**,** 296-9.

O'NEILL, L. A. & DINARELLO, C. A. 2000. The IL-1 receptor/toll-like receptor superfamily: crucial receptors for inflammation and host defense. *Immunol Today,* 21**,** 206-9.

OCHIENG, J., FRIDMAN, R., NANGIA-MAKKER, P., KLEINER, D. E., LIOTTA, L. A., STETLER-STEVENSON, W. G. & RAZ, A. 1994. Galectin-3 is a novel substrate for human matrix metalloproteinases-2 and -9. *Biochemistry,* 33**,** 14109-14.

ODERO-MARAH, V. A., KHALKHALI-ELLIS, Z., CHUNTHAPONG, J., AMIR, S., SEFTOR, R. E., SEFTOR, E. A. & HENDRIX, M. J. 2003. Maspin regulates different signaling pathways for motility and adhesion in aggressive breast cancer cells. *Cancer Biol Ther,* 2**,** 398-403.

OFFNER, F. A., FEICHTINGER, H., STADLMANN, S., OBRIST, P., MARTH, C., KLINGLER, P., GRAGE, B., SCHMAHL, M. & KNABBE, C. 1996. Transforming growth factor-beta synthesis by human peritoneal mesothelial cells. Induction by interleukin-1. *Am J Pathol,* 148**,** 1679-88.

OHTANI, Y. & OHTANI, O. 1997. Obliteration of the lymphatic trunks draining diaphragmatic lymph causes peritoneal fluid to enter the pleural cavity. *Arch Histol Cytol,* 60**,** 503-10.

OHTANI, Y., OHTANI, O. & NAKATANI, T. 1995. Microanatomy of the rat diaphragm with special reference to the lymphatics and mesothelial stomata. *Ital J Anat Embryol,* 100 Suppl 1**,** 143-53.

OHUCHI, E., IMAI, K., FUJII, Y., SATO, H., SEIKI, M. & OKADA, Y. 1997. Membrane type 1 matrix metalloproteinase digests interstitial collagens and other extracellular matrix macromolecules. *J Biol Chem,* 272**,** 2446-51.

OKAMURA, H., KATABUCHI, H. & OHBA, T. 2003. What we have learned from isolated cells from human ovary? *Mol Cell Endocrinol,* 202**,** 37-45.

OPDENAKKER, G., VAN DEN STEEN, P. E., DUBOIS, B., NELISSEN, I., VAN COILLIE, E., MASURE, S., PROOST, P. & VAN DAMME, J. 2001. Gelatinase B functions as regulator and effector in leukocyte biology. *J Leukoc Biol,* 69**,** 851-9.

OSTLUND FARRANTS, A. K., BLOMQUIST, P., KWON, H. & WRANGE, O. 1997. Glucocorticoid receptor-glucocorticoid response element binding stimulates nucleosome disruption by the SWI/SNF complex. *Mol Cell Biol,* 17**,** 895-905.

OTT, D. E. 2008. Laparoscopy and adhesion formation, adhesions and laparoscopy. *Semin Reprod Med,* 26**,** 322-30.

OVERALL, C. M., WRANA, J. L. & SODEK, J. 1989. Independent regulation of collagenase, 72-kDa progelatinase, and metalloendoproteinase inhibitor expression in human fibroblasts by transforming growth factor-beta. *J Biol Chem,* 264**,** 1860-9.

OWENS, M. W. & GRIMES, S. R. 1993. Pleural mesothelial cell response to inflammation: tumor necrosis factor-induced mitogenesis and collagen synthesis. *Am J Physiol,* 265**,** L382-8.

OWENS, M. W. & GRISHAM, M. B. 1993. Nitric oxide synthesis by rat pleural mesothelial cells: induction by cytokines and lipopolysaccharide. *Am J Physiol,* 265**,** L110-6.

PALAMAKUMBURA, A. H. & TRACKMAN, P. C. 2002. A fluorometric assay for detection of lysyl oxidase enzyme activity in biological samples. *Anal Biochem,* 300**,** 245-51.

PANCHENKO, M. V., STETLER-STEVENSON, W. G., TRUBETSKOY, O. V., GACHERU, S. N. & KAGAN, H. M. 1996. Metalloproteinase activity secreted by fibrogenic cells in the processing of prolysyl oxidase. Potential role of procollagen C-proteinase. *J Biol Chem,* 271**,** 7113-9.

PAPACLEOVOULOU, G. 2009. *Steroid signalling in the human ovarian surface epithelium wound healing.* Ph.D.

PAPACLEOVOULOU, G., HOGG, K., FEGAN, K. S., CRITCHLEY, H. O., HILLIER, S. G. & MASON, J. I. 2009. Regulation of 3beta-hydroxysteroid dehydrogenase type 1 and type 2 gene expression and function in the human ovarian surface epithelium by cytokines. *Mol Hum Reprod,* 15**,** 379-92.

PARKER, M. C., ELLIS, H., MORAN, B. J., THOMPSON, J. N., WILSON, M. S., MENZIES, D., MCGUIRE, A., LOWER, A. M., HAWTHORN, R. J., O'BRIENA, F., BUCHAN, S. & CROWE, A. M. 2001. Postoperative adhesions: ten-year follow-up of 12,584 patients undergoing lower abdominal surgery. *Dis Colon Rectum,* 44**,** 822-29; discussion 829-30.

PARKER, M. C., WILSON, M. S., MENZIES, D., SUNDERLAND, G., CLARK, D. N., KNIGHT, A. D. & CROWE, A. M. 2005. The SCAR-3 study: 5-year adhesion-related readmission risk following lower abdominal surgical procedures. *Colorectal Dis,* 7**,** 551-8.

PARKER, M. C., WILSON, M. S., MENZIES, D., SUNDERLAND, G., THOMPSON, J. N., CLARK, D. N., KNIGHT, A. D. & CROWE, A. M. 2004. Colorectal surgery: the risk and burden of adhesion-related complications. *Colorectal Dis,* 6**,** 506-11.

PATTERSON, M. L., ATKINSON, S. J., KNAUPER, V. & MURPHY, G. 2001. Specific collagenolysis by gelatinase A, MMP-2, is determined by the hemopexin domain and not the fibronectin-like domain. *FEBS Lett,* 503**,** 158-62.

PAYNE, S. L., FOGELGREN, B., HESS, A. R., SEFTOR, E. A., WILEY, E. L., FONG, S. F., CSISZAR, K., HENDRIX, M. J. & KIRSCHMANN, D. A. 2005. Lysyl oxidase regulates breast cancer cell migration and adhesion through a hydrogen peroxide-mediated mechanism. *Cancer Res,* 65**,** 11429-36.

PELIN, K., HIRVONEN, A. & LINNAINMAA, K. 1994. Expression of cell adhesion molecules and connexins in gap junctional intercellular communication deficient human mesothelioma tumour cell lines and communication competent primary mesothelial cells. *Carcinogenesis,* 15**,** 2673-5.

PELLEGRIN, S. & MELLOR, H. 2007. Actin stress fibres. *J Cell Sci,* 120**,** 3491-9.

PEPPER, M. S. 2001. Extracellular proteolysis and angiogenesis. *Thromb Haemost,* 86**,** 346-55.

PERFUMO, F., ALTIERI, P., DEGL'INNOCENTI, M. L., GHIGGERI, G. M., CARIDI, G., TRIVELLI, A. & GUSMANO, R. 1996. Effects of peritoneal effluents on mesothelial cells in culture: cell proliferation and extracellular matrix regulation. *Nephrol Dial Transplant,* 11**,** 1803-9.

PERIDES, G., ASHER, R. A., LARK, M. W., LANE, W. S., ROBINSON, R. A. & BIGNAMI, A. 1995. Glial hyaluronate-binding protein: a product of metalloproteinase digestion of versican? *Biochem J,* 312 (Pt 2)**,** 377-84.

PH, B. 2001. Disorders of collagen biosynthesis and structure. *In:* SCRIVER CR, E. A. (ed.) *The metabolic & Molecular Basis of Inherited Disease.* **.** New York: McGraw-Hill.

PIEK, E., MOUSTAKAS, A., KURISAKI, A., HELDIN, C. H. & TEN DIJKE, P. 1999. TGF-(beta) type I receptor/ALK-5 and Smad proteins mediate epithelial to mesenchymal transdifferentiation in NMuMG breast epithelial cells. *J Cell Sci,* 112 (Pt 24)**,** 4557-68.

PILCHER, B. K., DUMIN, J. A., SUDBECK, B. D., KRANE, S. M., WELGUS, H. G. & PARKS, W. C. 1997. The activity of collagenase-1 is required for keratinocyte migration on a type I collagen matrix. *J Cell Biol,* 137**,** 1445-57.

PINNELL, S. R. & MARTIN, G. R. 1968. The cross-linking of collagen and elastin: enzymatic conversion of lysine in peptide linkage to alpha-aminoadipic-delta-semialdehyde (allysine) by an extract from bone. *Proc Natl Acad Sci U S A,* 61**,** 708-16.

PITTAWAY, D. E., DANIELL, J. F. & MAXSON, W. S. 1985. Ovarian surgery in an infertility patient as an indication for a short-interval second-look laparoscopy: a preliminary study. *Fertil Steril,* 44**,** 611-4.

PLENZ, G. A., DENG, M. C., ROBENEK, H. & VOLKER, W. 2003. Vascular collagens: spotlight on the role of type VIII collagen in atherogenesis. *Atherosclerosis,* 166**,** 1-11.

PODOR, T. J., CAMPBELL, S., CHINDEMI, P., FOULON, D. M., FARRELL, D. H., WALTON, P. D., WEITZ, J. I. & PETERSON, C. B. 2002. Incorporation of vitronectin into fibrin clots. Evidence for a binding interaction between vitronectin and gamma A/gamma' fibrinogen. *J Biol Chem,* 277**,** 7520-8.

POLAND, C. A., DUFFIN, R., KINLOCH, I., MAYNARD, A., WALLACE, W. A., SEATON, A., STONE, V., BROWN, S., MACNEE, W. & DONALDSON, K. 2008. Carbon nanotubes introduced into the abdominal cavity of mice show asbestos-like pathogenicity in a pilot study. *Nat Nanotechnol,* 3**,** 423-8.

PRATT, W. B. & TOFT, D. O. 1997. Steroid receptor interactions with heat shock protein and immunophilin chaperones. *Endocr Rev,* 18**,** 306-60.

QU, P., DU, H., WANG, X. & YAN, C. 2009. Matrix metalloproteinase 12 overexpression in lung epithelial cells plays a key role in emphysema to lung bronchioalveolar adenocarcinoma transition. *Cancer Res,* 69**,** 7252-61.

QUAN, T. E., COWPER, S. E. & BUCALA, R. 2006. The role of circulating fibrocytes in fibrosis. *Curr Rheumatol Rep,* 8**,** 145-50.

QUINKLER, M., OELKERS, W. & DIEDERICH, S. 2001. Clinical implications of glucocorticoid metabolism by 11beta-hydroxysteroid dehydrogenases in target tissues. *Eur J Endocrinol,* 144**,** 87-97.

RADOJA, N., KOMINE, M., JHO, S. H., BLUMENBERG, M. & TOMIC-CANIC, M. 2000. Novel mechanism of steroid action in skin through glucocorticoid receptor monomers. *Mol Cell Biol,* 20**,** 4328-39.

RAE, M. T. & HILLIER, S. G. 2005. Steroid signalling in the ovarian surface epithelium. *Trends Endocrinol Metab,* 16**,** 327-33.

RAE, M. T., NIVEN, D., CRITCHLEY, H. O., HARLOW, C. R. & HILLIER, S. G. 2004a. Antiinflammatory steroid action in human ovarian surface epithelial cells. *J Clin Endocrinol Metab,* 89**,** 4538-44.

RAE, M. T., NIVEN, D., ROSS, A., FORSTER, T., LATHE, R., CRITCHLEY, H. O., GHAZAL, P. & HILLIER, S. G. 2004b. Steroid signalling in human ovarian surface epithelial cells: the response to interleukin-1alpha determined by microarray analysis. *J Endocrinol,* 183**,** 19-28.

RAFTERY, A. T. 1973a. An enzyme histochemical study of mesothelial cells in rodents. *J Anat,* 115**,** 365-73.

RAFTERY, A. T. 1973b. Regeneration of parietal and visceral peritoneum. A light microscopical study. *Br J Surg,* 60**,** 293-9.

RAMIREZ, F., FOWELL, D. J., PUKLAVEC, M., SIMMONDS, S. & MASON, D. 1996. Glucocorticoids promote a TH2 cytokine response by CD4+ T cells in vitro. *J Immunol,* 156**,** 2406-12.

RATZINGER, S., EBLE, J. A., PASOLDT, A., OPOLKA, A., ROGLER, G., GRIFKA, J. & GRASSEL, S. 2010. Collagen XVI induces formation of focal contacts on intestinal myofibroblasts isolated from the normal and inflamed intestinal tract. *Matrix Biol,* 29**,** 177-93.

RAY, A. & PREFONTAINE, K. E. 1994. Physical association and functional antagonism between the p65 subunit of transcription factor NF-kappa B and the glucocorticoid receptor. *Proc Natl Acad Sci U S A,* 91**,** 752-6.

REED, K. L., STUCCHI, A. F., LEEMAN, S. E. & BECKER, J. M. 2008. Inhibitory effects of a neurokinin-1 receptor antagonist on postoperative peritoneal adhesion formation. *Ann N Y Acad Sci,* 1144**,** 116-26.

REINHARD, C., SHAMOON, B., SHYAMALA, V. & WILLIAMS, L. T. 1997. Tumor necrosis factor alpha-induced activation of c-jun N-terminal kinase is mediated by TRAF2. *EMBO J,* 16**,** 1080-92.

REKAWIECKI, R., KOWALIK, M. K., SLONINA, D. & KOTWICA, J. 2008. Regulation of progesterone synthesis and action in bovine corpus luteum. *J Physiol Pharmacol,* 59 Suppl 9**,** 75-89.

RENNARD, S. I., JAURAND, M. C., BIGNON, J., KAWANAMI, O., FERRANS, V. J., DAVIDSON, J. & CRYSTAL, R. G. 1984. Role of pleural mesothelial cells in the production of the submesothelial connective tissue matrix of lung. *Am Rev Respir Dis,* 130**,** 267-74.

REPNIK, U., KNEZEVIC, M. & JERAS, M. 2003. Simple and cost-effective isolation of monocytes from buffy coats. *J Immunol Methods,* 278**,** 283-92.

ROBERTS, A. B. 1999. TGF-beta signaling from receptors to the nucleus. *Microbes Infect,* 1**,** 1265-73.

ROBSON, M. C., STEED, D. L. & FRANZ, M. G. 2001. Wound healing: biologic features and approaches to maximize healing trajectories. *Curr Probl Surg,* 38**,** 72-140.

RODRIGUEZ-MANZANEQUE, J. C., WESTLING, J., THAI, S. N., LUQUE, A., KNAUPER, V., MURPHY, G., SANDY, J. D. & IRUELA-ARISPE, M. L. 2002. ADAMTS1 cleaves aggrecan at multiple sites and is differentially inhibited by metalloproteinase inhibitors. *Biochem Biophys Res Commun,* 293**,** 501-8.

ROSS, J. A., ANSELL, I., HJELLE, J. T., ANDERSON, J. D., MILLER-HJELLE, M. A. & DOBBIE, J. W. 1998. Phenotypic mapping of human mesothelial cells. *Adv Perit Dial,* 14**,** 25-30.

ROUGIER, J. P., GUIA, S., HAGEGE, J., NGUYEN, G. & RONCO, P. M. 1998. PAI-1 secretion and matrix deposition in human peritoneal mesothelial cell cultures: transcriptional regulation by TGF-beta 1. *Kidney Int,* 54**,** 87-98.

ROUGIER, J. P., MOULLIER, P., PIEDAGNEL, R. & RONCO, P. M. 1997. Hyperosmolality suppresses but TGF beta 1 increases MMP9 in human peritoneal mesothelial cells. *Kidney Int,* 51**,** 337-47.

SABA, A. A., GODZIACHVILI, V., MAVANI, A. K. & SILVA, Y. J. 1998. Serum levels of interleukin 1 and tumor necrosis factor alpha correlate with peritoneal adhesion grades in humans after major abdominal surgery. *Am Surg,* 64**,** 734-6; discussion 737.

SABA, A. A., KAIDI, A. A., GODZIACHVILI, V., DOMBI, G. W., DAWE, E. J., LIBCKE, J. H. & SILVA, Y. J. 1996. Effects of interleukin-6 and its neutralizing antibodies on peritoneal adhesion formation and wound healing. *Am Surg,* 62**,** 569-72.

SABEH, F., LI, X. Y., SAUNDERS, T. L., ROWE, R. G. & WEISS, S. J. 2009. Secreted versus membrane-anchored collagenases: relative roles in fibroblast-dependent collagenolysis and invasion. *J Biol Chem,* 284**,** 23001-11.

SAED, G. M., ZHANG, W., CHEGINI, N., HOLMDAHL, L. & DIAMOND, M. P. 1999. Alteration of type I and III collagen expression in human peritoneal mesothelial cells in response to hypoxia and transforming growth factor-beta1. *Wound Repair Regen,* 7**,** 504-10.

SAED, G. M., ZHANG, W., CHEGINI, N., HOLMDAHL, L. & DIAMOND, M. P. 2000. Transforming growth factor beta isoforms production by human peritoneal mesothelial cells after exposure to hypoxia. *Am J Reprod Immunol,* 43**,** 285-91.

SALTZMAN, A. K., OLSON, T. A., MOHANRAJ, D., CARSON, L. F. & RAMAKRISHNAN, S. 1996. Prevention of postoperative adhesions by an antibody to vascular permeability factor/vascular endothelial growth factor in a murine model. *Am J Obstet Gynecol,* 174**,** 1502-6.

SANES, J. R. 2003. The basement membrane/basal lamina of skeletal muscle. *J Biol Chem,* 278**,** 12601-4.

SANTIBANEZ, J. F. 2006. JNK mediates TGF-beta1-induced epithelial mesenchymal transdifferentiation of mouse transformed keratinocytes. *FEBS Lett,* 580**,** 5385-91.

SATO, M., SHEGOGUE, D., GORE, E. A., SMITH, E. A., MCDERMOTT, P. J. & TROJANOWSKA, M. 2002. Role of p38 MAPK in transforming growth factor beta stimulation of collagen production by scleroderma and healthy dermal fibroblasts. *J Invest Dermatol,* 118**,** 704-11.

SATO, S., SANJO, H., TAKEDA, K., NINOMIYA-TSUJI, J., YAMAMOTO, M., KAWAI, T., MATSUMOTO, K., TAKEUCHI, O. & AKIRA, S. 2005. Essential function for the kinase TAK1 in innate and adaptive immune responses. *Nat Immunol,* 6**,** 1087-95.

SCHAEFER, L. & SCHAEFER, R. M. 2010. Proteoglycans: from structural compounds to signaling molecules. *Cell Tissue Res,* 339**,** 237-46.

SCHEINMAN, R. I., COGSWELL, P. C., LOFQUIST, A. K. & BALDWIN, A. S., JR. 1995a. Role of transcriptional activation of I kappa B alpha in mediation of immunosuppression by glucocorticoids. *Science,* 270**,** 283-6.

SCHEINMAN, R. I., GUALBERTO, A., JEWELL, C. M., CIDLOWSKI, J. A. & BALDWIN, A. S., JR. 1995b. Characterization of mechanisms involved in transrepression of NF-kappa B by activated glucocorticoid receptors. *Mol Cell Biol,* 15**,** 943-53.

SCHULE, R., RANGARAJAN, P., KLIEWER, S., RANSONE, L. J., BOLADO, J., YANG, N., VERMA, I. M. & EVANS, R. M. 1990. Functional antagonism between oncoprotein c-Jun and the glucocorticoid receptor. *Cell,* 62**,** 1217-26.

SCHULTZ JEL, J., WITT, S. A., GLASCOCK, B. J., NIEMAN, M. L., REISER, P. J., NIX, S. L., KIMBALL, T. R. & DOETSCHMAN, T. 2002. TGF-beta1 mediates the hypertrophic cardiomyocyte growth induced by angiotensin II. *J Clin Invest,* 109**,** 787-96.

SCHULZE-OSTHOFF, K., BAKKER, A. C., VANHAESEBROECK, B., BEYAERT, R., JACOB, W. A. & FIERS, W. 1992. Cytotoxic activity of tumor necrosis factor is mediated by early damage of mitochondrial functions. Evidence for the involvement of mitochondrial radical generation. *J Biol Chem,* 267**,** 5317-23.

SECKL, J. R. & WALKER, B. R. 2001. Minireview: 11beta-hydroxysteroid dehydrogenase type 1- a tissue-specific amplifier of glucocorticoid action. *Endocrinology,* 142**,** 1371-6.

SELLAK, H., FRANZINI, E., HAKIM, J. & PASQUIER, C. 1994. Reactive oxygen species rapidly increase endothelial ICAM-1 ability to bind neutrophils without detectable upregulation. *Blood,* 83**,** 2669-77.

SEMPOWSKI, G. D., BECKMANN, M. P., DERDAK, S. & PHIPPS, R. P. 1994. Subsets of murine lung fibroblasts express membrane-bound and soluble IL-4 receptors. Role of IL-4 in enhancing fibroblast proliferation and collagen synthesis. *J Immunol,* 152**,** 3606-14.

SHAPIRO, S. D., KOBAYASHI, D. K. & LEY, T. J. 1993. Cloning and characterization of a unique elastolytic metalloproteinase produced by human alveolar macrophages. *J Biol Chem,* 268**,** 23824-9.

SHAULIAN, E. & KARIN, M. 2002. AP-1 as a regulator of cell life and death. *Nat Cell Biol,* 4**,** E131-6.

SHAVELL, V. I., SAED, G. M. & DIAMOND, M. P. 2009. Review: Cellular metabolism: contribution to postoperative adhesion development. *Reprod Sci,* 16**,** 627-34.

SHEPPARD, K. A., ROSE, D. W., HAQUE, Z. K., KUROKAWA, R., MCINERNEY, E., WESTIN, S., THANOS, D., ROSENFELD, M. G., GLASS, C. K. & COLLINS, T. 1999. Transcriptional activation by NF-kappaB requires multiple coactivators. *Mol Cell Biol,* 19**,** 6367-78.

SHI-WEN, X., STANTON, L. A., KENNEDY, L., PALA, D., CHEN, Y., HOWAT, S. L., RENZONI, E. A., CARTER, D. E., BOU-GHARIOS, G., STRATTON, R. J., PEARSON, J. D., BEIER, F., LYONS, K. M., BLACK, C. M., ABRAHAM, D. J. & LEASK, A. 2006. CCN2 is necessary for adhesive responses to transforming growth factor-beta1 in embryonic fibroblasts. *J Biol Chem,* 281**,** 10715-26.

SHIMADA, T., NAKAMURA, H., OHUCHI, E., FUJII, Y., MURAKAMI, Y., SATO, H., SEIKI, M. & OKADA, Y. 1999. Characterization of a truncated recombinant form of human membrane type 3 matrix metalloproteinase. *Eur J Biochem,* 262**,** 907-14.

SHIMAOKA, M., XIAO, T., LIU, J. H., YANG, Y., DONG, Y., JUN, C. D., MCCORMACK, A., ZHANG, R., JOACHIMIAK, A., TAKAGI, J., WANG, J. H. & SPRINGER, T. A. 2003.

Structures of the alpha L I domain and its complex with ICAM-1 reveal a shape-shifting pathway for integrin regulation. *Cell,* 112**,** 99-111.

SHINDO, T., KURIHARA, H., KUNO, K., YOKOYAMA, H., WADA, T., KURIHARA, Y., IMAI, T., WANG, Y., OGATA, M., NISHIMATSU, H., MORIYAMA, N., OH-HASHI, Y., MORITA, H., ISHIKAWA, T., NAGAI, R., YAZAKI, Y. & MATSUSHIMA, K. 2000. ADAMTS-1: a metalloproteinase-disintegrin essential for normal growth, fertility, and organ morphology and function. *J Clin Invest,* 105**,** 1345-52.

SHIPLEY, J. M., WESSELSCHMIDT, R. L., KOBAYASHI, D. K., LEY, T. J. & SHAPIRO, S. D. 1996. Metalloelastase is required for macrophage-mediated proteolysis and matrix invasion in mice. *Proc Natl Acad Sci U S A,* 93**,** 3942-6.

SHUMKO, J. Z., FEINBERG, R. N., SHALVOY, R. M. & DEFOUW, D. O. 1993. Responses of rat pleural mesothelia to increased intrathoracic pressure. *Exp Lung Res,* 19**,** 283-97.

SIEGEL, R. C. 1974. Biosynthesis of collagen crosslinks: increased activity of purified lysyl oxidase with reconstituted collagen fibrils. *Proc Natl Acad Sci U S A,* 71**,** 4826-30.

SILVERSTEIN, R. L., LEUNG, L. L., HARPEL, P. C. & NACHMAN, R. L. 1984. Complex formation of platelet thrombospondin with plasminogen. Modulation of activation by tissue activator. *J Clin Invest,* 74**,** 1625-33.

SIMANTOV, R. & SILVERSTEIN, R. L. 2003. CD36: a critical anti-angiogenic receptor. *Front Biosci,* 8**,** s874-82.

SIME, P. J., MARR, R. A., GAULDIE, D., XING, Z., HEWLETT, B. R., GRAHAM, F. L. & GAULDIE, J. 1998. Transfer of tumor necrosis factor-alpha to rat lung induces severe pulmonary inflammation and patchy interstitial fibrogenesis with induction of transforming growth factor-beta1 and myofibroblasts. *Am J Pathol,* 153**,** 825-32.

SIMPSON, D. M. & ROSS, R. 1972. The neutrophilic leukocyte in wound repair a study with antineutrophil serum. *J Clin Invest,* 51**,** 2009-23.

SIMS, J. E., GAYLE, M. A., SLACK, J. L., ALDERSON, M. R., BIRD, T. A., GIRI, J. G., COLOTTA, F., RE, F., MANTOVANI, A., SHANEBECK, K. & ET AL. 1993. Interleukin 1 signaling occurs exclusively via the type I receptor. *Proc Natl Acad Sci U S A,* 90**,** 6155-9.

SIMS, J. E., MARCH, C. J., COSMAN, D., WIDMER, M. B., MACDONALD, H. R., MCMAHAN, C. J., GRUBIN, C. E., WIGNALL, J. M., JACKSON, J. L., CALL, S. M. & ET AL. 1988. cDNA expression cloning of the IL-1 receptor, a member of the immunoglobulin superfamily. *Science,* 241**,** 585-9.

SIMSIR, A., FETSCH, P., MEHTA, D., ZAKOWSKI, M. & ABATI, A. 1999. E-cadherin, N-cadherin, and calretinin in pleural effusions: the good, the bad, the worthless. *Diagn Cytopathol,* 20**,** 125-30.

SITTER, T., SPANNAGL, M., SCHIFFL, H., HELD, E., VAN HINSBERGH, V. W. & KOOISTRA, T. 1995. Imbalance between intraperitoneal coagulation and fibrinolysis during peritonitis of CAPD patients: the role of mesothelial cells. *Nephrol Dial Transplant,* 10**,** 677-83.

SITTER, T., TOET, K., FRICKE, H., SCHIFFL, H., HELD, E. & KOOISTRA, T. 1996. Modulation of procoagulant and fibrinolytic system components of mesothelial cells by inflammatory mediators. *Am J Physiol,* 271**,** R1256-63.

SITTER, T., TOET, K., QUAX, P. & KOOISTRA, T. 1999. Fibrinolytic activity of human mesothelial cells is counteracted by rapid uptake of tissue-type plasminogen activator. *Kidney Int,* 55**,** 120-9.

SMITH, M. L., GOURDON, D., LITTLE, W. C., KUBOW, K. E., EGUILUZ, R. A., LUNA-MORRIS, S. & VOGEL, V. 2007. Force-induced unfolding of fibronectin in the extracellular matrix of living cells. *PLoS Biol,* 5**,** e268.

SONNENBERG, A., LINDERS, C. J., MODDERMAN, P. W., DAMSKY, C. H., AUMAILLEY, M. & TIMPL, R. 1990. Integrin recognition of different cell-binding fragments of laminin (P1, E3, E8) and evidence that alpha 6 beta 1 but not alpha 6 beta 4 functions as a major receptor for fragment E8. *J Cell Biol,* 110**,** 2145-55.

SOUNG, Y. H., GIL, H. J., CLIFFORD, J. L. & CHUNG, J. 2011. Role of alpha6beta4 integrin in cell motility, invasion and metastasis of mammary tumors. *Curr Protein Pept Sci,* 12**,** 23-9.

SPORN, M. B. & ROBERTS, A. B. 1992. Transforming growth factor-beta: recent progress and new challenges. *J Cell Biol,* 119**,** 1017-21.

STOENICA, L., SENKOV, O., GERARDY-SCHAHN, R., WEINHOLD, B., SCHACHNER, M. & DITYATEV, A. 2006. In vivo synaptic plasticity in the dentate gyrus of mice deficient in the neural cell adhesion molecule NCAM or its polysialic acid. *Eur J Neurosci,* 23**,** 2255-64.

STOVALL, T. G., ELDER, R. F. & LING, F. W. 1989. Predictors of pelvic adhesions. *J Reprod Med,* 34**,** 345-8.

STRACKE, J. O., FOSANG, A. J., LAST, K., MERCURI, F. A., PENDAS, A. M., LLANO, E., PERRIS, R., DI CESARE, P. E., MURPHY, G. & KNAUPER, V. 2000a. Matrix metalloproteinases 19 and 20 cleave aggrecan and cartilage oligomeric matrix protein (COMP). *FEBS Lett,* 478**,** 52-6.

STRACKE, J. O., HUTTON, M., STEWART, M., PENDAS, A. M., SMITH, B., LOPEZ-OTIN, C., MURPHY, G. & KNAUPER, V. 2000b. Biochemical characterization of the catalytic domain of human matrix metalloproteinase 19. Evidence for a role as a potent basement membrane degrading enzyme. *J Biol Chem,* 275**,** 14809-16.

STRATTON, R., RAJKUMAR, V., PONTICOS, M., NICHOLS, B., SHIWEN, X., BLACK, C. M., ABRAHAM, D. J. & LEASK, A. 2002. Prostacyclin derivatives prevent the fibrotic response to TGF-beta by inhibiting the Ras/MEK/ERK pathway. *FASEB J,* 16**,** 1949-51.

STRIPPOLI, R., BENEDICTO, I., PEREZ LOZANO, M. L., CEREZO, A., LOPEZ-CABRERA, M. & DEL POZO, M. A. 2008. Epithelial-to-mesenchymal transition of peritoneal mesothelial cells is regulated by an ERK/NF-kappaB/Snail1 pathway. *Dis Model Mech,* 1**,** 264-74.

STUPACK, D. G. & CHERESH, D. A. 2002. Get a ligand, get a life: integrins, signaling and cell survival. *J Cell Sci,* 115**,** 3729-38.

STYLIANOU, E., O'NEILL, L. A., RAWLINSON, L., EDBROOKE, M. R., WOO, P. & SAKLATVALA, J. 1992. Interleukin 1 induces NF-kappa B through its type I but not its type II receptor in lymphocytes. *J Biol Chem,* 267**,** 15836-41.

SULAIMAN, H., DAWSON, L., LAURENT, G. J., BELLINGAN, G. J. & HERRICK, S. E. 2002. Role of plasminogen activators in peritoneal adhesion formation. *Biochem Soc Trans,* 30**,** 126-31.

SULAIMAN, H., GABELLA, G., DAVIS, C., MUTSAERS, S. E., BOULOS, P., LAURENT, G. J. & HERRICK, S. E. 2000. Growth of nerve fibres into murine peritoneal adhesions. *J Pathol,* 192**,** 396-403.

SUN, L., DENG, L., EA, C. K., XIA, Z. P. & CHEN, Z. J. 2004. The TRAF6 ubiquitin ligase and TAK1 kinase mediate IKK activation by BCL10 and MALT1 in T lymphocytes. *Mol Cell,* 14**,** 289-301.

SUZUKI, K., ENGHILD, J. J., MORODOMI, T., SALVESEN, G. & NAGASE, H. 1990. Mechanisms of activation of tissue procollagenase by matrix metalloproteinase 3 (stromelysin). *Biochemistry,* 29**,** 10261-70.

SUZUKI, N., YOKOYAMA, F. & NOMIZU, M. 2005. Functional sites in the laminin alpha chains. *Connect Tissue Res,* 46**,** 142-52.

TANAKA, M., FUENTES, M. E., YAMAGUCHI, K., DURNIN, M. H., DALRYMPLE, S. A., HARDY, K. L. & GOEDDEL, D. V. 1999. Embryonic lethality, liver degeneration, and impaired NF-kappa B activation in IKK-beta-deficient mice. *Immunity,* 10**,** 421-9.

TANAKA, S., CHOE, N., IWAGAKI, A., HEMENWAY, D. R. & KAGAN, E. 2000. Asbestos exposure induces MCP-1 secretion by pleural mesothelial cells. *Exp Lung Res,* 26**,** 241-55.

TAYLOR-ROBINSON, D., STACEY, C. M., JENSEN, J. S., THOMAS, B. J. & MUNDAY, P. E. 2009. Further observations, mainly serological, on a cohort of women with or without pelvic inflammatory disease. *Int J STD AIDS,* 20**,** 712-8.

THAI, S. N. & IRUELA-ARISPE, M. L. 2002. Expression of ADAMTS1 during murine development. *Mech Dev,* 115**,** 181-5.

TIEDEMANN, K. 1976. On the yolk sac of the cat. Endoderm and mesothelium. *Cell Tissue Res,* 173**,** 109-27.

TOLHURST CLEAVER, C. L., HOPKINS, A. D., KEE KWONG, K. C. & RAFTERY, A. T. 1974. The effect of postoperative peritoneal lavage on survival, peritoneal wound healing and adhesion formation following fecal peritonitis: an experimental study in the rat. *Br J Surg,* 61**,** 601-4.

TOPLEY, N., JORRES, A., LUTTMANN, W., PETERSEN, M. M., LANG, M. J., THIERAUCH, K. H., MULLER, C., COLES, G. A., DAVIES, M. & WILLIAMS, J. D. 1993. Human peritoneal mesothelial cells synthesize interleukin-6: induction by IL-1 beta and TNF alpha. *Kidney Int,* 43**,** 226-33.

TOPLEY, N., PETERSEN, M. M., MACKENZIE, R., NEUBAUER, A., STYLIANOU, E., KAEVER, V., DAVIES, M., COLES, G. A., JORRES, A. & WILLIAMS, J. D. 1994. Human peritoneal mesothelial cell prostaglandin synthesis: induction of cyclooxygenase mRNA by peritoneal macrophage-derived cytokines. *Kidney Int,* 46**,** 900-9.

TORRE, M., FAVRE, A., PINI PRATO, A., BRIZZOLARA, A. & MARTUCCIELLO, G. 2002. Histologic study of peritoneal adhesions in children and in a rat model. *Pediatr Surg Int,* 18**,** 673-6.

TRACKMAN, P. C., BEDELL-HOGAN, D., TANG, J. & KAGAN, H. M. 1992. Post-translational glycosylation and proteolytic processing of a lysyl oxidase precursor. *J Biol Chem,* 267**,** 8666-71.

TRACKMAN, P. C., PRATT, A. M., WOLANSKI, A., TANG, S. S., OFFNER, G. D., TROXLER, R. F. & KAGAN, H. M. 1990. Cloning of rat aorta lysyl oxidase cDNA: complete codons and predicted amino acid sequence. *Biochemistry,* 29**,** 4863-70.

TRAUTMANN, A., TOKSOY, A., ENGELHARDT, E., BROCKER, E. B. & GILLITZER, R. 2000. Mast cell involvement in normal human skin wound healing: expression of monocyte chemoattractant protein-1 is correlated with recruitment of mast cells which synthesize interleukin-4 in vivo. *J Pathol,* 190**,** 100-6.

TSILIBARY, E. C. & WISSIG, S. L. 1977. Absorption from the peritoneal cavity: SEM study of the mesothelium covering the peritoneal surface of the muscular portion of the diaphragm. *Am J Anat,* 149**,** 127-33.

TSILIBARY, E. C. & WISSIG, S. L. 1983. Lymphatic absorption from the peritoneal cavity: regulation of patency of mesothelial stomata. *Microvasc Res,* 25**,** 22-39.

TZU, J. & MARINKOVICH, M. P. 2008. Bridging structure with function: structural, regulatory, and developmental role of laminins. *Int J Biochem Cell Biol,* 40**,** 199-214.

URIA, J. A. & LOPEZ-OTIN, C. 2000. Matrilysin-2, a new matrix metalloproteinase expressed in human tumors and showing the minimal domain organization required for secretion, latency, and activity. *Cancer Res,* 60**,** 4745-51.

UZEL, M. I., SCOTT, I. C., BABAKHANLOU-CHASE, H., PALAMAKUMBURA, A. H., PAPPANO, W. N., HONG, H. H., GREENSPAN, D. S. & TRACKMAN, P. C. 2001. Multiple bone morphogenetic protein 1-related mammalian metalloproteinases process pro-lysyl oxidase at the correct physiological site and control lysyl oxidase activation in mouse embryo fibroblast cultures. *J Biol Chem,* 276**,** 22537-43.

VALCOURT, U., KOWANETZ, M., NIIMI, H., HELDIN, C. H. & MOUSTAKAS, A. 2005. TGF-beta and the Smad signaling pathway support transcriptomic reprogramming during epithelial-mesenchymal cell transition. *Mol Biol Cell,* 16**,** 1987-2002.

VAN DER BURG, B. & VAN DER SAAG, P. T. 1996. Nuclear factor-kappa-B/steroid hormone receptor interactions as a functional basis of anti-inflammatory action of steroids in reproductive organs. *Mol Hum Reprod,* 2**,** 433-8.

VAN DER LAAN, S. & MEIJER, O. C. 2008. Pharmacology of glucocorticoids: beyond receptors. *Eur J Pharmacol,* 585**,** 483-91.

VANDEN BERGHE, W., DE BOSSCHER, K., BOONE, E., PLAISANCE, S. & HAEGEMAN, G. 1999. The nuclear factor-kappaB engages CBP/p300 and histone acetyltransferase activity for transcriptional activation of the interleukin-6 gene promoter. *J Biol Chem,* 274**,** 32091-8.

VARGA, J. & JIMENEZ, S. A. 1986. Stimulation of normal human fibroblast collagen production and processing by transforming growth factor-beta. *Biochem Biophys Res Commun,* 138**,** 974-80.

VASSALLI, J. D., SAPPINO, A. P. & BELIN, D. 1991. The plasminogen activator/plasmin system. *J Clin Invest,* 88**,** 1067-72.

VAZQUEZ, F., HASTINGS, G., ORTEGA, M. A., LANE, T. F., OIKEMUS, S., LOMBARDO, M. & IRUELA-ARISPE, M. L. 1999. METH-1, a human ortholog of ADAMTS-1, and METH-2 are members of a new family of proteins with angio-inhibitory activity. *J Biol Chem,* 274**,** 23349-57.

VELNAR, T., BAILEY, T. & SMRKOLJ, V. 2009. The wound healing process: an overview of the cellular and molecular mechanisms. *J Int Med Res,* 37**,** 1528-42.

VERRECCHIA, F., CHU, M. L. & MAUVIEL, A. 2001. Identification of novel TGF-beta /Smad gene targets in dermal fibroblasts using a combined cDNA microarray/promoter transactivation approach. *J Biol Chem,* 276**,** 17058-62.

VICENTE-MANZANARES, M., WEBB, D. J. & HORWITZ, A. R. 2005. Cell migration at a glance. *J Cell Sci,* 118**,** 4917-9.

VISSE, R. & NAGASE, H. 2003. Matrix metalloproteinases and tissue inhibitors of metalloproteinases: structure, function, and biochemistry. *Circ Res,* 92**,** 827-39.

VISSER, C. E., BROUWER-STEENBERGEN, J. J., SCHADEE-EESTERMANS, I. L., MEIJER, S., KREDIET, R. T. & BEELEN, R. H. 1996. Ingestion of Staphylococcus aureus, Staphylococcus epidermidis, and Escherichia coli by human peritoneal mesothelial cells. *Infect Immun,* 64**,** 3425-8.

VISSER, C. E., STEENBERGEN, J. J., BETJES, M. G., MEIJER, S., ARISZ, L., HOEFSMIT, E. C., KREDIET, R. T. & BEELEN, R. H. 1995. Interleukin-8 production by human mesothelial cells after direct stimulation with staphylococci. *Infect Immun,* 63**,** 4206-9.

VISSER, C. E., TEKSTRA, J., BROUWER-STEENBERGEN, J. J., TUK, C. W., BOORSMA, D. M., SAMPAT-SARDJOEPERSAD, S. C., MEIJER, S., KREDIET, R. T. & BEELEN, R. H. 1998a. Chemokines produced by mesothelial cells: huGRO-alpha, IP-10, MCP-1 and RANTES. *Clin Exp Immunol,* 112**,** 270-5.

VISSER, J., VAN BOXEL-DEZAIRE, A., METHORST, D., BRUNT, T., DE KLOET, E. R. & NAGELKERKEN, L. 1998b. Differential regulation of interleukin-10 (IL-10) and IL-12 by glucocorticoids in vitro. *Blood,* 91**,** 4255-64.

VU, T. H. & WERB, Z. 2000. Matrix metalloproteinases: effectors of development and normal physiology. *Genes Dev,* 14**,** 2123-33.

WAJANT, H., HAAS, E., SCHWENZER, R., MUHLENBECK, F., KREUZ, S., SCHUBERT, G., GRELL, M., SMITH, C. & SCHEURICH, P. 2000. Inhibition of death receptor-mediated gene induction by a cycloheximide-sensitive factor occurs at the level of or upstream of Fas-associated death domain protein (FADD). *J Biol Chem,* 275**,** 24357-66.

WAJANT, H., PFIZENMAIER, K. & SCHEURICH, P. 2003. Tumor necrosis factor signaling. *Cell Death Differ,* 10**,** 45-65.

WALLWIENER, C. W., KRAEMER, B., WALLWIENER, M., BROCHHAUSEN, C., ISAACSON, K. B. & RAJAB, T. K. 2010. The extent of adhesion induction through electrocoagulation and suturing in an experimental rat study. *Fertil Steril,* 93**,** 1040-4.

WANG, J. & SPRINGER, T. A. 1998. Structural specializations of immunoglobulin superfamily members for adhesion to integrins and viruses. *Immunol Rev,* 163**,** 197-215.

WANG, N. S. 1974. The regional difference of pleural mesothelial cells in rabbits. *Am Rev Respir Dis,* 110**,** 623-33.

WANG, N. S. 1975. The preformed stomas connecting the pleural cavity and the lymphatics in the parietal pleura. *Am Rev Respir Dis,* 111**,** 12-20.

WANG, Q., USINGER, W., NICHOLS, B., GRAY, J., XU, L., SEELEY, T. W., BRENNER, M., GUO, G., ZHANG, W., OLIVER, N., LIN, A. & YEOWELL, D. 2011. Cooperative

interaction of CTGF and TGF-beta in animal models of fibrotic disease. *Fibrogenesis Tissue Repair,* 4**,** 4.

WANG, S. X., MURE, M., MEDZIHRADSZKY, K. F., BURLINGAME, A. L., BROWN, D. E., DOOLEY, D. M., SMITH, A. J., KAGAN, H. M. & KLINMAN, J. P. 1996. A crosslinked cofactor in lysyl oxidase: redox function for amino acid side chains. *Science,* 273**,** 1078-84.

WANG, T., CHEN, Y. H., HONG, H., ZENG, Y., ZHANG, J., LU, J. P., JEANSONNE, B. & LU, Q. 2009. Increased nucleotide polymorphic changes in the 5'-untranslated region of delta-catenin (CTNND2) gene in prostate cancer. *Oncogene,* 28**,** 555-64.

WANG, X., YI, J., LEI, J. & PEI, D. 1999a. Expression, purification and characterization of recombinant mouse MT5-MMP protein products. *FEBS Lett,* 462**,** 261-6.

WANG, Y., JOHNSON, A. R., YE, Q. Z. & DYER, R. D. 1999b. Catalytic activities and substrate specificity of the human membrane type 4 matrix metalloproteinase catalytic domain. *J Biol Chem,* 274**,** 33043-9.

WARN, R., HARVEY, P., WARN, A., FOLEY-COMER, A., HELDIN, P., VERSNEL, M., ARAKAKI, N., DAIKUHARA, Y., LAURENT, G. J., HERRICK, S. E. & MUTSAERS, S. E. 2001. HGF/SF induces mesothelial cell migration and proliferation by autocrine and paracrine pathways. *Exp Cell Res,* 267**,** 258-66.

WATTERS, W. B. & BUCK, R. C. 1973. Mitotic activity of peritoneum in contact with a regenerating area of peritoneum. *Virchows Arch B Cell Pathol,* 13**,** 48-54.

WEIBEL, M. A. & MAJNO, G. 1973. Peritoneal adhesions and their relation to abdominal surgery. A postmortem study. *Am J Surg,* 126**,** 345-53.

WENSTRUP, R. J., FLORER, J. B., DAVIDSON, J. M., PHILLIPS, C. L., PFEIFFER, B. J., MENEZES, D. W., CHERVONEVA, I. & BIRK, D. E. 2006. Murine model of the Ehlers-Danlos syndrome. col5a1 haploinsufficiency disrupts collagen fibril assembly at multiple stages. *J Biol Chem,* 281**,** 12888-95.

WERB, Z., BANDA, M. J. & JONES, P. A. 1980. Degradation of connective tissue matrices by macrophages. I. Proteolysis of elastin, glycoproteins, and collagen by proteinases isolated from macrophages. *J Exp Med,* 152**,** 1340-57.

WERNER, S. & GROSE, R. 2003. Regulation of wound healing by growth factors and cytokines. *Physiol Rev,* 83**,** 835-70.

WESCHE, H., HENZEL, W. J., SHILLINGLAW, W., LI, S. & CAO, Z. 1997. MyD88: an adapter that recruits IRAK to the IL-1 receptor complex. *Immunity,* 7**,** 837-47.

WHAWELL, S. A. & THOMPSON, J. N. 1995. Cytokine-induced release of plasminogen activator inhibitor-1 by human mesothelial cells. *Eur J Surg,* 161**,** 315-8.

WHITAKER, D., MANNING, L., ROBINSON, B. & SHILKIN, K. 1992. The pathobiology of the mesothelium.

. *In:* HENDERSON DW, S. K., LANGLOIS SLEP, WHITAKER D (EDS). (ed.) *Malignant Mesothelioma. .* New York: Hemisphere Publishing.

WHITAKER, D. & PAPADIMITRIOU, J. 1985. Mesothelial healing: morphological and kinetic investigations. *J Pathol,* 145**,** 159-75.

WHITAKER, D., PAPADIMITRIOU, J. M. & WALTERS, M. N. 1980. The mesothelium: a histochemical study of resting mesothelial cells. *J Pathol,* 132**,** 273-84.

WHITAKER, D., PAPADIMITRIOU, J. M. & WALTERS, M. N. 1982. The mesothelium and its reactions: a review. *Crit Rev Toxicol,* 10**,** 81-144.

WHITE, D. P., CASWELL, P. T. & NORMAN, J. C. 2007. alpha v beta3 and alpha5beta1 integrin recycling pathways dictate downstream Rho kinase signaling to regulate persistent cell migration. *J Cell Biol,* 177**,** 515-25.

WIGHT, T. N. 2002. Versican: a versatile extracellular matrix proteoglycan in cell biology. *Curr Opin Cell Biol,* 14**,** 617-23.

WILL, H., ATKINSON, S. J., BUTLER, G. S., SMITH, B. & MURPHY, G. 1996. The soluble catalytic domain of membrane type 1 matrix metalloproteinase cleaves the propeptide of progelatinase A and initiates autoproteolytic activation. Regulation by TIMP-2 and TIMP-3. *J Biol Chem,* 271**,** 17119-23.

WILLIAMS, G. T. & WILLIAMS, W. J. 1983. Granulomatous inflammation--a review. *J Clin Pathol,* 36**,** 723-33.

WILLIAMS, R. S., ROSSI, A. M., CHEGINI, N. & SCHULTZ, G. 1992. Effect of transforming growth factor beta on postoperative adhesion formation and intact peritoneum. *J Surg Res,* 52**,** 65-70.

WILSON, M. S., MENZIES, D., KNIGHT, A. D. & CROWE, A. M. 2002. Demonstrating the clinical and cost effectiveness of adhesion reduction strategies. *Colorectal Dis,* 4**,** 355-360.

WITTE, M. B. & BARBUL, A. 1997. General principles of wound healing. *Surg Clin North Am,* 77**,** 509-28.

WOLFFE, A. P., WONG, J. & PRUSS, D. 1997. Activators and repressors: making use of chromatin to regulate transcription. *Genes Cells,* 2**,** 291-302.

WOODARD, B. H., ROSENBERG, S. I., FARNHAM, R. & ADAMS, D. O. 1982. Incidence and nature of primary granulomatous inflammation in surgically removed material. *Am J Surg Pathol,* 6**,** 119-29.

WYNN, T. A. 2004. Fibrotic disease and the T(H)1/T(H)2 paradigm. *Nat Rev Immunol,* 4**,** 583-94.

WYNN, T. A. 2008. Cellular and molecular mechanisms of fibrosis. *J Pathol,* 214**,** 199-210.

WYNN, T. A. & BARRON, L. 2010. Macrophages: master regulators of inflammation and fibrosis. *Semin Liver Dis,* 30**,** 245-57.

WYSK, M., YANG, D. D., LU, H. T., FLAVELL, R. A. & DAVIS, R. J. 1999. Requirement of mitogen-activated protein kinase kinase 3 (MKK3) for tumor necrosis factor-induced cytokine expression. *Proc Natl Acad Sci U S A,* 96**,** 3763-8.

XIA, M., LEPPERT, D., HAUSER, S. L., SREEDHARAN, S. P., NELSON, P. J., KRENSKY, A. M. & GOETZL, E. J. 1996. Stimulus specificity of matrix metalloproteinase dependence of human T cell migration through a model basement membrane. *J Immunol,* 156**,** 160-7.

XING, Z., GAULDIE, J., COX, G., BAUMANN, H., JORDANA, M., LEI, X. F. & ACHONG, M. K. 1998. IL-6 is an antiinflammatory cytokine required for controlling local or systemic acute inflammatory responses. *J Clin Invest,* 101**,** 311-20.

XIONG, J. P., STEHLE, T., ZHANG, R., JOACHIMIAK, A., FRECH, M., GOODMAN, S. L. & ARNAOUT, M. A. 2002. Crystal structure of the extracellular segment of integrin alpha Vbeta3 in complex with an Arg-Gly-Asp ligand. *Science,* 296**,** 151-5.

XU, J., LAMOUILLE, S. & DERYNCK, R. 2009. TGF-beta-induced epithelial to mesenchymal transition. *Cell Res,* 19**,** 156-72.

YAMADA, Y., KIRILLOVA, I., PESCHON, J. J. & FAUSTO, N. 1997. Initiation of liver growth by tumor necrosis factor: deficient liver regeneration in mice lacking type I tumor necrosis factor receptor. *Proc Natl Acad Sci U S A,* 94**,** 1441-6.

YANEZ-MO, M., LARA-PEZZI, E., SELGAS, R., RAMIREZ-HUESCA, M., DOMINGUEZ-JIMENEZ, C., JIMENEZ-HEFFERNAN, J. A., AGUILERA, A., SANCHEZ-TOMERO, J. A., BAJO, M. A., ALVAREZ, V., CASTRO, M. A., DEL PESO, G., CIRUJEDA, A., GAMALLO, C., SANCHEZ-MADRID, F. & LOPEZ-CABRERA, M. 2003. Peritoneal dialysis and epithelial-to-mesenchymal transition of mesothelial cells. *N Engl J Med,* 348**,** 403-13.

YANG, K. L., CHANG, W. T., CHUANG, C. C., HUNG, K. C. & LI, E. I. 2008. Antagonizing TGF-beta induced liver fibrosis by a retinoic acid derivative through regulation of ROS and calcium influx. *Biochem Biophys Res Commun,* 365**,** 484-9.

YANG, W. S., KIM, B. S., LEE, S. K., PARK, J. S. & KIM, S. B. 1999. Interleukin-1beta stimulates the production of extracellular matrix in cultured human peritoneal mesothelial cells. *Perit Dial Int,* 19**,** 211-20.

YAO, C. C., ZIOBER, B. L., SQUILLACE, R. M. & KRAMER, R. H. 1996. Alpha7 integrin mediates cell adhesion and migration on specific laminin isoforms. *J Biol Chem,* 271**,** 25598-603.

YAO, V., PLATELL, C. & HALL, J. C. 2003. Role of peritoneal mesothelial cells in peritonitis. *Br J Surg,* 90**,** 1187-94.

YAO, V., PLATELL, C. & HALL, J. C. 2004. Peritoneal mesothelial cells produce inflammatory related cytokines. *ANZ J Surg,* 74**,** 997-1002.

YAP, A. S., BRIEHER, W. M. & GUMBINER, B. M. 1997. Molecular and functional analysis of cadherin-based adherens junctions. *Annu Rev Cell Dev Biol,* 13**,** 119-46.

YEH, Y. Y., CHIAO, C. C., KUO, W. Y., HSIAO, Y. C., CHEN, Y. J., WEI, Y. Y., LAI, T. H., FONG, Y. C. & TANG, C. H. 2008. TGF-beta1 increases motility and alphavbeta3 integrin up-regulation via PI3K, Akt and NF-kappaB-dependent pathway in human chondrosarcoma cells. *Biochem Pharmacol,* 75**,** 1292-301.

YESILDAGLAR, N. & KONINCKX, P. R. 2000. Adhesion formation in intubated rabbits increases with high insufflation pressure during endoscopic surgery. *Hum Reprod,* 15**,** 687-91.

YOKOYAMA, H., WADA, T., KOBAYASHI, K., KUNO, K., KURIHARA, H., SHINDO, T. & MATSUSHIMA, K. 2002. A disintegrin and metalloproteinase with thrombospondin motifs (ADAMTS)-1 null mutant mice develop renal lesions mimicking obstructive nephropathy. *Nephrol Dial Transplant,* 17 Suppl 9**,** 39-41.

YOSHINAGA, S. K., PETERSON, C. L., HERSKOWITZ, I. & YAMAMOTO, K. R. 1992. Roles of SWI1, SWI2, and SWI3 proteins for transcriptional enhancement by steroid receptors. *Science,* 258**,** 1598-604.

YU, L., HEBERT, M. C. & ZHANG, Y. E. 2002. TGF-beta receptor-activated p38 MAP kinase mediates Smad-independent TGF-beta responses. *EMBO J,* 21**,** 3749-59.

YUASA, T., OHNO, S., KEHRL, J. H. & KYRIAKIS, J. M. 1998. Tumor necrosis factor signaling to stress-activated protein kinase (SAPK)/Jun NH2-terminal kinase (JNK) and p38. Germinal center kinase couples TRAF2 to mitogen-activated protein kinase/ERK kinase kinase 1 and

SAPK while receptor interacting protein associates with a mitogen-activated protein kinase kinase kinase upstream of MKK6 and p38. *J Biol Chem,* 273**,** 22681-92.

YUNG, S., THOMAS, G. J. & DAVIES, M. 2000. Induction of hyaluronan metabolism after mechanical injury of human peritoneal mesothelial cells in vitro. *Kidney Int,* 58**,** 1953-62.

YUNG, S., THOMAS, G. J., STYLIANOU, E., WILLIAMS, J. D., COLES, G. A. & DAVIES, M. 1995. Source of peritoneal proteoglycans. Human peritoneal mesothelial cells synthesize and secrete mainly small dermatan sulfate proteoglycans. *Am J Pathol,* 146**,** 520-9.

ZEILLEMAKER, A. M., MUL, F. P., HOYNCK VAN PAPENDRECHT, A. A., KUIJPERS, T. W., ROOS, D., LEGUIT, P. & VERBRUGH, H. A. 1995. Polarized secretion of interleukin-8 by human mesothelial cells: a role in neutrophil migration. *Immunology,* 84**,** 227-32.

ZEISBERG, E. M., TARNAVSKI, O., ZEISBERG, M., DORFMAN, A. L., MCMULLEN, J. R., GUSTAFSSON, E., CHANDRAKER, A., YUAN, X., PU, W. T., ROBERTS, A. B., NEILSON, E. G., SAYEGH, M. H., IZUMO, S. & KALLURI, R. 2007. Endothelial-to-mesenchymal transition contributes to cardiac fibrosis. *Nat Med,* 13**,** 952-61.

ZEISBERG, M. & KALLURI, R. 2004. The role of epithelial-to-mesenchymal transition in renal fibrosis. *J Mol Med,* 82**,** 175-81.

ZEYNELOGLU, H. B., SELI, E., SENTURK, L. M., GUTIERREZ, L. S., OLIVE, D. L. & ARICI, A. 1998. The effect of monocyte chemotactic protein 1 in intraperitoneal adhesion formation in a mouse model. *Am J Obstet Gynecol,* 179**,** 438-43.

ZHANG, J. Y., WANG, Y., ZHANG, D., YANG, Z. Q., DONG, X. J., JIANG, G. Y., ZHANG, P. X., DAI, S. D., DONG, Q. Z., HAN, Y., ZHANG, S., CUI, Q. Z. & WANG, E. H. 2010. delta-Catenin promotes malignant phenotype of non-small cell lung cancer by non-competitive binding to E-cadherin with p120ctn in cytoplasm. *J Pathol,* 222**,** 76-88.

ZHANG, Q. X., MAGOVERN, C. J., MACK, C. A., BUDENBENDER, K. T., KO, W. & ROSENGART, T. K. 1997. Vascular endothelial growth factor is the major angiogenic factor in omentum: mechanism of the omentum-mediated angiogenesis. *J Surg Res,* 67**,** 147-54.

ZHANG, W., ZHANG, Z. & ZHANG, Y. 2011. The application of carbon nanotubes in target drug delivery systems for cancer therapies. *Nanoscale Res Lett,* 6**,** 555.

ZHU, Z., HOMER, R. J., WANG, Z., CHEN, Q., GEBA, G. P., WANG, J., ZHANG, Y. & ELIAS, J. A. 1999. Pulmonary expression of interleukin-13 causes inflammation, mucus hypersecretion, subepithelial fibrosis, physiologic abnormalities, and eotaxin production. *J Clin Invest,* 103**,** 779-88.

Appendix 1

Negative control (Rabbit IgG) for LOX antibodies on NT-treated diaphragm section (X4)

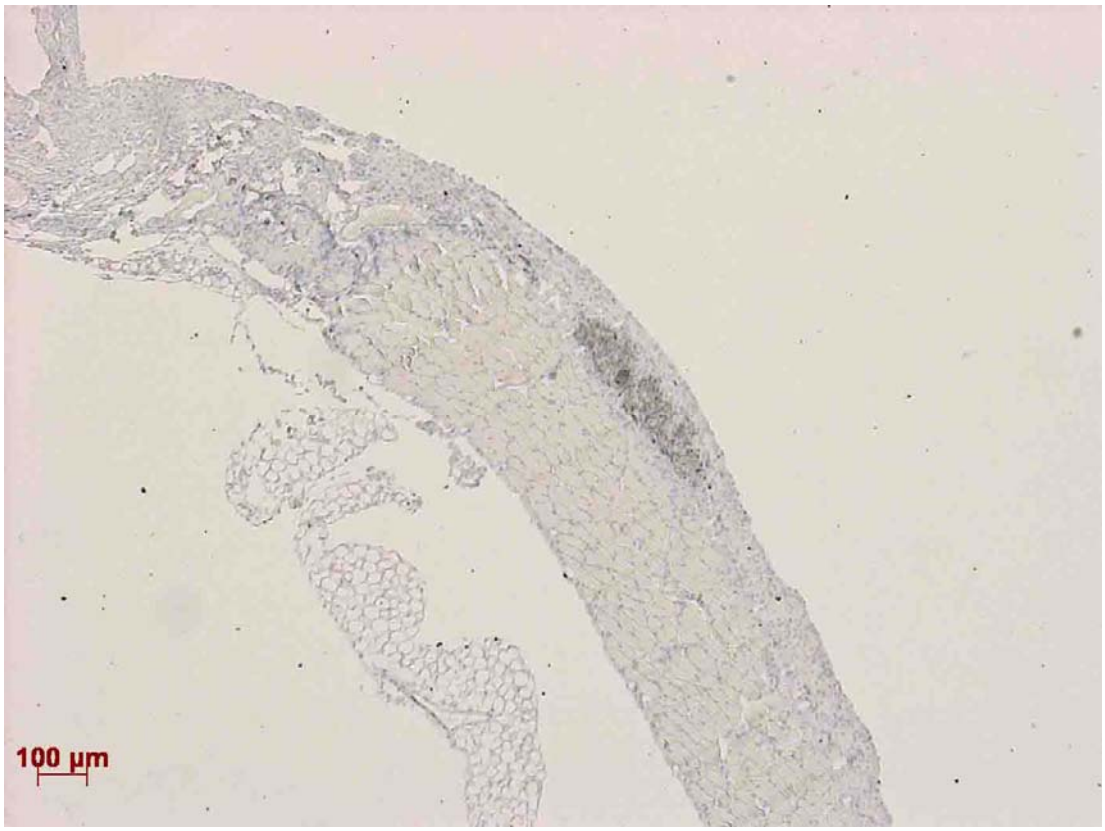

Appendix 2

Histology sections of mouse diaphragm stained with picrosirius red

Diaphrams were recovered from mice following 7 days treatment of the following groups: A: BAPN, animal treated with 0.5ml saline on day 1 and daily 200µl i.p. injections of BAPN (1g/kg) for 7 days. B: DEX, animal treated with 0.5ml saline on day 1 and daily 200µl i.p. injections of DEX (1mg/kg) for 7 days. or C: BAPN+DEX

A BAPN

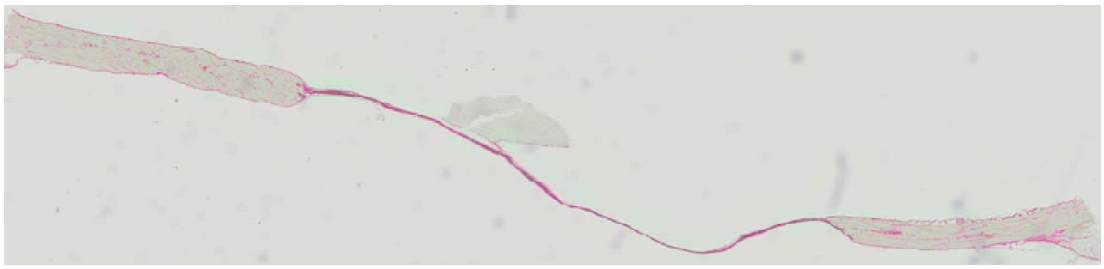

B DEX

C BAPN+DEX